

Design and Synthesis of Donor-Acceptor Functionalized Phenothiazines

Ph.D. Thesis

By
Madhurima Poddar



DISCIPLINE OF CHEMISTRY
INDIAN INSTITUTE OF TECHNOLOGY INDORE

Design and Synthesis of Donor-Acceptor Functionalized Phenothiazines

A THESIS

*Submitted in partial fulfillment of the
requirements for the award of the degree*

of
DOCTOR OF PHILOSOPHY

by

Madhurima Poddar



DISCIPLINE OF CHEMISTRY
INDIAN INSTITUTE OF TECHNOLOGY INDORE

June 2020



INDIAN INSTITUTE OF TECHNOLOGY INDORE

CANDIDATE'S DECLARATION

I hereby certify that the work which is being presented in the thesis entitled **Design and Synthesis of Donor-Acceptor Functionalized Phenothiazines** in the partial fulfillment of the requirements for the award of the degree of **DOCTOR OF PHILOSOPHY** and submitted in the **DISCIPLINE OF CHEMISTRY, Indian Institute of Technology Indore**, is an authentic record of my own work carried out during the time period from **July 2015 to June 2020** under the supervision of Dr. Rajneesh Misra, Professor, Discipline of Chemistry, IIT Indore.

The matter presented in this thesis has not been submitted by me for the award of any other degree of this or any other institute.

Madhurima Poddar 26.06.2020

**Signature of the student with date
(MADHURIMA PODDAR)**

This is to certify that the above statement made by the candidate is correct to the best of my/our knowledge.

Rajneesh Misra 26.06.2020

**Signature of Thesis Supervisor with date
(Dr. RAJNEESH MISRA)**

MADHURIMA PODDAR has successfully given her Ph.D. Oral Examination held on **01.12.2020**

| | | |
|---|---|---|
| Signature of Chairperson (OEB) Date: 01.12.2020 | Signature of External Examiner Date: 01.12.2020 | Signature(s) of Thesis Supervisor(s) Date: 01.12.2020 |
| Signature of PSPC Member #1 Date: 01.12.2020 | Signature of PSPC Member #2 Date: 01.12.2020 | Signature of Convener, DPGC Date: 01.12.2020 |

Signature of Head of Discipline
Date: **01.12.2020**

ACKNOWLEDGEMENTS

The work described in this thesis would not have been possible without my close association with numerous people who were always there when I required them the most. I take this opportunity to acknowledge them and extend my sincere gratitude for helping me make this Ph.D. thesis a possibility.

First and foremost, I would like to extend my sincere gratitude to the person who made the biggest difference in my life, my mentor and supervisor, Prof. Rajneesh Misra. He has been there, throughout my Ph.D., motivating and inspiring every bit of me towards new possibilities in life. His enthusiasm, integral view on research and his mission for providing high-quality work, has made a deep impression on me. He has been living role model to me, as I have learnt extensively from him including how to raise new possibilities, how to regard an old question from a new perspective, how to approach a problem by systematic thinking, data-driven decision making and exploiting serendipity. I am indebted to him for his support, motivation and better understanding. I am glad to be associated with a person like Prof. Rajneesh Misra in my life.

I express my heart-felt gratitude to Dr. Shaikh M. Mobin for single crystal X-ray support and his valuable guidance. I would also like to extend my gratitude to my PSpC members Dr. Sampak Samanta and Dr. Abhishek Srivastava for their valuable suggestions, guidance, and support.

With great pleasure, I express my respect to Prof. Nilesh Jain [Director (Officiating), Indian Institute of Technology Indore] for his unending encouragement and providing all the facilities at Indian Institute of Technology Indore.

I am grateful to Dr. Biswarup Pathak (Head, Discipline of Chemistry, Indian Institute of Technology Indore) for his suggestions and guidance in various aspects. I am also grateful to Dr. Suman Mukhopadhyay, Dr. Tridib K. Sarma, Dr. Anjan Chakraborty, Dr. Sampak Samanta, Dr. Shaikh M. Mobin, Dr. Tushar Kanti Mukherjee, Dr. Apurba K Das, Dr. Sanjay Singh, Dr. Satya Bulusu, Dr. Chelvam Venkatesh, Dr. Amrendra Kumar Singh, Dr. Abhinav Raghuvanshi, Dr.

Dipak Kumar Roy, Dr. Selvakumar Sermadurai and Dr. Umesh A. Kshirsagar for their guidance and help during various activities.

I would like to acknowledge all the teachers I learnt from since my childhood, I would not have been here without their guidance, blessing and support.

I extend my profound thanks to my group members, Dr. Bhausahab Dhokale, Dr. Prabhat Gautam, Dr. Thaksen Jadav, Dr. Ramesh Maragani, Dr. Rekha Sharma, Dr. Yuvraj Patil, Dr. Ramana Reddi, Dr. Gangala Sivakumar, Dr. Shubhra Bikash Maity, Dr. Ramireddy Eda, Yogajivan, Bijesh, Anupama, Charu, Jivan, Manju, Indresh, Faizal, Wazid, Pankaj, Nikhilji, Rahul, Shalu, Priyanka, Hariom, Karishma, Haripriya, Vinay, Vivek and Nitin for their generous co-operation and help to make my work successful.

I am also thankful to all my friends who helped me directly-indirectly during my Ph. D. I am thankful to Ms. Sarita Batra, Mr. Kinney Pandey, Mr. Ghanshyam Bhavsar, Mr. Manish Kushwaha, Mr. Rameshwar and Ms. Vinita Kothari for their technical help and support.

I would like to express my thanks to IIT Indore for infrastructure and Ministry of Human Resource Development (MHRD) for my Fellowship and all others who helped and supported me directly or indirectly.

A special mention of thanks to my flatmates Dr. Deepika Tyagi, Dr. Camellia Sarkar, Dr. Suchismita Behera, Dr. Pragati Sahoo, Dr. Aparna Rai and our cutest Coco for their constant support, guidance and cooperation during my Ph.D. Their extended sisterly love towards me made my journey much easier.

I would also like to thank few of my close friends for providing a stimulating and fun filled environment. My thanks go in particular to Dr. Saptarshi, Priodyuti, Debapriya, Piyalidi, Momisa, Damayitri, Pratyusa, Samapika.

My heart-felt thanks to my splendid juniors and seniors at IIT Indore for their generous co-operation and help.

My heartfelt regard goes to my father Mr. Ranjit Poddar, mother Ms. Susmita Poddar, father-in-law Mr. Nripendra Nath Sarkar, mother-in-law Ms.

Sangita Sarkar, my husband Mr. Anirban Sarkar, my uncles (Mr. Biswajit Choudhury, Mr. Ranjan Sarkar and Mr. Abhijit Poddar), aunts (Ms Basabi Choudhury, Ms Jayanti Sarkar and Late Keya Poddar), sisters (Bulti, Rina, Rini, Rimpa, Riya, Boni, Babi, Rai, Banti, Poulami, Tua), sister-in-law Ms. Tamallika Sarkar, brothers (Asim and Asit) for their love and moral support and I must mention the youngest members Hampu, Hampi, Abir, Writ, Chini and Topor for their smiley support. I deeply express my love and gratitude to my lovable family.

Most importantly none of these would have been possible without the blessing of my grandfathers (Late Mr. Amarendra Poddar, Late Mr. Prafullya Choudhury, Mr. Narayan Poddar, Late Mr. Bikash Saha and Late Mr. Parimal Saha) and my grandmothers (Ms. Gita Poddar, Ms. Rekha Choudhury, Ms. Polly Poddar and Late Ms. Manjusree Saha). I doubt that I will ever be able to convey my appreciation fully, but I owe them my eternal gratitude.

Finally, I thank the Almighty for giving me the strength and patience to work through all these years.

DEDICATED TO

My Grandparents

Late Amarendra Narayan Poddar

Late Prafulla Chandra Choudhury

Gita Poddar

Rekha Choudhury

– MADHURIMA PODDAR

Synopsis

Phenothiazine is a class of fused heteroaromatic compound, containing sulfur (S) and nitrogen (N) atoms in the central ring (Figure 1). Phenothiazine acts as a strong donor which has been used as a building block to develop optoelectronic materials. Phenothiazine derivatives possess high chemical and thermal stability, low reversible oxidation potential, strong absorption, high luminescence and photo-conductivities. The most common approach for tuning the photophysical and electrochemical properties of the phenothiazine is to link donor/acceptor units directly or by π -spacer at the 3- and 7- positions of phenothiazine (Figure 2). The donor–acceptor functionalized phenothiazines exhibit strong absorption in the near-infrared region and low HOMO–LUMO gap which are used as potential candidates for the applications in dye sensitized solar cells (DSSCs), bulk heterojunction organic solar cells (BHJOSCs), OLEDs, NLOs, OFETs, hole transporting materials (HTMs), sensing, bioimaging, photodynamic therapy *etc.*

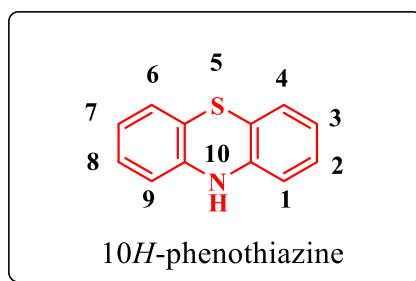


Figure 1. The molecular structure of phenothiazine core.

In order to improve the photonic and electronic properties of phenothiazines a variety of donors (ferrocene, triphenylamine, carbazole) and acceptors (BODIPY, 1,8-naphthalimide, 1,1,2,2-tetracyanoethylene and 7,7,8,8-tetracyanoquinodimethane) have been introduced to the phenothiazine core. The photophysical and electrochemical properties of the donor–acceptor functionalized phenothiazines were investigated.

The main objectives of the current work are:

- To design and synthesize donor–acceptor functionalized phenothiazine derivatives for optoelectronic applications.
- To synthesize symmetrical and unsymmetrical phenothiazine derivatives by varying the donor/acceptor units in a systematic way.
- To study the effect of substitution pattern of donor–acceptor phenothiazines on their photophysical and electrochemical properties.
- To fine tune the HOMO–LUMO gap by altering the donor/acceptor strength or π -linker on the phenothiazine core.
- To investigate the structural and photophysical properties of the donor–acceptor functionalized phenothiazines *via* density functional theory (DFT) and time-dependent density functional theory (TD-DFT) calculations and compare with the experimental data.

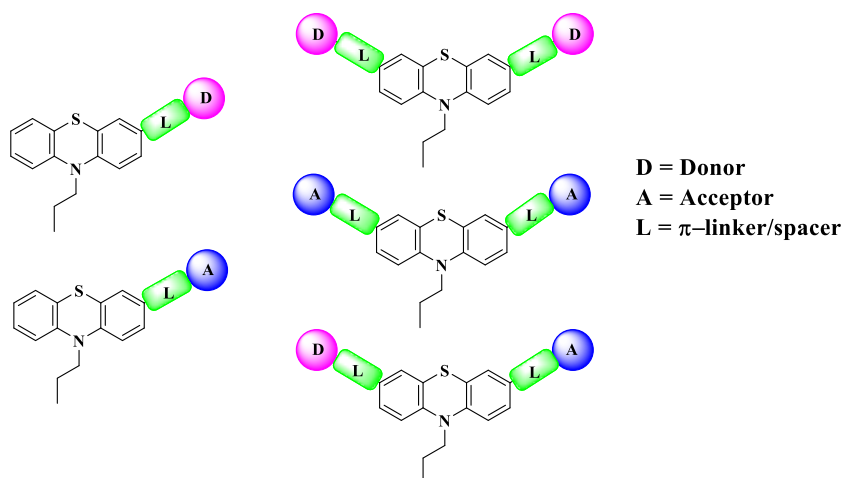


Figure 2. General classification of donor-acceptor functionalized phenothiazines in this work.

Chapter 1: Introduction

This chapter describes the synthesis and functionalization strategies of phenothiazine derivatives and their applications in various fields.

Chapter 2: Materials and Experimental Techniques

This chapter summarizes the general experimental methods, characterization techniques and details of instruments used for characterization.

Chapter 3: Aryl-Substituted Phenothiazines: Design, Synthesis and Properties

Chapter 3 describes the design and synthesis of a series of aryl substituted phenothiazine-based fluorophores **4a–4f** *via* Pd-catalyzed Sonogashira cross-coupling reactions by attaching appropriately substituted intermediates (phenyl, naphthalene, methoxy naphthalene, anthracene, phenanthrene and pyrene) with the substituted phenothiazine core. The substitution of aryl groups on the phenothiazine core was found to perturb its photophysical and electrochemical properties. The absorption spectrum of the fluorophores showed strong $\pi \rightarrow \pi^*$ transition in the range of 368–440 nm, which may be due to good electronic communication between phenothiazine and aryl moieties. The emission maxima of the fluorophores were bathochromically shifted by increasing the solvent polarity. The fluorophores showed large stoke shift values in the range of 109–215 nm in polar solvents (Figure 3). The fluorophores were also emissive in solid-state where the anthracene, phenanthrene and pyrene substituted phenothiazines showed red shifted emission maxima in the solid state as compared to the solution phase indicating considerable π - π staking in the solid-state. The anthracene substituted phenothiazine exhibited redshifted absorption and emission which may be due to the extended π -conjugation in the molecule, resulting in low HOMO–LUMO energy gap. In order to explore the geometrical structure and the electronic properties of the phenothiazines (**4a–4f**), theoretical studies were performed by using density functional theory (DFT) and time dependent density functional theory (TD-DFT) calculations.

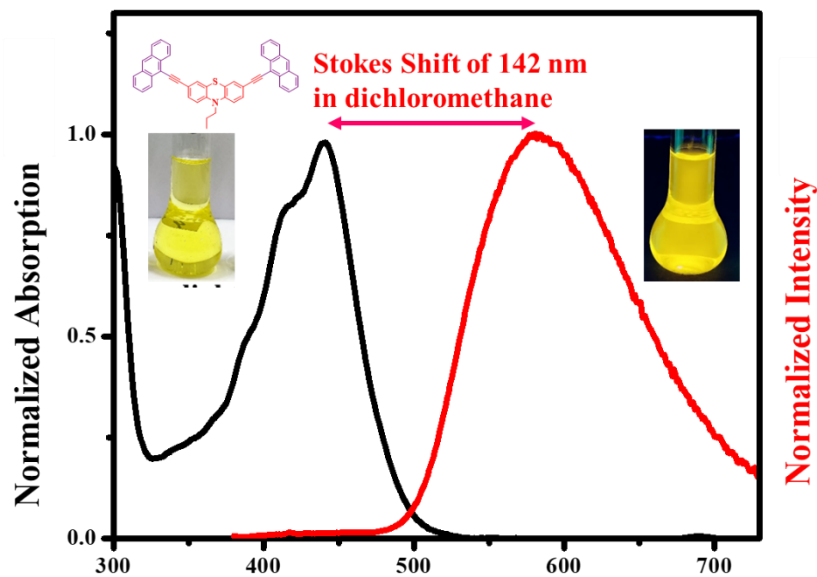


Figure 3. Normalized electronic absorption and emission spectra of anthracene substituted phenothiazine **4d**.

Chapter 4: Design and Synthesis of Donor–Acceptor Based Ferrocene Substituted Phenothiazines: Tuning of HOMO–LUMO gap

Chapter 4 summarizes the design and synthesis of a series of unsymmetrical (D–A–D1, D1– π –D–A–D1 and D1–A1–D–A2–D1) and symmetrical (D1–A–D–A–D1) type of phenothiazines **4b**, **4c**, **4c'**, **5b**, **5c**, **5d**, **5d'**, **5e**, **5e'**, **5f** and **5f'** by [2 + 2] cycloaddition–electrocyclic ring-opening reaction of ferrocenyl substituted phenothiazines with tetracyanoethylene (TCNE) and 7,7,8,8–tetracyanoquinodimethane (TCNQ). The photophysical, electrochemical and computational studies show strong charge-transfer (CT) interaction in the phenothiazine derivatives which can be tuned by the variation of number of TCNE/TCNQ acceptors. The phenothiazines **4b**, **4c**, **4c'**, **5b**, **5c**, **5d**, **5d'**, **5e**, **5e'**, **5f** and **5f'** show red shifted absorption in 400–900 nm region (Figure 4), resulting in low HOMO–LUMO gap which is supported by TD-DFT calculations. The electrochemical study exhibits reduction waves at low potential

due to strong 1,1,4,4-tetracyanobuta-1,3-diene (TCBD) and cyclohexa-2,5-diene-1,4-ylidene-expanded TCBD acceptors. The incorporation of cyclohexa-2,5-diene-1,4-ylidene-expanded TCBD stabilizes the LUMO energy level to greater extent as compared to TCBD.

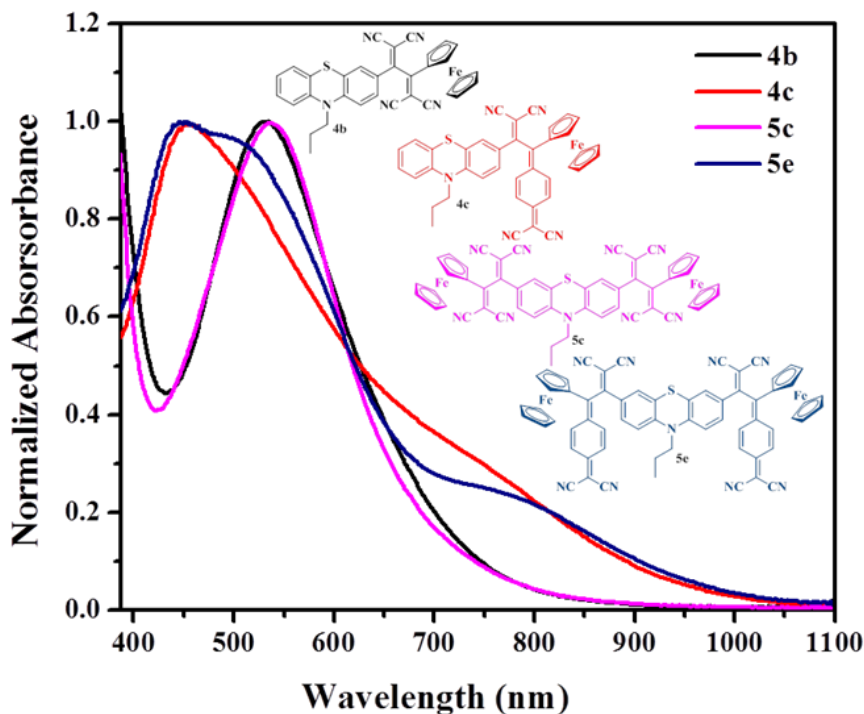


Figure 4. Normalized electronic absorption spectra of TCBD and cyclohexa-2,5-diene-1,4-ylidene-expanded TCBD substituted ferrocenyl phenothiazines.

Chapter 5: Donor-Acceptor Based BODIPY Functionalized Phenothiazines

Chapter 5 reports the design and synthesis of a set of unsymmetrical and symmetrical difluoro-4-bora-3a,4a-diaza-s-indacene (BODIPY) substituted phenothiazines of type D-A, D- π -A and A-D-A, A- π -D- π -A by condensation and Pd-catalyzed Sonogashira cross-coupling reactions. Their photophysical and electrochemical properties were investigated. The electronic absorption spectra showed that the acetylene linked phenothiazine functionalized BODIPYs **7a** and **7b** exhibited bathochromic shift as compared to directly linked phenothiazine

functionalized BODIPYs **4a** and **4b**. The density functional theory (DFT) calculation showed that the incorporation of acetylene linkage between phenothiazine and BODIPYs induced coplanarity and resulted lower HOMO–LUMO gap which leads to red shifted absorption. The unsymmetrical phenothiazine functionalized BODIPYs exhibited higher thermal stability as compared to symmetrical analogous and follow the order **7a** > **4a** > **4b** > **7b**.

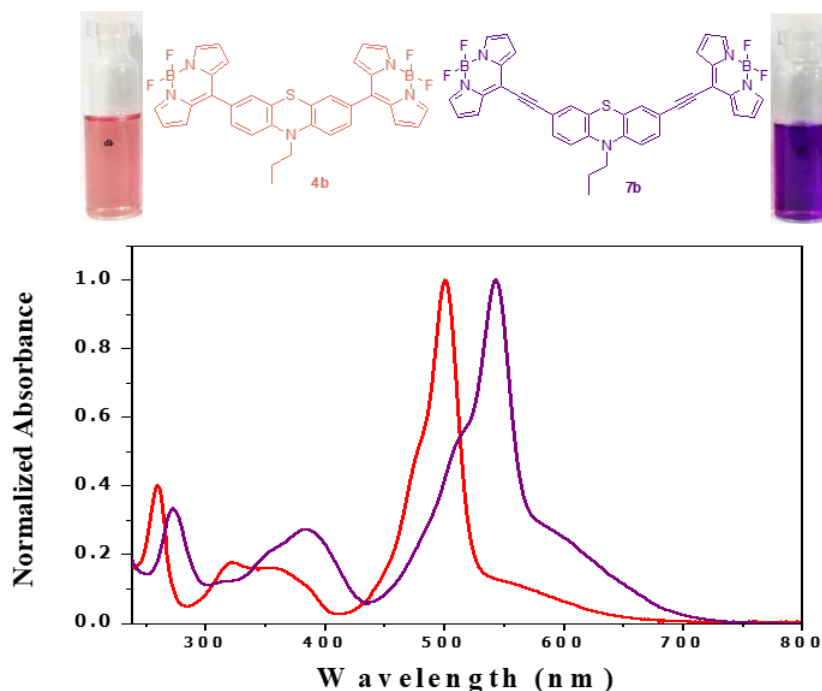


Figure 5. Normalized electronic absorption spectra of BODIPY functionalized phenothiazines **4b** and **7b**.

Chapter 6: 1,1,4,4-Tetracyanobuta-1,3-Diene (TCBD)- and Cyclohexa-2,5-Diene-1,4-Diylidene-Expanded TCBD-Substituted BODIPY-Phenothiazines: Tuning of HOMO–LUMO gap

Chapter 6 describes the synthesis of a set of donor–acceptor based 1,1,4,4-tetracyanobuta-1,3-diene (TCBD) and cyclohexa-2,5-diene-1,4-ylidene-expanded TCBD substituted BODIPY-phenothiazines **1–3**, *via* Pd-catalyzed Sonogashira

cross-coupling reaction and [2+2] cycloaddition–electrocyclic ring-opening reaction. The incorporation of TCBD and cyclohexa-2,5-diene-1,4-ylidene-expanded TCBD (abbreviated as DCNQ = dicyanodiquinodimethane) in BODIPY functionalized phenothiazine resulted in significant perturbation on the optical and electronic properties. The absorption spectrum of both the compounds **2** and **3** showed red shifted absorption as compared to compound **1**. Additionally, both **2** and **3** exhibited a distinct intramolecular charge transfer (ICT) transition in the near-infrared region more so for compound **3**. The electrochemical study revealed multi-redox processes due to the presence of redox-active phenothiazine, BODIPY, TCBD or DCNQ entities. The result revealed that the incorporation of DCNQ resulted in stronger D–A interaction as compared to TCBD.

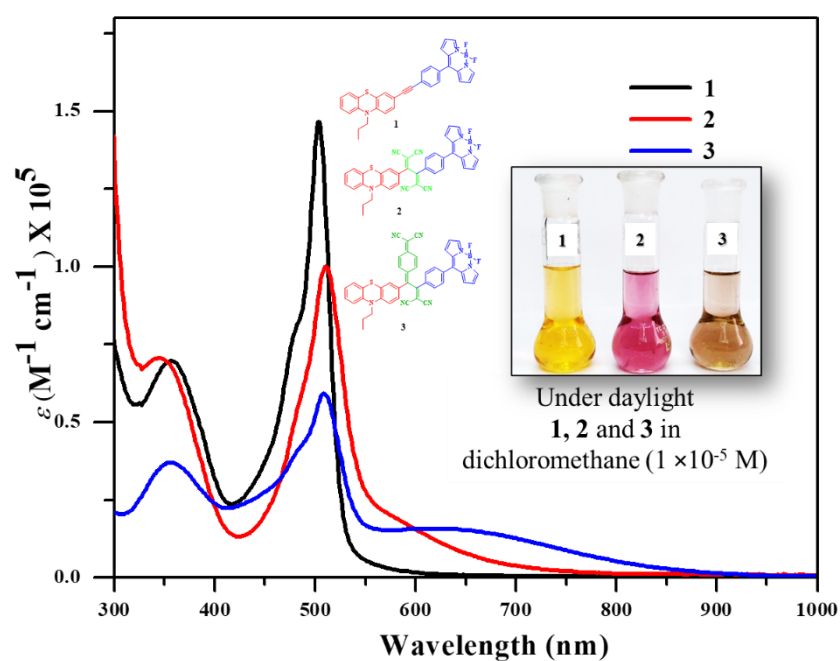


Figure 6. Electronic absorption spectra of phenothiazines **1–3**.

Chapter 7: Donor-Acceptor based 1,8-Naphthalimide Substituted Phenothiazines: Tuning of HOMO-LUMO gap

Chapter 7 describes the design and synthesis of a series of donor-acceptor (D-A) substituted phenothiazine based chromophores (D- π -D- π -A, D'- π -D- π -A, D-A'-D- π -A and D'-A'-D- π -A). The phenothiazine was substituted with the 4-ethynyl-1,8-naphthalimide (NPI) on one side whereas a variety of donors (phenothiazine, carbazole, ferrocene and triphenylamine) were introduced on the other side of phenothiazine via Pd-catalyzed Sonogashira cross-coupling reaction. In order to tune the photophysical and electrochemical properties of the phenothiazine-based chromophores, cyano-based acceptor 1,1,4,4-tetracyanobuta-1,3-diene (TCBD) was incorporated in compounds **12-15** by the [2+2] cycloaddition-electrocyclic ring-opening reaction of compounds **8-11** and tetracyanoethylene (TCNE), respectively. The photophysical and electrochemical studies showed that the incorporation of TCBD acceptor in the compounds **12-15** facilitated the donor-acceptor strength to greater extent. The electronic absorption spectra exhibited red shifted absorption bands for the TCBD substituted phenothiazines as compared to the alkynylated phenothiazines which led to much lower optical band gaps in the formers. Similarly, the electrochemical properties showed that the TCBD substituted compounds **12-15** showed low first reduction potential values as compared to compounds **8-11** which reveals that the incorporation of TCBD acceptor in the former stabilized the LUMO energy level of compounds **12-15** to greater extent. The experimental values were further supported by the DFT and TDDFT calculations.

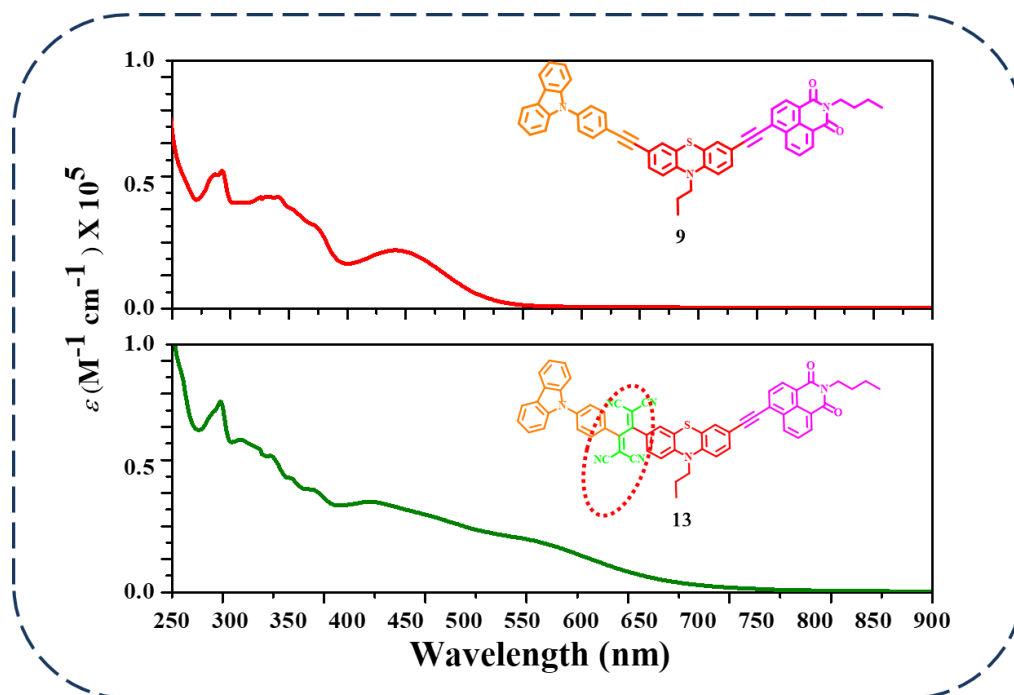


Figure 7. Electronic absorption spectra of donor–acceptor substituted NPI-phenothiazine based compounds **9** and **13**.

Chapter 8: Conclusions and Future Scope.

Chapter 8 summarizes the salient features of the work and its prospects to develop the new materials for optoelectronic applications.

LIST OF PUBLICATIONS

- [1] **Poddar, M.**, Gautam, P., Rout, Y., Misra, R. (2017), Donor–acceptor phenothiazine functionalized BODIPYs, *Dyes and Pigments*, 146, 368–373 (DOI: 10.1016/j.dyepig.2017.07.017). †(Impact Factor = 3.767)
- [2] **Poddar, M.**, Misra, R. (2017), NIR-Absorbing Donor–Acceptor Based 1,1,4,4-Tetracyanobuta-1,3-Diene (TCBD)- and Cyclohexa-2,5-Diene-1,4-Ylidene-Expanded TCBD-Substituted Ferrocenyl Phenothiazines, *Chem. Asian J.*, 12, 2908–2915 (DOI: 10.1002/asia.201700879). † (Impact Factor = 3.692)

- [3] **Poddar, M.**, Sharma, V., Mobin, S. M., Misra, R. (2018), 1,8-Naphthalimide-Substituted BODIPY Dyads: Synthesis, Structure, Properties, and Live-Cell Imaging, *Chem. Asian J.*, 13, 2881–2890 (DOI: 10.1002/asia.201800816). (Impact Factor = 3.698)
- [4] **Poddar, M.**, Sivakumar, G., Misra, R. (2019), Donor–acceptor substituted 1,8-naphthalimides: design, synthesis, and structure–property relationship, *J. Mater. Chem. C*, 7, 14798–14815 (DOI: 10.1039/C9TC02634G). (Impact Factor = 6.641)
- [5] Carlotti, B., **Poddar, M.**, Elisei, F., Spalletti, A., Misra, R. (2019), Energy-Transfer and Charge-Transfer Dynamics in Highly Fluorescent Naphthalimide–BODIPY Dyads: Effect of BODIPY Orientation, *J. Phys. Chem. C*, 123, 24362 (DOI: 10.1021/acs.jpcc.9b05851). (Impact Factor = 4.309)
- [6] **Poddar, M.**,^{\$} Jang, Y.,^{\$} Misra, R., D’Souza, F. (2020), Excited State Electron Transfer in 1,1,4,4-Tetracyanobuta-1,3-Diene (TCBD)- and Cyclohexa-2,5-Diene-1,4-Diylidene-Expanded TCBD–Substituted BODIPY Phenothiazines Donor-Acceptor Conjugates, *Chem. Eur. J.*, 26, 30, 6869 (DOI: 10.1002/chem.202000346). † (Impact Factor = 5.160)
- [7] **Poddar, M.**, Misra, R. (2020), Recent Advances of BODIPY based derivatives for Optoelectronic Applications, *Coordination Chemistry Reviews*, 421, 213462 (DOI: 10.1016/j.ccr.2020.213462). (Impact Factor = 13.476)
- [8] **Poddar, M.**, Cesaretti, A., Ferraguzzi, E., Carlotti, B., Misra, R. (2020), Highly Emissive Aryl–Substituted Phenothiazines: Synthesis and Photophysical Properties, *J. Phys. Chem. C*, 124, 17864 (DOI: 10.1021/acs.jpcc.0c01786). (Impact Factor = 4.270)
- [9] Chaudhary, A.,^{\$} **Poddar, M.**,^{\$} Pathak, D. K., Mishra, R., Kumar, R. (2020), Electron Donor Ferrocenyl Phenothiazine: Counter Ion for Improving All-Organic Electrochromism, *ACS Appl. Electron. Mater.*, 2, 2994, DOI: 10.1021/acsaelm.0c00606.

† Papers pertaining to the thesis.

\$ Authors having equal contribution.

CONFERENCE/SYMPOSIUM PRESENTATION

▪ **International:**

- 1) **M. Poddar**, V. Sharma, S. M. Mobin, R. Misra, Design and Synthesis of 1,8-Naphthalimide Substituted BODIPY Dyads: Structure, Properties and Live-Cell Imaging, 14th International Symposium on Functional π -Electron Systems (F π 14), Berlin, Germany, (2nd -7th June, 2019); Poster Presented.
- 2) **M. Poddar**, R. Misra, Design and Synthesis of Donor–Acceptor Based 1,1,4,4–Tetracyanobuta–1,3–Diene (TCBD) and Cyclohexa–2,5–Diene–1,4–Ylidene–Expanded TCBD Functionalized Ferrocenyl Phenothiazines, Emerging Trends in Chemistry 2019, IIT Indore, India, (12th-15th July, 2019); Poster Presented.

▪ **National:**

- 1) **M. Poddar**, P. Gautam, Y. Rout, A. Ekbote, R. Misra, Donor–Acceptor Phenothiazine Functionalized BODIPYs, 6th Industry-Academia Conclave Indian Institute of Technology Indore, India, (20th Nov., 2018); Poster Presented.
- 2) **M. Poddar**, P. Gautam, Y. Rout, R. Misra, Donor–Acceptor Phenothiazine Functionalized BODIPYs, In-house Chemistry Symposium "CHEM-2019", Indian Institute of Technology Indore, India (28th Feb 2019); Given Oral Presentation.
- 3) **M. Poddar**, V. Sharma, S. M. Mobin, R. Misra, Design and Synthesis of 1,8-Naphthalimide Substituted BODIPY Dyads: Structure, Properties and Live-Cell Imaging, In-house Chemistry Symposium "CHEM-2020", Indian Institute of Technology Indore, India (12th Feb 2020); Given Oral Presentation.

TABLE OF CONTENTS

| | |
|---------------------------|--------|
| 1. List of Figures | xxvi |
| 2. List of Schemes | xxix |
| 3. List of Tables | xxxii |
| 4. List of Charts | xxxiii |
| 5. Acronyms | xxxiv |
| 6. Nomenclature | xxxiv |

Chapter 1: Introduction

| | |
|--|----|
| 1.1. Background | 1 |
| 1.2. Phenothiazine | 3 |
| 1.3. Classification of donor-acceptor functionalized phenothiazine | 4 |
| 1.4. Synthesis of phenothiazine core | 5 |
| 1.4.1. History | 5 |
| 1.4.2. From 2-aminobenzenethiol | 5 |
| 1.4.3. From 2-bromobenzenethiol | 6 |
| 1.5. Synthesis of Phenothiazine Precursors | 7 |
| 1.5.1. Bromination of 10-propyl-10H-phenothiazine | 7 |
| 1.5.2. Vilsmeier-Haack formylation of 10-propyl-10H-phenothiazine | 8 |
| 1.6. Synthesis of Phenothiazine Derivatives | 8 |
| 1.6.1. Knoevenagel condensation reaction of phenothiazine | 8 |
| 1.6.2. Cross-Coupling Reactions of Phenothiazines | 9 |
| 1.6.2.1. Sonogashira Cross-Coupling Reaction | 9 |
| 1.6.2.2. Suzuki Cross-Coupling Reaction | 10 |
| 1.6.2.3. Stille Cross-Coupling Reaction | 11 |
| 1.6.2.4. Heck Cross-Coupling Reaction | 12 |
| 1.7. Applications of Phenothiazine Derivatives | 13 |

| | |
|---|----|
| 1.7.1. Dye sensitized solar cells (DSSCs) | 13 |
| 1.7.2. Bulk Heterojunction Organic Solar Cells (BHJOSCs) | 14 |
| 1.7.3. Perovskite Solar Cell (PSCs) | 15 |
| 1.7.4. Organic Light Emitting Diodes (OLEDs) | 16 |
| 1.7.5. Nonlinear Optical Materials (NLOs) | 16 |
| 1.7.6. Sensing | 17 |
| 1.8. Current Work | 17 |
| 1.9. Organization of thesis | 18 |
| 1.10. References | 20 |
| | |
| Chapter 2: Materials and experimental techniques | |
| 2.1. Introduction | 31 |
| 2.2. Chemicals for synthesis | 31 |
| 2.3. Spectroscopic measurements | 31 |
| 2.3.1. NMR spectroscopy | 31 |
| 2.3.2. Mass spectrometry | 32 |
| 2.3.3. UV–vis spectroscopy | 32 |
| 2.3.4. Fluorescence spectroscopy | 33 |
| 2.4. Electrochemical studies | 33 |
| 2.5. Single crystal X-ray diffraction studies | 33 |
| 2.6. Computational calculations | 33 |
| 2.7. References | 34 |
| | |
| Chapter 3: Aryl–Substituted Phenothiazines: Design, Synthesis and Properties | |
| 3.1. Introduction | 35 |
| 3.2. Results and discussions | 37 |
| 3.3. Photophysical properties | 38 |
| 3.4. Electrochemical Properties | 44 |

| | | |
|-------------------|---|-----|
| 3.5. | Theoretical Calculations | 44 |
| 3.6. | Experimental Section | 47 |
| 3.7. | Conclusion | 50 |
| 3.8. | References | 50 |
| | | |
| Chapter 4: | Design and Synthesis of Donor–Acceptor Based Ferrocene Substituted Phenothiazines: Tuning of HOMO–LUMO gap | |
| 4.1. | Introduction | 59 |
| 4.2. | Results and discussion | 61 |
| 4.3. | Photophysical properties | 64 |
| 4.4. | Electrochemical Properties | 65 |
| 4.5. | Theoretical Calculations | 70 |
| 4.6. | Experimental section | 76 |
| 4.7. | Conclusions | 80 |
| 4.8. | References | 81 |
| | | |
| Chapter 5: | Donor–Acceptor Based BODIPY Functionalized Phenothiazines | |
| 5.1. | Introduction | 91 |
| 5.2. | Results and discussion | 92 |
| 5.3. | Thermogravimetric Analysis | 93 |
| 5.4. | Photophysical properties | 94 |
| 5.5. | Electrochemical properties | 96 |
| 5.6. | Theoretical calculations | 98 |
| 5.7. | Experimental details | 100 |
| 5.8. | Conclusions | 103 |
| 5.9. | References | 104 |

| | | |
|-------------------|--|-----|
| Chapter 6: | 1,1,4,4-Tetracyanobuta-1,3-Diene (TCBD)- and Cyclohexa-2,5-Diene-1,4-Diylidene-Expanded TCBD-Substituted BODIPY-Phenothiazines: Tuning of HOMO-LUMO gap | |
| 6.1. | Introduction | 109 |
| 6.2. | Results and discussion | 110 |
| 6.3. | Photophysical properties | 111 |
| 6.4. | Theoretical calculations | 113 |
| 6.5. | Experimental section | 115 |
| 6.6. | Conclusions | 117 |
| 6.7. | References | 117 |
| Chapter 7: | Donor-Acceptor based 1,8-Naphthalimide Substituted Phenothiazines: Tuning of HOMO-LUMO gap | |
| 7.1. | Introduction | 127 |
| 7.2. | Results and discussion | 138 |
| 7.3. | Photophysical properties | 132 |
| 7.4. | Electrochemical Properties | 135 |
| 7.5. | Theoretical calculations | 138 |
| 7.6. | Experimental section | 141 |
| 7.7. | Conclusions | 146 |
| 7.8. | References | 147 |
| Chapter 8: | Conclusions and future scope | |
| 8.1. | Conclusions | 153 |
| 8.2. | Future scope | 155 |
| 8.3. | References | 156 |

LIST OF FIGURES

Chapter 1. Introduction

- Figure 1.1.** Schematic representation of donor and acceptor molecular systems and their frontier molecular orbital diagram. 1
- Figure 1.2.** The molecular structure of phenothiazine core. 3
- Figure 1.3.** General classification of donor-acceptor functionalized phenothiazines in this work. 4

Chapter 3: Aryl-Substituted Phenothiazines: Design, Synthesis and Properties

- Figure 3.1.** Pictorial representation of phenothiazines **4a–4f** in dichloromethane at 1.0×10^{-5} M concentration. 38
- Figure 3.2.** Electronic absorption spectra of aryl-substituted phenothiazines **4a–4f** in dichloromethane at 1.0×10^{-5} M concentration. 39
- Figure 3.3.** Emission spectra of aryl-substituted phenothiazines **4a–4f** in different solvents. 41
- Figure 3.4.** Solid-state emission spectra of aryl-substituted phenothiazine **4a–4f**. 43
- Figure 3.5.** Cyclic voltammograms of phenothiazines **4a–4f** 0.01 M concentration in 0.1 M tri-tert-butylphosphonium tetrafluoroborate in dichloromethane recorded at a scan rate of 100 mV s^{-1} . 44
- Figure 3.6.** Energy diagram showing the HOMO and LUMO wave functions and energies of phenothiazines **4a–4f** as determined at B3LYP/6-31G** level. 45
- Figure 3.7.** Theoretical absorption spectra of phenothiazine **4d**. 47

Chapter 4: Design and Synthesis of Donor–Acceptor Based Ferrocene Substituted Phenothiazines: Tuning of HOMO–LUMO gap

- Figure 4.1.** The electronic absorption spectra of phenothiazines (i) **4b**, **5b** and **5c**, and (ii) **4c**, **5d**, **5e** and **5f** in dichloromethane (1×10^{-5} M). 65
- Figure 4.2.** CV and DPV plots of phenothiazine **4b**. 67
- Figure 4.3.** CV and DPV plots of phenothiazine **4c**. 68
- Figure 4.4.** CV and DPV plots of phenothiazine **5b**. 69
- Figure 4.5.** CV and DPV plots of phenothiazines **5c**. 69
- Figure 4.6.** CV and DPV plots of phenothiazine **5d**. 69
- Figure 4.7.** CV and DPV plots of phenothiazine **5e**. 70
- Figure 4.8.** CV and DPV plots of phenothiazines **5f**. 70
- Figure 4.9.** Energy diagram showing the HOMO and LUMO wave functions and energies of phenothiazines **4b**, **4c** and **5b–5f** as determined at B3LYP/6-31G** level. 71

Chapter 5: Donor–Acceptor Based BODIPY Functionalized Phenothiazines

- Figure 5.1.** Thermogravimetric analysis of phenothiazine functionalized BODIPYs **4a**, **4b**, **7a** and **7b** measured at a heating rate of $10 \text{ }^\circ\text{C min}^{-1}$ under nitrogen atmosphere. 94
- Figure 5.2.** Electronic absorption spectra of (a) **4a** and **7a** and (b) **4b** and **7b** in dichloromethane (1×10^{-5} M). 95
- Figure 5.3.** Absorption curves of phenothiazine functionalized BODIPYs **4a**, **4b**, **7a** and **7b** in different solvents. 96
- Figure 5.4.** Cyclic Voltammogram plot of **4a**, **4b**, **7a** and **4b** in dichloromethane. 96
- Figure 5.5.** Energy diagram showing the HOMO and LUMO wave functions and energies of phenothiazine functionalized BODIPYs **4a**, **4b**, **7a** and **7b** as determined at B3LYP/6-31G** level. 99

Chapter 6: 1,1,4,4-Tetracyanobuta-1,3-Diene (TCBD)- and Cyclohexa-2,5-Diene-1,4-Diylidene-Expanded TCBD-Substituted BODIPY-Phenothiazines: Tuning of HOMO-LUMO gap

Figure 6.1. The electronic absorption spectra of phenothiazines **1**, **2** and **3** in dichloromethane (1×10^{-5} M). 112

Figure 6.2. Energy diagram showing the HOMO and LUMO wave functions and energies of phenothiazines **1-3** as determined at B3LYP/6-31G** level. 114

Figure 6.3. Theoretically optimized structures of phenothiazines **1-3** by B3LYP/6-31+G** basis set. 114

Chapter 7: Donor-Acceptor based 1,8-Naphthalimide Substituted Phenothiazines: Tuning of HOMO-LUMO gap

Figure 7.1. Crystal structures of compound **3**: (i) front view, (ii) side view. 130

Figure 7.1. The electronic absorption spectra of phenothiazines **8-11** in dichloromethane (1×10^{-5} M). 132

Figure 7.3. The electronic absorption spectra of phenothiazines **12-15** in dichloromethane (1×10^{-5} M). 133

Figure 7.4. Cyclic voltammograms of phenothiazines **8-11** (0.01 M) in dichloromethane with 0.1 M TBAPF₆ at a scan rate of 100 mVs⁻¹ versus a standard calomel electrode (SCE) at 25 °C. 136

Figure 7.5. Cyclic voltammograms of phenothiazines **12-15** (0.01 M) in dichloromethane with 0.1 M TBAPF₆ at a scan rate of 100 mVs⁻¹ versus a standard calomel electrode (SCE) at 25 °C. 137

Figure 7.6. Energy diagram showing the HOMO and LUMO wave functions and energies of phenothiazines **8-15** as determined at B3LYP/6-31G** level. 139

LIST OF SCHEMES

Chapter 1: Introduction

| | | |
|---------------------|---|----|
| Scheme 1.1. | Discovery of phenothiazine. | 5 |
| Scheme 1.2. | Synthesis of phenothiazine from 2-aminobenzenethiol. | 6 |
| Scheme 1.3. | Synthesis of phenothiazine from 2-aminobenzenethiol. | 6 |
| Scheme 1.4. | Synthesis of phenothiazine from 2-bromobenzenethiol. | 6 |
| Scheme 1.5. | Synthesis of phenothiazine from 2-bromobenzenethiol. | 6 |
| Scheme 1.6. | Synthesis of 10-propyl-10 <i>H</i> -phenothiazine. | 7 |
| Scheme 1.7. | Synthesis of 3-bromo-10-propyl-10 <i>H</i> -phenothiazine and 3,7-dibromo-10-propyl-10 <i>H</i> -phenothiazine. | 7 |
| Scheme 1.8. | Synthesis of 10-propyl-10 <i>H</i> -phenothiazine-3-carbaldehyde and 3,7-dibromo-10-propyl-10 <i>H</i> -phenothiazine-3,7-dicarbaldehyde. | 8 |
| Scheme 1.9. | Synthesis of compounds 4 , 8 and 9 . | 9 |
| Scheme 1.10. | Synthesis of compounds 4–8 . | 10 |
| Scheme 1.11. | Synthesis of compounds 4–8 . | 11 |
| Scheme 1.12. | Synthesis of compounds 4 . | 11 |
| Scheme 1.13. | Synthesis of compounds 7–11 . | 12 |
| Scheme 1.14. | Synthesis of compound 1 for NLO application. | 17 |
| Scheme 1.15. | Synthesis of compounds 2 and 4 for sensing. | 17 |

Chapter 3: Aryl-Substituted Phenothiazines: Design, Synthesis and Properties

| | | |
|--------------------|---|----|
| Scheme 3.1. | Synthesis of Aryl-Substituted Phenothiazines 4a–4f . | 37 |
|--------------------|---|----|

Chapter 4: Design and Synthesis of Donor-Acceptor Based Ferrocene Substituted Phenothiazines: Tuning of HOMO-LUMO gap

| | | |
|--------------------|---|----|
| Scheme 4.1. | Synthetic route for ferrocenyl phenothiazines 4a and 5a . | 61 |
| Scheme 4.2. | Synthetic route for ferrocenyl phenothiazines 4b , 4c and 4c' . | 62 |
| Scheme 4.3. | Synthetic route for ferrocenyl phenothiazines 5b , 5c , 5d , 5d' , 5e and 5e' . | 63 |

| | | |
|--------------------|--|-----|
| Scheme 4.4. | Synthetic route for ferrocenyl phenothiazines 5f and 5f . | 63 |
| Chapter 5: | Donor–Acceptor Based BODIPY Functionalized Phenothiazines | |
| Scheme 5.1. | Synthesis of phenothiazine functionalized BODIPYs 4a and 4b . | 92 |
| Scheme 5.2. | Synthesis of phenothiazine functionalized BODIPYs 7a and 7b . | 93 |
| Chapter 6: | 1,1,4,4-Tetracyanobuta-1,3-Diene (TCBD)- and Cyclohexa-2,5-Diene-1,4-Diylidene-Expanded TCBD–Substituted BODIPY-Phenothiazines: Tuning of HOMO–LUMO gap | |
| Scheme 6.1. | Synthesis of phenothiazines 1 , 2 and 3 . | 111 |
| Chapter 7: | Donor-Acceptor based 1,8-Naphthalimide Substituted Phenothiazines: Tuning of HOMO-LUMO gap | |
| Scheme 7.1. | Synthetic route of compound 3 . | 129 |
| Scheme 7.2. | Synthetic route of compounds 8–11 . | 129 |
| Scheme 7.3. | Synthetic route of compounds 12–15 . | 130 |

LIST OF TABLES

Chapter 3: Aryl-Substituted Phenothiazines: Design, Synthesis and Properties

| | | |
|-------------------|---|----|
| Table 3.1. | Photophysical and Electrochemical Properties of phenothiazines 4a-4f in dichloromethane. | 40 |
| Table 3.2. | Solvent dependent studies of phenothiazines 4a-4f in different solvents. | 42 |
| Table 3.3. | Calculated electronic transitions for phenothiazines 4a-4f in dichloromethane. | 46 |

Chapter 4: Design and Synthesis of Donor-Acceptor Based Ferrocene Substituted Phenothiazines: Tuning of HOMO-LUMO gap

| | | |
|-------------------|--|----|
| Table 4.1. | Photophysical and electrochemical properties of phenothiazines 4b, 4c, 4c', 5b, 5c, 5d, 5d', 5e, 5e', 5f and 5f' . | 67 |
| Table 4.2. | FMO of regioisomeric phenothiazines 4c and 4c' . | 72 |
| Table 4.3. | FMO of regioisomeric phenothiazines 5d and 5d' . | 72 |
| Table 4.4. | FMO of regioisomeric phenothiazines 5e and 5e' . | 73 |
| Table 4.5. | FMO of regioisomeric phenothiazines 5f and 5f' . | 74 |
| Table 4.6. | Calculated electronic transitions for phenothiazines 4b, 4c, 4c', 5b, 5c, 5d, 5d', 5e, 5e', 5f and 5f' in dichloromethane. | 75 |

Chapter 5: Donor-Acceptor Based BODIPY Functionalized Phenothiazines

| | | |
|-------------------|--|-----|
| Table 5.1. | The photophysical and electrochemical properties of phenothiazine functionalized BODIPYs 4a, 4b, 7a and 7b . | 97 |
| Table 5.2. | Absorption maxima of phenothiazine functionalized BODIPYs 4a, 4b, 7a and 7b in different solvents. | 98 |
| Table 5.3. | Calculated electronic transition of phenothiazine functionalized BODIPYs 4a, 4b, 7a and 7b . | 100 |

Chapter 6: 1,1,4,4-Tetracyanobuta-1,3-Diene (TCBD)- and Cyclohexa-2,5-Diene-1,4-Diylidene-Expanded TCBD-Substituted BODIPY-Phenothiazines: Tuning of HOMO-LUMO gap

Table 6.1. Photophysical and theoretical properties of phenothiazines **1–3**. 113

Chapter 7: Donor-Acceptor based 1,8-Naphthalimide Substituted Phenothiazines: Tuning of HOMO-LUMO gap

Table 7.1. Crystal structure data and refinement parameters. 131

Table 7.2. Photophysical properties of compounds **8–15** in dichloromethane. 134

Table 7.3. Calculated electronic transition of compounds **8–15**. 140

LIST OF CHARTS

Chapter 1: Introduction

Chart 1.1. Examples of donor and acceptor moieties. 2

Chart 1.2. Molecules for DSSCs. 14

Chart 1.3. Molecules for BHJOSCs. 15

Chart 1.4. Molecules for PSCs. 15

Chart 1.5. Molecules for OLEDs. 16

Chapter 3: Aryl-Substituted Phenothiazines: Design, Synthesis and Properties

Chart 3.1. Structures of aryl substituted phenothiazines **4a–4f**. 36

ACRONYMS

| | |
|-------------------|---|
| D–A | Donor–acceptor |
| SCXRD | Single Crystal X-ray diffraction |
| NMR | Nuclear Magnetic Resonance |
| PPh ₃ | Triphenylphosphin |
| DMF | Dimethylformamide |
| DCM | Dichloromethane |
| TGA | Thermogravimetric Analysis |
| Ph | phenyl |
| IR | Infrared |
| UV-Vis | UV-Visible Spectroscopy |
| Calcd. | Calculated |
| CDCl ₃ | Chloroform-d |
| ESI-MS | Electrospray Ionization- Mass Spectrometry |
| EtOH | Ethanol |
| MeOH | Methanol |
| THF | Tetrahydrofuran |
| TLC | Thin Layer Chromatography |
| TEA | Triethylamine |

NOMENCLATURE

| | |
|--------------------|----------------------------|
| λ | Wavelength |
| ε | Extinction coefficient |
| α | Alfa |
| β | Beta |
| γ | Gamma |
| π | Pi |
| ϕ | Fluorescence quantum yield |
| σ | Sigma |
| \AA | Angstrom |
| nm | Nanometer |
| cm | Centimeter |
| $^{\circ}$ | Degree |
| $^{\circ}\text{C}$ | Degree Centigrade |
| mmol | Millimol |
| mL | Milliliter |
| μL | Microliter |
| a. u. | Arbitrary Unit |

Chapter 1

Introduction

1.1. Background

The design and synthesis of π -conjugated donor–acceptor (D–A) molecular systems have attracted considerable attention of multidisciplinary scientific community due their vast applications in the field of organic photonics and electronics as well as biological studies.^[1] The development of D–A molecules induces narrow HOMO–LUMO gap in the molecular system, which could be attributed to the intermolecular charge transfer between the donor and acceptor moieties.^[2] The photonic and electronic properties of the D–A molecules are dependent on the HOMO–LUMO energy gap which can be easily modified by (a) changing the π -bridge between the D–A molecular systems or by (b) varying the strength of the donor/acceptor units.^[3]

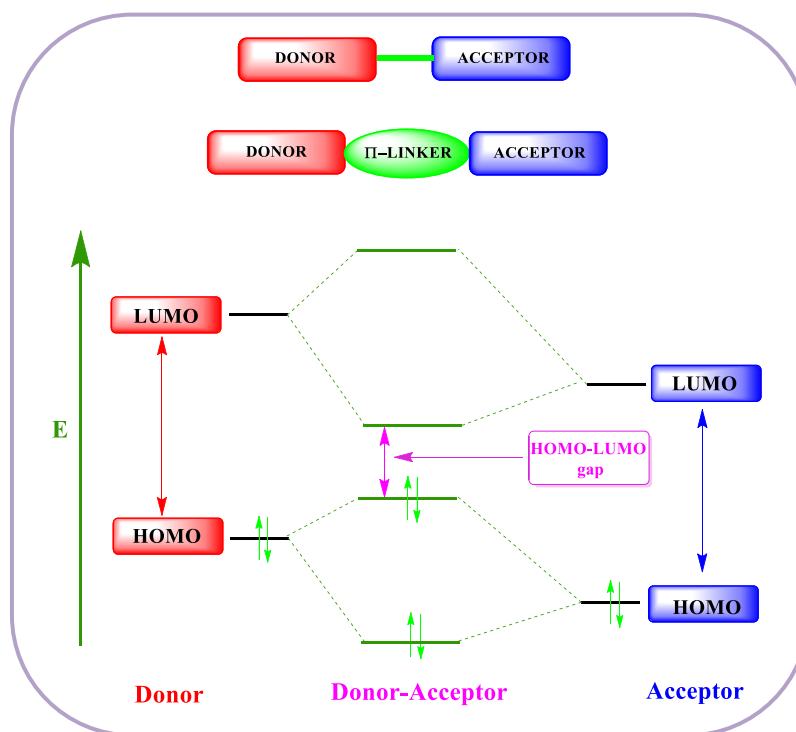


Figure 1.1. Schematic representation of donor and acceptor molecular systems and their frontier molecular orbital diagram.

In the D–A molecules, the electron rich moiety which donates the electron to another moiety is known as donor and the electron deficient moiety which withdraws the electron from the donor is known as acceptor. There are several examples of donor and acceptor moieties which are shown in Chart 1.1.

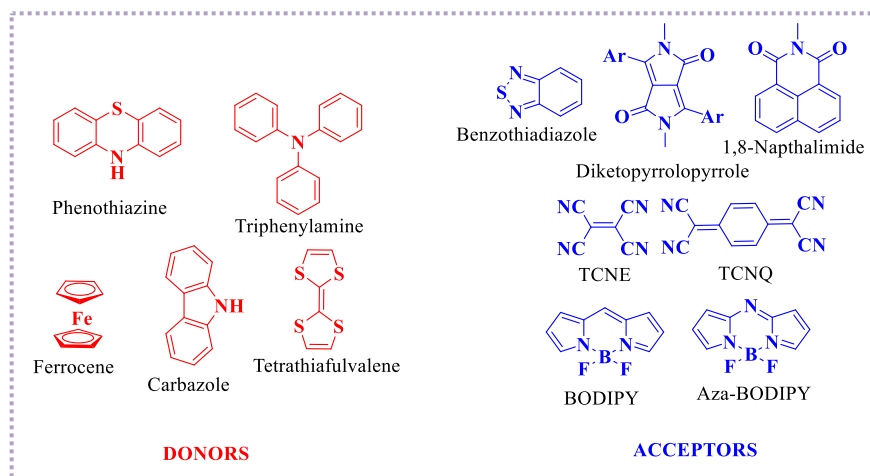


Chart 1.1. Examples of donor and acceptor moieties.

The couplings of orbitals of donor and acceptor moieties are depicted in Figure 1.1 where the electron donating groups raise the HOMO energy levels whereas the electron withdrawing group lower the LUMO energy levels. The hybridization of the donor and acceptor increases the energy level of HOMO and decreases the energy level of LUMO resulting in a low HOMO–LUMO gap with a broad absorption spectrum.^[4]

These kinds of D–A molecular systems with low HOMO–LUMO gap and broad absorption spectra are of great interest because of their applications in diverse fields, e.g.

- Dye sensitized solar cells (DSSCs)^[5]
- Bulk heterojunction organic solar cells (BHJOSCs)^[6]
- Perovskite solar cells (PSCs)^[7]
- Organic light emitting diodes (OLEDs)^[8]
- Non-linear optics (NLOs)^[9]
- Organic field effect transistors (OFETs)^[10]

- Biological imaging and photodynamic therapy.^[11]

1.2. Phenothiazine

Among various heterocyclic compounds, phenothiazines have attracted the attention of researchers for their extensive use as an active chromophore in organic photonics and electronics (Figure 1.2).^[12] Phenothiazines have fused tricyclic heteroaromatic rings which contain electron rich S- and N-atoms in the middle ring endowing phenothiazines with strong electron donating ability.^[13]

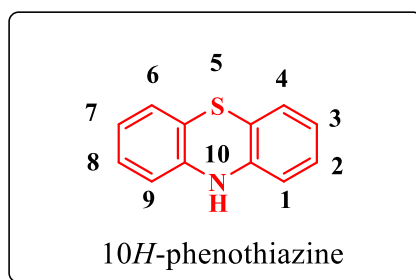


Figure 1.2. The molecular structure of phenothiazine core.

The nonplanar heteroanthracene structure of phenothiazine shows twisted butterfly like conformations.^[14] Phenothiazines can be functionalized at the N-position and aromatic ring.^[15, 16] It allows electrophilic substitution at aromatic positions, nucleophilic substitution at N-position and oxidation at the S-position.^[15, 16] The most common approach is the electrophilic substitution reaction at the 3, 7 -positions of phenothiazine.^[17] The phenothiazine derivatives exhibit several spectacular properties^[18] like:

- Electron rich S-atoms and N-atoms substituted heterocyclic phenothiazines exhibit strong electron donating ability.
- Synthetic modifications of phenothiazines are easy and cost effective.
- The low reversible oxidation potential of phenothiazine derivatives makes them suitable electrophores in optoelectronics.
- Phenothiazines possess high chemical and thermal stability.
- Phenothiazine derivatives show intense luminescence and high photo-conductivities.

- Phenothiazine derivatives exhibit tunable photophysical and electrochemical properties by incorporating suitable functionalities at the 3,7-positions.

1.3. Classification of donor-acceptor functionalized phenothiazine

In this work, the classification of donor-acceptor phenothiazine has been done on the substituents at the 3,7-positions of the phenothiazine core. The mono substituted phenothiazines were synthesized by the incorporation of donor/acceptor at the 3-position of phenothiazine. The substitution of donor/acceptor at the 3,7-positions of the phenothiazine core resulted in disubstituted phenothiazines. In all the cases, donor/acceptor substituents were introduced to the phenothiazines either *via* spacer (π -linker) or without spacer (Figure 1.3).

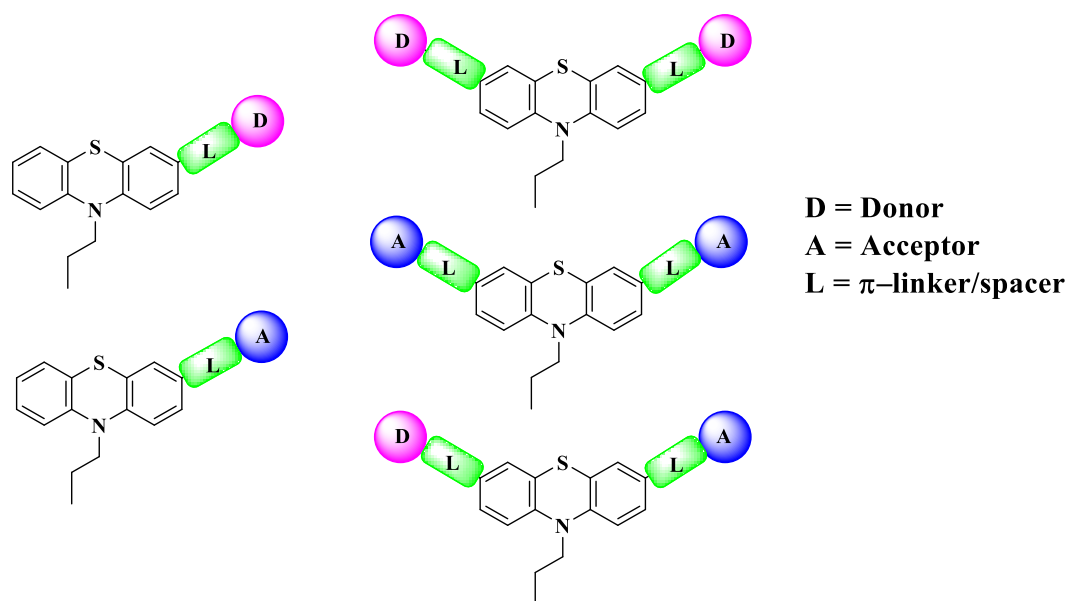


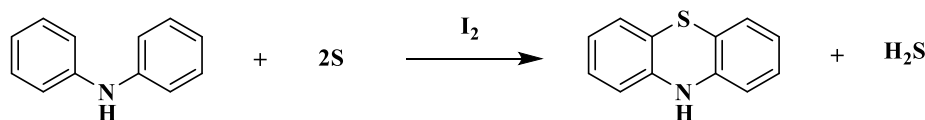
Figure 1.3. General classification of donor-acceptor functionalized phenothiazines in this work.

1.4. Synthesis of Phenothiazine Core

The highly rigid electroactive molecular backbone with high molar extinction coefficient (ϵ) and intense luminescence properties of phenothiazines make them excellent candidates for the optoelectronic applications as well as in biological studies.^[19] In the past few decades, researchers have extensively explored donor–acceptor substituted phenothiazine for a wide variety of applications such as, dye sensitized solar cells (DSSCs),^[20] bulk heterojunction organic solar cells (BHJOSCs),^[21] OLEDs,^[22] NLOs,^[23] OFETs,^[24] hole transporting materials (HTMs),^[25] sensing,^[26] bioimaging,^[27] photodynamic therapy,^[28] *etc.* The methodology of synthesizing the phenothiazine core is discussed in the following section.

1.4.1. History

In 1883, Brenthsen *et. al.* have synthesized 10*H*-phenothiazine for the first time by heating sulfur and diphenylamine at 200–300 °C.^[29] The drawback of the reaction was the poor yield of thionation. Further Ackermann and Knoevenagel improved the reaction by adding 1% iodine as catalyst (Scheme 1.1).^[30]



Scheme 1.1. Discovery of phenothiazine.

In 1954, Massie *et al.* have made a comprehensive study on the chemical reactivity of phenothiazine.^[31] Since then, many significant results have been reported which are of interest not only for researchers working with phenothiazine-based derivatives but also for the entire heterocyclic chemistry.

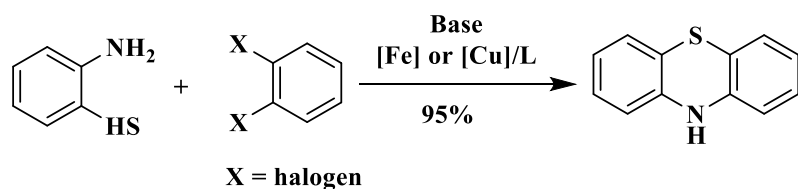
1.4.2. From 2-aminobenzenethiol

The condensation of 2-aminobenzenethiol and cyclohexanone in presence of thiol additives [DMSO (10 mol%)] resulted in phenothiazine (Scheme 1.2).^[32]



Scheme 1.2. Synthesis of phenothiazine from 2-aminobenzenethiol.

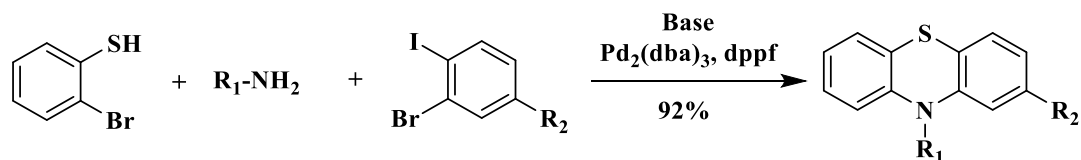
Recently, copper or iron catalysed coupling reaction of 2-aminobenzenethiol and 1,2-dihalobenzene have been reported to synthesize phenothiazine with good regioselectivity (Scheme 1.3).^[33, 34]



Scheme 1.3. Synthesis of phenothiazine from 2-aminobenzenethiol.

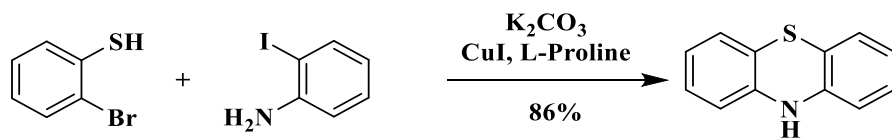
1.4.3. From 2-bromobenzenethiol

The palladium-catalyzed coupling reaction of 1-bromo-2-iodobenzenes, 2-bromobenzenethiol and primary amines resulted in phenothiazine (Scheme 1.4).^[35]



Scheme 1.4. Synthesis of phenothiazine from 2-bromobenzenethiol.

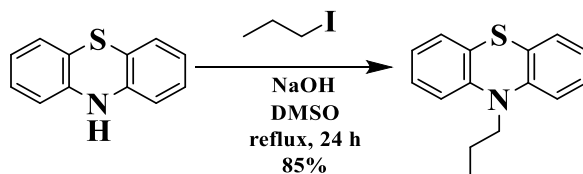
2-bromobenzenethiol also reacted with 2-iodoanilines in presence of CuI/L-proline-catalyst gave phenothiazine in good regioselectivity (Scheme 1.5).^[36]



Scheme 1.5. Synthesis of phenothiazine from 2-bromobenzenethiol.

1.5. Synthesis of Phenothiazine Precursors

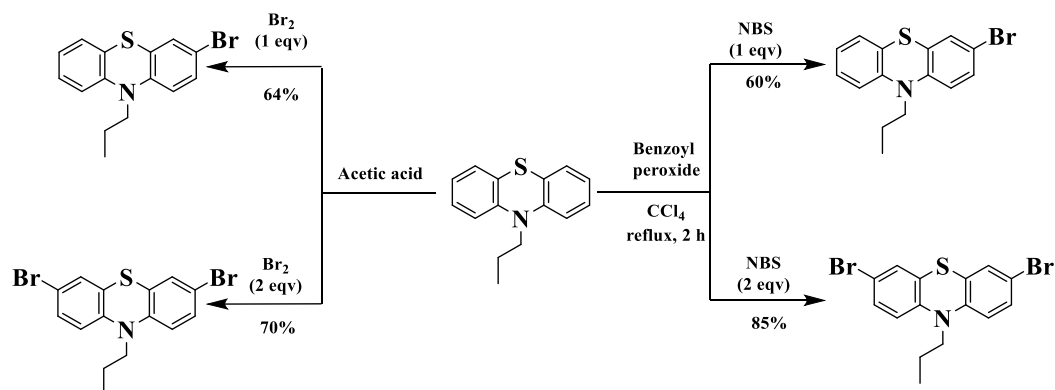
The parent compound 10*H*-phenothiazine can be easily alkylated at the N-position. The reaction of 10*H*-phenothiazine, 1-iodopropane and sodium hydroxide in presence of dry DMSO resulted in 10-propyl-10*H*-phenothiazine (Scheme 1.6).^[37] Phenothiazine is highly susceptible towards electrophilic substitution reaction at the 3,7-positions. The 3,7-brominated and formylated phenothiazines are the most commonly used precursors.



Scheme 1.6. Synthesis of 10-propyl-10*H*-phenothiazine.

1.5.1. Bromination of 10-propyl-10*H*-phenothiazine

The precursors 3-bromo-10-propyl-10*H*-phenothiazine and 3,7-dibromo-10-propyl-10*H*-phenothiazine can be synthesized in two different pathways (Scheme 1.7). **Pathway I:** The reaction of 10-propyl-10*H*-phenothiazine with bromine (1 equivalent) in acetic acid or dichloromethane results in mono brominated phenothiazine whereas the addition of 2 equivalent of bromine results in dibrominated phenothiazine.^[38,39]

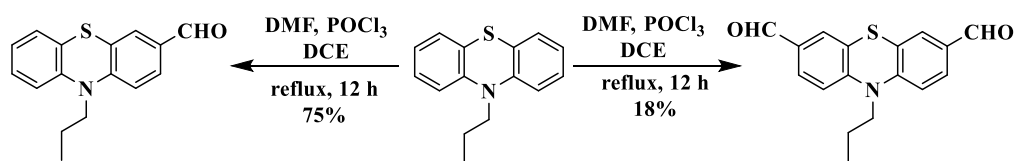


Scheme 1.7. Synthesis of 3-bromo-10-propyl-10*H*-phenothiazine and 3,7-dibromo-10-propyl-10*H*-phenothiazine.

Pathway II: The reaction of 10-propyl-10*H*-phenothiazine with *N*-bromosuccinimide (NBS) (1 equivalent for monobromination and 2 equivalents for dibromination) in presence of catalytic amount of benzoyl peroxide in CCl₄ results in 3-bromo-10-propyl-10*H*-phenothiazine and 3,7-dibromo-10-propyl-10*H*-phenothiazine, respectively.^[40]

1.5.2. Vilsmeier-Haack formylation of 10-propyl-10*H*-phenothiazine

The mono- and di-formylated phenothiazines are prepared by dropwise addition of POCl₃ to a mixture of DMF and 1,2-dichloroethane at 0°C, followed by the addition of alkylated phenothiazine to the Vilsmeier reagent under vigorous stirring and refluxed for 12 h (Scheme 1.8).^[41, 42]



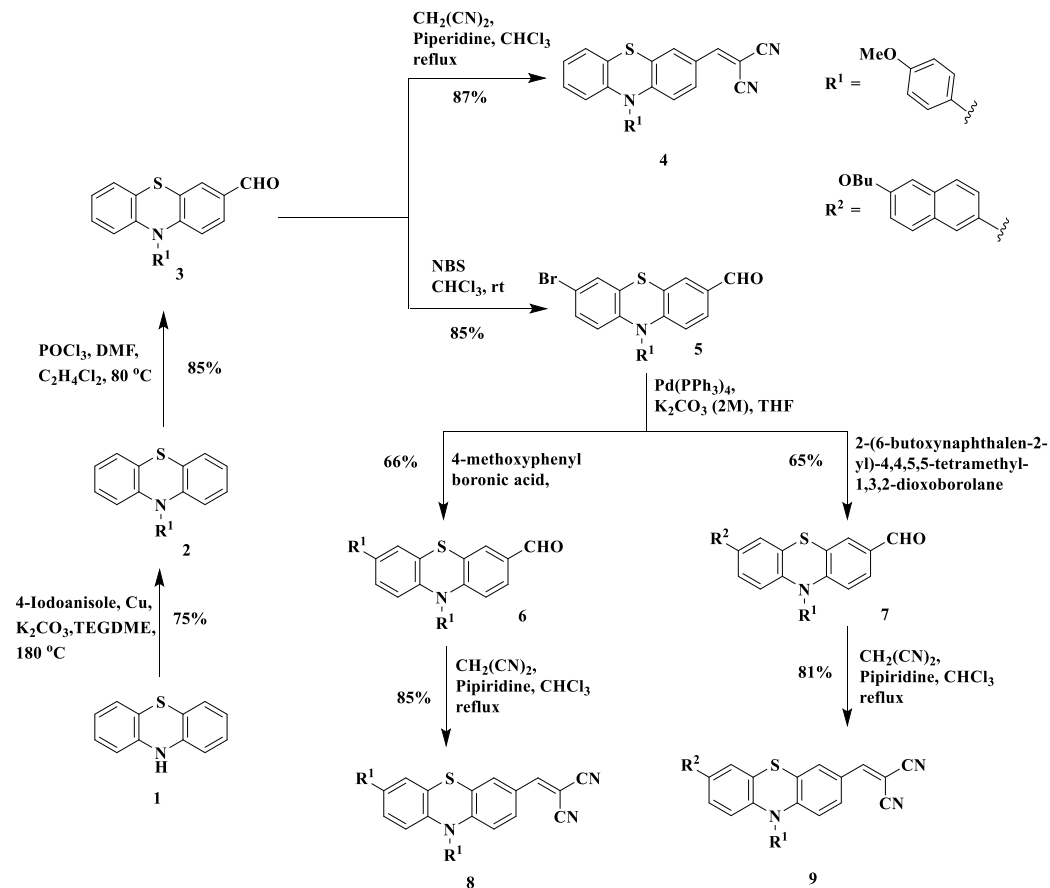
Scheme 1.8. Synthesis of 10-propyl-10*H*-phenothiazine-3-carbaldehyde and 3,7-dibromo-10-propyl-10*H*-phenothiazine-3,7-dicarbaldehyde.

1.6. Synthesis of Phenothiazine Derivatives

The synthetic methodologies of different type of phenothiazine-based derivatives are summarized in the following sections.

1.6.1. Knoevenagel condensation reaction of phenothiazine

Shinde et al. have synthesized a series of phenothiazine based organic semiconductors **4**, **8** and **9** via Knoevenagel-condensation reaction and investigated their photophysical and electrochemical properties for hole mobility (Scheme 1.9). The mixture of formylated phenothiazines and malononitrile in chloroform were refluxed for 12 h to obtain the compounds **4**, **8** and **9** in 81–87% yield.^[43]



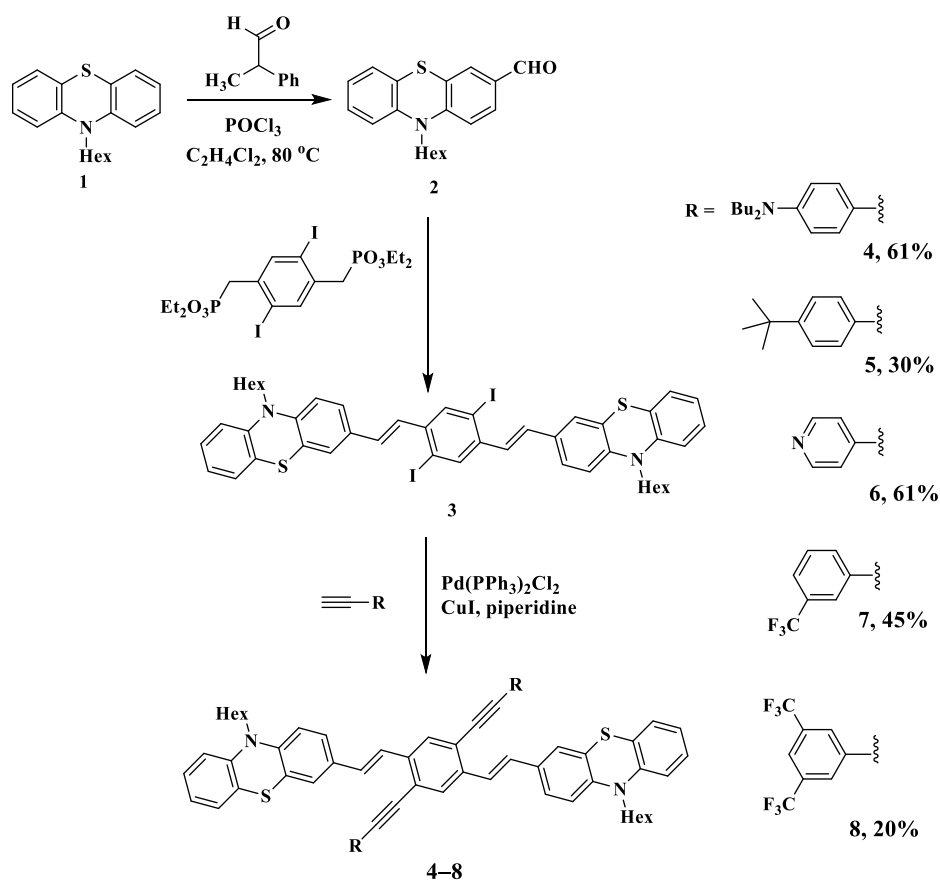
Scheme 1.9. Synthesis of compounds **4**, **8** and **9**.

1.6.2. Cross-Coupling Reactions of Phenothiazines

The most common approach of designing donor–acceptor based phenothiazines includes the cross-coupling reaction. The mono and di-bromo/iodo phenothiazines undergo various cross-coupling reactions, e.g. Sonogashira coupling, Suzuki coupling, Heck coupling and Stille coupling.

1.6.2.1. Sonogashira Cross-Coupling Reaction

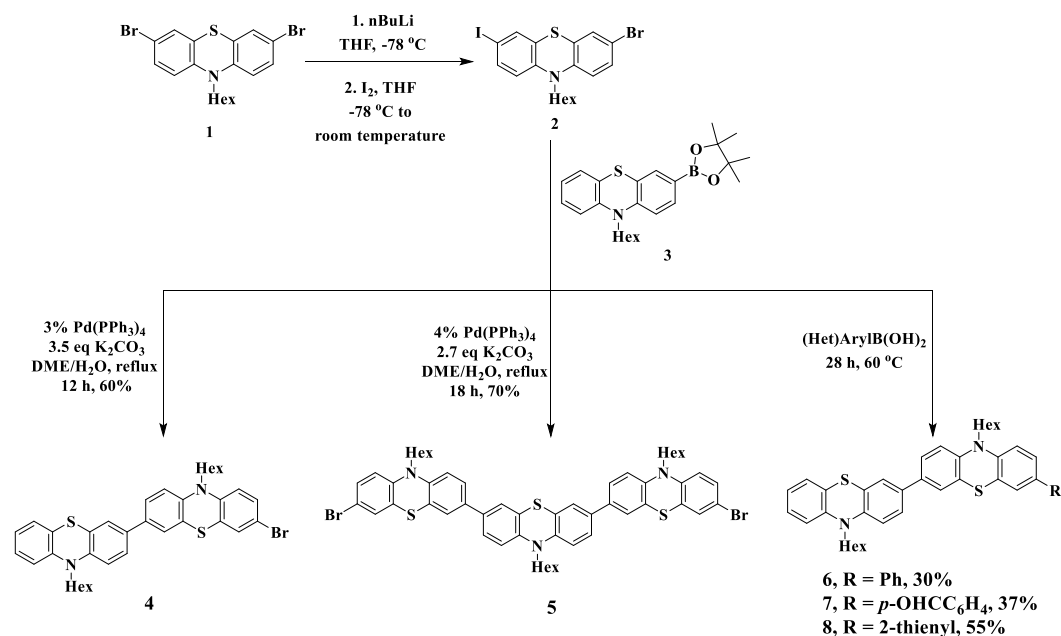
Hauck *et al.* have synthesized a series of phenothiazine-based molecules **4–8** via Sonogashira cross-coupling reaction and investigated their photophysical and electrochemical properties for metal cation sensing applications. The reaction of iodinated phenothiazine with the series of alkynes in presence Pd catalyst and piperidine gives molecules **4–8** in 20–61% yield (Scheme 1.10).^[16a]



Scheme 1.10. Synthesis of compounds **4–8**.

1.6.2.2. Suzuki Cross-Coupling Reaction

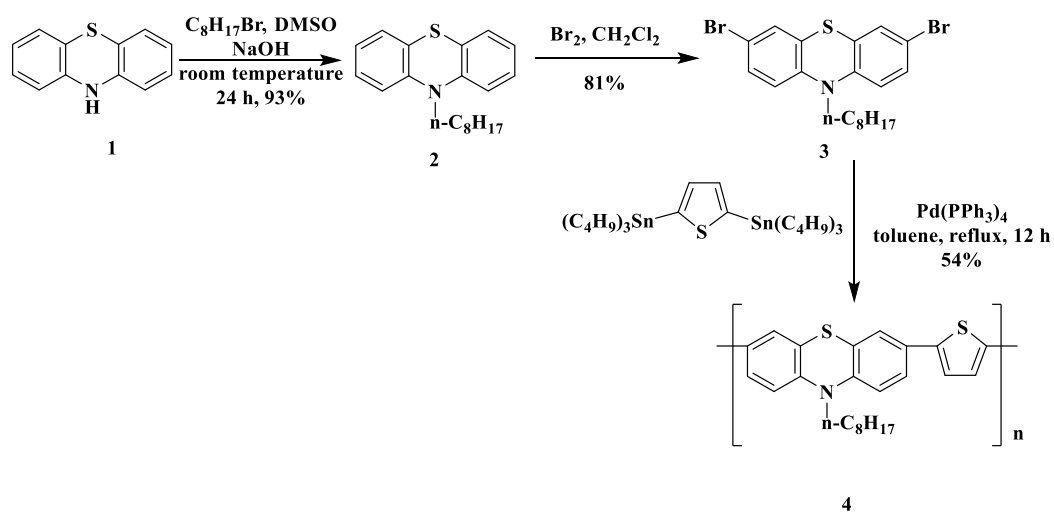
Müller and co-workers have synthesized a series of phenothiazine derivatives **4–8** via Pd-catalyzed Suzuki coupling reaction. The bromiodo derivative of phenothiazine was reacted with the mono- and bisboronic esters of phenothiazines in presence of Pd catalyst, potassium carbonate and DME, for 18 h under reflux condition and resulted in derivatives **4–8** in 30–70% yield (Scheme 1.11).^[12b]



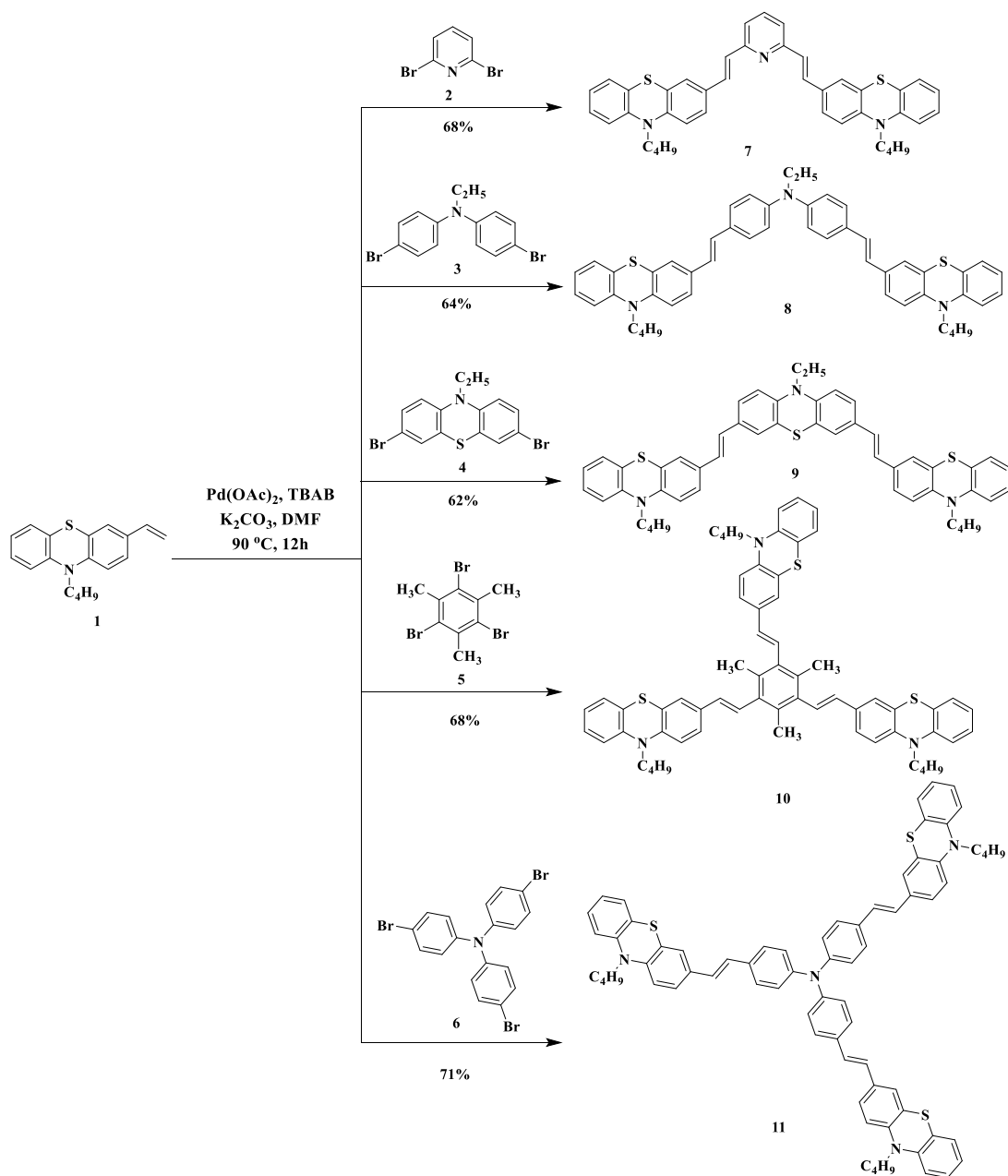
Scheme 1.11. Synthesis of compounds 4–8.

1.6.2.3. Stille Cross-Coupling Reaction

Sang *et al.* have synthesized thiophene based phenothiazine derivatives **4** via Stille coupling reaction and investigated the photophysical and electrochemical properties for photovoltaic application. The reaction of dibromo phenothiazine with the stannyl thiophene in presence of $\text{Pd}(\text{PPh}_3)_4$ and toluene resulted in **4** in 54% yield (Scheme 1.12).^[44]



Scheme 1.12. Synthesis of compounds **4**.



Scheme 1.13. Synthesis of compounds 7–11.

1.6.2.4. Heck Cross-Coupling Reaction

Ravivarma *et al.* have reported a series of phenothiazine-based derivatives 7–11 for DSSC applications. The derivatives 7–11 were synthesized *via* Heck cross-coupling reaction. The brominated aryl groups reacted with vinyl functionalized phenothiazines in presence of Pd(OAc)_2 , K_2CO_3 and

tetrabutylammonium bromide to give derivatives **7–11** in 62–85% yield (Scheme 1.13).^[45]

1.7. Applications of Phenothiazine Derivatives

The donor–acceptor substituted phenothiazine derivatives have a wide range of applications in optoelectronics and biological studies. Some of the important applications are discussed below.

1.7.1. Dye sensitized solar cells (DSSCs)

Dye sensitized solar cells (DSSCs) have attracted the attention of researchers due to their easy tunable molecular architectures, low cost and high efficiency. In this regard, the electron rich phenothiazine is one of the most promising cores for DSSC application. The most common approach to synthesize phenothiazine-based donor–acceptor architectures is to design D–A, D–A– π –A, A–D–A type of derivatives. A series of dithieno[3,2-b:2',3'-d]pyrrole (DTP) functionalized phenothiazines **1–4** were designed and synthesized by *Han et al.* and used for DSSCs (Chart 1.2). The photophysical and electrochemical study exhibited that the incorporation of auxiliary acceptors and alkyl chains stabilized the LUMO energy to great extent and resulted in improved photovoltaic performance. Among all the dyes phenothiazine **3** showed the highest power conversion efficiency (PCE) of 10.06% with J_{sc} of 19.18 mA cm⁻², V_{oc} of 829 mV, and FF of 0.63 whereas phenothiazine **1**, **2** and **4** showed the PCE of 9.42%, 9.25% and 8.19%, respectively.^[46]

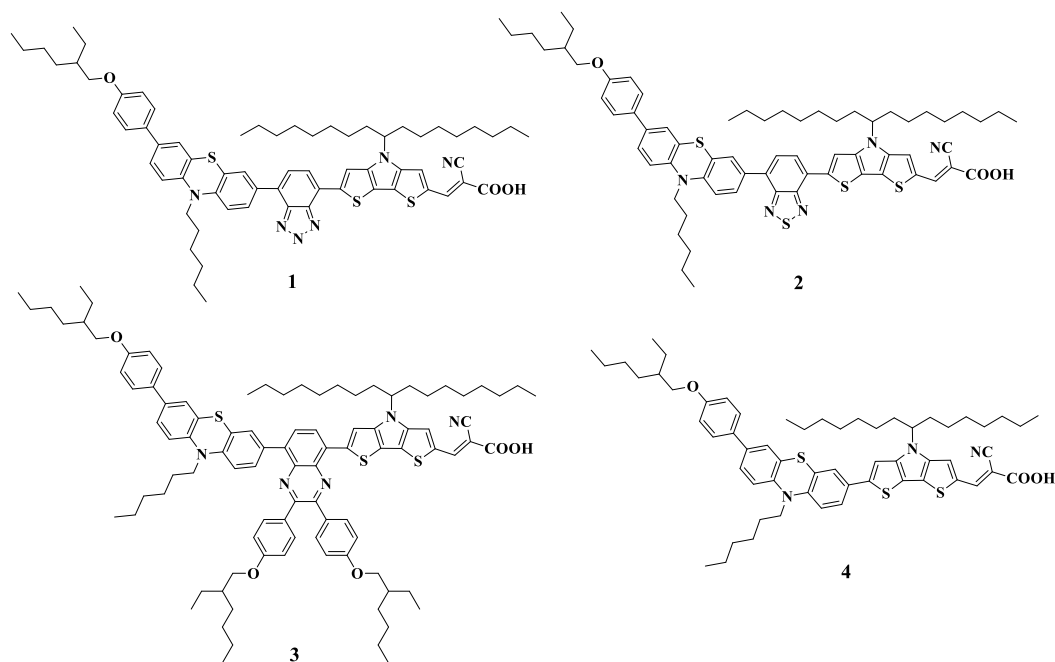


Chart 1.2. Molecules for DSSCs.

1.7.2. Bulk Heterojunction Organic Solar Cells (BHJOSCs)

The bulk heterojunction organic solar cells are comprised of electron donor and acceptor materials which are blended together to form a film. Researchers are interested in developing active layer donor materials to achieve broad absorption spectra with good charge transport and low HOMO–LUMO gap. The electron rich phenothiazine acts as a building block which combines with the electron deficient materials by providing push-pull dyes with low HOMO–LUMO gap. Revoju *et al.* have reported two compounds **1** and **2** where two phenothiazine moieties are linked *via* central benzodithiophene (phenothiazine-benzodithiophene-phenothiazine) with electron acceptors 1,3-indanedione and malononitrile as end capping units (Chart 1.3). The compounds **1** and **2** showed high thermal stability, broad and strong absorption band, deep-lying HOMO energy levels and high hole mobility. The organic solar cells based on the active layer of **1:PC71BM** and **2:PC71BM** showed the PCE of 6.20% ($J_{sc} = 11.18$ mA/cm², $V_{oc} = 0.99$ V and FF = 0.56) and 7.45% ($J_{sc} = 12.06$ mA/cm², $V_{oc} = 1.04$ V and FF = 0.60), respectively.^[47]

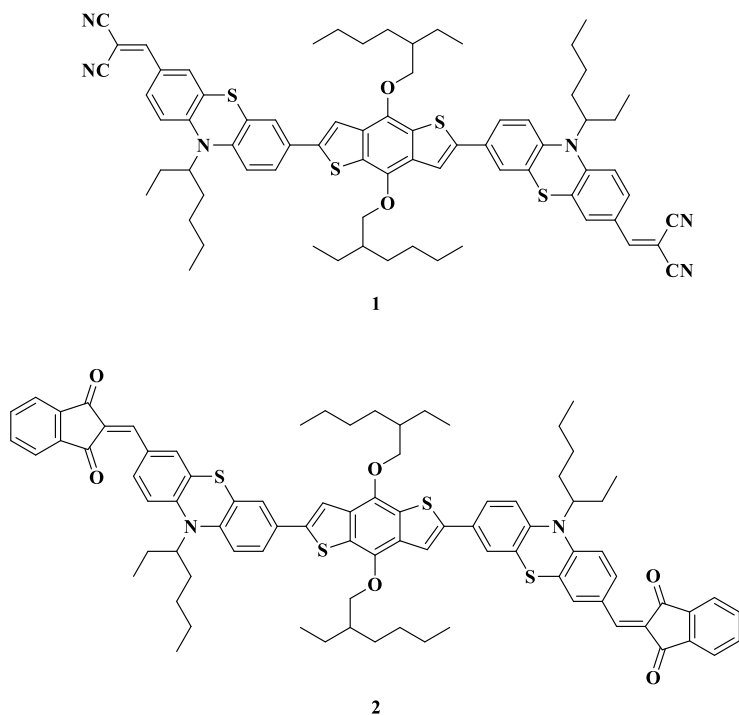


Chart 1.3. Molecules for BHJOSCs.

1.7.3. Perovskite Solar Cell (PSCs)

In 2017, two phenothiazine-based materials **1** and **2** were introduced by Grisorio *et al.* as hole transporting materials for perovskite solar cell application (Chart 1.4). The photophysical and electrochemical properties of **1** and **2** revealed that the presence of phenylene spacer in **2** improved the photovoltaic performance drastically. The compound **1** exhibited the PCE of 2.10% whereas compound **2** showed the PCE of 17.6%.^[48]

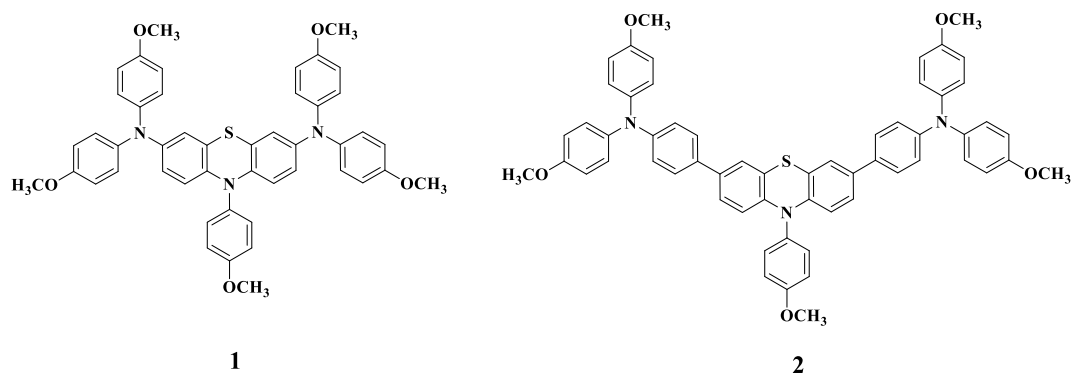


Chart 1.4. Molecules for PSCs.

1.7.4. Organic Light Emitting Diodes (OLEDs)

Phenothiazine based materials have been used for OLED application due to their low cost, tunable mechanical and electroluminescence properties with high thermal robustness. Adachi and coworkers have synthesized a phenothiazine based fluorescent molecule **1**, where the 2,4,6-triphenyl-1,3,5-triazine moiety is attached with three phenothiazine moieties. The molecule **1** showed dual emission and TADF properties (Chart 1.5). The OLED based on molecule **1** exhibited yellowish green electroluminescence [CIE coordinates (0.23, 0.75)] with a high EQE of 17.40% where turn-on voltage of 4.20 V, maximum luminance of 7430 cd m⁻² and maximum current efficiency of 58.60 cd A⁻¹ were obtained.^[49]

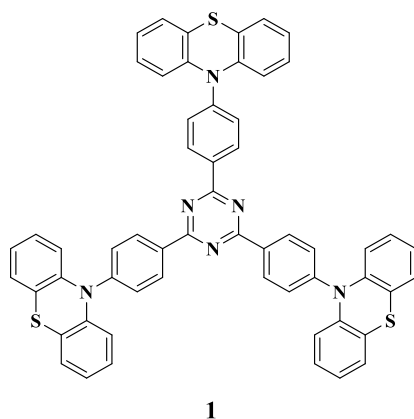
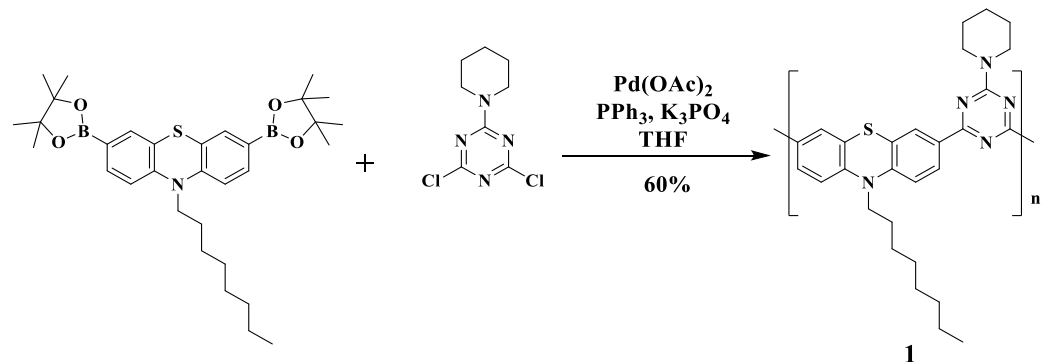


Chart 1.5. Molecules for OLEDs.

1.7.5. Nonlinear Optical Materials (NLOs)

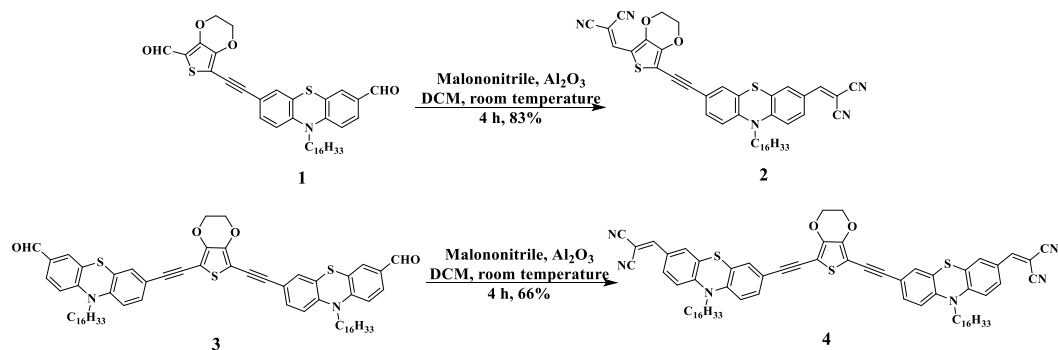
The high luminescence, low oxidation potential and high photoconductivity of phenothiazines, makes them attractive candidates for NLO applications. Sreekumar *et al.* have reported phenothiazine-based copolymer **1** where the phenothiazine-N-piperidine is attached to the triazine moiety *via* Suzuki coupling reaction (Scheme 1.14). The phenothiazine copolymer showed optical band gap of 2.5 eV. The third-order nonlinear optical properties of the phenothiazine copolymer by Z-scan technique. The results exhibited the nonlinear refractive index and absorption values of -0.58×10^{-10} esu and 3.75×10^{-10} m/W, respectively.^[50]



Scheme 1.14. Synthesis of compound **1** for NLO application.

1.7.6. Sensing

The tunable photoluminescence properties of phenothiazines make them suitable for sensing applications. Ramchandran *et al.* have synthesized a series of phenothiazine-based molecules **1–4** for cyanide ion sensing where the phenothiazine is attached with ethylenedioxythiophene and dicyanovinyl groups (Scheme 1.14). The compounds **2** and **4** showed high selectivity and sensitivity towards cyanide ions with the detection limit of 8 ppb and 14 ppb, respectively indicating “turn-on” fluorescence.^[51]



Scheme 1.15. Synthesis of compounds **2** and **4** for sensing.

1.8. Current Work

The donor–acceptor based molecules with low HOMO–LUMO gap are emerging class of materials for their application in optoelectronics. In order to fine tune the photonic properties and HOMO–LUMO gap, a wide variety of

donors (ferrocene, triphenylamine, carbazole) and acceptors (BODIPY, 1,8-naphthalimide, TCNE, TCNQ) have been introduced to the phenothiazine core. The photophysical and electrochemical properties of the phenothiazines were studied.

The main objectives of the current work are:

- To design and synthesize donor–acceptor functionalized phenothiazine derivatives for optoelectronic applications.
- To synthesize symmetrical and unsymmetrical phenothiazine derivatives by varying the donor/acceptor units in a systematic way.
- To study the effect of substitution pattern of donor–acceptor phenothiazines on their photophysical and electrochemical properties.
- To fine tune the HOMO–LUMO gap by altering the donor/acceptor strength or π -linker on the phenothiazine core.
- To investigate the structural and photophysical properties of the donor–acceptor functionalized phenothiazines by using density functional theory (DFT) and time-dependent density functional theory (TD-DFT) calculations and compare with the experimental data.

1.9. Organization of thesis

Chapter 1 of the thesis gives general introduction of the phenothiazine, followed by the historical background, various synthetic strategies for the design of phenothiazine derivatives. A brief literature survey of the applications of the phenothiazine derivatives in various fields is outlined.

Chapter 2 of the thesis describes the instrumentation and general methods used for the present study.

Chapter 3 of the thesis describes the design and synthesis of a series of aryl substituted phenothiazine-based fluorophores *via* Pd-catalyzed Sonogashira

cross-coupling reactions by attaching appropriately substituted intermediates (phenyl, naphthalene, methoxy naphthalene, anthracene, phenanthrene and pyrene) with the substituted phenothiazine core. Their photophysical and electrochemical properties were studied.

Chapter 4 of the thesis summarizes the design and synthesis of a series of 1,1,4,4-tetracyanobuta-1,3-diene (TCBD) and cyclohexa-2,5-diene-1,4-ylidene-expanded TCBD acceptors substituted ferrocenyl using [2 + 2] cycloaddition–electrocyclic ring-opening reaction. The effect of the incorporation of TCBD and cyclohexa-2,5-diene-1,4-ylidene-expanded TCBD on the photonic and electronic properties of ferrocenyl phenothiazines were investigated.

Chapter 5 of the thesis describes the design and synthesis of a set of unsymmetrical and symmetrical difluoro-4-bora-3a,4a-diaza-s-indacene (BODIPY) substituted phenothiazines by using condensation and Pd-catalyzed Sonogashira cross-coupling reactions. The effect of acetylene linkage between phenothiazine and BODIPYs on the thermal, photophysical and electrochemical properties of phenothiazines were investigated.

Chapter 6 of the thesis reports the synthesis of a set of TCBD and cyclohexa-2,5-diene-1,4-ylidene-expanded TCBD substituted BODIPY-phenothiazines, *via* Pd-catalyzed Sonogashira cross-coupling reaction and [2+2] cycloaddition–electrocyclic ring-opening reaction. The significant perturbation on the optical and electronic properties of the phenothiazines were explored.

Chapter 7 of the thesis describes the design and synthesis of a series of donor substituted 4-ethynyl-1,8-naphthalimide (NPI) phenothiazine-based chromophores and their TCBD derivatives *via* Pd-catalyzed Sonogashira cross-coupling reactions and [2 + 2] cycloaddition–electrocyclic ring-opening reaction. The effect of the donor (phenothiazine, carbazole, ferrocene and triphenylamine) on the photonic and electronic properties of the NPI-phenothiazine and further

effect of the TCBD acceptor on the donor substituted NPI-phenothiazine were also explored.

Chapter 8 of the thesis summarizes the noticeable features of the work and prospects.

1.10. References

- [1] (a) Bent, H. A. (1968), Structural chemistry of donor-acceptor interactions, *Chem. Rev.*, 68, 5, 587-648 (DOI: 10.1021/cr60255a003); (b) Morokuma, K. (1977), Why do molecules interact? The origin of electron donor-acceptor complexes, hydrogen bonding and proton affinity, *Acc. Chem. Res.*, 10, 8, 294-300 (DOI: 10.1021/ar50116a004); (c) Zhang, J., Xu, W., Sheng, P., Zhao, G., Zhu, D. (2017), Organic Donor–Acceptor Complexes as Novel Organic Semiconductors, *Acc. Chem. Res.*, 50, 7, 1654-1662 (DOI: 10.1021/acs.accounts.7b00124); (d) Deibel, C., Strobel, T., Dyakonov, V. (2010), Role of the charge transfer state in organic donor-acceptor solar cells, *Adv Mater.*, 22(37), 4097-4111 (DOI: 10.1002/adma.201000376); (e) Sommer, M., Huettnerab, S., Thelakkat, M. (2010), Donor–acceptor block copolymers for photovoltaic applications, *J. Mater. Chem.*, 20, 10788-10797 (DOI: 10.1039/C0JM00665C); (f) Yao, S., Ahn, H.-Y., Wang, X., Fu, J., Stryland, E. W. V., Hagan, D. J., Belfield, K. D. (2010), Donor–Acceptor–Donor Fluorene Derivatives for Two-Photon Fluorescence Lysosomal Imaging, *J. Org. Chem.*, 75, 12, 3965-3974 (DOI: 10.1021/jo100554j).
- [2] (a) Kivala, M., Boudon, C., Gisselbrecht, J.-P., Seiler, P., Gross, M., Diederich, F. (2007), A novel reaction of 7,7,8,8-tetracyanoquinodimethane (TCNQ): charge-transfer chromophores by [2 + 2] cycloaddition with alkynes, *Chem. Commun.*, 4731-4733 (DOI: 10.1039/B713683H); (b) Reutenauer, P., Kivala, M., Jarowski, P. D., Boudon, C., Gisselbrecht, J.-P., Gross, M., Diederich, F. (2007), New

- strong organic acceptors by cycloaddition of TCNE and TCNQ to donor-substituted cyanoalkynes, *Chem. Commun.*, 4898-4900 (DOI: 10.1039/B714731G). (c) Beaujuge, P. M., Amb, C. M., Reynolds, J. R. (2010), Spectral Engineering in π -Conjugated Polymers with Intramolecular Donor–Acceptor Interactions, *Acc. Chem. Res.*, 43, 11, 1396-1407 (DOI: 10.1021/ar100043u).
- [3] (a) Bures, F., Schweizer, W. B., May, J. C., Boudon, C., Gisselbrecht, J.-P., Gross, M., Biaggio, I., Diederich, F. (2007), Property Tuning in Charge-Transfer Chromophores by Systematic Modulation of the Spacer between Donor and Acceptor. *Chem. Eur. J.*, 13, 5378–5387 (DOI: 10.1002/chem.200601735); (b) Wang, J.-L., Xiao, Q., Pei, J. (2010), Benzothiadiazole-Based D– π -A– π -D Organic Dyes with Tunable Band Gap: Synthesis and Photophysical Properties. *Org. Lett.*, 12, 4164–4167 (DOI: 10.1021/ol101754q).
- [4] (a) Qian G., Wang Z. Y. (2010), Near-infrared organic compounds and emerging applications, *Chem. Asian J.*, 5, 1006-1029 (DOI: 10.1002/asia.200900596); (b) Roncali, J. (2007), Molecular engineering of the band gap of π -conjugated systems: facing technological applications, *Macromol. Rapid Commun.*, 28, 1761-1775 (DOI: 10.1002/marc.200700345).
- [5] (a) Fang, Z., Eshbaugh, A. A., Schanze, K. S. (2011), Low-Bandgap Donor–Acceptor Conjugated Polymer Sensitizers for Dye-Sensitized Solar Cells, *J. Am. Chem. Soc.*, 133, 9, 3063-3069 (DOI: 10.1021/ja109926k); (b) Yao, Z., Zhang, M., Wu, H., Yang, L., Li, R., Wang, P. (2015), Donor/Acceptor Indenoperylene Dye for Highly Efficient Organic Dye-Sensitized Solar Cells, *J. Am. Chem. Soc.*, 137, 11, 3799-3802 (DOI: 10.1021/jacs.5b01537).
- [6] (a) Liu, Q., Jiang, K., Guan, B., Tang, Z., Pei, J., Song, Y. (2011), A novel bulk heterojunction solar cell based on a donor–acceptor conjugated triphenylamine dye, *Chem. Commun.*, 47, 740-742 (DOI: 10.1039/C0CC03925J); (b) Vandewal, K., Tvingstedt, K., Gadisa, A.,

- Inganäs, O., Manca, J. V. (2010), Relating the open-circuit voltage to interface molecular properties of donor:acceptor bulk heterojunction solar cells, *Phys. Rev. B*, 81, 125204 (DOI: 10.1103/PhysRevB.81.125204).
- [7] (a) Zhao, L., Lin, Y. L., Kim, H., Giebink, N. C., Rand, B. P. (2018), Donor/Acceptor Charge-Transfer States at Two-Dimensional Metal Halide Perovskite and Organic Semiconductor Interfaces, *ACS Energy Lett.*, 3, 11, 2708-2712 (DOI: 10.1021/acsenergylett.8b01722); (b) Kim, G.-W., Kim, J., Lee, G.-Y., Kang, G., Lee, J., Park, T. (2015) A Strategy to Design a Donor- π -Acceptor Polymeric Hole Conductor for an Efficient Perovskite Solar Cell, *Adv. Energy Mater.*, 5, 1500471 (DOI: 10.1002/aenm.201500471).
- [8] (a) Olivier, Y., Moral, M., Muccioli, L., Sancho-García, J.-C. (2017), Dynamic nature of excited states of donor-acceptor TADF materials for OLEDs: how theory can reveal structure-property relationships, *J. Mater. Chem. C*, 5, 5718-5729 (DOI: 10.1039/C6TC05075A); (b) Sommer, G. A., Mataranga-Popa, L. N., Czerwieńiec, R., Hofbeck, T., Homeier, H. H. H., Müller, T. J. J., Yersin, H. (2018), Design of Conformationally Distorted Donor-Acceptor Dyads Showing Efficient Thermally Activated Delayed Fluorescence, *J. Phys. Chem. Lett.*, 9, 13, 3692-3697 (DOI: 10.1021/acs.jpcclett.8b01511).
- [9] (a) Malaun, M., Reeves, Z. R., Paul, R. L., Jeffery, J. C., McCleverty, J. A., Ward, M. D., Asselberghs, I., Clays, K., Persoons, A. (2001), Reversible switching of the first hyperpolarisability of an NLO-active donor-acceptor molecule based on redox interconversion of the octamethylferrocene donor unit, *Chem. Commun.*, 49-50 (DOI: 10.1039/B008056J); (b) Huo, F., Zhang, H., Chen, Z., Qiu, L., Liu, J., Bo, S., Kityk, I. V. (2019), Novel nonlinear optical push-pull fluorene dyes chromophore as promising materials for telecommunications, *J Mater Sci: Mater Electron*, 30, 12180-12185 (DOI: 10.1007/s10854-019-01576-7).
- [10] (a) Huang, J., Pei, M., Kim, H. S., Yang, H., Hwang, D.-H. (2019), Dithienobenzothiadiazole-Based Donor-Acceptor Polymer: Synthesis and

- Characterization for Organic Field-Effect Transistor, *Macromol. Res.*, 27, 227–231 (DOI: 10.1007/s13233-019-7055-y); (b) Chen, C.-H., Wang, Y., Michinobu, T., Chang, S.-W., Chiu, Y.-C., Ke, C.-Y., Liou, G.-S. (2020), Donor–Acceptor Effect of Carbazole-Based Conjugated Polymer Electrets on Photoresponsive Flash Organic Field-Effect Transistor Memories, *ACS Appl. Mater. Interfaces*, 12, 5, 6144–6150 (DOI: 10.1021/acsami.9b20960).
- [11] (a) Crossley, D. L., Urbano, L., Neumann, R., Bourke, S., Jones, J., Dailey, L. A., Green, M., Humphries, M. J., King, S. M., Turner, M. L., Ingleson, M. J. (2017), Post-polymerization C–H Borylation of Donor–Acceptor Materials Gives Highly Efficient Solid State Near-Infrared Emitters for Near-IR-OLEDs and Effective Biological Imaging, *ACS Appl. Mater. Interfaces*, 9, 34, 28243–28249 (DOI: 10.1021/acsami.7b08473); (b) Zhao, Y., Zhang, Z., Lu, Z., Wang, H., Tang, Y. (2019), Enhanced Energy Transfer in a Donor–Acceptor Photosensitizer Triggers Efficient Photodynamic Therapy, *ACS Appl. Mater. Interfaces*, 11, 42, 38467–38474 (DOI: 10.1021/acsami.9b12375).
- [12] (a) Massie, S. P. (1954), The chemistry of phenothiazine, *Chem. Rev.*, 54 (5) 797–833 (DOI: 10.1021/cr60171a003) (b) Sailer, M., Gropeanu, R.-A., Müller, T. J. J. (2003) Practical Synthesis of Iodo Phenothiazines. A Facile Access to Electrophore Building Blocks, *J. Org. Chem.*, 68, 7509–7512 (DOI: 10.1021/jo034555z); (c) Krämer, C. S., Müller, T. J. J. (2003), Synthesis and Electronic Properties of Alkynylated Phenothiazines, *Eur. J. Org. Chem.*, 3534–3548 (DOI: 10.1002/ejoc.200300250)
- [13] (a) Hauck, M., Stolte, M., Schenhaber, J., Kuball, H.-G., Müller, T. J. J. (2011) Synthesis, Electronic, and Electro-Optical Properties of Emissive Solvatochromic Phenothiazinyl Merocyanine, *Dyes. Chem. Eur. J.*, 17, 9984–9998 (DOI: 10.1002/chem.201100592); (b) Krämer, C. S., Zeitler, K., Müller, T. J. J. (2000), Synthesis of Functionalized Ethynylphenothiazine Fluorophores, *Org. Lett.*, 2, 3723–3726 (DOI: 10.1021/ol0066328).

- [14] Bejan, A., Shova, S., Damaceanu, M.-D., Simionescu, B. C., Marin L. (2016), Structure-Directed Functional Properties of Phenothiazine Brominated Dyes: Morphology and Photophysical and Electrochemical Properties, *Cryst. Growth Des.*, 16, 3716–3730 (DOI: 10.1021/acs.cgd.6b00212).
- [15] (a) Konidena, R. K., Thomas, K. R. J., Kumar, S., Wang, Y.-C., Li, C.-J., Jou, J.-H. (2015), Phenothiazine Decorated Carbazoles: Effect of Substitution Pattern on the Optical and Electroluminescent Characteristics, *J. Org. Chem.*, 80, 5812–5823 (DOI: 10.1021/acs.joc.5b00787); (b) Wang, W., Li, X., Lan, J., Wu, D., Wang, R., You, J. (2018), Construction of 3,7-Dithienyl Phenothiazine-Based Organic Dyes via Multistep Direct C–H Arylation Reactions *J. Org. Chem.*, 83, 8114–8126 (DOI: 10.1021/acs.joc.8b00915).
- [16] (a) Hauck, M., Schonhaber, J., Zuccherro, A. J., Hardcastle, K. I., Müller, T. J. J., Bunz, U. H. F. (2007), Phenothiazine Cruciforms: Synthesis and Metallochromic Properties. *J. Org. Chem.*, 72, 6714–6725 (DOI: 10.1021/jo070922i); (b) Gupta, R. R.; Ojha, K. G. (1988), In Phenothiazines and 1,4-Benzothiazines: Chemical and Biochemical Aspects. Gupta, R. R., ed.; *Elsevier: Amsterdam*, 163–269.
- [17] (a) Wang, W., Li, X., Lan, J., Wu, D., Wang, R., You, J. (2018), Construction of 3,7-Dithienyl Phenothiazine-Based Organic Dyes via Multistep Direct C–H Arylation Reactions, *J. Org. Chem.*, 83, 8114–8126 (DOI: 10.1021/acs.joc.8b00915); (b) Rechmann, J., Sarfraz, A., Götzinger, A. C., Dirksen, E., Müller, T. J. J., Erbe A. (2015), Surface Functionalization of Oxide-Covered Zinc and Iron with Phosphonated Phenylethynyl Phenothiazine, *Langmuir*, 31, 7306–7316 (DOI: 10.1021/acs.langmuir.5b01370).
- [18] (a) Rajakumar P., Kanagalatha, R. (2007), Synthesis and optoelectrochemical properties of novel phenothiazinophanes, *Tetrahedron Letters*, 48, 8496–8500 (DOI: 10.1016/j.tetlet.2007.09.161); (b) Hsieh, T.-S., Wu, J.-Y., Chang, C.-C. (2015), Multiple fluorescent

- behaviors of phenothiazine-based organic molecules, *Dyes and Pigments*, 112, 34-41 (DOI: 10.1016/j.dyepig.2014.06.017); (c) Han, F., Chi, L., Wu, W., Liang, X., Fua, M., Zhao, J. (2008), Environment sensitive phenothiazine dyes strongly fluorescence in protic solvents, *Journal of Photochemistry and Photobiology A: Chemistry*, 196, 10–23 (DOI: 10.1016/j.jphotochem.2007.11.007); (d) Miles, D. T., Murray, R. W. Redox and Double-Layer Charging of Phenothiazine Functionalized Monolayer-Protected Clusters, *Anal. Chem.* 2001, 73, 921-929 (DOI: 10.1021/ac0012647); (e) Hayen, H., Karst, U. (2003), Analysis of Phenothiazine and Its Derivatives Using LC/Electrochemistry/MS and LC/Electrochemistry/Fluorescence, *Anal. Chem.*, 75, 4833-4840 (DOI: 10.1021/ac0346050); (f) Okamoto, T., Kuratsu, M., Kozaki, M., Hirotsu, K., Ichimura, A., Matsushita, T., Okada, K. (2004), Remarkable Structure Deformation in Phenothiazine Trimer Radical Cation, *Org. Lett.*, 6, 20, 3493-3496 (DOI: 10.1021/ol048698z); (g) Lebedev, A. Y., Izmer, V. V., Kazyul'kin, D. N., Beletskaya, I. P., Voskoboynikov, A. Z. (2002), Palladium-Catalyzed Stereocontrolled Vinylation of Azoles and Phenothiazine, *Org. Lett.*, 4, 4, 623-626 (DOI: 10.1021/ol0172370); (h) Zhang, G., Sun, J., Xue, P., Zhang, Z., Gong, P., Peng, J., Lu, R. (2015), Phenothiazine modified triphenylacrylonitrile derivatives: AIE and mechanochromism tuned by molecular conformation, *J. Mater. Chem. C*, 3, 2925-2932 (DOI: 10.1039/c4tc02925a).
- [19] (a) Luo, J.-S., Wan, Z.-Q., Jia, C.-Y. (2016), Recent advances in phenothiazine-based dyes for dye-sensitized solar cells, *Chinese Chemical Letters*, 27, 1304–1318 (DOI: 10.1016/j.ccllet.2016.07.002); (b) Thokala, S., Singh, S. P. (2020), Phenothiazine-Based Hole Transport Materials for Perovskite Solar Cells, *ACS Omega*, 5, 5608–5619 (DOI: 10.1021/acsomega.0c00065); (c) Huang, Z.-S., Meier, H., Cao, D. (2016), Phenothiazine-based dyes for efficient dye-sensitized solar cells, *J. Mater. Chem. C*, 4, 2404-2426 (DOI: 10.1039/c5tc04418a); (d) Al-Busaidi, I. J., Haque, A., Rasbi, N. K. A., Khan M. S. (2019), Phenothiazine-based

- derivatives for optoelectronic applications: A review, *Synthetic Metals*, 257, 116189 (DOI: 10.1016/j.synthmet.2019.116189); (e) Varga, B., Csonka, Á., Csonka, A., Molnár, J., Amaral, L., Spengler, G. (2017), Possible Biological and Clinical Applications of Phenothiazines, *Anticancer Res.*, 37 (11), 5983-5993 (DOI: 10.21873/anticancer.12045); (f) Aaron, J. J., Seye, M. D. G., Trajkovska, S., Motohashi, N. (2008), Bioactive Phenothiazines and Benzo[a]phenothiazines: Spectroscopic Studies, and Biological and Biomedical Properties and Applications, In: Motohashi N. (eds) *Bioactive Heterocycles VII. Topics in Heterocyclic Chemistry*, vol 16. *Springer*, Berlin, Heidelberg.
- [20] (a) Nagarajan, B., Kushwaha, S., Elumalai, R., Mandal, S., Ramanujam, K., Raghavachari, D. (2017), Novel ethynyl-pyrene substituted phenothiazine based metal free organic dyes in DSSC with 12% conversion efficiency, *J. Mater. Chem. A*, 5, 10289-10300 (DOI: 10.1039/C7TA01744H); (b) Yang, C.-J., Chang, Y. J., Watanabe, M., Hon, Y.-S., Chow, T. J. (2012), Phenothiazine derivatives as organic sensitizers for highly efficient dye-sensitized solar cells, *J. Mater. Chem.*, 22, 4040-4049 (DOI: 10.1039/C2JM13961H).
- [21] (a) Blanco, G. D., Hiltunen, A. J., Lim, G. N., KC, C. B., Kaunisto, K. M., Vuorinen, T. K., Nesterov, V. N., Lemmetyinen, H. J., D'Souza, F. (2016), Syntheses, Charge Separation, and Inverted Bulk Heterojunction Solar Cell Application of Phenothiazine–Fullerene Dyads, *ACS Appl. Mater. Interfaces*, 8, 13, 8481-8490 (DOI: 10.1021/acsami.6b00561); (b) Maglione, C., Carella, A., Centore, R., Chávez, P., Lévêque, P., Fall, S., Leclercb, N. (2017), Novel low bandgap phenothiazine functionalized DPP derivatives prepared by direct heteroarylation: Application in bulk heterojunction organic solar cells, *Dyes and Pigments*, 141, 169-178 (DOI: 10.1016/j.dyepig.2017.02.012).
- [22] (a) Aizawa, N., Tsou, C.-J., Park, I. S., Yasuda, T. (2017), Aggregation-induced delayed fluorescence from phenothiazine-containing donor–acceptor molecules for high-efficiency non-doped organic light-emitting

- diodes, *Polym J*, 49, 197–202 (DOI: 10.1038/pj.2016.82); (b) Marghad, I., Bencheikh, F., Wang, C., Manolikakes, S., Rérat, A., Gosmini, C., Kim, D. h., Ribierre, J.-C., Adachi, C. (2019), Control of the dual emission from a thermally activated delayed fluorescence emitter containing phenothiazine units in organic light-emitting diodes, *RSC Adv.*, 9, 4336–4343 (DOI: 10.1039/C8RA10393C).
- [23] Huang, W., Helvenston, M., Casson, J. L., Wang, R., Bardeau, J.-F., Lee, Y., Johal, M. S., Swanson, B. I., Robinson, J. M., Li, D. (1999), Synthesis, Characterization, and NLO Properties of a Phenothiazine–Stilbazole Monolayer, *Langmuir*, 15, 19, 6510–6514 (DOI: 10.1021/la990237c).
- [24] Zou, Y., Wu, W., Sang, G., Yang, Y., Liu, Y., Li, Y. (2007), Polythiophene Derivative with Phenothiazine–Vinylene Conjugated Side Chain: Synthesis and Its Application in Field-Effect Transistors, *Macromolecules*, 40, 20, 7231–7237 (DOI: 10.1021/ma071402v).
- [25] Liu, X., Tan, X., Chen, Q., Shan, H., Liu, C., Xu, J., Chen, Z.-K., Huang, W., Xu, Z.-X. (2017), Facile synthesis of a dopant-free hole transporting material with a phenothiazine core for planar perovskite solar cells, *RSC Adv.*, 7, 53604–53610 (DOI: 10.1039/C7RA10677G).
- [26] Hou, P., Wang, J., Fu, S., Liu, L., Chen, S. (2019), Highly sensitive fluorescent probe based on a novel phenothiazine dye for detection of thiophenols in real water samples and living cells, *Anal Bioanal Chem* 411, 935–942 (DOI:10.1007/s00216-018-1525-5).
- [27] Wang, J., Niu, Q., Hu, T., Li, T., Wei, T. (2019), A new phenothiazine-based sensor for highly selective, ultrafast, ratiometric fluorescence and colorimetric sensing of Hg²⁺: Applications to bioimaging in living cells and test strips, *Journal of Photochemistry & Photobiology A: Chemistry*, 384, 112036 (DOI: 10.1016/j.jphotochem.2019.112036).
- [28] Gorman, S. A., Brown, S. B., Griffiths, J. (2006), An overview of synthetic approaches to porphyrin, phthalocyanine, and phenothiazine photosensitizers for photodynamic therapy, *J Environ Pathol Toxicol*

- Oncol.*, 25, 79-108 (DOI: 10.1615/jenviropatholtoxicoloncol.v25.i1-2.50).
- [29] Bernthsen, A., (1883), Zur Kenntniss des Methylenblau und verwandter Farbstoffe, *Ber. Dtsch. Chem. Ges.*, 16 (2), 2896-2904.
- [30] (a) Ackermann (1909), *German Patent*, 224, 348. (b) Knoevenagel (1914), *J. prakt. Chem.*, 89 (2), 1.
- [31] Massie, S. P. (1954), The Chemistry of Phenothiazine, *Chem. Rev.*, 54, 5, 797-833 (DOI: 10.1021/cr60171a003).
- [32] Liao, Y., Jiang, P., Chen, S., Xiao, F., Deng, G.-J. (2013), Synthesis of phenothiazines from cyclohexanones and 2-aminobenzenethiols under transition-metal-free conditions, *RSC Adv.*, 3, 18605–18608 (DOI: 10.1039/c3ra43989e).
- [33] Dai, C., Sun, X., Tu, X., Wu, L., Zhan, D., Zeng, Q. (2012), Synthesis of phenothiazines via ligand-free CuI-catalyzed cascade C–S and C–N coupling of aryl ortho-dihalides and ortho-aminobenzenethiols, *Chem. Commun.*, 48, 5367–5369 (DOI: 10.1039/c2cc30814b).
- [34] Hu, W., Zhang, S. (2015), Method for the Synthesis of Phenothiazines via a Domino Iron-Catalyzed C–S/C–N Cross-Coupling Reaction, *J. Org. Chem.*, 80, 12, 6128-6132 (DOI: 10.1021/acs.joc.5b00568).
- [35] Dahl, T., Tornøe, C. W., Banz-Andersen, B., Nielsen, P., Jørgensen, M. (2008), Palladium-catalyzed three-component approach to promazine with formation of one carbon-sulfur and two carbon-nitrogen bonds, *Angew Chem Int Ed Engl.*, 47(9), 1726-1728 (DOI: 10.1002/anie.200705209).
- [36] Ma, D., Geng, Q., Zhang, H., Jiang, Y. (2010), Assembly of Substituted Phenothiazines by a Sequentially Controlled CuI/l-Proline-Catalyzed Cascade CS and CN Bond Formation, *Angew. Chem. Int. Ed.*, 49, 1291 – 1294 (DOI: 10.1002/anie.200905646).
- [37] Kim, S. H., Sakong, C., Chang, J. B., Kim, B., Ko, M. J., Kim, D. H., Hong, K. S., Kim, J. P. (2013), The effect of N-substitution and ethylthio substitution on the performance of phenothiazine donors in dye-sensitized

- solar cells, *Dyes and Pigments*, 97, 262-271 (DOI: 10.1016/j.dyepig.2012.12.007).
- [38] Sailer, M., Franz, A. W., Muller, T. J. J. (2008), Synthesis and Electronic Properties of Monodisperse Oligophenothiazines, *Chem. Eur. J.*, 14, 2602–2614.
- [39] Doskocz, J., Sołoducho, J., Cabaj, J., Łapkowski, M., Golba, S., Palewska, K. (2007), Development in Synthesis, Electrochemistry, LB Moieties of Phenothiazine Based Units, *Electroanalysis*, 19, 1394-1401.
- [40] Bieliauskas, A., Martynaitis, V., Getautis, V., Malinauskas, T., Jankauskas, V., Kamarauskas, E., Holzer, W., Sackus, A. (2012), Synthesis of electroactive hydrazones derived from 3-(10-alkyl-10H-phenothiazin-3-yl)-2-propenals and their corresponding 3,3'-bispropenals, *Tetrahedron*, 68, 3552-3559 (DOI: 10.1016/j.tet.2012.03.010).
- [41] Lee, S. K., Cho, M. J., Yoon, H., Lee, S. H., Kim, J. H., Zhang, Q., Choi, D. H. (2004), Electro-optic Properties of a Guest-Host System Containing a Phenothiazine-based Chromophore: Effect of the Chromophore Density on the Macroscopic Optical Nonlinearity, *Macromol. Res.*, 12, 5, 484-489 (DOI: 10.1007/BF03218431).
- [42] Marin, L., Bejan, A., Ailincăi, D., Belei, D. (2017), Poly(azomethine-phenothiazine)s with efficient emission in solid state, *European Polymer Journal*, 95, 127–137 (DOI: 10.1016/j.eurpolymj.2017.08.006).
- [43] Shinde, D. B., Salunke, J. K., Candeias, N. R., Tinti, F., Gazzano, M., Wadgaonkar, P. P., Priimagi, A., Camaioni, N., Vivo, P. (2017), Crystallisation-enhanced bulk hole mobility in phenothiazine-based organic semiconductors, *Sci Rep*, 7, 46268 (DOI: 10.1038/srep46268).
- [44] Sang, G., Zou, Y., Li, Y. (2008), Two Polythiophene Derivatives Containing Phenothiazine Units: Synthesis and Photovoltaic Properties, *J. Phys. Chem. C*, 112, 12058–12064 (DOI: 10.1021/jp803187u).
- [45] Ravivarma, M., Satheeshkumar, C., Ganesan, S., Rajakumar, P. (2017), Synthesis and application of stilbenoid phenothiazine dendrimers as

- additives for dye-sensitized solar cells, *Mater. Chem. Front.*, 1, 2117-2124 (DOI: 10.1039/C7QM00238F).
- [46] Han, M.-L., Zhu, Y.-Z., Liu, S., Liu, Q.-L., Ye, D., Wang, B., Zheng, J.-Y. (2018), The improved photovoltaic performance of phenothiazine-dithienopyrrole based dyes with auxiliary acceptors, *Journal of Power Sources*, 387, 117–125 (DOI: 10.1016/j.jpowsour.2018.03.059).
- [47] Revoju, S., Biswas, S., Eliasson, B., Sharma, G. D. (2018), Effect of acceptor strength on optical, electrochemical and photovoltaic properties of phenothiazine-based small molecule for bulk heterojunction organic solar cells, *Dyes and Pigments*, 149, 830–842 (DOI: 10.1016/j.dyepig.2017.11.048).
- [48] Grisorio, R., Roose, B., Colella, S., Listorti, A., Suranna, G. P., Abate, A. (2017), Molecular Tailoring of Phenothiazine-Based Hole-Transporting Materials for High-Performing Perovskite Solar Cells, *ACS Energy Lett.*, 2, 1029–1034 (DOI: 10.1021/acseenergylett.7b00054).
- [49] Marghad, I., Kim, D. H., Tian, X., Mathevet, F., Gosmini, C., Ribierre, J.-C., Adachi, C. (2018), Synthesis by a Cost-Effective Method and Electroluminescence of a Novel Efficient Yellowish-Green Thermally Activated Delayed Fluorescent Molecule, *ACS Omega*, 3, 2254–2260 (DOI: 10.1021/acsomega.7b01570).
- [50] Narayanan, S., Abbas, A., Kartha, C. S., Joseph, R., Devaky, K. S., Sreekumard, K. (2018), Low Band Gap Donor-Acceptor Phenothiazine Copolymer with Triazine Segment: Design, Synthesis and Application for Optical Limiting Devices, *Journal of Luminescence*, 198, 449–456 (DOI: 10.1016/j.jlumin.2018.01.044).
- [51] Ramachandran, E., Vandarkuzhali, S. A. A., Sivaraman, G., Dhamodharan, R. (2018), Phenothiazine Based Donor–Acceptor Compounds with Solid- State Emission in the Yellow to NIR Region and Their Highly Selective and Sensitive Detection of Cyanide Ion in ppb Level, *Chem. Eur. J.*, 24, 11042–11050 (DOI: 10.1002/chem.201800216).

Chapter 2

Materials and Experimental Techniques

2.1. Introduction

The materials, general synthetic procedures, characterization techniques and the instrumentation employed in this thesis are described in this chapter.

2.2. Chemicals for synthesis

The common solvents used for syntheses were purified according to established procedures.^[1] 10*H*-phenothiazine was obtained from TCI chemicals. Iodopropane, trimethylsilylacetylene, pyrrole, benzaldehyde, thiophosgene, phosphorus oxychloride and boron trifluoride etherate were obtained from Spectrochem India. CuI, Pd(PPh₃)₄ and PdCl₂(PPh₃)₂ were purchased from Aldrich chemicals USA and Spectrochem India.

The solvents and reagents were used as received unless otherwise indicated. Photophysical and electrochemical studies were performed with spectroscopic grade solvents.

Dry solvents such as, dichloromethane, 1,2-dichloroethane, chloroform, tetrahydrofuran (THF), triethylamine, dimethylformamide (DMF), ethanol, acetonitrile and methanol were obtained from Spectrochem, Advent Chembio Pvt. Ltd. and S. D. Fine chem. Ltd.

Silica gel (100–200 mesh and 230–400 mesh) were purchased from Rankem chemicals, India. TLC pre-coated silica gel plates (Kieselgel 60F254, Merck) were obtained from Merck, India. All the oxygen or moisture sensitive reactions were performed under nitrogen/argon atmosphere using standard Schlenk method.

2.3. Spectroscopic measurements

2.3.1. NMR spectroscopy

¹H NMR (400 MHz), and ¹³C NMR (100 MHz) spectra were recorded on the Bruker Avance (III) 400 MHz, using CDCl₃ as solvent. ¹H NMR (500 MHz),

and ^{13}C NMR (125 MHz) spectra were recorded on the Bruker-500 MHz Ascend FT NMR, using CDCl_3 as solvent. Chemical shifts in ^1H , and ^{13}C NMR spectra were reported in parts per million (ppm). In ^1H NMR chemical shifts are reported relative to the residual solvent peak (CDCl_3 , 7.26 ppm). Multiplicities are given as: s (singlet), d (doublet), t (triplet), q (quartet), m (multiplet), and the coupling constants J , are given in Hz. ^{13}C NMR chemical shifts are reported relative to the solvent residual peak (CDCl_3 , 77.36 ppm).

2.3.2. Mass spectrometry

High resolution mass spectra (HRMS) were recorded on Bruker-Daltonics, micrOTOF-Q II mass spectrometer using positive and negative mode electrospray ionizations.

2.3.3. UV-Vis spectroscopy

UV-Vis absorption spectra were recorded using a Varian Cary100 Bio UV-Vis and Perkin Elmer LAMBDA 35 UV/Vis spectrophotometer.

2.3.4. Fluorescence spectroscopy

Fluorescence emission spectra were recorded upon specific excitation wavelength on a Horiba Scientific Fluoromax-4 spectrophotometer. The slit width for the excitation and emission was set at 2 nm.

The fluorescence quantum yields (ϕ_F)

The fluorescence quantum yields (ϕ_F) of compounds were calculated by the steady-state comparative method using following equation,

$$\phi_F = \phi_{st} \times S_u/S_{st} \times A_{st}/A_u \times n_2 D_u/n_1 D_{st} \dots\dots\dots (\text{Eq. 1})$$

Where ϕ_F is the emission quantum yield of the sample, ϕ_{st} is the emission quantum yield of the standard, A_{st} and A_u represent the absorbance of the standard and sample at the excitation wavelength, respectively, while S_{st} and S_u are the integrated emission band areas of the standard and sample, respectively, and nD_{st}

and n_{D_u} the solvent refractive index of the standard and sample, u and st refer to the unknown and standard, respectively.

2.4. Electrochemical studies

Cyclic voltamograms (CVs) were recorded on CHI620D electrochemical analyzer using Glassy carbon as working electrode, Pt wire as the counter electrode, and Saturated Calomel Electrode (SCE) as the reference electrode. The scan rate was 100 mVs^{-1} . A solution of tetrabutylammonium hexafluorophosphate (TBAPF₆) in CH₂Cl₂ (0.1 M) was employed as the supporting electrolyte.

2.5. Single crystal X-ray diffraction studies.

Single crystal X-ray diffraction studies were performed on SUPER NOVA diffractometer. The strategy for the Data collection was evaluated by using the CrysAlisPro CCD software. The data were collected by the standard 'phi-omega scan techniques, and were scaled and reduced using CrysAlisPro RED software. The structures were solved by direct methods using SHELXS-97, and refined by full matrix least-squares with SHELXL-97, refining on F^2 .¹ The positions of all the atoms were obtained by direct methods. All non-hydrogen atoms were refined anisotropically. The remaining hydrogen atoms were placed in geometrically constrained positions, and refined with isotropic temperature factors, generally $1.2U_{eq}$ of their parent atoms. The CCDC numbers contain the respective supplementary crystallographic data. These data can be obtained free of charge via www.ccdc.cam.ac.uk/conts/retrieving.html (or from the Cambridge Crystallographic 42 Data Centre, 12 union Road, Cambridge CB21 EZ, UK; Fax: (+44) 1223-336-033; or deposit@ccdc.cam.ac.uk).

2.6. Computational calculations

The density functional theory (DFT) calculation were carried out at the B3LYP/6-31G** level for C, N, S, H, and Lan12DZ level for Zn in the Gaussian 09 program.^[2]

2.7. References

- [1] (a) Vogel A. I., Tatchell A. R., Furnis B. S., Hannaford A. J., & Smith, P. W. G. (1996), *Vogel's Textbook of Practical Organic Chemistry (5th Edition)* (5th ed.). (b) Wei Ssberger A. Proskraner E. S. Riddick J. A., Toppos Jr. E. F. (1970). *Organic Solvents in Techniques of Organic Chemistry*, Vol. IV, 3rd Edition, Inc. New York.
- [2] (a) Lee C., Yang W., & Parr R. G. (1988). Development of the Colle-Salvetti correlation-energy formula into a functional of the electron density. *Physical Review B*, 37(2), 785–789 (DOI: 10.1103/PhysRevB.37.785). (b) A. D. Becke (1993), A new mixing of Hartree-Fock and local densityfunctional theories, *J. Chem. Phys.* 98 (2), 1372–377 (DOI: 10.1063/1.464304). (c) Frisch M. J., Trucks G. W., Schlegel H. B., Scuseria G. E., Robb M. A., Cheeseman J. R., Scalmani G., Barone V., Mennucci B., Petersson G. A., Nakatsuji H., Caricato M., Li X., Hratchian H. P., Izmaylov A. F., Bloino J., Zheng G., Sonnenberg J. L., Hada M., Ehara M., Toyota K., Fukuda R., Hasegawa J., Ishida M. Nakajima T., Honda Y., Kitao O., Nakai H., Vreven T., Montgomery J. A. Jr., Peralta J. E., Ogliaro F., Bearpark M., Heyd J. J., Brothers E., Kudin K. N., Staroverov V. N., Kobayashi R., Normand J., Raghavachari K., Rendell A., Burant J. C., Iyengar S. S., Tomasi J., Cossi M., Rega N., Millam N. J., Klene M., Knox J. E., Cross J. B., Bakken V., Adamo C., Jaramillo J., Gomperts R., Stratmann R. E., Yazyev O., Austin A. J., Cammi R., Pomelli C.; Ochterski J. W., Martin R. L., Morokuma K., Zakrzewski V. G., Voth G. A., Salvador P., Dannenberg J. J., Dapprich S., Daniels A. D., Farkas O., Foresman J. B., Ortiz J. V., Cioslowski J., Fox D. J. (2009), *Gaussian 09, revision A.02; Gaussian, Inc.:Wallingford, CT.*

Chapter 3

Aryl-Substituted Phenothiazines: Design, Synthesis and Properties

3.1. Introduction

The research in the field of solar light harvesting is of significant interest for a sustainable society, where artificial systems mimic natural photosynthetic systems by transforming the solar light into storable electric or chemical energy.¹⁻³ In this regard, the development of multichromophoric π -conjugated molecules as artificial systems has attracted the attention of researchers for fast-responding optoelectronic devices, such as organic light emitting diodes (OLEDs), organic photovoltaics (OPVs) and organic luminescent displays.⁴⁻⁶ The advantages of using these π -conjugated molecules are their excellent thermal, photophysical and electrochemical properties, which can be easily modified.⁷ π -conjugated small molecules, which are able to give photoinduced electron transfer, are of extreme interest for light-to-electricity conversion in OPV devices.⁸⁻¹⁰ On the other hand, not only have highly fluorescent organic molecules been employed in first generation OLED devices, but also organic donor-acceptor systems showing thermally activated delayed fluorescence (TADF) have been used in the active layer of extremely efficient third generation OLEDs.¹¹⁻¹⁵

π -conjugated small-molecule-based organic fluorophores possess high fluorescence quantum yields, absorption bands in the visible region along with high molar extinction coefficients as well as large Stokes shift values.¹⁶⁻¹⁸ Organic fluorophores with large Stokes shifts are valuable for biological studies as an alternative to fluorescent proteins, metal complexes, quantum dots, or UV absorbing chromophores.¹⁷⁻²¹ The major benefit of utilizing fluorophores with large Stokes shifts is to minimize the interference or cross-talk between the excitation source and the emission for bioimaging applications with high signal-

to-noise ratio.²² The mostly used fluorophores, such as rhodamine, fluorescein, cyanine, oxazine, BODIPY, exhibit small Stokes shift values of less than 40 nm which can cause poor signal-to-noise ratio and self-quenching.²³ In this respect, the possibility of multiphoton excitation for these fluorophores^{24–25} is an added value to improve the imaging resolution, also allowing increased penetration depth for the infrared exciting light in biological tissues. The design and synthesis of small-molecule-based organic fluorophores with high quantum yields, large and tunable Stokes shifts, strong two photon absorption are therefore desirable for biological applications.²⁶

Phenothiazine is a tricyclic moiety containing sulfur (S) and nitrogen (N) heteroatoms. The electron rich S and N atoms make phenothiazine an excellent donor with low oxidation potential values.^{27–31} The incorporation of heterocyclic phenothiazines in molecular systems leads to high chemical and thermal stability.^{27–31} Benzene,^{32–34} naphthalene,³⁵ anthracene,^{36–38} phenanthrene³⁹ and pyrene^{40, 41} are well established conjugated systems and have been explored in the field of optoelectronic and biological applications. In fact, our group has already reported a variety of phenothiazine-based π -conjugated molecular systems for optoelectronics.^{42–46}

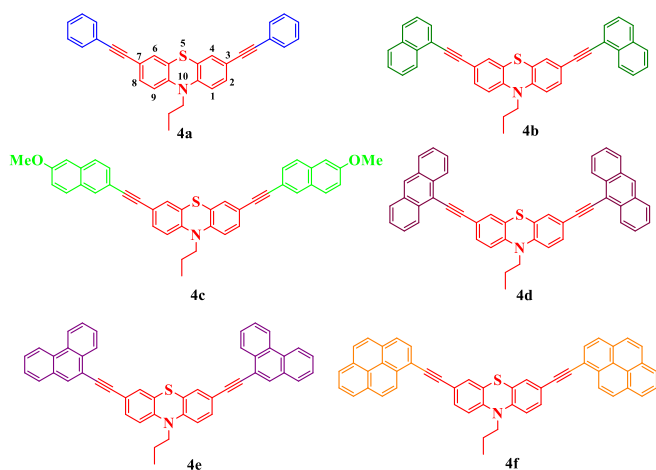
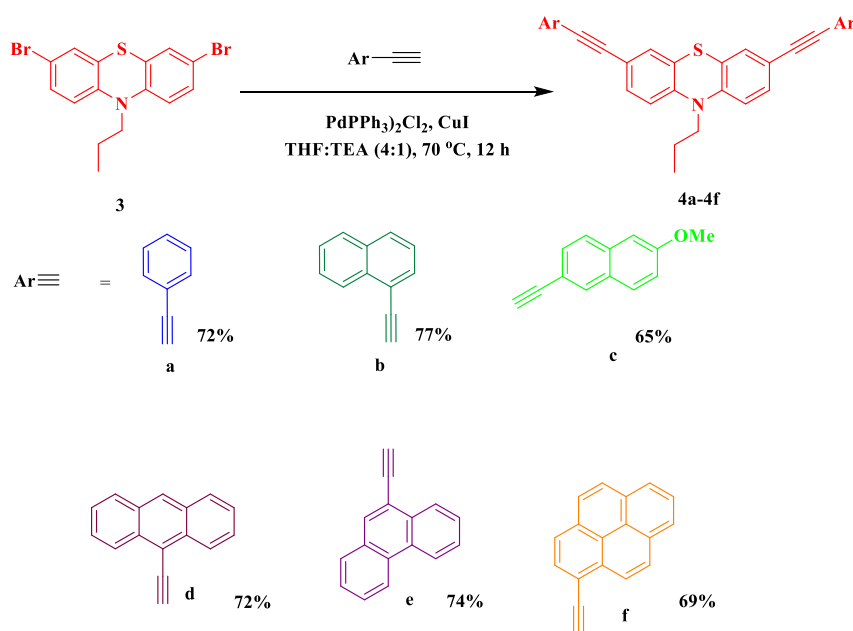


Chart 3.1. Structures of aryl substituted phenothiazines **4a–4f**.

In this chapter, we wish to report the synthesis of a series of aryl substituted symmetrical phenothiazine fluorophores *via* Pd-catalyzed Sonogashira cross-coupling reaction where the 3 and 7 positions of the phenothiazines are substituted with aryl moieties (Chart 3.1). In this work, our objective was to control the optical and electronic properties of the phenothiazines by perturbing the conjugation pattern on the phenothiazine core. We have incorporated ethynyl substituted simple acenes, such as benzene, naphthalene and anthracene, as well as large aromatic units, such as phenanthrene and pyrene, on the phenothiazine core. The photophysical and electrochemical properties were investigated for all the phenothiazines. The experimental study was carried out in a joint effort with DFT and TD-DFT calculations.

3.2. Results and discussions

Synthesis: The synthesis of aryl-substituted phenothiazines **4a–4f** is shown in Scheme 3.1. The alkylation was achieved by reaction of phenothiazine **1** with propyl-bromide in the presence of KOH and DMSO. The bromination of phenothiazine **2** with NBS resulted in dibromo-phenothiazine **3** with a 85% yield.^{27, 47}



Scheme 3.1. Synthesis of Aryl-Substituted Phenothiazines **4a–4f**.

The Pd-catalyzed Sonogashira cross-coupling reaction of dibromo substituted phenothiazine **3** with ethynyl derivatives **a–f**, resulted in phenothiazines **4a–4f** with 65–77% yields. All the phenothiazines **4a–4f** are soluble in common organic solvents such as toluene, dichloromethane, tetrahydrofuran, ethyl acetate, dimethylformamide, *etc.* The purification of the phenothiazines **4a–4f** were achieved by column chromatography. All the compounds were well-characterized by ^1H and ^{13}C NMR and HRMS techniques.

3.3. Photophysical properties

The electronic absorption and emission spectra of the aryl-substituted phenothiazines **4a–4f** were recorded in dichloromethane at room temperature (Figure 3.2 and Figure 3.3). The obtained results are compiled in Table 3.1. The photographs of the phenothiazines **4a–4f** in dichloromethane at 1.0×10^{-5} M concentration under daylight and UV-light are also displayed (Figure 3.1).

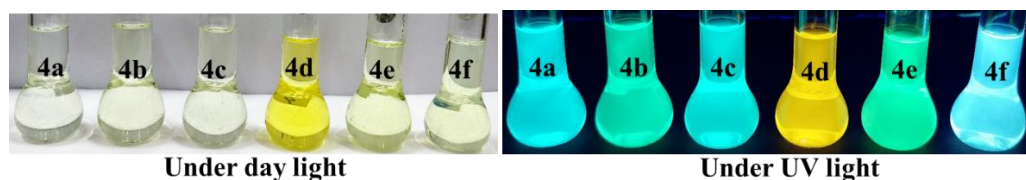


Figure 3.1. Pictorial representation of phenothiazines **4a–4f** in dichloromethane at 1.0×10^{-5} M concentration.

The absorption spectra of the phenothiazines **4a–4f** display characteristic bands both in the 360–540 nm range with lower molar extinction coefficient values, and in the 250–340 nm range with higher molar extinction coefficient values, which can be attributed to $\pi \rightarrow \pi^*$ transitions. The absorption bands of phenothiazines **4d–4f** bathochromically shift in comparison to the benzene and naphthalene substituted phenothiazines **4a–4c**. Among all the phenothiazines **4a–4f**, anthracene substituted phenothiazine **4d** shows the most red-shifted absorption band peaked at 440 nm. The optical band gap of the phenothiazines are in order **4a**>**4c**>**4b**>**4e**>**4f**>**4d**, following a trend that clearly indicates how the

substitution with the anthracene units results in better electronic communication and enhancement of conjugation leading to low optical band gap. The result was further supported by the TD-DFT calculations.

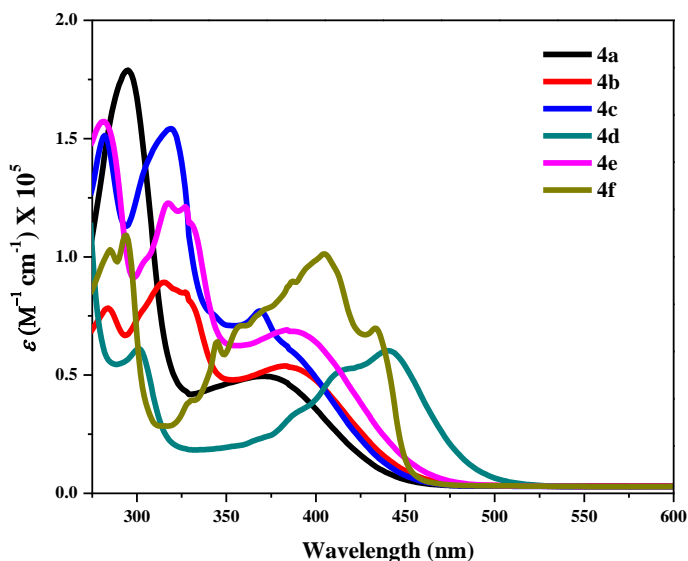


Figure 3.2. Electronic absorption spectra of aryl-substituted phenothiazines **4a–4f** in dichloromethane at 1.0×10^{-5} M concentration.

The fluorescence spectra of the phenothiazines **4a–4f** feature emission maxima in the range between 446 nm and 582 nm, with the most red-shifted emission band (peaking at 582 nm) being peculiar to **4d**. The phenothiazine fluorophores **4a–4e** show large Stokes shifts ranging from about 5500 cm^{-1} to 6000 cm^{-1} , with the exception of the pyrene substituted phenothiazine **4f** (Stokes shift value of 2200 cm^{-1}). Remarkable fluorescence quantum yields (between 40 and 82 %) were measured for these fluorophores in dichloromethane solution.

Solvatochromic Effect: The solvent effect was investigated for all the fluorophores **4a–4f** by studying the optical properties in different solvents (toluene, tetrahydrofuran (THF), dichloromethane (DCM) and dimethylformamide (DMF)). The absorption and emission spectra are shown in Figure 3.3 for all the solvents and the data are summarized in Table 3.2.

Table 3.1. Photophysical and Electrochemical Properties of phenothiazines **4a–4f** in dichloromethane.

| | Photophysical Data | | | | | Electrochemical Data | | |
|-----------|------------------------|-------------------------------------|-----------------------|------------|---------------------|------------------------------|-------------------|----------------|
| | λ_{abs} | ϵ | λ_{em} | | Stokes | $\Phi_{\text{F}}^{\text{d}}$ | Optical | E^{l} |
| | (nm) ^a | (M ⁻¹ cm ⁻¹) | (nm) ^b | | Shift | | Gap | Oxid |
| | | | A | B | (cm ⁻¹) | | (eV) ^c | |
| 4a | 374 295 | 49684 178808 | 483 | 482 | 6035 | 0.82 | 2.73 | 0.78 |
| 4b | 385 314 | 54240 89666 79194 | 497 | 497 | 5850 | 0.42 | 2.67 | 0.8 |
| 4c | 368 318 | 78107 155214 151270 | 487 | 479 | 6640 | 0.40 | 2.68 | 0.78 |
| 4d | 440 301 | 60380 62128 215526 | 582 | 594 | 5545 | 0.45 e | 2.46 | 0.78 |
| 4e | 388 318 | 70015 122440 157865 202403 | 502 | 542 | 5850 | 0.41 | 2.65 | 0.8 |
| 4f | 404 294 | 101392 109317 | 446 | 530 473 | 2230 | 0.67 | 2.61 | 0.83 |

a Absorbance measured in dichloromethane at 1×10^{-5} M concentration; b λ_{em} : emission wavelength; (A) = recorded in DCM solvent and (B) in Solid State; ϵ : extinction coefficient; c determined from onset wavelength of the UV/Vis absorption, d Determined using Quinine Sulphate as the standard ($\Phi = 0.54$, in 0.5 M H₂SO₄), e determined using Rhodamine 6G standard ($\Phi = 0.95$, in ethanol). f Calculated from DFT using B3LYP/6-31+G** level for B, C, F, H, N and S.

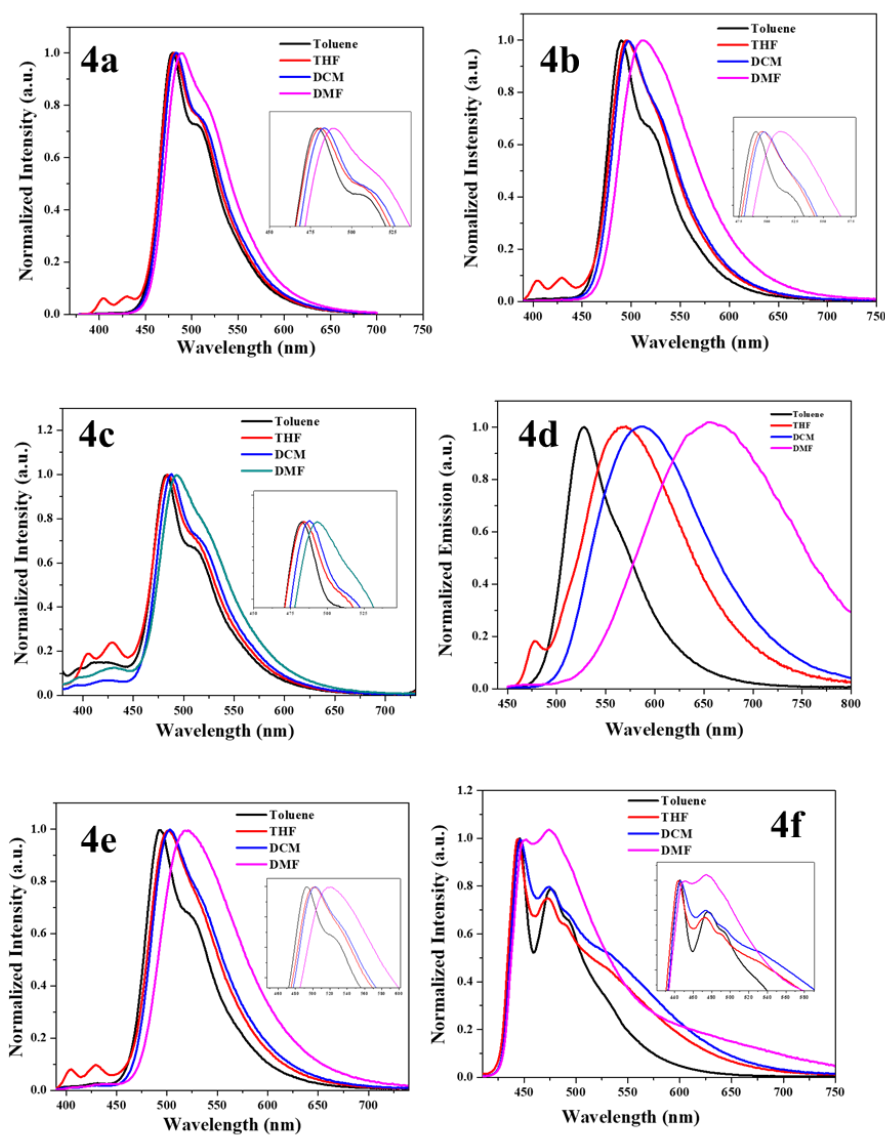


Figure 3.3. Emission spectra of aryl-substituted phenothiazines **4a–4f** in different solvents.

The absorption maxima of the fluorophores **4a–4f** are not heavily dependent on the solvent polarity. This finding is explained by the low polar ground state of phenothiazines.⁴⁸ On the other hand, the emission spectra of the fluorophores **4a–4e** are dependent on the solvent polarity. The increase in the solvent polarity resulted in the bathochromic spectral shift of the emission (Table 3.2). In particular, the fluorophore **4d** is greatly influenced by the solvent polarity as compared to the other fluorophores. The emission maxima of **4d** was observed

at 528 nm in toluene and at 657 nm in DMF, where the Stokes shift value reaches the highest value of 7350 cm⁻¹. This result suggests that fluorophore **4d** has a much larger dipole moment in the excited state with respect to the ground state. The fluorosolvatochromic effect on the fluorophores **4a–4e** is less important but again leads to higher Stokes shift in more polar solvents. The pyrene substituted fluorophore **4f** do not show solvent dependency of both the absorption and emission spectra which suggests lower dipole moments in both the ground and excited states.^{48–50}

Table 3.2. Solvent dependent studies of phenothiazines **4a–4f** in different solvents.

| Phenothiazines | Solvent | λ_{abs} (nm) | λ_{em} (nm) | Stokes Shift $\Delta\nu$ (cm ⁻¹) |
|----------------|---------|--------------------------------|-------------------------------|--|
| 4a | Toluene | 380 | 479 | 5440 |
| | THF | 371 | 480 | 6120 |
| | DCM | 374 | 483 | 6035 |
| | DMF | 377 | 489 | 6075 |
| 4b | Toluene | 381 | 490 | 5840 |
| | THF | 383 | 495 | 5910 |
| | DCM | 385 | 497 | 5850 |
| | DMF | 389 | 512 | 6180 |
| 4c | Toluene | 369 | 482 | 6355 |
| | THF | 367 | 484 | 6590 |
| | DCM | 368 | 487 | 6640 |
| | DMF | 369 | 493 | 6820 |
| 4d | Toluene | 439 | 528 | 3840 |
| | THF | 439 | 568 | 5173 |
| | DCM | 440 | 589 | 5750 |
| | DMF | 443 | 657 | 7350 |
| 4e | Toluene | 382 | 492 | 5850 |
| | THF | 383 | 501 | 6150 |
| | DCM | 388 | 502 | 5853 |
| | DMF | 393 | 520 | 6215 |
| 4f | Toluene | 406 | 446 | 2210 |
| | | | 476 | |
| | THF | 403 | 443 | 2240 |
| | | | 473 | |
| | DCM | 404 | 446 | 2330 |
| 474 | | | | |
| DMF | 405 | 450 | 2450 | |
| | | | 474 | |

Solid-State Emission: The solid-state emission spectra for the phenothiazines **4a–4f** were recorded at room temperature (Figure 3.4) and all the phenothiazines **4a–4f** were found to be emissive in the solid-state. The emission maxima of the fluorophores were observed at 482, 497, 479, 594, 542 and 530 nm for **4a**, **4b**, **4c**, **4d**, **4e** and **4f**, respectively.

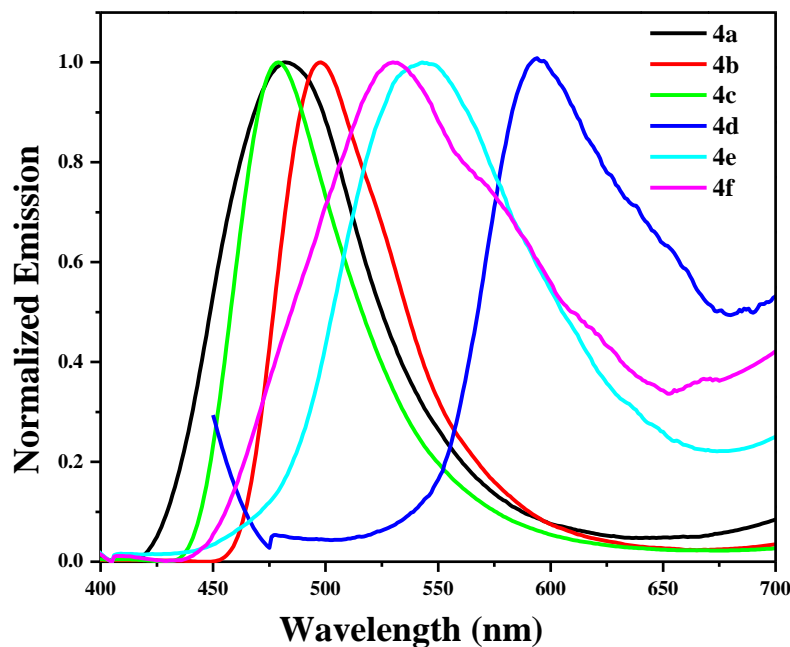


Figure 3.4. Solid-state emission spectra of aryl-substituted phenothiazine **4a–4f**.

The spectral data revealed that the benzene and naphthalene substituted phenothiazines **4a–4c** do not show any significant difference in the solid-state emission as compared to that of the solution phase (in dichloromethane). On the other hand, phenothiazines **4d–4f** show red-shifted emission maxima in solid-state relatively to their behavior in solution, which could be attributed to important π - π stacking interactions of the molecules in the solid-state. Notably, the pyrene substituted fluorophore **4f** shows highly red-shifted emission maxima (84 nm) in solid-state as compared to the solution, which may be due to the formation of characteristic pyrene excimers in the solid-state resulting from the extensive π - π stacking of the planar pyrene rings.^{48–50}

3.4. Electrochemical Properties

The electrochemical properties of aryl-substituted phenothiazines **4a–4f** were explored by cyclic voltammetry (CV) and differential pulse voltammetry (DPV) in dry dichloromethane (DCM) solution at room temperature using tri-*tert*-butylphosphonium tetrafluoroborate as a supporting electrolyte. The electrochemical data are compiled in Table 3.1, and the representative cyclic voltammograms are shown in Figure 3.5.

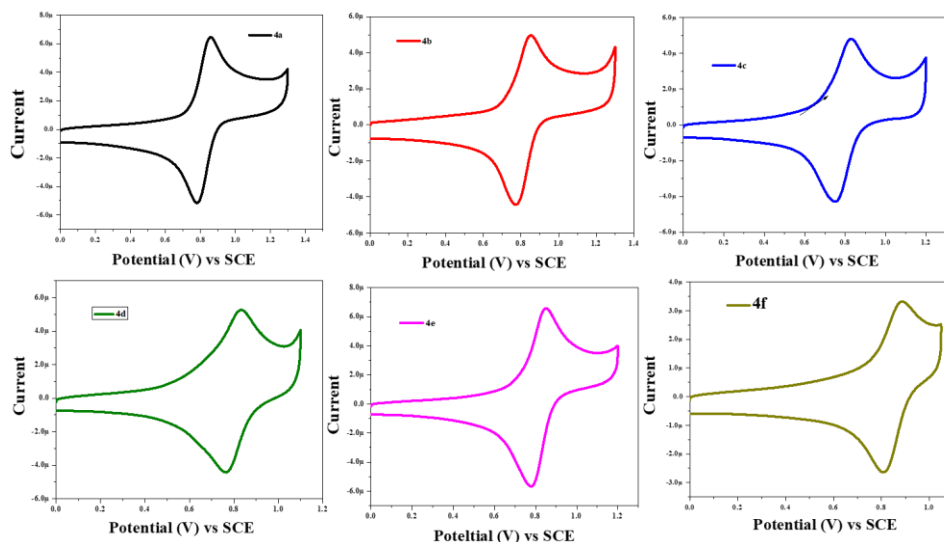


Figure 3.5. Cyclic voltammograms of phenothiazines **4a–4f** 0.01 M concentration in 0.1 M tri-*tert*-butylphosphonium tetrafluoroborate in dichloromethane recorded at a scan rate of 100 mV s^{-1} .

The electrochemical studies of the phenothiazine **4a–4f** conjugates exhibit reversible one electron oxidation wave due to the phenothiazinyl moiety, at about +0.80 V for all investigated molecules. The results of the electrochemical experiments thus agree with the observation of the phenothiazine radical cation during the femtosecond spectroscopic investigation.

3.5. Theoretical Calculations

The density functional theory calculations were performed to explore the geometrical structure and electronic properties of the phenothiazines **4a–4f** at

B3LYP/6-31+G** level for C, H, O, N and S.⁵¹ The energy diagram of the phenothiazines **4a–4f** are shown in Figure 3.6. The incorporation of anthracene, phenanthrene and pyrene in the phenothiazine core results in much stabilized LUMO energy levels leading to red-shifted absorption spectra.

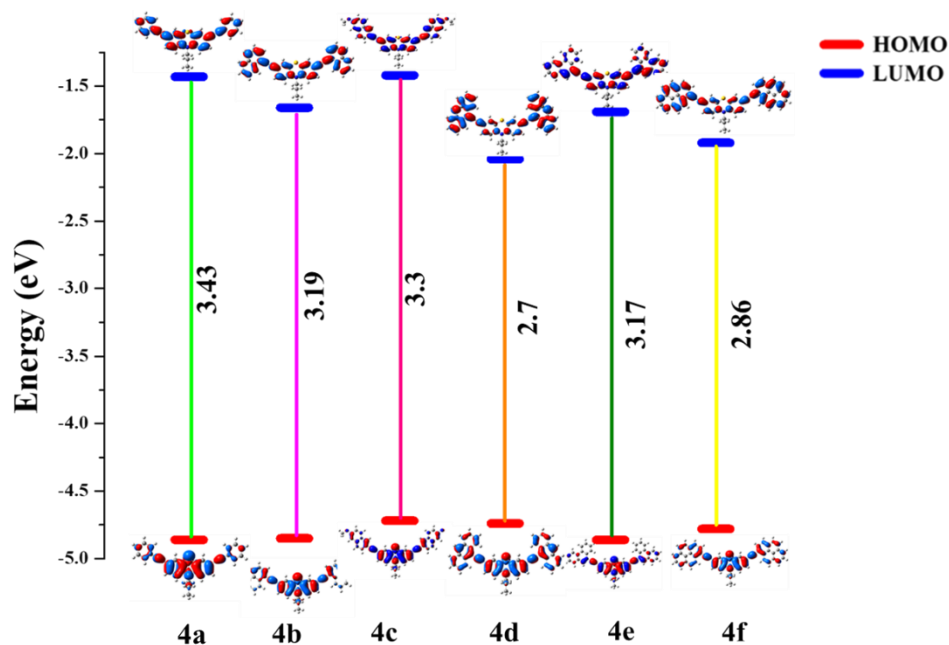


Figure 3.6. Energy diagram showing the HOMO and LUMO wave functions and energies of phenothiazines **4a–4f** as determined at B3LYP/6-31G** level.

The HOMOs of the phenothiazines **4a–4c** and **4e** are mainly localized on the phenothiazine moiety whereas the LUMOs are equally distributed both on the phenothiazine and the substituted benzene, naphthalene, methoxy-naphthalene and phenanthrene moieties. On the other hand, the anthracene and pyrene substituted phenothiazine **4d** and **4f** show comparatively much lower HOMO–LUMO energy gaps. The data show that the HOMOs are localized on the phenothiazine moiety but also partially situated on the lateral anthracene and pyrene for **4d** and **4f**, respectively. The LUMO is mainly distributed on the anthracene moiety for **4d** whereas for **4f** it is localized on the pyrene moiety. This indicates that the presence of anthracene and pyrene moieties in phenothiazine **4d** and **4f** lead to better electronic communication. This finding is in line with the

photoinduced electronic charge displacement from the phenothiazine to the lateral anthracenes speculated for **4d** from the ultrafast spectroscopic results.

Table 3.3. Calculated electronic transitions for phenothiazines **4a–4f** in dichloromethane

| Compounds | Wavelength (nm) | Composition | f^a | Assignment |
|-----------|--------------------|-----------------------|-------|-----------------|
| 4a | 363 | HOMO→LUMO (0.65) | 1.01 | π - π^* |
| | 289 | HOMO→LUMO+2 (0.61) | 0.75 | π - π^* |
| 4b | 376 | HOMO→LUMO (0.61) | 1.43 | π - π^* |
| | 306 | HOMO-2→LUMO (0.37) | 0.80 | π - π^* |
| 4c | 370 | HOMO→LUMO (0.62) | 1.42 | π - π^* |
| | 315 | HOMO→LUMO+1 (0.50) | 1.03 | π - π^* |
| 4d | 431 | HOMO→LUMO (0.56) | 1.45 | ICT |
| | 295 | HOMO→LUMO+6 (0.39) | 0.06 | π - π^* |
| 4e | 378 | HOMO→LUMO (0.60) | 1.70 | π - π^* |
| | 307 | HOMO-2→LUMO (0.38) | 1.03 | π - π^* |
| 4f | 405 | HOMO→LUMO (0.57) | 2.67 | π - π^* |
| | 291 | HOMO→LUMO+7 (0.47) | 0.08 | π - π^* |

f^a oscillator strength

TD-DFT calculations were performed for the phenothiazines **4a–4f** by using CAM-B3LYP/6-311G(d,p) basis set in dichloromethane. The transitions, with their composition, oscillator strength and assignment, are shown in Table 3.3. The TD-DFT calculations of the six phenothiazines **4a–4f** reveal two absorption bands, one at shorter wavelengths in the 290–315 nm region with lower oscillator strength values, and another at longer wavelengths in the 360–430 nm region with higher oscillator strengths. The data show that the transitions at longer wavelengths characterized by the largest oscillator strengths are mainly described by a HOMO→LUMO configuration for all the phenothiazines **4a–4f**. The theoretically calculated optical wavelengths of phenothiazines **4a–4f** are in

accordance with the experimental values. However, the calculated theoretical energies are slightly lower than the experimental ones, which may be due the effect of solvents, dipole moments, and temperature. The absorption spectra of phenothiazine **4d** calculated from TD-DFT shown in Figure 3.7.

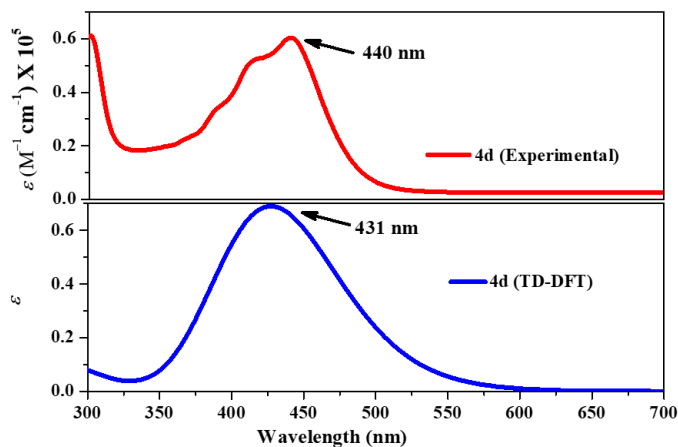


Figure 3.7. Theoretical absorption spectra of phenothiazine **4d**.

3.6. Experimental Section

General Methods. Chemicals were used as received unless otherwise indicated. All the oxygen or moisture sensitive reactions were carried out under argon atmosphere. ^1H NMR spectra were recorded using a 400 MHz spectrometer. Chemical shifts are reported in delta (δ) units, expressed in parts per million (ppm) downfield from tetramethylsilane (TMS) using residual protonated solvent as an internal standard $\{\text{CDCl}_3, 7.26 \text{ ppm}\}$. ^{13}C NMR spectra were recorded using a 400 MHz spectrometer. Chemical shifts are reported in delta (δ) units, expressed in parts per million (ppm) downfield from tetramethylsilane (TMS) using the solvent as internal standard $\{\text{CDCl}_3, 77.0 \text{ ppm}\}$. The ^1H NMR splitting patterns have been described as “s, singlet; d, doublet; t, triplet and m, multiplet”. UV/Vis spectrum of all compounds were recorded in dichloromethane solution. Cyclic voltammograms were recorded on electrochemical analyzer using Glassy carbon as working electrode, Pt wire as the counter electrode, and Saturated Calomel Electrode (SCE) as the reference electrode. The scan rate was 100mVs^{-1} for

Cyclic Voltammetry. A solution of tri-*tert*-butylphosphonium tetrafluoroborate in CH₂Cl₂ (0.1M) was used as supporting electrolyte.

General Procedure

3,7-Dibromo-10-propyl-10*H*-phenothiazine **3** (100 mg, 0.25 mmol), corresponding alkynes (0.55 mmol), PdCl₂(PPh₃)₂ (8.8 mg, 5 mol%), CuI (2.4 mg, 5 mol%) were dissolved in a mixture of dry THF (20 mL) and triethylamine (5 mL) under an argon atmosphere. The reaction mixture was stirred at 60 °C for 12 h. Following cooling to room temperature, the solvent was removed under reduced pressure, and the residue was purified by column chromatography on silica gel in a 4:1 mixture of hexane/ CH₂Cl₂ to get phenothiazines **4a–4f**.

Phenothiazine **4a**. Yellow colored solid. Yield: 80 mg (72%); ¹H NMR (400 MHz, CDCl₃): δ = 7.4961 (d, *J* = 6.28, 5H), 7.3384-7.2895 (m, 9H), 6.7886 (d, *J* = 7.28, 2H), 3.8196 (s, 2H), 1.8608-1.8075 (m, 2H), 1.0247 (t, *J* = 7.28, 3H); ¹³C NMR (100 MHz, CDCl₃): δ = 144.6, 131.4, 130.8, 130.2, 128.3, 128.1, 124.1, 123.3, 117.4, 115.1, 88.4, 88.7, 49.4, 20.0, 11.2; HRMS (ESI-TOF): *m/z* calculated for C₃₁H₂₃NS = 441.1630 [M]⁺, measured 441.1546 [M]⁺

Phenothiazine **4b**. Bright yellow colored solid. Yield: 105 mg (77%); ¹H NMR (400 MHz, CDCl₃): δ = 8.40 (d, *J* = 8.28, 2H), 7.87-7.82 (m, 4H), 7.73 (d, *J* = 7.04, 2H), 7.61-7.58 (m, 2H), 7.53 (t, *J* = 7.76, 2H), 7.47-7.40 (m, 6H), 6.85 (t, *J* = 8.28, 2H), 3.86 (t, *J* = 7.04, 2H), 1.92-1.83 (m, 2H), 1.05 (t, *J* = 7.24, 3H); ¹³C NMR (100 MHz, CDCl₃): δ = 144.7, 133.2, 130.9, 130.1, 128.6, 128.3, 126.7, 126.4, 126.2, 125.3, 124.2, 120.9, 117.6, 93.6, 87.6, 49.5, 20.1, 11.2; HRMS (ESI-TOF): *m/z* calculated for C₃₉H₂₇NS = 541.1857 [M]⁺, measured 541.1859 [M]⁺.

Phenothiazine **4c**. Pale yellow colored solid. Yield: 99 mg (65%); ¹H NMR (400 MHz, CDCl₃): δ = 8.0 (s, 1H), 7.94 (s, 2H), 7.69 (t, *J* = 8.8, 4H), 7.51 (d, *J* = 8.28, 2H), 7.34-7.30 (m, 3H), 7.17-7.11 (m, 4H), 6.80 (d, *J* = 8.28, 2H), 3.93 (s, 6H), 3.83 (s, 2H), 1.87-1.80 (m, 2H), 1.03 (t, *J* = 7.28, 3H); ¹³C NMR (100 MHz,

CDCl₃): δ = 158.3, 144.7, 143.8, 134.0, 131.0, 130.9, 130.2, 129.9, 129.6, 129.3, 128.9, 128.5, 126.8, 126.5, 124.1, 119.4, 118.2, 117.6, 116.6, 115.2, 114.8, 105.8, 90.0, 88.3, 55.3, 49.4, 19.9, 11.2; HRMS (ESI-TOF): m/z calculated for C₃₁H₂₃NO₂S= 602.2116 [M+H]⁺, measured 602.2146 [M+H]⁺.

Phenothiazine **4d**. Red colored solid. Yield: 117 mg (72%); ¹H NMR (400 MHz, CDCl₃): δ = 8.63 (d, J = 8.76, 4H), 8.43 (s, 2H), 8.02 (d, J = 8.28, 4H), 7.62-7.50 (m, 12H), 6.92 (d, J = 8.28, 4H), 3.92 (t, J = 7.04, 2H), 1.96-1.87 (m, 2H), 1.09 (t, J = 7.24, 3H); ¹³C NMR (100 MHz, CDCl₃): δ = 144.8, 132.5, 131.2, 130.9, 130.2, 128.7, 127.5, 126.8, 126.5, 125.8, 124.3, 117.8, 117.4, 115.4, 100.1, 86.5, 49.5, 20.1, 11.3; HRMS (ESI-TOF): m/z calculated for C₄₇H₃₁NS= 641.2173 [M]⁺, measured 641.2172 [M]⁺.

Phenothiazine **4e**. Yellowish orange colored solid. Yield: 120 mg (74%); ¹H NMR (400 MHz, CDCl₃): δ = 8.72-8.65 (m, 4H), 8.53-8.51 (m, 2H), 8.06, (s, 2H), 7.87 (d, J = 7.28, 2H), 7.72-7.59 (m, 8H), 7.48-7.44 (m, 4H), 6.85 (d, J = 8.28, 2H), 3.87 (t, J = 7.04, 2H), 1.93-1.84 (m, 2H), 1.06 (t, J = 7.28, 3H); ¹³C NMR (100 MHz, CDCl₃): δ = 144.7, 131.5, 131.3, 131.1, 130.9, 130.2, 130.1, 130.0, 128.5, 127.3, 127.0, 126.9, 124.2, 122.7, 122.6, 119.7, 117.5, 115.2, 93.3, 87.7, 49.4, 20.0, 11.2; HRMS (ESI-TOF): m/z calculated for C₄₇H₃₁NS= 642.2248 [M+H]⁺, measured 642.2250 [M+H]⁺.

Phenothiazine **4f**. Dark yellow colored solid. Yield: 120 mg (69%); ¹H NMR (400 MHz, CDCl₃): δ = 8.89 (d, J = 9.28, 1H), 8.70 (d, J = 9.04, 1H), 8.62 (d, J = 9.04, 1H), 8.40 (d, J = 7.76, 1H), 8.27-8.00 (m, 16H), 7.49-7.44 (m, 2H), 7.23 (s, 1H), 6.85 (d, J = 8.28, 1H), 6.70 (d, J = 8.28, 1H), 3.80 (t, J = 7.04, 2H), 1.87-1.78 (m, 2H), 1.02 (t, J = 7.28, 3H); ¹³C NMR (100 MHz, CDCl₃): δ = 144.9, 143.8, 131.9, 131.7, 131.3, 131.2, 131.1, 131.0, 130.5, 130.2, 129.9, 129.8, 129.7, 129.4, 128.8, 128.7, 128.5, 128.2, 128.1, 128.0, 127.3, 127.1, 126.5, 126.4, 126.2, 126.1, 125.9, 125.8, 125.7, 125.6, 125.5, 125.4, 124.6, 124.5, 124.3, 124.1, 118.1, 117.9, 117.6, 116.6, 115.3, 114.8, 94.4, 88.8, 49.4, 19.9, 11.2; HRMS (ESI-TOF): m/z calculated for C₅₁H₃₁NS= 689.2172 [M]⁺, measured 689.1940 [M]⁺.

3.7. Conclusions

A series of aryl substituted phenothiazines were synthesized *via* Pd-catalyzed Sonogashira cross-coupling reactions. The fluorescence study of the phenothiazines shows that all of them are highly emissive with remarkable quantum yields. The investigated molecules exhibit large Stokes shift values in solution, with the anthracene functionalized phenothiazine featuring strong positive fluorosolvatochromism and thus the largest Stokes shift in polar solvents (7350 cm⁻¹ in DMF). These fluorescent compounds are also highly emissive in the solid-state where the phenothiazine substituted with the largest aryl groups show marked red shifts of the emission maxima as compared to the solution, indicating considerable π - π stacking interactions. In particular, the anthracene substituted phenothiazine exhibits strongly redshifted absorption and emission wavelengths both in solid-state and in solution which implies pronounced electronic communication in this fluorophore. This finding agrees with the charge displacement predicted by the TD-DFT calculations as well as with the results of the cyclic voltammetry measurements. This work provides an outstanding strategy to synthesize organic fluorophores with high quantum yields and large Stokes shifts which are all excellent prerequisites for their possible use as promising fluorescent probes in bioimaging.

3.8. References

1. Wasielewski, M. R. (2009), Self-assembly strategies for integrating light harvesting and charge separation in artificial photosynthetic systems, *Acc. Chem. Res.*, 42, 1910–1921 (DOI: 10.1021/ar9001735).
2. Wasielewski, M. R. (1992), Photoinduced electron transfer in supramolecular systems for artificial photosynthesis, *Chem. Rev.*, 92, 435–461 (DOI: 10.1021/cr00011a005).
3. Gust, D., Moore, T. A., Moore, A. L. (1993), Molecular mimicry of photosynthetic energy and electron transfer, *Acc. Chem. Res.*, 26, 198–205 (DOI: 10.1021/ar00028a010).

4. Wang, C., Li, X., Pan, Y., Zhang, S. (2016), Highly efficient non-doped green organic light-emitting diodes with combination of high photoluminescence and high exciton utilization, *ACS Appl Mater Interfaces*, 8, 3041–3049 (DOI: 10.1021/acsami.5b10129).
5. Lin, Y., Li, Y., Zhan, X., (2012), Small molecule semiconductors for high-efficiency organic photovoltaics, *Chem. Soc. Rev.*, 41, 4245–4272 (DOI: 10.1039/C2CS15313K).
6. Chen, C.-T. (2004), Evolution of Red Organic Light-Emitting Diodes: Materials and Devices, *Chem. Mater*, 16, 4389–4400 (DOI: 10.1021/cm049679m).
7. Bures, F., Schweizer, W. B., May, J. C., Boudon, C., Gisselbrecht, J.-P., Gross, M., Biaggio, I., Diederich, F. (2007), Property Tuning in Charge-Transfer Chromophores by Systematic Modulation of the Spacer between Donor and Acceptor, *Chem.–Eur. J.*, 13, 5378–5387 (DOI: 10.1002/chem.200601735).
8. Blanco, G. D., Hiltunen, A. J., Lim, G. N., KC, C. B., Kaunisto, K. M., Vuorinen, T. K., Nesterov, V. N., Lemmetyinen, H. J., D’Souza, F. (2016), Syntheses, Charge Separation, and Inverted Bulk Heterojunction Solar Cell Application of Phenothiazine–Fullerene Dyads, *ACS Appl. Mater. Interfaces*, 8, 13, 8481–8490 (DOI: 10.1021/acsami.6b00561).
9. Daub, J., Engl, R., Kurzawa, J., Miller, S. E., Schneider, S., Stockmann, A., Wasielewski, M. R. (2001), Competition between Conformational Relaxation and Intramolecular Electron Transfer within Phenothiazine–Pyrene Dyads, *J. Phys. Chem. A*, 105, 23, 5655–5665 (DOI: 10.1021/jp0037293).
10. Christensen, J.A., Phelan, B. T., Chaudhuri, S., Acharya, A., Batista, V. S., Wasielewski, M. R. (2018), Phenothiazine Radical Cation Excited States as Super-oxidants for Energy-Demanding Reactions, *J. Am. Chem. Soc.*, 140, 15, 5290–5299 (DOI: 10.1021/jacs.8b01778).

11. Tang, G., Sukhanov, A. A., Zhao, J., Yang, W., Wang, Z., Liu, Q., Voronkova, V. K., Donato, M. D., Escudero, D., Jacquemin, D. (2019), Red Thermally Activated Delayed Fluorescence and the Intersystem Crossing Mechanisms in Compact Naphthalimide–Phenothiazine Electron Donor/Acceptor Dyads, *J. Phys. Chem. C*, 123, 30171–30186 (DOI: 10.1021/acs.jpcc.9b09335).
12. Okazaki, M., Takeda, Y., Data, P., Pander, P., Higginbotham, H., Monkman, A. P., Minakata, S. (2017), Thermally Activated Delayed Fluorescent Phenothiazine–dibenzo[a,j] phenazine–Phenothiazine Triads Exhibiting Tricolor Changing Mechanochromic Luminescence, *Chem. Sci.*, 8, 2677–2686 (DOI: 10.1039/C6SC04863C).
13. Aizawa, N., Tsou, C.-J., Park, I. S., Yasuda, T. (2017), Aggregation-induced delayed fluorescence from phenothiazine-containing donor–acceptor molecules for high-efficiency non-doped organic light-emitting diodes, *Polymer Journal*, 49, 197–202 (DOI: 10.1038/pj.2016.82).
14. Dias, F. B., Santos, J., Graves, D. R., Data, P., Nobuyasu, R. S., Fox, M. A., Batsanov, A. S., Palmeira, T., Berberan-Santos, M. N., Bryce, M. R., Monkman, A. P. (2016), The Role of Local Triplet Excited States and D-A Relative Orientation in Thermally Activated Delayed Fluorescence: Photophysics and Devices, *Adv. Sci.*, 3, 1600080, 1–10 (DOI: 10.1002/advs.201600080).
15. Marghad, I., Bencheikh, F., Wang, C., Manolikakes, S., Rérat, A., Gosmini, C., Kim, D. h., Ribierre, J.-C., Adachi, C. (2019), Control of the dual emission from a thermally activated delayed fluorescence emitter containing phenothiazine units in organic light-emitting diodes, *RSC Adv.*, 9, 4336–4343 (DOI: 10.1039/C8RA10393C).
16. Horváth, P., Šebej, P., Šolomek, T., Klán, P. (2015), Small-Molecule Fluorophores with Large Stokes Shifts: 9-Iminopyronin Analogues as Clickable Tags, *J. Org. Chem.*, 80, 1299–1311 (DOI: 10.1021/jo502213t).

17. Gao, Z., Hao, Y., Zheng, M., Chen, Y. (2017), A fluorescent dye with large Stokes shift and high stability: synthesis and application to live cell imaging, *RSC Adv.*, 7, 7604–7609 (DOI: 10.1039/C6RA27547H).
18. Zhou, L., Wang, Q., Tan, Y., Lang, M. J., Sun, H., Liu, X. (2017), Rational Development of Near-Infrared Fluorophores with Large Stokes Shifts, Bright One-Photon, and Two-Photon Emissions for Bioimaging and Biosensing Applications, *Chem.–Eur. J.*, 23, 8736–8740 (DOI: 10.1002/chem.201701365).
19. Nienhaus, K., Nienhaus, U. (2014), Fluorescent proteins for live-cell imaging with super-resolution, *Chem. Soc. Rev.*, 43, 1088–1106 (DOI: 10.1039/C3CS60171D).
20. Wang, F., Tan, W. B., Zhang, Y., Fan, X. P., Wang, M. Q. (2006), Luminescent nanomaterials for biological labelling, *Nanotechnology*, 17, R1 (DOI: 10.1088/0957-4484/17/1/R01).
21. Zems, Y., Moiseev, A. G., Perepichka, D. F. (2013), Convenient synthesis of a highly soluble and stable phosphorescent platinum porphyrin dye, *Org. Lett.*, 15, 5330–5333 (DOI: 10.1021/ol402590c).
22. Shcherbakova, D. M., Hink, M. A., Joosen, L., Gadella, T. W. J., Verkhusha, V. V. (2012), An Orange Fluorescent Protein with a Large Stokes Shift for Single-Excitation Multicolor FCCS and FRET Imaging, *J. Am. Chem. Soc.*, 134, 7913–7923 (DOI: 10.1021/ja3018972).
23. Jia, K., Wan, Y., Xia, A., Li, S., Gong, F., Yang, G. (2007), Characterization of Photoinduced Isomerization and Intersystem Crossing of the Cyanine Dye Cy3, *J. Phys. Chem. A*, 111, 1593–1597 (DOI: 10.1021/jp067843i).
24. Jia, X., Han, W., Xue, T., Zhao, D., Li, X., Nie, J., Wang, T. (2019), Diphenyl sulfone-based A- π -D- π -A dyes as efficient initiators for one photon and two photon initiated polymerization, *Polymer. Chem.*, 10, 2152–2161 (DOI: 10.1039/C8PY01778F).
25. Hao, F., Liu, Z., Zhang, M., Liu, J., Zhang, S., Wu, J., Zhou, H., Tian, Y.P. (2014), Four new two photon polymerization initiators with varying

- donor and conjugated bridge: synthesis and two photon activity, *Spectrochimica Acta A*, 118, 538–542 (DOI: 10.1016/j.saa.2013.09.051).
26. Carlotti, B., Poddar, M., Elisei, F., Spalletti, A., Misra, R. (2019), Energy-Transfer and Charge-Transfer Dynamics in Highly Fluorescent Naphthalimide–BODIPY Dyads: Effect of BODIPY Orientation, *J. Phys. Chem. C*, 123, 40, 24362–24374 (DOI: 10.1021/acs.jpcc.9b05851).
27. Sailer, M., Franz, A. W., Müller, T. J. J. (2008), Synthesis and Electronic Properties of Monodisperse Oligophenothiazines, *Chem. Eur. J.*, 14, 2602–2614 (DOI: 10.1002/chem.200701341).
28. Hauck, M., Schönhaber, J., Zuccherò, A. J., Hardcastle, K. I., Müller, T. J. J., Bunz, U. H. F. (2007), Phenothiazine Cruciforms: Synthesis and Metallochromic Properties, *J. Org. Chem.*, 72, 6714–6725 (DOI: 10.1021/jo0709221).
29. Franz, A. W., Rominger, F., Müller, T. J. J. (2008), Synthesis and Electronic Properties of Sterically Demanding N-Arylphenothiazines and Unexpected Buchwald-Hartwig Aminations, *J. Org. Chem.*, 73, 1795–1802 (DOI: 10.1021/jo702389v).
30. Krämer, C. S., Müller, T. J. J. (2003), Synthesis and Electronic Properties of Alkynylated Phenothiazines, *Eur. J. Org. Chem.*, 3534–3548 (DOI: 10.1002/ejoc.200300250).
31. Krämer, C. S., Zeitler, K., Müller, T. J. J. (2000), Synthesis of Functionalized Ethynylphenothiazine Fluorophores, *Org. Lett.*, 2, 3723–3726 (DOI: 10.1021/ol0066328).
32. Beppu, T., Tomiguchi, K., Masuhara, A., Pu, Y.-J., Katagiri, H. (2015), Single Benzene Green Fluorophore: Solid-State Emissive, WaterSoluble, and Solvent- and pH-Independent Fluorescence with Large Stokes Shifts, *Angew. Chem., Int. Ed.*, 54, 7332–7335 (DOI: 10.1002/anie.201502365).
33. Huang, R., Liu, B., Wang, C., Wang, Y., Zhang, H. Constructing Full-Color Highly Emissive Organic Solids Based on an X-Shaped Tetrasubstituted Benzene Skeleton, *J. Phys. Chem. C* **2018**, 122, 10510–10518 (DOI: 10.1021/acs.jpcc.8b01251).

34. Liu, B., Di, Q., Liu, W., Wang, C., Wang, Y., Zhang, H. (2019), Red-Emissive Organic Crystals of a Single-Benzene Molecule: Elastically Bendable and Flexible Optical Waveguide, *J. Phys. Chem. Lett.*, 10, 1437–1442 (DOI: 10.1021/acs.jpcllett.9b00196).
35. Pigot, C., Noirbent, G., Bui, T.-T., Péralta, S., Gigmes, D., Nechab, M., Dumur, F. (2019), Push-Pull Chromophores Based on the Naphthalene Scaffold: Potential Candidates for Optoelectronic Applications, *Materials*, 12, 1342 (DOI: 10.3390/ma12081342).
36. Lin, R. Y.-Y., Chuang, T.-M., Wu, F.-L., Chen, P.-Y., Chu, T.-C., Ni, J.-S., Fan, M.-S., Lo, Y.-H., Ho, K.-C., Lin, J. T. (2015), Anthracene/Phenothiazine π -Conjugated Sensitizers for Dye-Sensitized Solar Cells using Redox Mediator in Organic and Water-based Solvents, *ChemSusChem*, 8, 105–113 (DOI: 10.1002/cssc.201403016).
37. Li, X., Yang, L., Zhao, L., Wang, X.-L., Shao, K.-Z., Su, Z.-M. (2016), Luminescent Metal–Organic Frameworks with Anthracene Chromophores: Small-Molecule Sensing and Highly Selective Sensing for Nitro Explosives, *Cryst. Growth Des.*, 16, 4374–4382 (DOI: 10.1021/acs.cgd.6b00482).
38. Gray, V., Dzebo, D., Lundin, A., Alborzpour, J., Abrahamsson, M., Albinsson, B., Moth-Poulsen, K. (2015), Photophysical characterization of the 9,10-disubstituted anthracene chromophore and its applications in triplet–triplet annihilation photon upconversion, *J. Mater. Chem. C*, 3, 11111–11121 (DOI: 10.1039/C5TC02626A).
39. Wang, B., Qiao, X., Yang, Z., Wang, Y., Liu(Frank), S., Ma, D., Wang, Q. (2018), Realizing efficient red thermally activated delayed fluorescence organic light-emitting diodes using phenoxazine/phenothiazine-phenanthrene hybrids, *Organic Electronics*, 59, 32–38 (DOI: 10.1016/j.orgel.2018.04.045).
40. Thomas, K. R. J., Kapoor, N., Bolisetty, M. N. K. P., Jou, J.-H., Chen, Y.-L., Jou, Y.-C. (2012), Pyrene-Fluorene Hybrids Containing Acetylene

- Linkage as Color-Tunable Emitting Materials for Organic Light-Emitting Diodes, *J. Org. Chem.*, 77, 3921–3932 (DOI: 10.1021/jo300285v).
41. Bains, G. K., Kim, S. H., Sorin, E. J., Narayanaswami, V. (2012), The Extent of Pyrene Excimer Fluorescence Emission Is a Reflector of Distance and Flexibility: Analysis of the Segment Linking the LDL Receptor-Binding and Tetramerization Domains of Apolipoprotein E3, *Biochemistry*, 51, 6207–6219 (DOI: 10.1021/bi3005285).
 42. Poddar, M., Gautam, P.; Rout, Y.; Misra, R. Donor–acceptor phenothiazine functionalized BODIPYs. *Dyes and Pigments* **2017**, 146, 368–373.
 43. Poddar, M.; Misra, R. (2017), NIR-Absorbing Donor–Acceptor Based 1,1,4,4-Tetracyanobuta-1,3-Diene (TCBD)- and Cyclohexa-2,5-Diene-1,4-Ylidene-Expanded TCBD-Substituted Ferrocenyl Phenothiazines, *Chem. Asian J.*, 12, 2908–2915 (DOI: 10.1002/asia.201700879).
 44. Rout, Y., Gautam, P., Misra, R. (2017), Unsymmetrical and Symmetrical Push–Pull Phenothiazines, *J. Org. Chem.*, 82, 6840–6845 (DOI: 10.1021/acs.joc.7b00991).
 45. Khan, F., Ekbote, A., Misra, R. (2019), Reversible mechanochromism and aggregation induced enhanced emission in phenothiazine substituted tetraphenylethylene, *New J. Chem.*, 43, 16156–16163 (DOI: 10.1039/C9NJ03290H).
 46. Ekbote, A., Mobin, S. M., Misra, R. (2020), Stimuli-responsive phenothiazine-based donor–acceptor isomers: AIE, mechanochromism and polymorphism, *J. Mater. Chem. C*, 8, 3589–3602 DOI: 10.1039/C9TC05192A (DOI: 10.1039/C9TC05192A).
 47. Doskocz, J., Soloducho, J., Cabaj, J., Lapkowski, M., Golba, S., Palewska, K. (2007), Development in Synthesis, Electrochemistry, LB Moieties of Phenothiazine Based Units, *Electroanalysis*, 19, 1394–1401 (DOI: 10.1002/elan.200703866).
 48. Lakowicz, J. R. (2007), Principles of Fluorescence Spectroscopy, Springer Science & Business Media, 3rd Edition,.

49. Lehrer, S. S. (1995), Pyrene excimer fluorescence as a probe of protein conformational change, *Subcell. Biochem.*, 24, 115–132 (DOI: 10.1007/978-1-4899-1727-0_5).
50. Birks, J. B. (1970), Photophysics of aromatic molecules, *New York: Wiley-Interscience, London.*
51. Frisch M. J., Trucks G. W., Schlegel H. B., Scuseria G. E., Robb M. A., Cheeseman J. R., Scalmani G., Barone V., Mennucci B., Petersson G. A., Nakatsuji H., Caricato M., Li X., Hratchian H. P., Izmaylov A. F., Bloino J., Zheng G., Sonnenberg J. L., Hada M., Ehara M., Toyota K., Fukuda R., Hasegawa J., Ishida M. Nakajima T., Honda Y., Kitao O., Nakai H., Vreven T., Montgomery J. A. Jr., Peralta J. E., Ogliaro F., Bearpark M., Heyd J. J., Brothers E., Kudin K. N., Staroverov V. N., Kobayashi R., Normand J., Raghavachari K., Rendell A., Burant J. C., Iyengar S. S., Tomasi J., Cossi M., Rega N., Millam N. J., Klene M., Knox J. E., Cross J. B., Bakken V., Adamo C., Jaramillo J., Gomperts R., Stratmann R. E., Yazyev O., Austin A. J., Cammi R., Pomelli C.; Ochterski J. W., Martin R. L., Morokuma K., Zakrzewski V. G., Voth G. A., Salvador P., Dannenberg J. J., Dapprich S., Daniels A. D., Farkas O., Foresman J. B., Ortiz J. V., Cioslowski J., Fox D. J. (2009), *Gaussian 09, revision A.02; Gaussian, Inc.:Wallingford, CT.*

Chapter 4

Design and Synthesis of Donor–Acceptor Based Ferrocene Substituted Phenothiazines: Tuning of HOMO–LUMO gap

4.1. Introduction

π -Conjugated molecular systems containing sulfur (S) and nitrogen (N) atoms are of significant interest for various optoelectronic applications.^[1] A wide variety of S and N based heterocyclic units such as thiazoles, benzothiazoles, benzothiadiazole, phenothiazines and many more have been explored for non-linear optics (NLO), organic light emitting diodes (OLEDs), organic photovoltaics (OPVs) and organic field-effect transistors (OFETs).^[2] The tuning of the photonic properties of these systems can be achieved by altering the strength of donor or acceptor units, and the connecting π -linker.^[3] Our group is interested in the design and synthesis of small molecule based heterocyclic π -conjugated molecular systems for organic photovoltaics.^[4]

The incorporation of heterocyclic moiety into the chromophore backbone leads to higher chemical and thermal robustness.^[5] Phenothiazines are interesting mainly because of their inherent folded conformation (folding angle of 158.58°). It can be transformed into a planar conformation by the substitution of different functionalities in the N position of the phenothiazine moiety.^[6] Phenothiazine allows variety of reactions including electrophilic substitution at the aromatic position, nucleophilic reaction at the N position, oxidation at the sulfur, *etc.*^[6c] In addition, phenothiazines possess low reversible oxidation potential which makes them suitable as electrophores in organic materials.^[7] The ferrocene is a strong electron donor and its derivatives play an important role in NLO, superconductor, magnetic, semiconductor, and redox catalyst materials.^[8] We were interested to incorporate cyano based 1,1,4,4-tetracyanobuta-1,3-diene (TCBD) and cyclohexa-2,5-diene-1,4-ylidene-expanded TCBD acceptors on the ferrocenyl phenothiazine derivatives to study the effect of the acceptors on photonic and electrochemical properties of ferrocenyl phenothiazine. Cyano-based acceptors

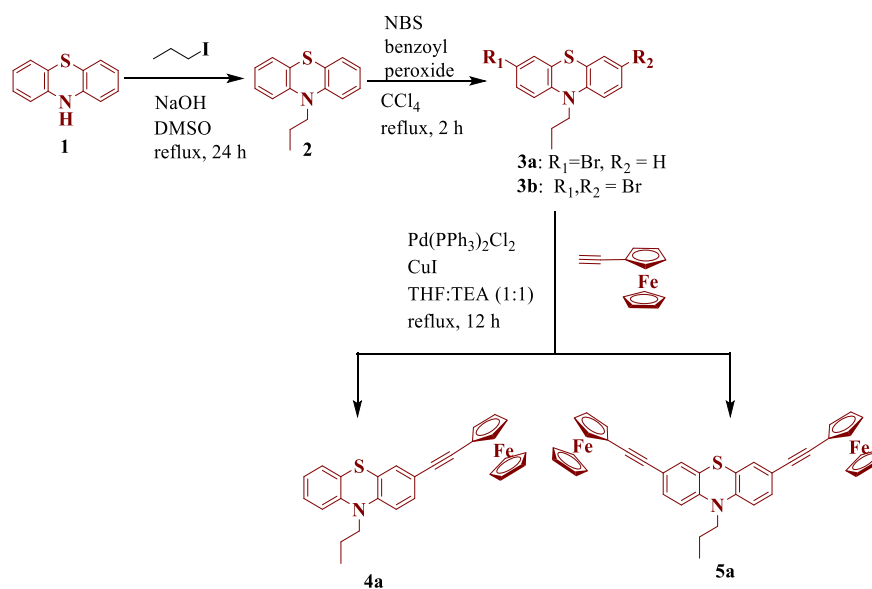
are one of the most powerful unit for the application in organic electronic devices.^[9] The [2+2] cycloadditions of tetracyanoethylene (TCNE) and 7,7,8,8-tetracyanoquinodimethane (TCNQ) with the electron rich alkynes followed by the electrocyclic ring-opening results in donor–acceptor type molecular systems.^[10, 11, 12] These cyano based acceptors have been used to form charge transfer (CT) complexes with a variety of electron-rich organic and organometallic compounds which exhibit a number of interesting properties such as electric conductivity.^[10] Diederich *et al.* are pioneer in the field of TCBD and cyclohexa–2,5–diene–1,4–ylidene–expanded TCBD chemistry and have studied a large variety of TCBD and cyclohexa–2,5–diene–1,4–ylidene–expanded TCBD derivatives.^[11, 12]

Michinobu *et al.* have extensively explored the TCBD and cyclohexa–2,5–diene–1,4–ylidene–expanded TCBD substituted polymers which are supposed to be promising materials for photovoltaic applications.^[13] Shoji *et al.* have reported donor–acceptor based TCBD and cyclohexa–2,5–diene–1,4–ylidene–expanded TCBD molecules as redox active ICT chromophores.^[14] Butenschoen *et al.* have reported a variety of 1,1´-disubstituted ferrocenyl TCBD derivatives.^[15] Nakamura and coworkers have studied carbazole and its TCBD derivatives.^[16] Our group has reported a vast variety of TCBD functionalized chromophores for organic electronics.^[4f, 17]

Herein we wish to report the design and synthesis of unsymmetrical and symmetrical TCBD and cyclohexa–2,5–diene–1,4–ylidene–expanded TCBD chromophores where phenothiazine and ferrocene are acting as strong donors. In this chapter our objective was to improve the photonic and electronic properties of ferrocene substituted phenothiazines by incorporating TCNE and TCNQ in between phenothiazine and ferrocene building blocks. We have further explored a comparative photophysical and electrochemical studies by varying the number of TCBD and cyclohexa–2,5–diene–1,4–ylidene–expanded TCBD acceptor as well as ferrocene donor on the phenothiazine moiety. Additionally, theoretical calculations were performed in order to study the conformation and the photonic properties of phenothiazines.

4.2. Results and Discussion

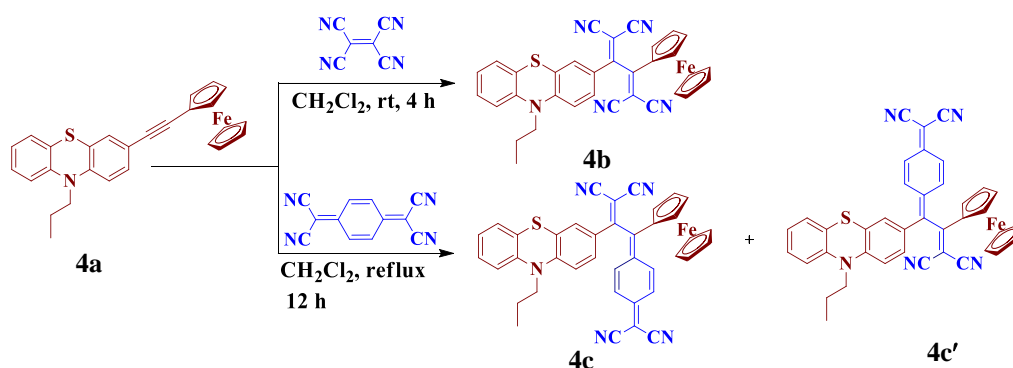
The TCBD and cyclohexa-2,5-diene-1,4-ylidene-expanded TCBD substituted ferrocenyl phenothiazines **4b**, **4c**, **4c'**, **5b**, **5c**, **5d**, **5d'**, **5e**, **5e'**, **5f** and **5f'** were designed and synthesized by the [2 + 2] cycloaddition–electrocyclic ring-opening reaction of ferrocenyl phenothiazines **4a** and **5a** with TCNE and TCNQ (Scheme 4.2, Scheme 4.3 and Scheme 4.4). The ferrocenyl phenothiazines **4a** and **5a** were synthesized by the Sonogashira cross-coupling reaction of 3-bromo-10-propylphenothiazine and 3,7-dibromo-10-propylphenothiazines with the ethynyl ferrocene.^[18] The Pd-catalyzed Sonogashira cross-coupling reaction of phenothiazines **3a** and **3b** with ethynyl ferrocene at 60 °C resulted ferrocenyl phenothiazines **4a** and **5a** in 50% and 51% yields respectively (Scheme 4.1).



Scheme 4.1. Synthetic route for ferrocenyl phenothiazines **4a** and **5a**.

In order to explore the effect of number of TCBD and cyclohexa-2,5-diene-1,4-ylidene-expanded TCBD acceptors on the ferrocenyl phenothiazines the mono-(**4b**, **4c**, **4c'**, **5b** and **5d**, **5d'**) and di-(**5c**, **5e**, **5e'**, **5f** and **5f'**) substituted ferrocenyl phenothiazines were synthesized. The precursors **4a** and **5a** undergo the [2 + 2] cycloaddition–electrocyclic ring-opening reaction with TCNE at room temperature within 4 hours in CH₂Cl₂ solvent, resulted TCBD functionalized

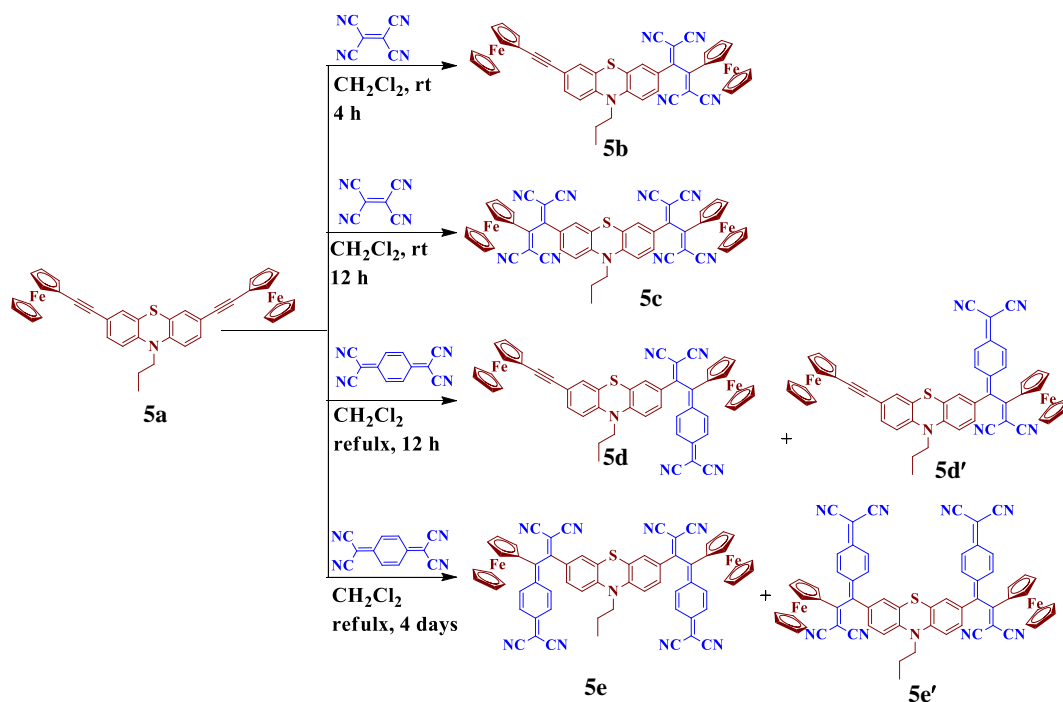
phenothiazines **4b** and **5b** in 83% and 85% yield, respectively (Scheme 4.2 and Scheme 4.3). The ferrocenyl phenothiazine **5a** undergoes a similar transformation by using excess amount of TCNE which resulted phenothiazine **5c** in 90% yield at 40 °C, for 12 hours in CH₂Cl₂ solvent. The derivatives of cyclohexa–2,5–diene–1,4–ylidene–expanded TCBDs were obtained as non-separable regioisomeric mixtures. The reaction of ferrocenyl phenothiazine **4a** with 1 equivalent of TCNQ at 40 °C, for 12 hours in CH₂Cl₂ solvent results in 40.5:59.5 regioisomeric phenothiazines **4c** and **4c'** in 85% yield. The reaction of ferrocenyl phenothiazine **5a** with 1 equivalent of TCNQ at 40 °C, for 12 hours in CH₂Cl₂ solvent results in 37.5:62.5 regioisomeric phenothiazines **5d** and **5d'** in 80% yield. The phenothiazines **5e** and **5e'** was obtained in 45.1:54.9 regioisomeric mixtures by the similar reaction of excess amount of TCNQ with phenothiazine **5a** at 40 °C, for 4 days in CH₂Cl₂ solvent and resulted in 70% yield (Scheme 4.3).



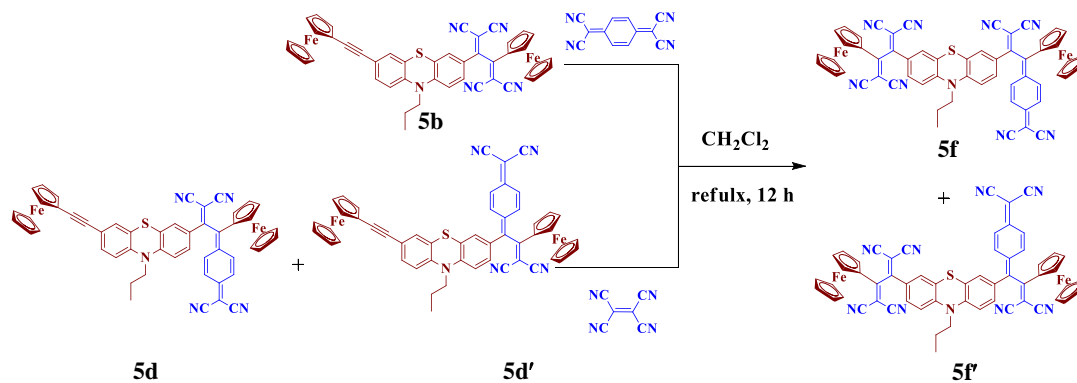
Scheme 4.2. Synthetic route for ferrocenyl phenothiazines **4b**, **4c** and **4c'**.

The reaction of isomeric cyclohexa–2,5–diene–1,4–ylidene–expanded TCBDs functionalized phenothiazine **5d** and **5d'** with TCNE at 40 °C, for 12 hours in CH₂Cl₂ solvent results in 33.1:66.9 regioisomeric phenothiazine **5f** and **5f'** in 80% yield. The phenothiazines **5f** and **5f'** was also synthesized from TCBD functionalized phenothiazine **5b** with TCNQ at 40 °C, for 12 hours in CH₂Cl₂ solvent which resulted in 33.1:66.9 regioisomeric mixtures with 81% yield, (Scheme 4.4). The ferrocenyl phenothiazines as well as TCBD and cyclohexa–

2,5–diene–1,4–ylidene–expanded TCBD functionalized ferrocenyl phenothiazines **4b**, **4c**, **4c'**, **5b**, **5c**, **5d**, **5d'**, **5e**, **5e'**, **5f** and **5f'** are soluble in common organic solvents such as dichloromethane, chloroform, tetrahydrofuran, toluene and were well characterized by ^1H NMR, ^{13}C NMR and HRMS techniques.



Scheme 4.3. Synthetic route for ferrocenyl phenothiazines **5b**, **5c**, **5d**, **5d'**, **5e** and **5e'**.



Scheme 4.4. Synthetic route for ferrocenyl phenothiazines **5f** and **5f'**.

4.3. Photophysical Properties

The electronic absorption spectra of the ferrocenyl phenothiazines and their TCBD and cyclohexa-2,5-diene-1,4-ylidene-expanded TCBD conjugates **4b**, **4c** and **5b–5f** were recorded in dichloromethane at room temperature (Figure 4.1), and the data are compiled in Table 4.1.

The TCBD functionalized phenothiazines **4b**, **5b** and **5c** exhibit ICT transition at 531 nm, 547 nm and 537 nm respectively which indicates that the incorporation of TCBD unit results in strong donor-acceptor interaction. On the other hand, the cyclohexa-2,5-diene-1,4-ylidene-expanded TCBD substituted phenothiazines **4c**, **5d** and **5e** exhibit two strong absorption bands due to the strong electron accepting capability of cyclohexa-2,5-diene-1,4-ylidene-expanded TCBD.

The absorption band between 454–468 nm and 737–794 nm can be attributed to the π - π^* transition band and CT band, respectively. The TCBD/cyclohexa-2,5-diene-1,4-ylidene-expanded TCBD substituted phenothiazine **5f** exhibit π - π^* transition band and CT band at 524 nm and 800 nm respectively. It also shows a shoulder band at 439 nm which may be due to the presence of two different acceptors in phenothiazine **5f**. The incorporation of the TCBD and cyclohexa-2,5-diene-1,4-ylidene-expanded TCBD acceptor units resulted in strong donor-acceptor interaction which was further explained by TD-DFT calculation in dichloromethane phase.

The optical band gap of phenothiazines **4b**, **4c** and **5b–5f** follow the order **4b**>**5c**>**5b**>**5f**>**4c**>**5e**>**5d**. The trend clearly indicates the influence of TCBD and cyclohexa-2,5-diene-1,4-ylidene-expanded TCBD on ferrocenyl phenothiazines leading to the red shifted electronic absorption and low optical band gap which is further explained by TDDFT calculations where the effect of regioisomeric mixture on the electronic spectra is also discussed.

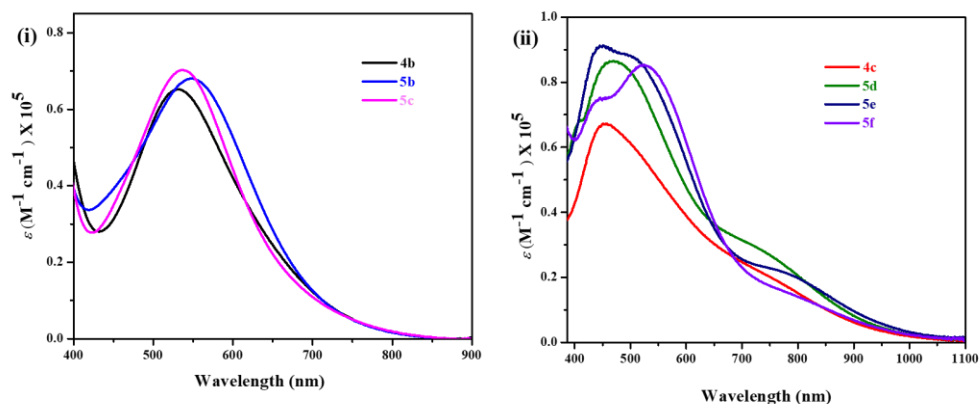


Figure 4.1. The electronic absorption spectra of phenothiazines (i) **4b**, **5b** and **5c**, and (ii) **4c**, **5d**, **5e** and **5f** in dichloromethane (1×10^{-5} M).

4.4. Electrochemical Properties

The electrochemical properties of ferrocenyl phenothiazines **4b**, **4c** and **5b–5f** were explored by cyclic voltammetry (CV) and differential pulse voltammetry (DPV) in dry dichloromethane (DCM) solution at room temperature using tetrabutylammonium hexafluorophosphate (TBAPF₆) as a supporting electrolyte. The electrochemical data are compiled in Table 4.1, and the representative CV and DPV plots are shown in Figure 4.2–4.8.

In general, phenothiazine shows one reversible oxidation wave.^[19] The TCBD and cyclohexa-2,5-diene-1,4-ylidene-expanded TCBD substituted ferrocenyl phenothiazines show an additional reversible oxidation wave which corresponds to the oxidation of ferrocenyl ring.

The phenothiazines **4c**, **5c** and **5e** show two oxidation potentials at (+0.68 V, +0.95 V), (+0.55 V, +0.66 V) and (+0.54 V, +0.79 V) respectively, where the first oxidation potentials are attributed to the ferrocenyl moiety and the second oxidation potentials are due to the phenothiazinyl moiety. The phenothiazine **4b** exhibits only one oxidation wave at +0.71 V due to the simultaneous reversible oxidation of ferrocene and phenothiazine units.^[17a-c] The phenothiazines **5b**, **5d** and **5f** show three oxidation peaks at (+0.33 V, +0.68 V and +0.81 V), (+0.32V,

+0.55V, +0.68 V) and (+0.56 V, +0.67V and +0.85 V), respectively where the first two oxidation potentials correspond to the ferrocene moiety and the third oxidation potential can be attributed to the phenothiazine moiety. The trend in the first oxidation potential of the phenothiazines **4b**, **4c** and **5b–5f** follows the order **4b>5c>5f>4c>5e>5b>5d**.

The TCBD functionalized phenothiazines **4b**, **5b** and **5c** exhibit a reversible two-step reduction wave attributed to one-electron transfer in each step and show the reduction potential value at (–0.75 V, –1.04 V), (–0.76 V, –1.06 V) and (–0.72 V, –1.07 V), respectively due to the TCBD units. The two reduction waves correspond to the formation of radical anions and dianions. A positive shift in the first reduction potential was observed in phenothiazine **5c** because of the presence of two electron withdrawing TCBD units. This indicates that increasing the number of TCBD unit enhances the π -accepting properties. The cyclohexa–2,5–diene–1,4–ylidene–expanded TCBD adduct of phenothiazines **4c**, **5d** and **5e** show only one reduction wave, whose potentials were identified at –0.56 V, –0.55 V and –0.56 V, respectively which is due to the simultaneous electrochemical reduction of cyclohexa–2,5diene–1,4ylidene–expanded TCBD units.^[17a-c] The phenothiazine **5f** shows three reduction wave at –0.54 V, –0.83 V, –1.11 V where the first reduction potential value corresponds to the cyclohexa–2,5diene–1,4ylidene–expanded TCBD moiety and potential at –0.83 V and –1.11 V could be attributed to the TCBD moiety. Therefore the introduction of cyclohexa–2,5–diene–1,4–ylidene–expanded TCBD adduct shows lower reduction potential as compared to TCBDs. The result reveals that the cyclohexa–2,5–diene–1,4–ylidene–expanded TCBD unit stabilizes the LUMO energy level to greater extent than that of TCBD. The HOMO and LUMO energy levels are calculated from the onset oxidation and reduction potentials. The corresponding HOMO and LUMO energy levels of phenothiazines **4b**, **4c**, **5b**, **5c**, **5d**, **5e** and **5f** are –4.98 eV, –4.83 eV, –4.53 eV, –4.91 eV, –4.62 eV, –4.84 eV, –4.86 eV and –3.82 eV, –3.94 eV, –3.79 eV, –3.81 eV, –3.96 eV, –4.00 eV, –3.88 eV, respectively.

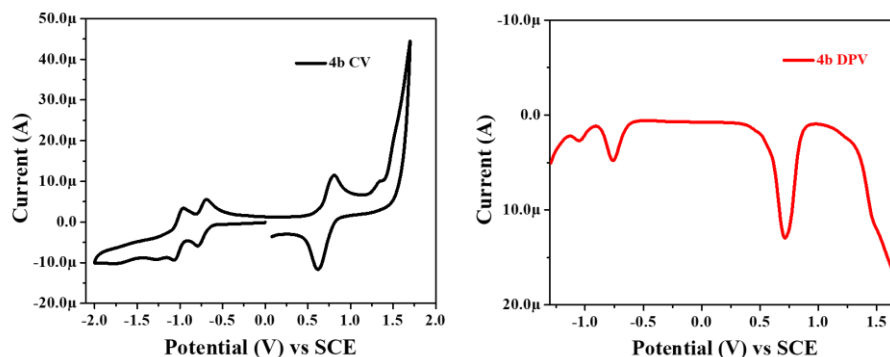


Figure 4.2. CV and DPV plots of phenothiazine **4b**.

Table 4.1. Photophysical and electrochemical properties of phenothiazines **4b**, **4c**, **4c'**, **5b**, **5c**, **5d**, **5d'**, **5e**, **5e'**, **5f** and **5f'**.

| Phenothiazines | Photophysical data ^a | | | Theoretical data ^c | Electrochemical data ^d | |
|----------------|---------------------------------|---|---------------------------------------|-------------------------------|-----------------------------------|----------------------------|
| | λ_{abs} (nm) | ϵ ($\text{M}^{-1}\text{cm}^{-1}$) | Optical Band Gap (eV) ^b | HOMO-LUMO energy gap (eV) | $E_{\text{ox}}(\text{V})$ | $E_{\text{red}}(\text{V})$ |
| 4b | 531 | 65323 | 1.59 | 2.64 | 0.71 | -0.75 -1.04 |
| 4c, 4c' | 454 | 60222 | 1.23 | 2.22, 2.04 | 0.55 0.65 | -0.56 |
| 5b | 547 | 68007 | 1.54 | 2.49 | 0.33 0.68 0.81 | -0.76 -1.06 |

| | | | | | | |
|----------------|-----|-------|------|------------|------|-------|
| 5c | 537 | 70166 | 1.57 | 2.63 | 0.68 | -0.72 |
| | | | | | 0.95 | -1.07 |
| 5d, 5d' | 468 | 77333 | 1.19 | 2.03, 1.87 | 0.32 | -0.55 |
| | | | | | 0.55 | |
| | | | | | 0.68 | |
| 5e, 5e' | 448 | 80368 | 1.21 | 2.24, 2.00 | 0.54 | -0.56 |
| | | | | | 0.79 | |
| 5f, 5f' | 524 | 77158 | 1.24 | 2.28, 2.11 | 0.56 | -0.54 |
| | | | | | 0.67 | -0.83 |
| | | | | | 0.85 | -1.11 |

^a Absorbance measured in dichloromethane at 1×10^{-5} M concentration; λ_{abs} : absorption wavelength; ϵ : extinction coefficient. ^b determined from onset wavelength of the UV/Vis absorption; ^c obtained from density functional theory calculations at B3LYP/6-31+G** level; ^d recorded by cyclic voltammetry, in 0.1 M solution of TBAPF₆ in DCM at 100 mV s^{-1} scan rate versus SCE electrode.

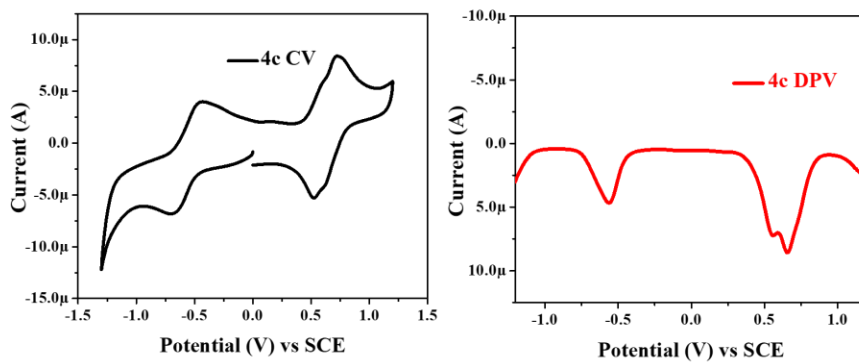


Figure 4.3. CV and DPV plots of phenothiazine **4c**.

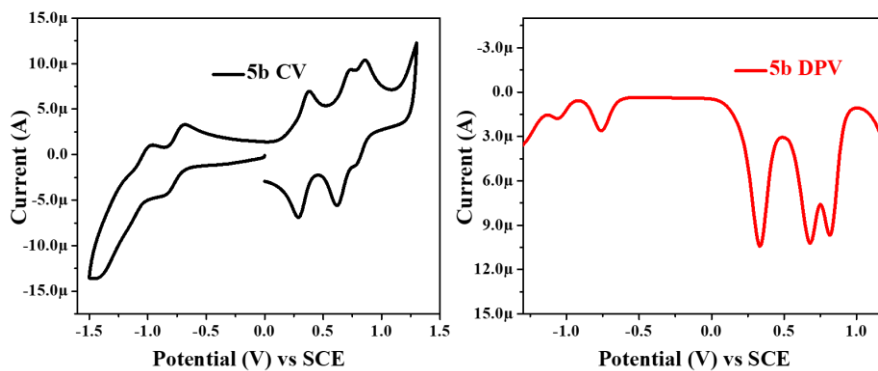


Figure 4.4. CV and DPV plots of phenothiazine **5b**.

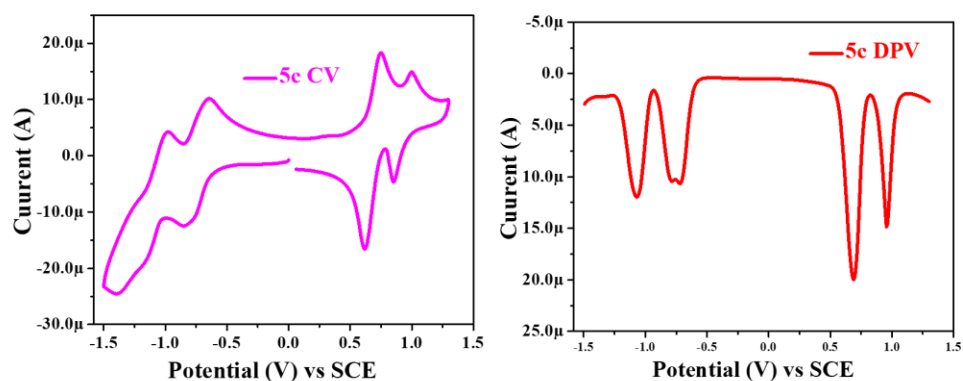


Figure 4.5. CV and DPV plots of phenothiazines **5c**.

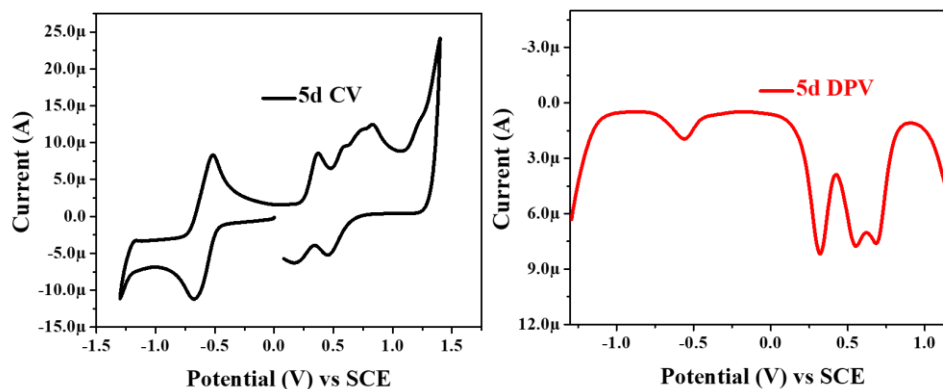


Figure 4.6. CV and DPV plots of phenothiazine **5d**.

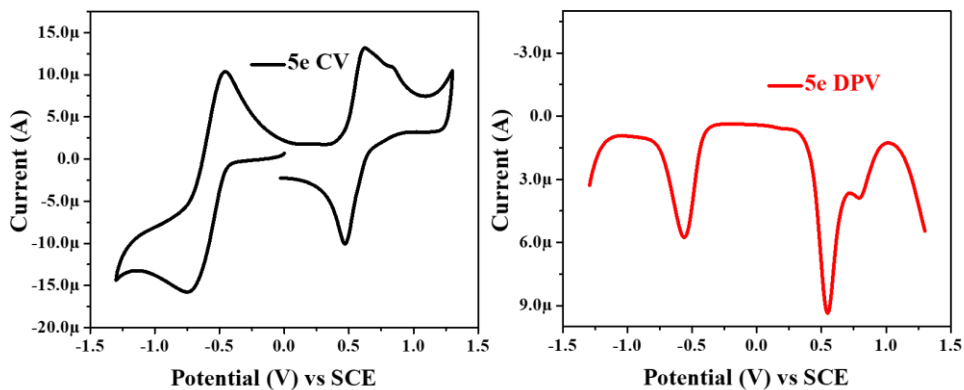


Figure 4.7. CV and DPV plots of phenothiazine **5e**.

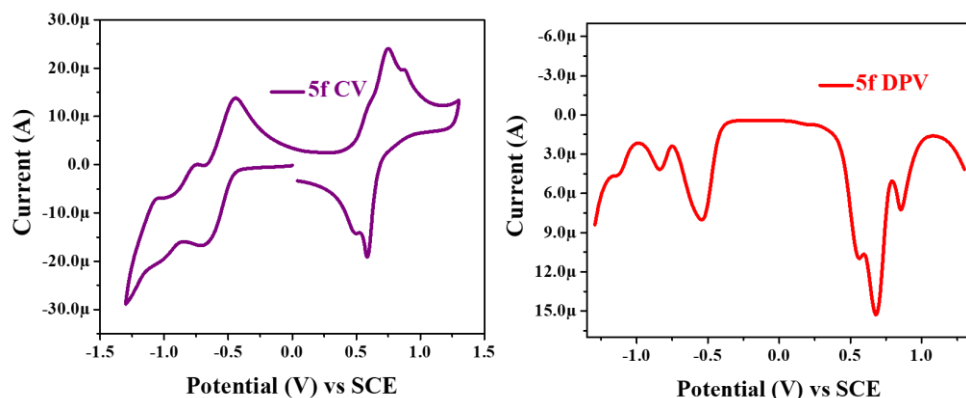


Figure 4.8. CV and DPV plots of phenothiazines **5f**.

4.5. Theoretical Calculations

The density functional theory calculation was performed on phenothiazines **4b**, **4c**, **5b**, **5c**, **5d**, **5e** and **5f** to explore the structure and electronic properties at B3LYP/6-31+G** level for B, C, F, H, N and S.^[20] The optimized structures of phenothiazines are nonplanar with twisted geometry. The incorporation of strong cyclohexa-2,5-diene-1,4-ylidene-expanded TCBD acceptor unit lower the LUMO energy level to greater extent as compared to TCBD, which results in low HOMO-LUMO gap and red shifted electronic absorption. The theoretically determined HOMO levels of phenothiazines **4b**, **4c**, **5b**, **5c**, **5d**, **5e** and **5f** are -5.53 eV, -5.62 eV, -5.41 eV, -5.95 eV, -5.39 eV, -6.03 eV and -6.0 eV whereas LUMO levels are -2.89 eV, -3.40 eV, -2.92 eV, -

3.31 eV, -3.36 eV, -3.79 eV and -3.72 eV (Figure 4.9). The comparison between FMOs of the isomeric phenothiazines (**4c** and **4c'**), (**5d** and **5d'**), (**5e** and **5e'**) and (**5f** and **5f'**) are shown in the Table 4.2–4.5, where the calculated HOMO levels of **4c'**, **5d'**, **5e'** and **5f'** are -5.45 eV, -5.29 eV, -5.87 eV and -5.93 eV, and the LUMO levels are -3.41 eV, -3.42 eV, -3.87 eV and -3.82 eV respectively. The data reveals that the LUMO energy levels of the isomeric phenothiazines **4c'**, **5d'**, **5e'** and **5f'** are more stabilized as compared to the **4c**, **5d**, **5e** and **5f**, respectively.

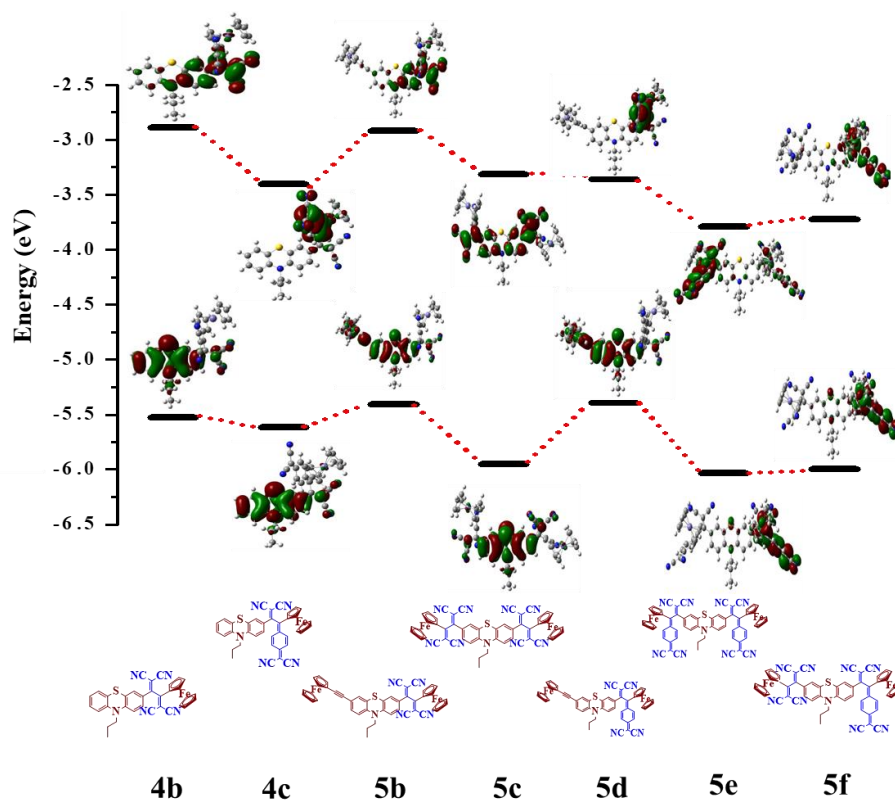


Figure 4.9. Energy diagram showing the HOMO and LUMO wave functions and energies of phenothiazines **4b**, **4c** and **5b–5f** as determined at B3LYP/6-31G** level.

The time-dependent DFT calculation was performed at the B3LYP/6-31G (d, p) level on optimized phenothiazines in dichloromethane to evaluate the absorption properties. The transitions with composition, oscillator strengths, and assignments are as shown in Table 4.6.

Table 4.2. FMO of regioisomeric phenothiazines **4c** and **4c'**.

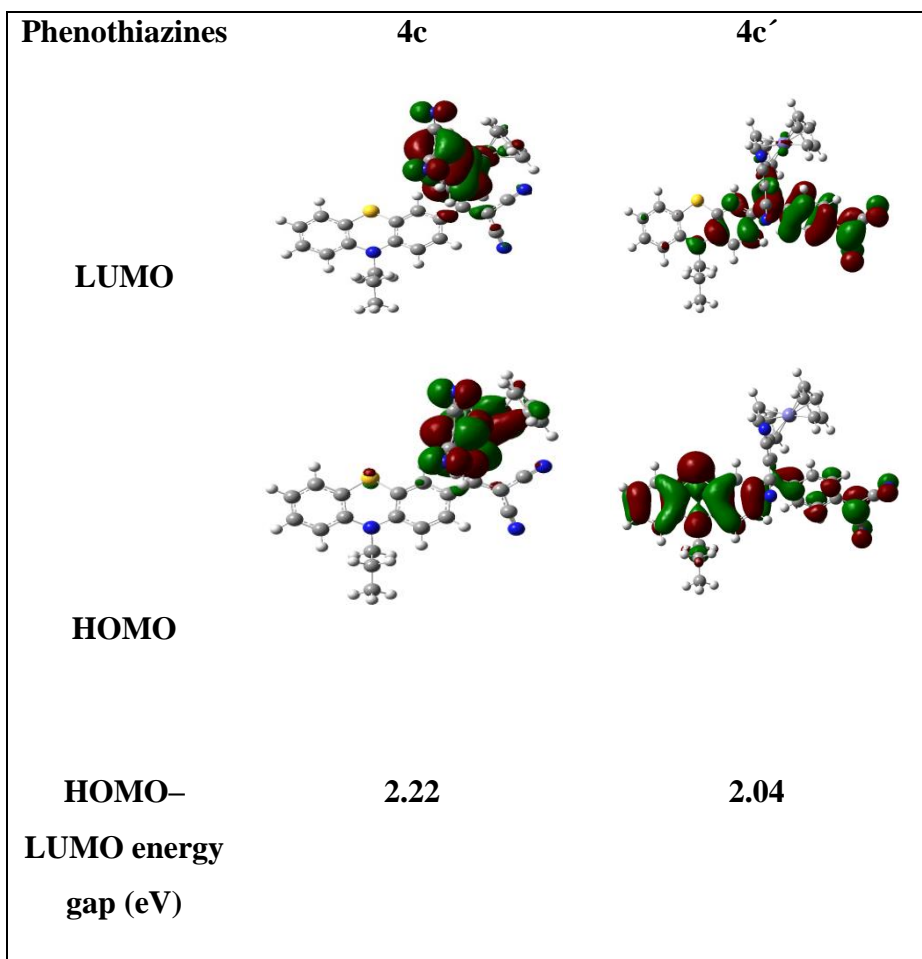
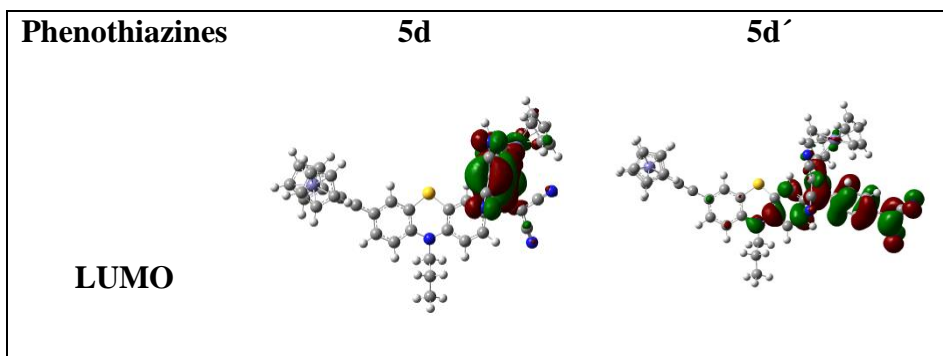


Table 4.3. FMO of regioisomeric phenothiazines **5d** and **5d'**.



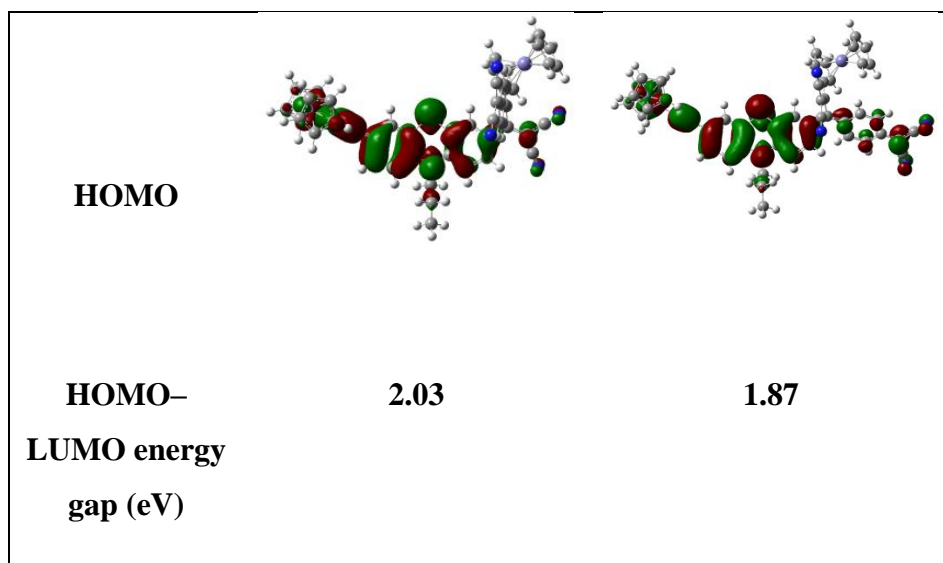


Table 4.4. FMO of regioisomeric phenothiazines **5e** and **5e'**.

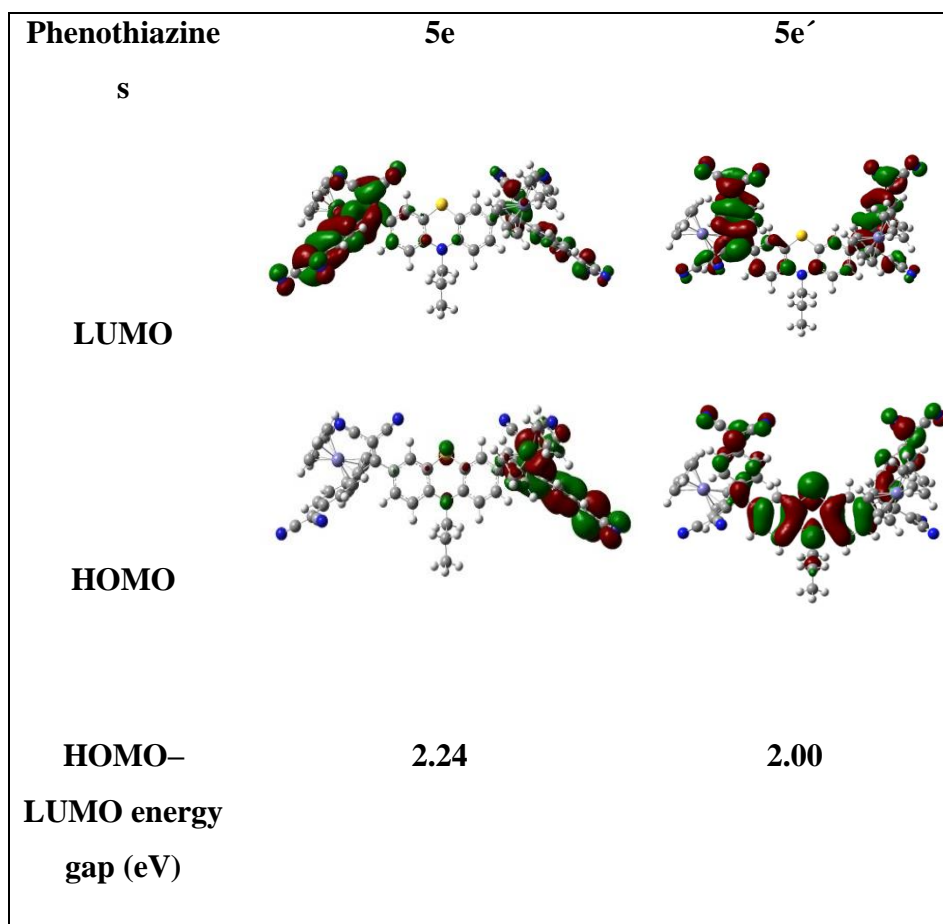
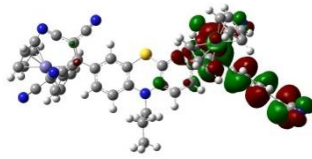
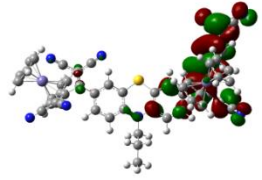
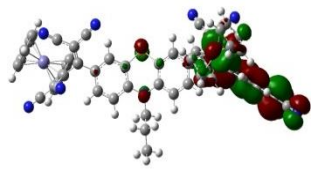
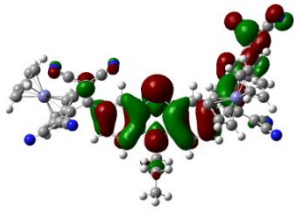


Table 4.5. FMO of regioisomeric phenothiazines **5f** and **5f'**.

| Phenothiazines | 5f | 5f' |
|------------------------------|---|--|
| LUMO |  |  |
| HOMO |  |  |
| HOMO–LUMO energy gap (eV) | 2.28 | 2.11 |

The TD-DFT calculation shows absorption band at 578, 625 and 602 nm respectively for phenothiazines **4b**, **5b** and **5c** due to the ICT, whereas the phenothiazines **4c**, **4c'**, **5d**, **5d'**, **5e**, **5e'**, **5f** and **5f'** exhibit two absorption bands in the visible region which can be attributed to the π – π^* transition at shorter wavelength and ICT at longer wavelength (Table 4.6). The main ICT transition for phenothiazine **4b** occurs from HOMO→LUMO+1, and HOMO→LUMO for phenothiazines **5b** and **5c**. The charge-transfer occurs from HOMO→LUMO+2, HOMO–3→LUMO, HOMO–2→LUMO and HOMO–1→LUMO in phenothiazines **4c**, **5d**, **5e** and **5f**, respectively whereas for **4c'**, **5d'**, **5e'** and **5f'** the charge-transfer occurs from HOMO→LUMO. The data shows that the isomeric phenothiazines **4c'**, **5d'**, **5e'** and **5f'** are red shifted as compared to **4c**, **5d**, **5e** and **5f**, respectively. The theoretical electronic absorption wavelengths were found to

be higher than those of experimental values which might be due to various factors, e.g. solvent effect, dipole moment and temperature.

Table 4.6. Calculated electronic transitions for phenothiazines **4b**, **4c**, **4c'**, **5b**, **5c**, **5d**, **5d'**, **5e**, **5e'**, **5f** and **5f'** in dichloromethane.

| Compounds | Wavelength (nm) | Composition | f ^a | Assignment |
|------------|-----------------|-------------------------|----------------|-----------------|
| 4b | 578 | HOMO→LUMO+1 (0.52) | 0.22 | ICT |
| 4c | 567 | HOMO→LUMO+2 (0.68) | 0.36 | ICT |
| | 480 | HOMO-3→LUMO (0.41) | 0.49 | π - π^* |
| 4c' | 743 | HOMO→LUMO (0.69) | 0.51 | ICT |
| | 483 | HOMO-3→LUMO (0.50) | 0.62 | π - π^* |
| 5b | 625 | HOMO→LUMO (0.65) | 0.35 | ICT |
| 5c | 602 | HOMO→LUMO (0.69) | 0.53 | ICT |
| 5d | 756 | HOMO-3→LUMO (0.48) | 0.05 | ICT |
| | 474 | HOMO-1→LUMO+1 (0.34) | 0.00 | π - π^* |
| 5d' | 795 | HOMO→LUMO (0.70) | 0.62 | ICT |
| | 482 | HOMO-4→LUMO (0.37) | 0.37 | π - π^* |
| 5e | 781 | HOMO-2→LUMO (0.38) | 0.23 | ICT |
| | 575 | HOMO-1→LUMO+1 (0.33) | 0.60 | π - π^* |
| 5e' | 824 | HOMO→LUMO (0.69) | 0.40 | ICT |

| | | | | |
|------------|-----|-------------------------|------|-------------|
| | 523 | HOMO→LUMO+1 (0.52) | 0.52 | $\pi-\pi^*$ |
| 5f | 782 | HOMO-1→LUMO (0.50) | 0.07 | ICT |
| | 526 | HOMO-1→LUMO+1 (0.34) | 0.10 | $\pi-\pi^*$ |
| 5f' | 769 | HOMO→LUMO (0.65) | 0.32 | ICT |
| | 503 | HOMO→LUMO+2 (0.59) | 0.47 | $\pi-\pi^*$ |

f^i oscillator strength

4.6. Experimental Section

General Methods. Chemicals were used as received unless otherwise indicated. All the oxygen or moisture sensitive reactions were carried out under argon atmosphere. ^1H NMR spectra were recorded using a 400 MHz spectrometer. Chemical shifts are reported in delta (δ) units, expressed in parts per million (ppm) downfield from tetramethylsilane (TMS) using residual protonated solvent as an internal standard $\{\text{CDCl}_3, 7.26 \text{ ppm}\}$. ^{13}C NMR spectra were recorded using a 400 MHz spectrometer. Chemical shifts are reported in delta (δ) units, expressed in parts per million (ppm) downfield from tetramethylsilane (TMS) using the solvent as internal standard $\{\text{CDCl}_3, 77.0 \text{ ppm}\}$. The ^1H NMR splitting patterns have been described as “s, singlet; d, doublet; t, triplet and m, multiplet”. UV/Vis spectrums of all compounds were recorded in dichloromethane solution. Cyclic voltammograms were recorded on electrochemical analyzer using Glassy carbon as working electrode, Pt wire as the counter electrode, and Saturated Calomel Electrode (SCE) as the reference electrode. The scan rate was 100mVs^{-1} for Cyclic Voltammetry. A solution of tetrabutylammonium hexafluorophosphate (TBAPF₆) in CH_2Cl_2 (0.1M) was used as supporting electrolyte.

Synthesis of 4b. Tetracyanoethylene (TCNE) (28.2 mg, 0.22 mmol) was added to a solution of compound **4a** (98.8 mg, 0.22 mmol) in CH_2Cl_2 (50 mL). The mixture was stirred at room temperature for 4 h. After the completion of the reaction the solvent was removed in vacuum, and the product was purified by column

chromatography with CH₂Cl₂ as the eluent which yield **4b** as a dark violet colored solid. Yield: 106.9 mg, 83%. ¹H NMR (400 MHz, CDCl₃): δ = 7.59 (d, *J* = 7.28 Hz, 1H), 7.30 (s, 1H), 7.16 (t, *J* = 7.56 Hz, 1H), 7.06-6.95 (m, 2H), 6.87-6.81 (m, 2H), 5.18 (s, 1H), 4.95 (s, 1H), 4.84 (s, 1H), 4.70 (s, 1H), 4.45-4.37 (m, 5H), 3.82 (t, *J*=7.04 Hz, 2H), 1.85-1.79 (m, 2H), 1.01 (t, *J* = 7.28 Hz, 3H); ¹³C NMR (100 MHz, CDCl₃): δ = 173.3, 163.5, 150.8, 142.2, 129.7, 128.6, 127.9, 127.6, 127.5, 125.3, 124.3, 124.2, 122.6, 116.1, 114.9, 113.7, 112.8, 112.5, 80.3, 79.1, 75.5, 75.4, 74.9, 72.7, 72.5, 72.0, 71.9, 71.5, 49.9, 19.9, 11.1; HRMS (ESI-TOF): *m/z* calculated for C₃₃H₂₃FeN₅S= 578.1097 [M+H]⁺, measured 578.1082 [M+H]⁺

Synthesis of 4c and 4c'. Tetracyanoquinodimethane (TCNQ) (44.9 mg, 0.22 mmol) was added to a solution of compound **4a** (98.8 mg, 0.22 mmol) in CH₂Cl₂ (50 mL). The mixture was refluxed at 40 °C for 12 h. After the completion of the reaction the solvent was removed in vacuum and the product was purified by column chromatography with CH₂Cl₂ as the eluent which yield **4c** and **4c'** in 40.5:59.5 calculated regioisomeric mixtures as a dark brown colored solid. Overall Yield: 122.0 mg, 85%. ¹H NMR (400 MHz, CDCl₃): δ = 8.31 (d, *J* = 9.28 Hz, 1H), 7.55 (d, *J* = 7.52 Hz, 1H), 7.45 (d, *J* = 9.52 Hz, 1H), 7.38 (d, *J* = 9.52 Hz, 1H), 7.23–7.10 (m, 9H), 7.02–6.95 (m, 4H), 6.89–6.77 (m, 5H), 4.97–4.76 (m, 7H), 4.42–4.26 (m, 11H), 3.85 (t, *J* = 7.04 Hz, 2H), 3.80 (t, *J* = 7.04 Hz, 2H), 1.87–1.77 (m, 4H), 1.04–0.98 (m, 6H); ¹³C NMR (100 MHz, CDCl₃): δ = 177.4, 167.4, 157.1, 154.6, 154.2, 150.4, 149.6, 148.5, 142.9, 142.3, 134.7, 135.2, 134.1, 131.6, 131.4, 130.6, 130.5, 129.9, 129.0, 128.9, 128.2, 127.9, 127.6, 126.7, 126.0, 125.6, 125.4, 125.1, 124.8, 124.2, 124.0, 123.8, 115.0, 114.9, 114.3, 113.8, 113.7, 113.5, 113.3, 80.0, 79.6, 79.5, 79.4, 77.8, 76.2, 76.1, 75.5, 75.0, 74.9, 74.8, 74.7, 73.9, 72.8, 72.6, 72.5, 72.4, 71.8, 71.1, 49.8, 49.4, 20.1, 20.0, 11.2, 11.1; HRMS (ESI-TOF): *m/z* calculated for C₃₉H₂₇FeN₅S= 676.1229 [M+Na]⁺, measured 676.1210 [M+Na]⁺

Synthesis of 5b. Tetracyanoethylene (TCNE) (19.2 mg, 0.15 mmol) was added to a solution of compound **5a** (98.6 mg, 0.15 mmol) in CH₂Cl₂ (50 mL). The mixture was stirred at room temperature for 4 h. After the completion of the reaction the

solvent was removed in vacuum, and the product was purified by column chromatography with CH₂Cl₂ as the eluent to yield **5b** as a dark violet colored solid. Yield: 100.10 mg, 85%; ¹H NMR (400 MHz, CDCl₃): δ = 7.58 (d, *J* = 8 Hz, 1H), 7.28 (s, 2H), 7.16 (s, 1H), 6.83–6.76 (m, 2H), 5.29 (s, 3H), 5.18 (s, 1H), 4.95 (s, 1H), 4.85 (s, 1H), 4.71 (s, 1H), 4.45 (s, 6H), 6.94 (s, 6H), 3.81 (t, *J* = 6.04 Hz, 2H), 1.83–1.79 (m, 2H), 1.02 (t, *J* = 6.76 Hz, 3H); ¹³C NMR (100 MHz, CDCl₃): δ = 173.3, 163.4, 150.2, 141.4, 130.9, 130.0, 129.7, 127.5, 124.8, 124.5, 122.6, 120.1, 115.8, 115.1, 113.7, 112.8, 112.7, 112.4, 89.5, 84.2, 80.6, 79.1, 75.5, 75.0, 72.5, 72.0, 71.4, 70.0, 68.9, 64.9, 49.9, 19.9, 11.1; HRMS (ESI-TOF): *m/z* calculated for C₄₅H₃₁Fe₂N₅S = 824.0633 [M+K]⁺, measured 824.0630 [M+K]⁺

Synthesis of 5c. Tetracyanoethylene (TCNE) (38.4 mg, 0.3 mmol) was added to a solution of compound **5a** (98.6 mg, 0.15 mmol) in CH₂Cl₂ (50 mL). The mixture was stirred at room temperature for 12 h. After the completion of the reaction the solvent was removed in vacuum, and the product was purified by column chromatography with CH₂Cl₂ as the eluent which yield **5c** as a dark violet colored solid. Yield: 123.4 mg, 90%; ¹H NMR (400 MHz, CDCl₃): δ = 7.54 (t, *J* = 8.28 Hz, 2H), 7.22 (d, *J* = 6.04 Hz, 2H), 6.89–6.86 (m, 2H), 5.30 (d, *J* = 7.76 Hz, 2H), 5.01 (s, 2H), 4.88 (s, 2H), 4.59 (d, *J* = 5.28 Hz, 2H), 4.46 (s, 8H), 3.82 (t, *J* = 7.04 Hz, 2H), 1.84–1.79 (m, 2H), 1.03 (t, *J* = 7.28 Hz, 3H); ¹³C NMR (100 MHz, CDCl₃): δ = 172.6, 163.5, 147.9, 147.8, 129.8, 127.5, 127.4, 126.2, 124.3, 116.1, 113.6, 112.8, 112.2, 111.9, 82.9, 78.8, 74.5, 72.7, 72.2, 71.8, 50.3, 19.9, 11.1; HRMS (ESI-TOF): *m/z* calculated for C₅₁H₃₁Fe₂N₉S = 952.0756 [M+K]⁺, measured 952.1018 [M+K]⁺

Synthesis of 5d and 5d'. Tetracyanoquinodimethane (TCNQ) (30.6 mg, 0.15 mmol) was added to a solution of compound **5a** (98.6 mg, 0.15 mmol) in CH₂Cl₂ (50 mL). The mixture was refluxed at 40 °C for 12 h. After the completion of the reaction the solvent was removed in vacuum and the product was purified by column chromatography with CH₂Cl₂ as the eluent which yield **5d** and **5d'** in 37.5:62.5 calculated regioisomeric mixtures as a dark brown colored solid. Overall Yield: 103.4 mg, 80%; ¹H NMR (400 MHz, CDCl₃): δ = 8.31 (d, *J* = 9.8

Hz, 1H), 7.56 (d, $J = 8.28$ Hz, 1H), 7.46 (d, $J = 9.52$ Hz, 2H), 7.38 (d, $J = 9.52$ Hz, 1H), 7.20 (t, $J = 8.76$ Hz, 5H), 7.13 (s, 1H), 7.03 (d, $J = 9.28$ Hz, 1H), 6.88 (d, $J = 8.52$ Hz, 1H), 6.80–6.74 (m, 5H), 5.28 (s, 2H), 4.93 (s, 1H), 4.83 (s, 3H), 4.76 (s, 1H), 4.45–4.20 (m, 31H), 3.84 (t, $J = 7.0$ Hz, 2H), 3.79 (t, $J = 7.04$ Hz, 2H), 1.87–1.77 (m, 4H), 1.05–0.98 (m, 6H); ^{13}C NMR (100 MHz, CDCl_3): $\delta = 167.3, 156.9, 154.6, 154.2, 149.8, 149.4, 147.9, 142.2, 141.5, 134.6, 134.1, 134.0, 131.5, 130.9, 130.5, 130.1, 130.0, 129.8, 129.2, 129.0, 128.2, 127.0, 126.1, 125.5, 125.1, 124.9, 124.6, 124.1, 122.9, 122.7, 119.9, 119.5, 115.7, 115.6, 115.3, 115.0, 114.3, 113.8, 113.6, 113.4, 113.2, 89.5, 89.4, 89.2, 84.2, 80.3, 79.5, 79.4, 77.9, 77.8, 76.1, 75.7, 74.9, 74.8, 73.8, 72.7, 72.6, 72.5, 72.4, 71.8, 71.3, 69.9, 49.8, 20.1, 19.9, 11.2, 11.1$; HRMS (ESI-TOF): m/z calculated for $\text{C}_{51}\text{H}_{35}\text{Fe}_2\text{N}_5\text{S} = 861.1309$ $[\text{M}]^+$, measured 861.1283 $[\text{M}]^+$.

Synthesis of 5e and 5e'. Tetracyanoquinodimethane (TCNQ) (61.2 mg, 0.3 mmol) was added to a solution of compound **5a** (98.6 mg, 0.15 mmol) in CH_2Cl_2 (50 mL). The mixture was refluxed at 40 °C for 4 days. After the completion of the reaction the solvent was removed in vacuum and the product was purified by column chromatography with CH_2Cl_2 as the eluent which yield **5e** and **5e'** in 45.1:54.9 calculated regioisomeric mixtures as a dark brown colored solid. Overall Yield: 111.9 mg, 70%; ^1H NMR (400 MHz, CDCl_3): $\delta = 8.30\text{--}8.26$ (m, 3H), 7.55–7.42 (m, 7H), 7.31–7.28 (m, 4H), 7.22–7.18 (m, 6H), 7.13 (s, 1H), 7.02 (s, 2H), 6.91–6.73 (m, 8H), 5.28 (s, 1H), 4.95–4.80 (m, 13H), 4.36–4.29 (m, 21H), 3.82 (t, $J = 8.0$ Hz, 2H), 3.75 (t, $J = 9.52$ Hz, 2H), 1.87–1.74 (m, 4H), 1.05–0.97 (m, 6H); ^{13}C NMR (100 MHz, CDCl_3): $\delta = 167.2, 156.3, 156.0, 154.4, 153.9, 148.3, 148.1, 147.5, 147.4, 145.4, 134.0, 133.8, 132.1, 131.5, 130.6, 130.5, 130.1, 129.9, 128.9, 128.6, 127.8, 125.0, 124.2, 123.9, 115.9, 115.8, 115.6, 115.0, 114.9, 113.4, 113.1, 112.9, 112.8, 112.7, 82.1, 81.7, 79.3, 79.1$; HRMS (ESI-TOF): m/z calculated for $\text{C}_{63}\text{H}_{39}\text{Fe}_2\text{N}_9\text{S} = 1088.1644$ $[\text{M}+\text{Na}]^+$, measured 1088.1651 $[\text{M}+\text{Na}]^+$.

Synthesis of 5f and 5f'. Tetracyanoethylene (TCNE) (15.4 mg, 0.12 mmol) was added to a solution of compound **5d** and **5d'** (103.4 mg, 0.12 mmol) in CH_2Cl_2

(50 mL). The mixture was refluxed at 40 °C for 12 h. After the completion of the reaction the solvent was removed in vacuum, and the product was purified by column chromatography with CH₂Cl₂ as the eluent which yield **5f** and **5f'** in 33.1:66.9 calculated regioisomeric mixtures as a dark colored solid. Overall Yield: 95 mg, 80%; ¹H NMR (400 MHz, CDCl₃): δ = 8.29 (d, *J* = 9.6 Hz, 1H), 7.58–7.45 (m, 5H), 7.34–7.28 (m, 2H), 7.21–7.07 (m, 6H), 6.93–6.75 (m, 5H), 5.28–5.23 (m, 3H), 4.99–4.81 (m, 11H), 4.65 (d, *J*=7.28 Hz, 1H), 4.57 (s, 2H), 4.44–4.30 (m, 20H), 3.85 (t, *J* = 6.52 Hz, 2H), 3.78 (t, *J* = 6.52 Hz, 2H), 1.84–1.75 (m, 4H), 1.05–0.99 (m, 6H); ¹³C NMR (100 MHz, CDCl₃): δ = 172.6, 172.5, 167.2, 163.5, 163.4, 158.2, 154.5, 153.9, 148.7, 148.3, 147.9, 147.4, 145.3, 134.2, 134.0, 133.9, 133.8, 132.1, 131.4, 130.7, 130.5, 129.9, 129.8, 129.7, 129.0, 128.7, 128.1, 128.0, 127.8, 127.5, 126.0, 125.8, 125.0, 124.2, 124.1, 123.9, 116.0, 115.9, 115.8, 115.0, 114.2, 113.7, 113.5, 113.4, 112.9, 112.8, 112.7, 112.4, 112.2, 111.9, 82.7, 82.6, 82.2, 82.1, 79.1, 78.9, 78.8, 75.8, 75.3, 75.1, 74.9, 73.9, 73.0, 72.7, 72.6, 72.1, 71.8, 71.7, 53.4, 50.2, 19.9, 19.8, 11.1, 11.0; HRMS (ESI-TOF): *m/z* calculated for C₅₈H₃₉Fe₂N₉S= 1012.1330 [M+Na]⁺, measured 1012.1462 [M+Na]⁺.

4.7. Conclusions

In summary, a series of TCBD and cyclohexa-2,5-diene-1,4-ylidene-expanded TCBD substituted phenothiazines **4b**, **4c**, **4c'**, **5b**, **5c**, **5d**, **5d'**, **5e**, **5e'**, **5f** and **5f'** were synthesized by [2+2] cycloaddition–electrocyclic ring-opening reactions. Their electrochemical properties reveal that the incorporation of strong acceptors TCBD and cyclohexa-2,5-diene-1,4-ylidene-expanded TCBD facilitates the reduction process of the ferrocenyl-phenothiazines which leads to low HOMO–LUMO gap. The electronic absorption spectra exhibit strong ICT at longer wavelength and strong donor–acceptor interactions. In particular, DFT and TDDFT calculations reveal a broad understanding of the electronic structure and absorption spectra of the phenothiazine chromophores which reveal that the incorporation of TCBD and cyclohexa-2,5-diene-1,4-ylidene-expanded TCBD acceptor group perturbs HOMO–LUMO gap of the phenothiazines to a greater

extent which is in a good agreement with the experimental values. The results provide an important procedure of designing new donor–acceptor chromophores with low band gaps.

3.8. References

- [1] (a) Kraft, A., Grimsdale, A. C., Holmes, A. B. (1998), Electroluminescent Conjugated Polymers–Seeing Polymers in a New Light. *Angew. Chem. Int. Ed.*, 37, 402–428 (DOI: 10.1002/(SICI)1521-3773(19980302)37:4<402::AID-ANIE402>3.0.CO;2-9); (b) Chen, C. H., Shi, J., Tang, C. W., Klubek, K. P. (2000), Recent developments in the synthesis of red dopants for Alq₃ hosted electroluminescence. *Thin Solid Films*, 363, 327–331 (DOI: 10.1016/S0040-6090(99)01010-X); (c) Ellinger, S., Graham, K. R.; Shi, P., Farley, R. T.; Steckler, T. T.; Brookins, R. N.; Taranekar, P.; Mei, J.; Padilha, L. A.; Ensley, T. R.; Hu, H.; Webster, S.; Hagan, D. J.; Stryland, E. W. V.; Schanze, K. S.; Reynolds, J. R. (2011), Donor–Acceptor–Donor-based π -Conjugated Oligomers for Nonlinear Optics and Near-IR Emission. *Chem. Mater.*, 23, 3805–3817 (DOI: 10.1021/cm201424a); (d) Roncali, J. (2009), Molecular Bulk Heterojunctions: An Emerging Approach to Organic Solar Cells. *Acc. Chem. Res.*, 42, 1719–1730 (DOI: 10.1021/ar900041b); (e) Li, Y., Liu, T., Liu, H., Tian, M.-Z., Li, Y. (2014), Self-Assembly of Intramolecular Charge-Transfer Compounds into Functional Molecular Systems. *Acc. Chem. Res.*, 47, 1186–1198 (DOI: 10.1021/ar400264e).
- [2] (a) Sonar, P., Singh, S. P., Li, Y., Soh, M. S., Dodabalapur, A. (2010), A low-bandgap diketopyrrolopyrrole-benzothiadiazole-based copolymer for high-mobility ambipolar organic thin-film transistors. *Adv. Mater.*, 22, 5409–5413 (DOI: 10.1002/adma.201002973); (b) Omer, K. M.; Ku, S. Y.; Wong, K. T., Bard, A. (2009), Green Electrogenerated Chemiluminescence of Highly Fluorescent Benzothiadiazole and Fluorene Derivatives. *J. J. Am. Chem. Soc.*, 131, 10733–10741 (DOI: 10.1021/ja904135y); (c) Kato, S-i.; Furuya, T., Kobayashi, A., Nitani, M.,

- le, Y., Aso, Y., Yoshihara, T., Tobita, S., Nakamura, Y. (2012), π -Extended Thiadiazoles Fused with Thienopyrrole or Indole Moieties: Synthesis, Structures, and Properties. *J. Org. Chem.*, 77, 7595–7606 (DOI: 10.1021/jo301458m); (d) Lin, Y., Fan, H.; Li, Y., Zhan, X. (2012), Thiazole-Based Organic Semiconductors for Organic Electronics. *Adv. Mater.*, 24, 3087–3106 (DOI: 10.1002/adma.201200721); (e) Chen, S., Li, Y., Yang, W., Chen, N., Liu, H., Li, Y. (2010), Synthesis and Tuning Optical Nonlinear Properties of Molecular Crystals of Benzothiadiazole. *J. Phys. Chem. C*, 114, 15109–15115 (DOI: 10.1021/jp103159b); (f) Meyer, T.; Ogermann, D.; Pankrath, A.; Kleinermanns, K.; Müller, T. J. J. (2012), Phenothiazinyl Rhodanylidene Merocyanines for Dye-Sensitized Solar Cells. *J. Org. Chem.*, 77, 3704–3715 (DOI: 10.1021/jo202608w); (g) Tian, H., Yang, X., Chen, R., Pan, Y., Li, L., Hagfeldt, A., Sun, L. (2007), Phenothiazine derivatives for efficient organic dye-sensitized solar cells. *Chem. Commun.*, 3741–3743 (DOI: 10.1039/B707485A).
- [3] (a) Bures, F., Schweizer, W. B., May, J. C., Boudon, C., Gisselbrecht, J.-P., Gross, M., Biaggio, I., Diederich, F. (2007), Property Tuning in Charge-Transfer Chromophores by Systematic Modulation of the Spacer between Donor and Acceptor. *Chem. Eur. J.*, 13, 5378–5387 (DOI: 10.1002/chem.200601735); (b) Wang, J.-L., Xiao, Q., Pei, J. (2010), Benzothiadiazole-Based D- π -A- π -D Organic Dyes with Tunable Band Gap: Synthesis and Photophysical Properties. *Org. Lett.*, 12, 4164–4167 (DOI: 10.1021/ol101754q); (c) Zhang, W.-W., Mao, W.-L., Hu, Y.-X., Tian, Z.-Q., Wang, Z.-L., Meng, Q.-J. (2009), Phenothiazine–Anthraquinone Donor–Acceptor Molecules: Synthesis, Electronic Properties and DFT-TDDFT Computational Study. *J. Phys. Chem. A*, 113, 9997–10004 (DOI: 10.1021/jp903390v).
- [4] (a) Misra, R., Gautam, P., Jadhav, T., Mobin, S. M. (2013), Donor–Acceptor Ferrocenyl-Substituted Benzothiadiazoles: Synthesis, Structure, and Properties. *J. Org. Chem.*, 78, 4940–4948 (DOI: 10.1021/jo4005734); (b) Misra, R., Gautam, P., Mobin, S. M. (2013), Aryl-Substituted

- Unsymmetrical Benzothiadiazoles: Synthesis, Structure, and Properties. *J. Org. Chem.*, 78, 12440–12452 (DOI: 10.1021/jo402111q); (c) Misra, R., Dhokale, B., Jadhav, T., Mobin, S. M. (2014), Heteroatom-Connected Ferrocenyl BODIPYs: Synthesis, Structure, and Properties. *Organometallics*, 33, 1867–1877 (DOI: 10.1021/om5002292); (d) Patil, Y., Jadhav, T., Dhokale, B., Misra, R. (2016), Tuning of the HOMO–LUMO Gap of Symmetrical and Unsymmetrical Ferrocenyl-Substituted Diketopyrrolopyrroles. *Eur. J. Org. Chem.*, 733–738 (DOI: 10.1002/ejoc.201501123); (e) Dhokale, B., Gautam, P., Misra, R. (2012), Donor–acceptor perylenediimide–ferrocene conjugates: synthesis, photophysical, and electrochemical properties. *Tetrahedron Lett.*, 53, 2352–2354 (DOI: 10.1016/j.tetlet.2012.02.107); (f) Jadhav, T., Maragani, R., Misra, R., Sreeramulu, V., Rao, D. N., Mobin, S. M. (2013), Design and synthesis of donor–acceptor pyrazabole derivatives for multiphoton absorption. *Dalton Trans.*, 42, 4340–4342 (DOI: 10.1039/C3DT33065F).
- [5] Bureš, F. (2014), Fundamental aspects of property tuning in push–pull molecules. *RSC Adv.*, 4, 58826–58851 (DOI: 10.1039/C4RA11264D).
- [6] (a) Massie, S. (1954), The Chemistry of Phenothiazine. *Chem. Rev.*, 54, 797–833 (DOI: 10.1021/cr60171a003); (b) Hauck, M., Schonhaber, J., Zuccherro, A. J., Hardcastle, K. I., Müller, T. J. J., Bunz, U. H. F. (2007), Phenothiazine Cruciforms: Synthesis and Metallochromic Properties. *J. Org. Chem.*, 72, 6714–6725 (DOI: 10.1021/jo0709221); (c) Gupta, R. R.; Ojha, K. G. (1988) In Phenothiazines and 1,4-Benzothiazines: Chemical and Biochemical Aspects. Gupta, R. R., ed.; *Elsevier: Amsterdam*, 163–269.
- [7] (a) Hauck, M., Stolte, M., Schçnhaber, J., Kuball, H.-G., Muller, T. J. J. (2011) Synthesis, Electronic, and Electro-Optical Properties of Emissive Solvatochromic Phenothiazinyl Merocyanine Dyes. *Chem. Eur. J.*, 17, 9984–9998 (DOI: 10.1002/chem.201100592); (b) Sailer, M., Gropeanu, R.-A., Müller, T. J. J. (2003) Practical Synthesis of Iodo Phenothiazines. A Facile Access to Electrophore Building Blocks. *J.*

- Org. Chem.*, 68, 7509–7512 (DOI: 10.1021/jo034555z); (c) Müller, T. J. J. (1999), First synthesis and electronic properties of ring-alkynylated phenothiazines. *Tetrahedron Lett.*, 40, 6563–6566 (DOI: 10.1016/S0040-4039(99)01402-1); (d) Krämer, C. S., Müller, T. J. J. (2003), Synthesis and Electronic Properties of Alkynylated Phenothiazines. *Eur. J. Org. Chem.*, 3534–3548 (DOI: 10.1002/ejoc.200300250); (e) Krämer, C. S., Zeitler, K., Müller, T. J. J. (2000), Synthesis of Functionalized Ethynylphenothiazine Fluorophores. *Org. Lett.*, 2, 3723–3726 (DOI: 10.1021/ol0066328).
- [8] (a) Green, M. L. H., Marder, S. R., Thompson, M. E., Bandy, J. A., Bloor, D., Kolinsky, P. V., Jones, R. J. (1987), Synthesis and structure of (cis)-[1-ferrocenyl-2-(4-nitrophenyl)ethylene], an organotransition metal compound with a large second-order optical nonlinearity. *Nature*, 330, 360–362 (DOI: 10.1038/330360a0); (b) Gautam, P., Dhokale, B., Shukla, V., Singh, C. P., Bindra, K. S., Misra, R. (2012), Optical limiting performance of meso-tetraferrocenyl porphyrin and its metal derivatives. *J. Photochem. Photobiol., A. Chem.*, 239, 24–27 (DOI: 10.1016/j.jphotochem.2012.04.020); (c) Sailer, M., Rominger, F., Müller, T. J. J. (2006), Ferrocenyl oligophenothiazines as organic–organometallic hybrid electrophores – Synthesis, structure, and electronic properties. *J. Organomet. Chem.*, 691, 299–308 (DOI: 10.1016/j.jorganchem.2005.08.012).
- [9] (a) Cairns, T. L., McKusick, B. C. (1961), Cyankohlenstoff-Chemie. *Angew. Chem.*, 73, 520–525 (DOI: 10.1002/ange.19610731503); (b) Webster, O. W. (2002), Cyanocarbons: A classic example of discovery-driven research. *J. Polym. Sci., Part A: Polym. Chem.*, 40, 210–221 (DOI: 10.1002/pola.10087); (c) Mochida, T., Yamazaki, S. (2002), Mono- and diferrocenyl complexes with electron-accepting moieties formed by the reaction of ferrocenylalkynes with tetracyanoethylene. *J. Chem. Soc., Dalton Trans.*, 3559–3564 (DOI: 10.1039/B204168E); (d) Wu, X., Wu, J., Liu, Y., Jen, A. K-Y. (1999), Highly Efficient, Thermally and Chemically

Stable Second Order Nonlinear Optical Chromophores Containing a 2-Phenyl-tetracyanobutadienyl Acceptor. *J. Am. Chem. Soc.*, 121, 472–473 (DOI: 10.1021/ja983537+); (c) Morioka, Y., Yoshizawa, N., Nishida, J.-i., Yamashita, Y. (2004), Novel Donor– π –Acceptor Compounds Containing 1,3-Dithiol-2-ylidene and Tetracyanobutadiene Units. *Chem. Lett.*, 33, 1190–1191 (DOI: 10.1246/cl.2004.1190); (d) Koszelewski, D., Nowak-Krol, A., Gryko, D. T. (2012), Selective Cycloaddition of Tetracyanoethene (TCNE) and 7,7,8,8-Tetracyano-*p*-quinodimethane (TCNQ) to Afford *meso*-Substituted Phenylethynyl Porphyrins. *Chem. Asian J.*, 7, 1887–1894 (DOI: 10.1002/asia.201200179); (e) García, R., Herranz, M. Á., Torres, M. R., Bouit, P.-A., Delgado, J. L., Calbo, J., Viruela, P. M., Ortí, E., Martín, N. (2012), Tuning the Electronic Properties of Nonplanar exTTF-Based Push–Pull Chromophores by Aryl Substitution. *J. Org. Chem.*, 77, 10707–10717 (DOI: 10.1021/jo302047m); (f) Sasaki, S.-i., Mizutani, K., Kunieda, M., Tamiaki, H. (2013), Cycloaddition to a C3-ethynylated chlorophyll derivative and self-aggregation of zinc chlorin–pyrazole/triazole conjugates. *Tetrahedron*, 69, 9772–9778 (DOI: 10.1016/j.tet.2013.09.007); (g) Betou, M., Kerisit, N., Meledje, E., Leroux, Y. R., Katan, C., Halet, J.-F., Guillemin, J.-C., Trolez, Y. (2014), High-Yield Formation of Substituted Tetracyanobutadienes from Reaction of Ynamides with Tetracyanoethylene. *Chem. Eur. J.*, 20, 9553–9557 (DOI: 10.1002/chem.201402653); (h) Perrin, F. G., Kiefer, G., Jeanbourquin, L., Racine, S., Perrotta, D., Waser, J., Scopelliti, R., Severin, K. (2015), 1-Alkynyltriazenes as Functional Analogues of Ynamides. *Angew. Chem. Int. Ed.*, 54, 13393–13396 (DOI: 10.1002/anie.201507033).

- [10] (a) Vickers, E. B., Selby, T. D., Thorum, M. S., Taliaferro, M. L., Miller, J. S. (2004), Vanadium 7,7,8,8-Tetracyano-*p*-quinodimethane (V[TCNQ]₂)-Based Magnets. *Inorg. Chem.*, 43, 6414–6420 (DOI: 10.1021/ic049552z); (b) Hünig, S., Herberth, E. (2004), N,N'-

- Dicyanoquinone Diimines (DCNQIs): Versatile Acceptors for Organic Conductors. *Chem. Rev.*, 104, 5535–5563 (DOI: 10.1021/cr030637b); (c) Vickers, E. B., Giles, I. D., Miller, J. S. (2005), M[TCNQ]_y-Based Magnets (M = Mn, Fe, Co, Ni; TCNQ = 7,7,8,8-tetracyano-p-quinodimethane). *Chem. Mater.*, 17, 1667–1672 (DOI: 10.1021/cm047869r); (d) Pfeiffer, M., Leo, K., Zhou, X., Huang, J. S., Hofmann, M.; Werner, A.; Blochwitz-Nimoth, J. (2003), Doped organic semiconductors: Physics and application in light emitting diodes. *Org. Electron.*, 4, 89–103 (DOI: 10.1016/j.orgel.2003.08.004); (e) Ferraris, J.; Cowan, D. O., Walatka Jr, V., Perlstein, J. H. (1973), Electron transfer in a new highly conducting donor-acceptor complex. *J. Am. Chem. Soc.*, 95, 948–949 (DOI: 10.1021/ja00784a066); (f) Walzer, K., Maennig, B., Pfeiffer, M., Leo, K. (2007), Highly Efficient Organic Devices Based on Electrically Doped Transport Layers. *Chem. Rev.*, 107, 1233–1271 (DOI: 10.1021/cr050156n).
- [11] (a) Michinobu, T., May, J. C., Lim, J. H., Boudon, C., Gisselbrecht, J.-P., Seiler, P., Gross, M., Biaggio, I., Diederich, F. (2005), A new class of organic donor–acceptor molecules with large third-order optical nonlinearities. *Chem. Commun.*, 737–739 (DOI: 10.1039/B417393G); (b) Michinobu, T., Boudon, I., Gisselbrecht, J.-P., Seiler, P., Frank, B., Moonen, N. N. P., Gross, M., Diederich, F. (2006), Donor-Substituted 1,1,4,4-Tetracyanobutadienes (TCBDs): New Chromophores with Efficient Intramolecular Charge-Transfer Interactions by Atom-Economic Synthesis. *Chem.–Eur. J.*, 12, 1889–1905 (DOI: 10.1002/chem.200501113). (c) Kivala, M., Boudon, C., Gisselbrecht, J.-P., Seiler, P., Gross, M., Diederich, F. (2007), Charge-Transfer-Chromophore durch Cycloaddition-Retro- Elektrocyclisierung: multivalente Systeme und Kaskadenreaktionen *Angew. Chem.*, 119, 6473–6477 (DOI: 10.1002/ange.200701733).
- [12] (a) Kivala, M., Boudon, C., Gisselbrecht, J.-P., Seiler, P., Gross, M., Diederich, F. (2007), A novel reaction of 7,7,8,8-

- tetracyanoquinodimethane (TCNQ): charge-transfer chromophores by [2 + 2] cycloaddition with alkynes. *Chem. Commun.*, 4731–4733 (DOI: 10.1039/B713683H); (b) Reutenauer, P., Kivala, M., Jarowski, P. D., Boudon, C., Gisselbrecht, J., Gross, M., Diederich, F. (2007), New strong organic acceptors by cycloaddition of TCNE and TCNQ to donor-substituted cyanoalkynes. *Chem. Commun.*, 4898–4900 (DOI: 10.1039/B714731G); (c) Kato, S.-i., Kivala, M., Schweizer, W. B., Boudon, C., Gisselbrecht, J.-P., Diederich, F. (2009), Origin of Intense Intramolecular Charge-Transfer Interactions in Nonplanar Push–Pull Chromophores. *Chem.–Eur. J.*, 15, 8687–8691 (DOI: 10.1002/chem.200901630).
- [13] (a) Michinobu, T. (2008), Click-Type Reaction of Aromatic Polyamines for Improvement of Thermal and Optoelectronic Properties. *J. Am. Chem. Soc.*, 130, 14074–14075 (DOI: 10.1021/ja8061612); (b) Li, Y., Kazuma, T., Michinobu, T. (2010), Double Click Synthesis and Second-Order Nonlinearities of Polystyrenes Bearing Donor–Acceptor Chromophores. *Macromolecules*, 43, 5277–5286 (DOI: 10.1021/ma100869m); (c) Michinobu, T. (2011), Adapting semiconducting polymer doping techniques to create new types of click postfunctionalization. *Chem. Soc. Rev.*, 40, 2306–2316 (DOI: 10.1039/C0CS00205D); (d) Fujita, T., Tsuboi, K., Michinobu, T. (2011), High-Yielding Alkyne-Tetracyanoethylene Addition Reactions: A Powerful Tool for Analyzing Alkyne-Linked Conjugated Polymer Structures. *Macromol. Chem. Phys.*, 212, 1758–1766 (DOI: 10.1002/macp.201100198).
- [14] (a) Shoji, T., Ito, S., Toyota, K., Yasunami, M., Morita, N. (2008), Synthesis, Properties, and Redox Behavior of Mono-, Bis-, and Tris[1,1,4,4,-tetracyano-2-(1-azulenyl)-3-butadienyl] Chromophores Binding with Benzene and Thiophene Cores. *Chem.–Eur. J.*, 14, 8398–8408 (DOI: 10.1002/chem.200701981); (b) Shoji, T., Ito, S., Toyota, K., Iwamoto, T., Yasunami, M., Morita, N. (2009), Reactions between 1-Ethynylazulenes and 7,7,8,8-Tetracyanoquinodimethane (TCNQ):

- Preparation, Properties, and Redox Behavior of Novel Azulene-Substituted Redox-Active Chromophores. *Eur. J. Org. Chem.*, 4316–4324 (DOI: 10.1002/ejoc.200900539) (c) Shoji, T., Higashi, J., Ito, S., Okujima, T., Yasunami, M., Morita, N. (2012), Synthesis of donor–acceptor chromophores by the [2 + 2] cycloaddition of arylethynyl-2H-cyclohepta[b]furan-2-ones with 7,7,8,8-tetracyanoquinodimethane. *Org. Biomol. Chem.*, 10, 2431–2438 (DOI: 10.1039/C2OB06931H).
- [15] Krauß, N., Kielmann, M., Ma, J., Butenschön, H. (2015), Reactions of Alkynyl- and 1,1'-Dialkynylferrocenes with Tetracyanoethylene – Unanticipated Addition at the Less Electron-Rich of Two Triple Bonds. *Eur. J. Org. Chem.*, 2622–2631 (DOI: 10.1002/ejoc.201500105).
- [16] Kato, S.-i., Noguchi, H., Jin, S., Nakamura, Y. (2016), Synthesis and Electronic, Optical, and Electrochemical Properties of a Series of Tetracyanobutadiene-Substituted Carbazoles. *Asian J. Org. Chem.*, 5, 246–256 (DOI: 10.1002/ajoc.201500431).
- [17] (a) Misra, R., Gautam, P. (2014), Tuning of the HOMO–LUMO gap of donor-substituted symmetrical and unsymmetrical benzothiadiazoles. *Org. Biomol. Chem.*, 12, 5448–5457 (DOI: 10.1039/C4OB00629A); (b) Gautam, P., Maragani, R., Misra, R. (2014), Tuning the HOMO–LUMO gap of donor-substituted benzothiazoles. *Tetrahedron Letters*, 55, 6827–6830 (DOI: 10.1016/j.tetlet.2014.10.094); (c) Dhokale, B., Jadhav, T., Mobin, S. M., Misra, R. (2016), Tetracyanobutadiene functionalized ferrocenyl BODIPY dyes. *Dalton Trans.*, 45, 1476–1483 (DOI: 10.1039/C5DT04037J); (d) Rout, Y., Gautam, P., Misra, R. (2017), Unsymmetrical and Symmetrical Push–Pull Phenothiazines. *J. Org. Chem.*, 82, 6840–6845 (DOI: 10.1021/acs.joc.7b00991); (e) Gautam, P., Sharma, R., Misra, R., Keshtov, M. L., Kuklin, S. A., Sharma, G. D. (2017), Donor–acceptor–acceptor (D–A–A) type 1,8-naphthalimides as non-fullerene small molecule acceptors for bulk heterojunction solar cells. *Chem. Sci.*, 8, 2017–2024 (DOI: 10.1039/C6SC04461A); (f) Patil, Y., Misra, R., Singhal, R., Sharma, G. D. (2017), Ferrocene-

- diketopyrrolopyrrole based non-fullerene acceptors for bulk heterojunction polymer solar cells. *J. Mater. Chem. A*, 5, 13625–13633 (DOI: 10.1039/C7TA03322B).
- [18] Zhang, W.-W., Yu, Y.-G., Lu, Z.-D., Mao, W.-L., Li, Y.-Z., Meng, Q.-J. (2007), Ferrocene–Phenothiazine Conjugated Molecules: Synthesis, Structural Characterization, Electronic Properties, and DFT-TDDFT Computational Study. *Organometallics*, 26, 865–873 (DOI: 10.1021/om060923o).
- [19] (a) Lai, R. Y., Fabrizio, E. F., Lu, L., Jenekhe, S. A., Bard, A. J. (2001), Synthesis, Cyclic Voltammetric Studies, and Electrogenenerated Chemiluminescence of a New Donor-Acceptor Molecule: 3,7-[Bis[4-phenyl-2-quinolyl]]-10-methylphenothiazine. *J. Am. Chem. Soc.*, 123, 9112–9118 (DOI: 10.1021/ja0102235); (b) Kulkarni, A. P., Wu, P.-T., Kwon, T. W., Jenekhe, S. A. (2005), Phenothiazine-Phenylquinoline Donor–Acceptor Molecules: Effects of Structural Isomerism on Charge Transfer Photophysics and Electroluminescence. *J. Phys. Chem. B*, 109, 19584–19594 (DOI: 10.1021/jp0529772).
- [20] Frisch M. J., Trucks G. W., Schlegel H. B., Scuseria G. E., Robb M. A., Cheeseman J. R., Scalmani G., Barone V., Mennucci B., Petersson G. A., Nakatsuji H., Caricato M., Li X., Hratchian H. P., Izmaylov A. F., Bloino J., Zheng G., Sonnenberg J. L., Hada M., Ehara M., Toyota K., Fukuda R., Hasegawa J., Ishida M. Nakajima T., Honda Y., Kitao O., Nakai H., Vreven T., Montgomery J. A. Jr., Peralta J. E., Ogliaro F., Bearpark M., Heyd J. J., Brothers E., Kudin K. N., Staroverov V. N., Kobayashi R., Normand J., Raghavachari K., Rendell A., Burant J. C., Iyengar S. S., Tomasi J., Cossi M., Rega N., Millam N. J., Klene M., Knox J. E., Cross J. B., Bakken V., Adamo C., Jaramillo J., Gomperts R., Stratmann R. E., Yazyev O., Austin A. J., Cammi R., Pomelli C.; Ochterski J. W., Martin R. L., Morokuma K., Zakrzewski V. G., Voth G. A., Salvador P., Dannenberg J. J., Dapprich S., Daniels A. D., Farkas O., Foresman J. B.,

Ortiz J. V., Cioslowski J., Fox D. J. (2009), *Gaussian 09, revision A.02*;
Gaussian, Inc.:Wallingford, CT.

Chapter 5

Donor–Acceptor Based BODIPY Functionalized Phenothiazines

5.1. Introduction

π -conjugated donor-acceptor (D-A) molecular systems have been explored for various applications in optoelectronics.^[1] The photonic properties of donor-acceptor systems can be significantly improved by varying the donor/acceptor unit or the π -linker.^[2]

BODIPY is a strong electron acceptor and possesses unique spectroscopic and photophysical properties, such as strong absorption in the visible region with high molar extinction coefficient, and high fluorescence quantum yield.^[3] The BODIPY moiety exhibit tunable redox potentials together with robustness against light and chemicals.^[4] The photonic properties of BODIPY can be tuned by functionalizing it with donor molecules at the *meso*- and the pyrrolic positions (α and β positions).^[5]

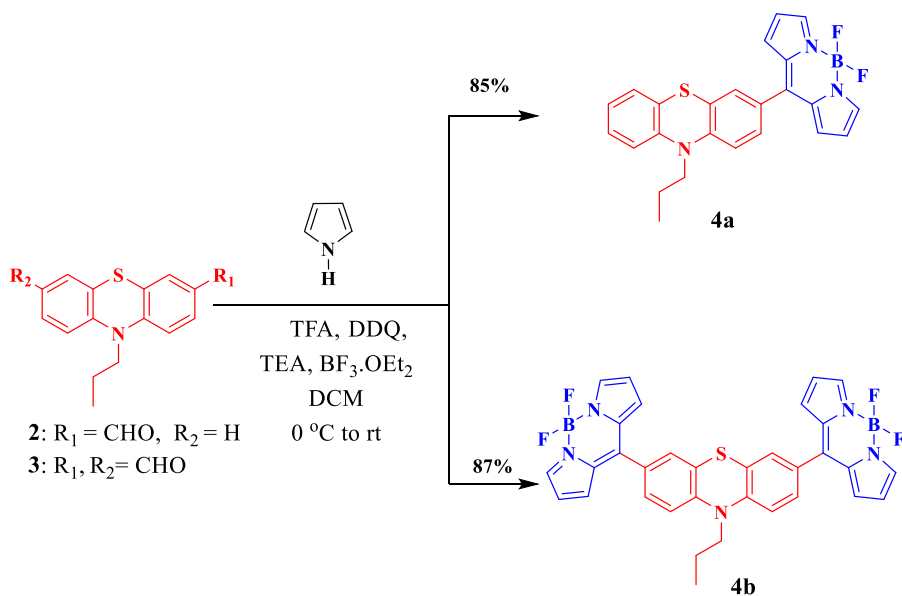
Phenothiazines are important class of heterocycles with low reversible oxidation potential which makes them suitable electrophores in organic materials.^[6] Phenothiazine is a strong donor due to its electron rich nitrogen and sulfur atoms and has been used to design molecular systems for organic light-emitting diodes (OLEDs), photovoltaic cells and organic field effect transistors.^[7] Müller *et al.* have reported various phenothiazine derivatives and explored their properties.^[8] We have reported design and synthesis of variety of β and *meso* substituted ferrocenyl BODIPYs.^[9] Therefore we were interested to incorporate the donor phenothiazine unit at the *meso* position of BODIPY directly and via ethynyl spacer. Giribabu *et al.* have synthesized directly linked mono-phenothiazine BODIPYs at the N- and 3 position of phenothiazine donor moiety.^[10]

In this chapter we wish to report the design and synthesis unsymmetrical D–A, D– π –A and symmetrical A–D–A, A– π –D– π –A type of BODIPY

functionalized phenothiazines and investigated the effect of ethynyl spacer on the photonic properties and HOMO–LUMO gap.

5.2. Results and Discussion

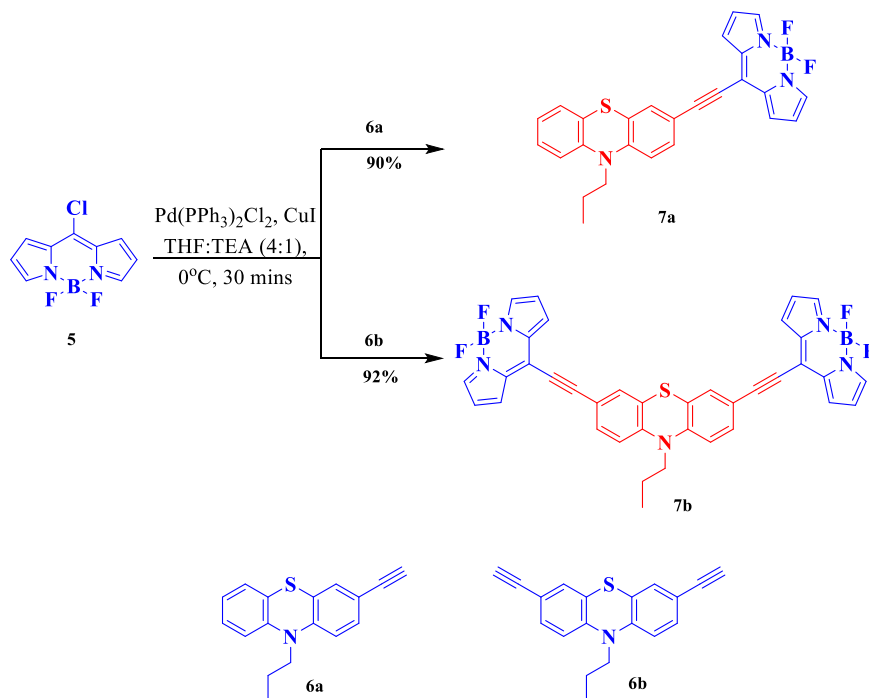
The synthetic route of BODIPY functionalized phenothiazines **4a** and **4b** are shown in Scheme 5.1. The condensation reaction of formylated phenothiazines **2/3** with excess pyrrole in the presence of catalytic amount of trifluoroacetic acid (TFA), followed by oxidation using 2,3-dichloro-5,6-dicyano-1,4-benzoquinone (DDQ) and complexation with boron trifluoride etherate ($\text{BF}_3 \cdot \text{OEt}_2$) resulted **4a** and **4b** in 85% and 87% yields respectively.



Scheme 5.1. Synthesis of phenothiazines **4a** and **4b**.

The phenothiazines **6a** and **6b** were obtained from the Sonogashira cross-coupling reaction of mono and di-brominated phenothiazines with trimethylsilylacetylene (TMS), followed by the de-protection of TMS using K_2CO_3 .^[8c] The precursor 8-chloro BODIPY **5** was obtained by the reaction of dipyrrolylketone with POCl_3 followed by the complexation with $\text{BF}_3 \cdot \text{OEt}_2$ in presence of triethylamine.^[11] The Pd-catalyzed Sonogashira cross-coupling reaction of phenothiazines **6a** and **6b** with 8-chloro BODIPY **5** at 0 °C resulted phenothiazine functionalized BODIPYs **7a** and **7b** in 90% and 92% yields

respectively (Scheme 5.2). The BODIPY functionalized phenothiazines **4a**, **4b**, **7a** and **7b** are soluble in common organic solvents such as dichloromethane, chloroform, tetrahydrofuran, toluene and were well characterized by ^1H NMR, ^{13}C NMR and HRMS techniques.



Scheme 5.2. Synthesis of phenothiazines **7a** and **7b**.

5.3. Thermogravimetric Analysis

The thermal stability of BODIPY functionalized phenothiazines **4a**, **4b**, **7a** and **7b** were investigated by the thermogravimetric analysis (TGA) at a heating rate of $10^\circ\text{C min}^{-1}$, under nitrogen atmosphere (Figure 5.1). The decomposition temperatures (T_d) values for 10% weight loss in monosubstituted phenothiazine functionalized BODIPYs **4a** and **7a** show decomposition temperature above 580°C whereas disubstituted phenothiazine functionalized BODIPYs **4b** and **7b** with two acceptor units show the decomposition temperature above 366°C . The trend in thermal stability of the phenothiazine functionalized BODIPYs follows the order **7a** > **4a** > **4b** > **7b**. This indicates that increase in the number of BODIPY units leads to decrease in thermal stability.

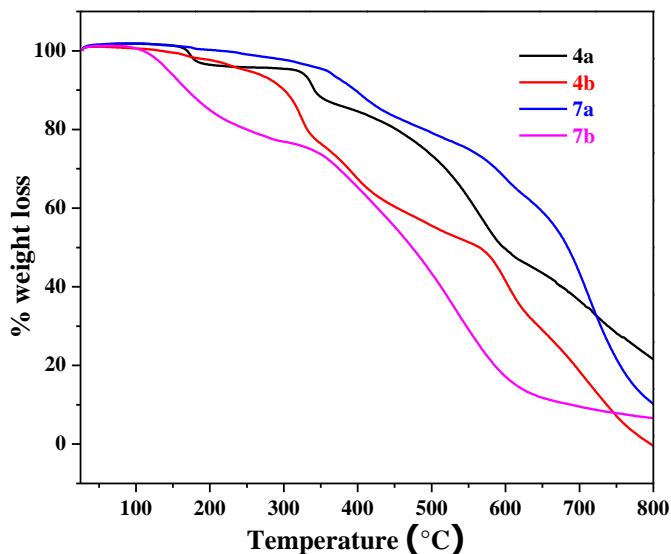


Figure 5.1. Thermogravimetric analysis of BODIPY functionalized phenothiazines **4a**, **4b**, **7a** and **7b** measured at a heating rate of $10\text{ }^{\circ}\text{C min}^{-1}$ under nitrogen atmosphere.

5.4. Photophysical Properties

The electronic absorption spectra of the BODIPY functionalized phenothiazines **4a**, **4b**, **7a** and **7b** were recorded in dry dichloromethane (Figure 5.2) and the data are summarized in Table 1. The BODIPY functionalized phenothiazines **4a**, **4b**, **7a** and **7b** exhibit weak absorption bands at 235–440 nm region and strong absorption bands at 450–580 nm region which corresponds to $\pi\rightarrow\pi^*$ transitions.^[5b, 12] The incorporation of acetylenic linkage between phenothiazine and BODIPY moieties in **7a** and **7b** results in redshift of 40 nm in the absorption maxima, as compared to directly linked BODIPYs **4a** and **4b**. The BODIPY functionalized phenothiazines **4a** and **4b** show charge transfer (CT) band between 530–670 nm whereas **7a** and **7b** show CT band between 572–723 nm which is supported by TD-DFT calculation. The trend in the optical HOMO–LUMO gap values exhibits the order **4b** > **4a** > **7b** > **7a**. These data revealed that

incorporation of acetylenic linkage between the phenothiazine and BODIPY units decreases the HOMO–LUMO gap values.

The solvent dependent absorption spectra show negative solvatochromic effect. The increase in solvent polarity (from toluene to methanol) exhibit blue shifted absorption curves in BODIPY functionalized phenothiazines **4a**, **4b**, **7a** and **7b** (Figure 5.3 and Table 5.2).

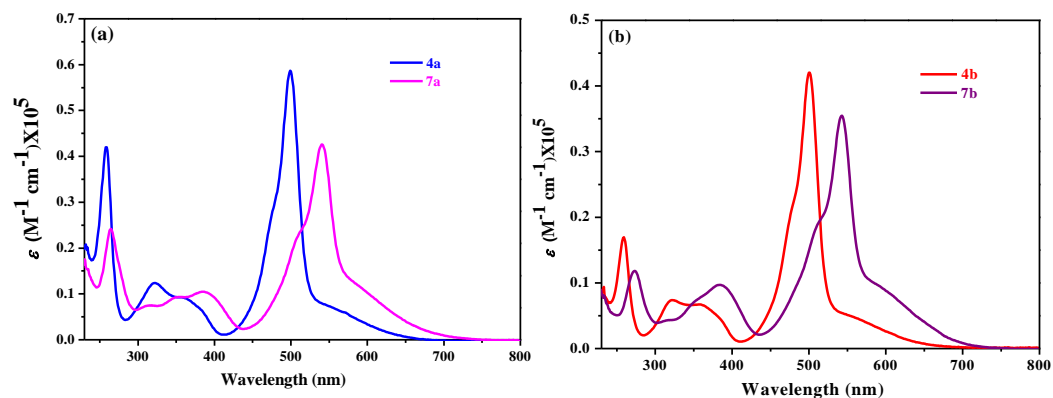


Figure 5.2. Electronic absorption spectra of (a) **4a** and **7a** and (b) **4b** and **7b** in dichloromethane (1×10^{-5} M).

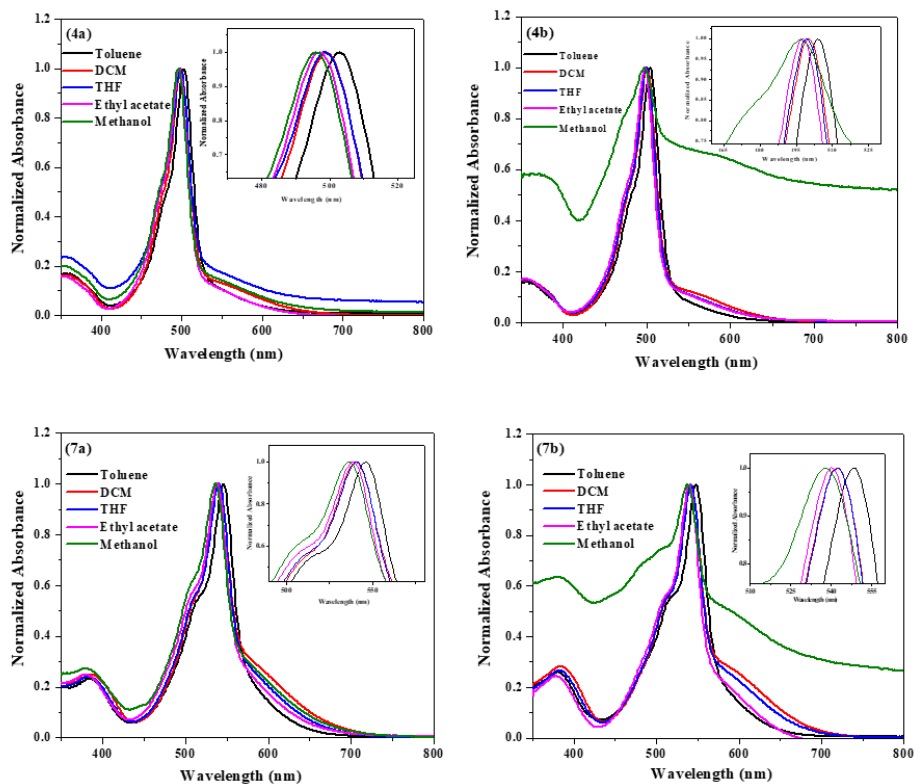


Figure 5.3. Absorption curves of BODIPY functionalized phenothiazines **4a**, **4b**, **7a** and **7b** in different solvents.

5.5. Electrochemical Properties

The electrochemical properties of BODIPY functionalized phenothiazines **4a**, **4b**, **7a** and **7b** were recorded by cyclic voltammetry (CV) technique in dichloromethane using tetrabutylammoniumhexafluorophosphate (TBAPF₆) as a supporting electrolyte. The representative CV plot is shown in Figure 5.4 and the data are summarized in Table 5.1.

The BODIPY functionalized phenothiazines **4a**, **4b**, **7a** and **7b** show one reversible oxidation peak in the range of 1.25 to 0.6 V. The compounds **4a** and **4b** show oxidation peaks at 0.85 V and 0.95 V, whereas acetylene linked BODIPY functionalized phenothiazines **7a** and **7b** show oxidation peaks at 0.87 V and 0.98 V respectively. The oxidation peak of BODIPYs follow the order **7b** > **4b** > **7a** > **4a**. This indicates that the incorporation of two acceptor BODIPY units decreases the electron density on phenothiazine and results in higher oxidation potential.

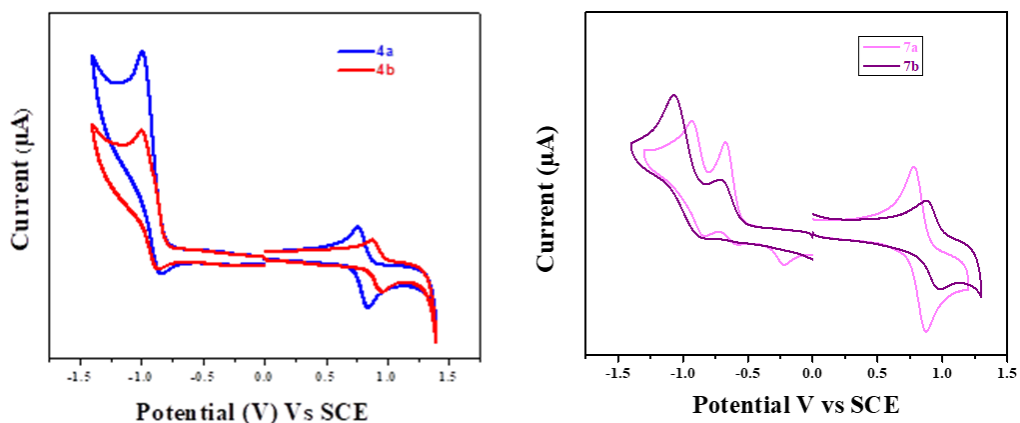


Figure 5.4. Cyclic Voltammogram plot of **4a**, **4b**, **7a** and **7b** in dichloromethane.

The BODIPYs **4a** and **4b** show reduction peaks at -0.91 V and -0.93 V, whereas the acetylene linked phenothiazine functionalized BODIPYs **7a** and **7b** show first reduction peaks at -0.59 V and -0.70 V, and the second reduction peaks at -0.83 V and -0.87 V which is due to the BODIPY unit. The reduction

potential values of BODIPYs **7a** and **7b** are lower as compared to BODIPYs **4a** and **4b** which indicates the electron deficient nature in the formers.^[13]

The calculated electrochemical band gap (E_{gap}) of BODIPY functionalized phenothiazines **4a**, **4b**, **7a** and **7b** are 1.51 eV, 1.63 eV, 1.25 eV and 1.49 eV respectively. The E_{gap} values follow the trend **4b** > **4a** > **7b** > **7a** which is in agreement with the optical and theoretical HOMO–LUMO gap.

Table 5.1. The photophysical and electrochemical properties of BODIPY functionalized phenothiazines **4a**, **4b**, **7a** and **7b**.

| Compound | Photophysical data | | | Electrochemical data ^c | | | T_d (°C) ^d | HOMO–LUMO Gap ^e (eV) |
|-----------|--|--|-------------------------------|-----------------------------------|----------------------|------------------------------------|-------------------------|---------------------------------|
| | λ_{abs} (nm) ^a | ϵ (M ⁻¹ cm ⁻¹) | Optical Gap (eV) ^b | E_{ox} (V) | E_{red} (V) | E_{gap} (eV) ^c | | |
| 4a | 258 | 41990 | | | | | | |
| | 322 | 12370 | 2.02 | 0.85 | -0.91 | 1.51 | 580 | 2.72 |
| | 499 | 58608 | | | | | | |
| 4b | 258 | 16942 | | | | | | |
| | 322 | 7353 | 1.95 | 0.95 | -0.93 | 1.63 | 415 | 2.83 |
| | 500 | 41962 | | | | | | |
| 7a | 264 | 24180 | | | | | | |
| | 384 | 10417 | 1.75 | 0.87 | -0.59 | 1.25 | 671 | 2.54 |
| | 540 | 42560 | | | -0.83 | | | |
| 7b | 271 | 11800 | | | | | | |
| | 383 | 9699 | 1.79 | 0.98 | -0.70 | 1.49 | 366 | 2.61 |
| | 542 | 35370 | | | -0.87 | | | |

^a Absorbance measured in dichloromethane at 1×10^{-5} M concentration; λ_{abs} : absorption wavelength; ϵ : extinction coefficient. ^b determined from onset wavelength of the UV/Vis absorption; ^c recorded by cyclic voltammetry, in 0.1 M solution of TBAPF₆ in DCM at 100 mV s⁻¹ scan rate versus SCE electrode; ^d decomposition temperatures for 10% weight loss under N₂ atmosphere at heating rate of 10 °C min⁻¹; ^e theoretical HOMO–LUMO gap obtained from DFT calculation

Table 5.2. Absorption maxima of BODIPY functionalized phenothiazines **4a**, **4b**, **7a** and **7b** in different solvents.

| Compounds | λ_{max} (nm) | | | | |
|-----------|-----------------------------|-----|-----|---------------|----------|
| | Toluene | DCM | THF | Ethyl acetate | Methanol |
| 4a | 502 | 499 | 498 | 496 | 495 |
| 4b | 503 | 500 | 499 | 497 | 496 |
| 7a | 545 | 540 | 540 | 538 | 536 |
| 7b | 548 | 542 | 541 | 540 | 537 |

5.6. Theoretical Calculations

The density functional theory calculations were performed to explore the geometrical and electronic structures of the BODIPY functionalized phenothiazines **4a**, **4b**, **7a** and **7b** at B3LYP/6-31+G** level for B, C, F, H, N and S.^[14] The frontier molecular orbitals (FMOs) of **4a**, **4b**, **7a** and **7b** are shown in Figure 5.5. The HOMO orbitals of BODIPY functionalized phenothiazines **4a**, **4b**, **7a** and **7b** are mainly localized on phenothiazine unit and LUMO orbitals on BODIPY unit, clearly indicates strong donor-acceptor interaction between phenothiazine and BODIPY unit. The calculated HOMO levels of **4a**, **4b**, **7a** and **7b** are -5.43eV , -5.76eV , -5.48eV and -5.8eV respectively and the corresponding LUMO levels are -2.71eV , -2.93eV , -2.94eV and -3.2eV respectively. The theoretical HOMO–LUMO gap values for **4a**, **4b**, **7a** and **7b** are 2.72, 2.83, 2.54 and 2.61, respectively and follow the order **4b** > **4a** > **7b** > **7a**. The data reveals that acetylene linked BODIPY functionalized phenothiazines **7a** and **7b** exhibit lower HOMO and LUMO energy levels than those of directly linked **4a** and **4b**. The HOMO–LUMO gap values from the DFT calculations were found to be in good agreement with the optical bandgap (E_{gap}) values calculated from the UV/Vis absorption spectrum (Table 5.1).

The time-dependent DFT (TD-DFT) calculations were performed at the B3LYP/6-31G (d, p) level to explain the electronic transitions. The results indicate that BODIPY functionalized phenothiazines show two main electronic transitions in the visible region. The transitions with oscillator strengths, assignments and composition are shown in Table 5.3. The transition that occurs from HOMO to LUMO in the longer-wavelength region is associated with the ICT transition of the phenothiazine and BODIPY unit, whereas the other transition in the short-wavelength region is related to π - π^* transition (Table 5.3). The main charge-transfer transition in BODIPY functionalized phenothiazines **4a**, **4b**, **7a** and **7b** occurs from HOMO→LUMO whereas the π - π^* transition occurs from HOMO-1→LUMO, HOMO-2→LUMO+1, HOMO-2→LUMO and HOMO-3→LUMO, respectively.

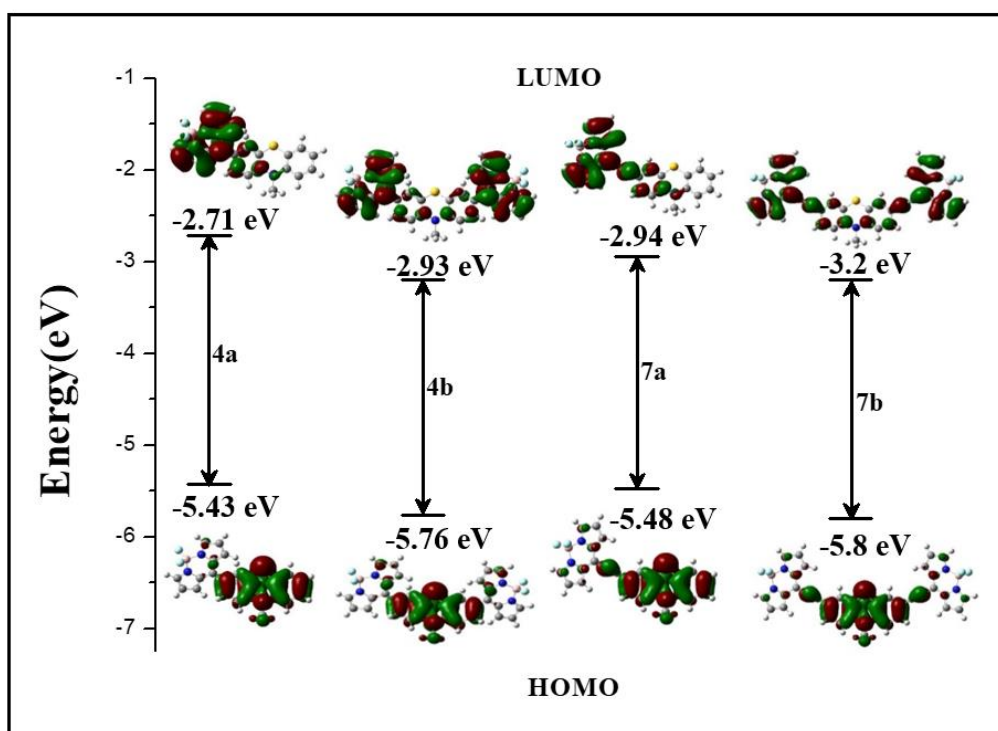


Figure 5.5. Energy diagram showing the HOMO and LUMO wave functions and energies of BODIPY functionalized phenothiazines **4a**, **4b**, **7a** and **7b** as determined at B3LYP/6-31G** level.

Table 5.3. Calculated electronic transition of BODIPY functionalized phenothiazines **4a**, **4b**, **7a** and **7b**.

| Compound | Wavelength | Composition | f^a | Assignment |
|-----------|------------|-----------------------------|-------|-------------|
| | ds | | | |
| 4a | 590 | HOMO→LUMO (0.70) | 0.15 | ICT |
| | 415 | HOMO-1→LUMO (0.68) | 0.43 | $\pi-\pi^*$ |
| 4b | 578 | HOMO→LUMO (0.70) | 0.24 | ICT |
| | 414 | HOMO-2→LUMO+1 (0.58) | 0.58 | $\pi-\pi^*$ |
| 7a | 617 | HOMO→LUMO (0.70) | 0.46 | ICT |
| | 425 | HOMO-2→LUMO (0.70) | 0.38 | $\pi-\pi^*$ |
| 7b | 624 | HOMO→LUMO (0.70) | 0.85 | ICT |
| | 418 | HOMO-3→LUMO (0.68) | 0.54 | $\pi-\pi^*$ |

f^a oscillator strength

5.7. Experimental Section

General Methods

Chemicals were used as received unless otherwise indicated. All the oxygen or moisture sensitive reactions were carried out under argon atmosphere. ^1H NMR spectra were recorded using a 400 MHz spectrometer. Chemical shifts are reported in delta (δ) units, expressed in parts per million (ppm) downfield from tetramethylsilane (TMS) using residual protonated solvent as an internal standard $\{\text{CDCl}_3, 7.26 \text{ ppm}\}$. ^{13}C NMR spectra were recorded using a 400 MHz spectrometer. Chemical shifts are reported in delta (δ) units, expressed in parts per million (ppm) downfield from tetramethylsilane (TMS) using the solvent as internal standard $\{\text{CDCl}_3, 77.0 \text{ ppm}\}$. The ^1H NMR splitting patterns have been described as “s, singlet; d, doublet; t, triplet and m, multiplet”. UV/Vis spectrums of all compounds were recorded in dichloromethane solution. Cyclic voltammograms were recorded on electrochemical analyzer using Glassy carbon

as working electrode, Pt wire as the counter electrode, and Saturated Calomel Electrode (SCE) as the reference electrode. The scan rate was 100mVs⁻¹ for Cyclic Voltammetry. A solution of tetrabutylammonium hexafluorophosphate (TBAPF₆) in DCM (0.1M) was used as supporting electrolyte.

Synthesis of 3-(4,4-difluoro-4-bora-3a,4a-diaza-s-indacene)-10-propyl-10H-phenothiazine (4a)

To a stirred solution of compound **2** (0.5 g, 1.85 mmol) and pyrrole (2.48 g, 37.0 mmol) acid catalyst (trifluoroacetic acid, 0.001 mL) was added at room temperature. The reaction mixture was allowed to stir at room temperature for 2 h under argon atmosphere. The excess pyrrole was removed by distillation under reduced pressure. To purify the dipyrromethane intermediate column chromatography was done with DCM/hexane (1:1). In a 100 mL round bottomed flask dipyrromethane intermediate (200 mg, 0.518 mmol) was dissolved in dichloromethane (50 mL) and oxidized with DDQ (141.23 mg, 0.621 mmol) The reaction were allowed to stir for 1 h at room temperature. Then trimethylamine (209.06 mg, 2.07 mmol) was added to the reaction mixture followed by BF₃.OEt₂ (293.79 mg, 2.07 mmol). The stirring was continued for another 1 hr. Then the mixture was evaporated and the crude was purified by silica gel column chromatography with hexane/CH₂Cl₂ (1:1) to get the desired compound **4a** as a dark colored solid, Yield 0.189 g (85%); mp 145 °C. ¹H NMR (400 MHz, CDCl₃): δ 7.92 (2H, s), 7.41-7.35 (2H, m), 7.22-7.15 (2H, m), 7.02-6.91 (5H, m), 6.55 (2H, d, *J* = 4 Hz), 3.90 (2H, t, *J* = 8 Hz), 1.95-1.88 (2H, m), 1.07 (3H, t, *J* = 8 Hz); ¹³C NMR (100 MHz, CDCl₃): δ 148.2, 146.3, 143.9, 134.4, 134.5, 131.1, 130.5, 129.3, 127.9, 127.6, 125.1, 123.8, 123.3, 118.2, 115.8, 114.8, 49.4, 20.1, 11.3; HRMS (ESI-TOF): *m/z* calculated for C₂₄H₂₀BF₂N₃S= 431.1336 [M+H]⁺, measured 431.1332 [M+H]⁺.

Synthesis of 3,7-bis(4,4-difluoro-4-bora-3a,4a-diaza-s-indacene)-10-propyl-10H-phenothiazine (4b)

To a stirred solution of compound **3** (0.5g, 1.85mmol) and pyrrole (4.96g, 74.0mmol) acid catalyst (trifluoroacetic acid, 0.002mL) was added at room temperature. The reaction mixture was allowed to stir at room temperature for 2 h

under argon atmosphere. The excess pyrrole was removed by distillation under reduced pressure. To purify the dipyrromethane intermediate column chromatography was done with DCM/hexane (1:1). In a 100 mL round bottomed flask dipyrromethane intermediate (200 mg, 0.518 mmol) was dissolved in dichloromethane (50 mL) and oxidized with DDQ (282.46 mg, 1.24 mmol). The reaction was allowed to stir for 1 h at room temperature. Then trimethylamine (418.12 mg, 4.14 mmol) was added to the reaction mixture followed by BF₃.OEt₂ (587.58 mg, 4.14 mmol). The stirring was continued for another 1 h. Then the mixture was evaporated and the crude was purified by silica gel column chromatography with hexane/CH₂Cl₂ (1:1) to get the desired compound **4b** as a dark colored solid, Yield 0.279 g (87%); mp >250 °C. ¹H NMR (400 MHz, CDCl₃): δ 7.94 (4H, s), 7.46-7.43 (2H, dd), 7.37 (2H, s), 7.03 (6H, d, *J* = 8 Hz), 6.56 (4H, d, *J* = 4 Hz), 3.97 (2H, t, *J* = 8 Hz), 2.02-1.95 (2H, m), 1.14 (3H, t, *J* = 8 Hz); ¹³C NMR (100 MHz, CDCl₃): δ 147.0, 146.1, 144.1, 134.8, 131.3, 131.0, 129.7, 124.4, 118.8, 115.6, 50.2, 30.0, 20.4, 11.6; HRMS (ESI-TOF): *m/z* calculated for C₃₃H₂₅B₂F₄N₅S = 644.1856 [M+Na]⁺, measured 644.1852 [M+Na]⁺.

Synthesis of 3-(4,4-difluoro-4-bora-3a,4a-diaza-s-indacene)-ethynyl-10-propyl-10H-phenothiazine (7a)

In a 100 mL round bottomed flask 8-Chloro BODIPY **5** (88.14 mg, 0.39 mmol) and 3-ethynyl-10-propyl-10H-phenothiazine **6a** (100 mg, 0.39 mmol) were dissolved in THF–triethylamine (4 : 1, v/v; 5 ml), and in an ice bath the mixture was cooled to 0 °C. The reaction mixture was purged with argon, and Pd(PPh₃)₂Cl₂ (13.68 mg, 5 mol%), and CuI (3.6 mg, 5 mol%) were added. The reaction mixture was stirred at 0 °C for 30 min. Upon the completion of the reaction, the mixture was evaporated and purified by silica gel column chromatography with hexane/CH₂Cl₂ (1:4) to get the desired compound **7a** as a dark colored solid. Yield 0.159 g (90%); mp 150 °C. ¹H NMR (400 MHz, CDCl₃): δ 7.81 (2H, s), 7.45 (1H, d, *J* = 8 Hz), 7.38 (3H, s), 7.19 (1H, t, 8 Hz), 7.13 (1H, d, *J* = 8 Hz) 6.99 (1H, t, *J* = 8 Hz), 6.91-6.88 (2H, m), 6.55 (2H, d, *J* = 7.7 Hz), 3.87 (2H, t, *J* = 8 Hz), 1.91-1.81(2H, m), 1.05 (3H, t, *J* = 4 Hz); ¹³C

NMR (100 MHz, CDCl₃): δ 148.0, 143.6, 142.8, 136.2, 132.7, 131.2, 128.5, 127.7, 127.6, 127.5, 125.1, 123.5, 123.4, 118.0, 115.9, 115.1, 114.1, 107.3, 85.6, 49.5, 20.0, 11.2; HRMS (ESI-TOF): m/z calculated for C₂₆H₂₀BF₂N₂S= 455.1438 [M+H]⁺, measured 455.1473 [M+H]⁺.

Synthesis of 3,7-bis(4,4-difluoro-4-bora-3a,4a-diaza-s-indacene)-bis(ethene-1,2-diyl)-10-propyl-10H-phenothiazine (7b)

In a 100 mL round bottomed flask 8-Chloro BODIPY **5** (176.28 mg, 0.78 mmol) and 3,7-diethynyl-10-propyl-10H-phenothiazine **6a** (100 mg, 0.39 mmol) were dissolved in THF–triethylamine (10 : 1, v/v; 5 ml), and in an ice bath the mixture was cooled to 0 °C. The reaction mixture was purged with argon, and Pd(PPh₃)₂Cl₂ (13.68 mg, 5 mol%), and CuI (3.6 mg, 5 mol%) were added. The reaction mixture was stirred at 0 °C for 30 min. Upon the completion of the reaction, the mixture was evaporated and purified by silica gel column chromatography with hexane/CH₂Cl₂ (1:4) to get the desired compound **7b** as a dark colored solid. Yield: 0.25 g (92%); mp >250 °C. ¹H NMR (400 MHz, CDCl₃): δ 7.81 (4H, s), 7.46 (3H, d, J = 8 Hz), 7.36 (5H, s), 6.88 (2H, d, J = 12 Hz), 6.54 (4H, s), 3.89 (2H, t, J = 4 Hz), 1.90-1.82 (2H, m), 1.06 (2H, t, J = 8 Hz); ¹³C NMR (100 MHz, CDCl₃): δ 146.3, 143.2, 136.3, 132.9, 131.2, 128.7, 127.3, 124.2, 118.2, 115.7, 115.4, 105.8, 85.6, 49.9, 20.0, 11.1; HRMS (ESI-TOF): m/z calculated for C₃₇H₂₀B₂F₄N₅S= 692.1857 [M+Na]⁺, measured 692.1852 [M+Na]⁺.

5.8. Conclusions

In summary, a series of donor-acceptor BODIPY functionalized phenothiazines were designed and synthesized by the condensation and Pd-catalyzed Sonogashira cross-coupling reaction. The photophysical and electrochemical studies show strong donor-acceptor interactions between phenothiazine and BODIPY. The optimized structure of acetylene linked phenothiazine BODIPY shows co-planar orientation of the phenothiazine donor and the BODIPY acceptor units which leads to extension of conjugation and significant red shift of the absorption bands in **7a** and **7b**. The calculated HOMO–

LUMO gap values were lower in acetylene linked phenothiazine BODIPYs. The increase in acceptor units of BODIPY functionalized phenothiazines lowers the thermal stability. Further studies into the synthesis of phenothiazine derivatives with other acceptor units and their application for organic electronic devices are ongoing in our laboratory.

3.9. References

- [1] (a) Kraft A., Grimsdale A. C., Holmes A. B. (1998), Electroluminescent Conjugated Polymers—Seeing Polymers in a New Light, *Angew. Chem. Int. Ed.*, 37, 402–428 (DOI: 10.1002/(SICI)1521-3773(19980302)37:4<402::AID-ANIE402>3.0.CO;2-9). (b) Chen C. H., Shi J., Tang C. W., Klubek K. P. (2000), Recent developments in the synthesis of red dopants for Alq₃ hosted electroluminescence, *Thin Solid Films*, 363, 327–331 (DOI: 10.1016/S0040-6090(99)01010-X). (c) Kobayashi N., Inagaki S., Nemykin V. N., Nonomura T. (2001), A Novel Hemiporphyrzine Comprising Three Isoindolediimine and Three Thiadiazole Units, *Angew. Chem. Int. Ed.*, 40, 2710–2712 (DOI: 10.1002/1521-3773(20010716)40:14<2710::AID-ANIE2710>3.0.CO;2-A). (d) Ji C., Yin L., Li K., Wang L., Jiang X., Suna Y., Li Y. (2015), D– π –A– π –D-type low band gap diketopyrrolopyrrole based small molecules containing an ethynyl-linkage: synthesis and photovoltaic properties, *RSC Adv.*, 5, 31606–31614 (DOI: 10.1039/c5ra01946j). (e) Wong W. Y., Wong W. K., Raithby P. R. (1998), Synthesis, characterisation and properties of platinum(II) acetylide complexes of ferrocenylfluorene: novel soluble donor–acceptor heterometallic materials, *J. Chem. Soc. Dalton Trans.*, 2761–2766 (DOI: 10.1039/A803168A).
- [2] (a) Zhang W.-W., Mao W.-L., Hu Y.-X., Tian Z.-Q., Wang Z.-L., Meng Q.-J. J. (2009), Phenothiazine-anthraquinone donor-acceptor molecules: synthesis, electronic properties and DFT-TDDFT computational study, *Phys. Chem. A*, 113, 9997–10004 (DOI:

- 10.1021/jp903390v). (b) Lu H., Mack J., Yang Y., Shen Z. (2014), Structural modification strategies for the rational design of red/NIR region BODIPYs, *Chem. Soc. Rev.*, 43, 4778–4823 (DOI: 10.1039/c4cs00030g).
- (c) Loudet A., Burgess K. (2007), BODIPY Dyes and Their Derivatives: Syntheses and Spectroscopic Properties, *Chem. Rev.*, 107, 4891–4932 (DOI: 10.1021/cr078381n). (d) Han J., Burgess K. (2010), Fluorescent Indicators for Intracellular pH, *Chem. Rev.*, 110, 2709–2728 (DOI: 10.1021/cr900249z).
- [3] (a) Boens N., Leen V., Dehaen W. (2012), Fluorescent indicators based on BODIPY, *Chem. Soc. Rev.*, 41, 1130–1172 (DOI: 10.1039/C1CS15132K). (b) Kim H. S., Pham T. C. T., Yoon K. B. (2012), A novel class of nonlinear optical materials based on host–guest composites: zeolites as inorganic crystalline hosts, *Chem. Commun.*, 48, 4659–4673 (DOI: 10.1039/C2CC30919J). (c) Dhokale B., Jadhav T., Mobin S. M., Misra R. (2014), Meso enamine substituted BODIPYs, *Chem. Commun.*, 50, 9119–9121 (DOI: 10.1039/C4CC03857F).
- [4] (a) Yokoi H., Wachi N., Hiroto S., Shinokubo H. (2014), Oxidation of 2-amino-substituted BODIPYs providing pyrazine-fused BODIPY trimmers, *Chem. Commun.*, 50, 2715–2717 (DOI: 10.1039/c3cc48738e). (b) Bessette A., Hanan G. S. (2014), Design, synthesis and photophysical studies of dipyrromethene-based materials: insights into their applications in organic photovoltaic devices, *Chem. Soc. Rev.*, 43, 3342–3405 (DOI: 10.1039/c3cs60411j). (c) Zhao N., Xuan S., Fronczek F. R., Smith K. M., Vicente M. G. H. (2015), Stepwise Polychlorination of 8 - Chloro-BODIPY and Regioselective Functionalization of 2,3,5,6,8-Pentachloro-BODIPY, *J. Org. Chem.*, 80, 8377–8383 (DOI: 10.1021/acs.joc.5b01147). (d) Ulrich G., Ziessel R., Harriman A. (2008), The chemistry of fluorescent bodipy dyes: versatility unsurpassed, *Angew. Chem. Int. Ed.*, 47, 1184–1201 (DOI: 10.1002/anie.200702070).
- [5] (a) Zatsikha Y. V., Holstrom C. D., Chanawanno K., Osinski A. J., Ziegler C. J., Nemykin V. N. (2017), Observation of the Strong Electronic

Coupling in Near-Infrared-Absorbing Tetraferrocene aza-Dipyrromethene and aza-BODIPY with Direct Ferrocene- α - and Ferrocene- β -Pyrrole Bonds: Toward Molecular Machinery with Four-Bit Information Storage Capacity, *Inorg. Chem.*, 56(2), 991–1000 (DOI: 10.1021/acs.inorgchem.6b02806). (b) Zatsikha Y. V., Maligaspe E., Purchel A. A., Didukh N. O., Wang Y., Kovtun Y. P., Blank D. A. Nemykin V. N. (2015), Tuning Electronic Structure, Redox, and Photophysical Properties in Asymmetric NIR-Absorbing Organometallic BODIPYs, *Inorg. Chem.*, 54(16), 7915–7928 (DOI: 10.1021/acs.inorgchem.5b00992). (c) Uchida T., Ito M., Kozawa K. (1983), Crystal Structure and Related Properties of Phenothiazine Cation Radical-Hexachloroantimonate. Monoclinic(I) Form, *Bull. Chem. Soc. Jpn.* 56, 577–582 (DOI: 10.1246/bcsj.56.577). (d) Lu, H., Mack, J., Yang, Y., Shen, Z. (2014), Structural modification strategies for the rational design of red/NIR region BODIPYs, *Chem. Soc. Rev.*, 43, 4778–4823 (DOI: 10.1039/C4CS00030G).

- [6] (a) Kim G. W., Cho M. J., Yu Y. J., Kim Z. H., Jin J. I., Kim D. Y., Choi D. H. (2007), Red Emitting Phenothiazine Dendrimers Encapsulated 2-[2-[2-(4-Dimethylaminophenyl)vinyl]-6-methylpyran-4-ylidene] malononitrile Derivatives, *Chem. Mater.*, 19, 42–50 (DOI: 10.1021/cm0618493). (b) Achar B. N., Ashok M. A., (2008), Electrical measurements and thermal kinetics study of phenothiazine and a few of its derivatives, *Mater. Chem. Phys.*, 108, 8–15 (DOI:10.1016/j.matchemphys.2007.08.039). (c) Hauck M., Schonhaber J., Zuccherro A. J., Hardcastle K. I., Müller T. J. J., Bunz U. H. F. (2007), Phenothiazine Cruciforms: Synthesis and Metallochromic Properties, *J. Org. Chem.*, 72, 6714–6725 (DOI: 10.1021/jo0709221).
- [7] Hart A. S., KC C. B., Subbaiyan N. K., Karr P. A., D’Souza F. (2012), Phenothiazine-Sensitized Organic Solar Cells: Effect of Dye Anchor Group Positioning on the Cell Performance, *ACS Appl. Mater. Interfaces*, 4, 5813–5820 (DOI: 10.1021/am3014407).

- [8] (a) Hauck M., Stolte M., Schçnhaber J., Kuball H.-G., Müller T. J. J. (2011), Synthesis, Electronic, and Electro-Optical Properties of Emissive Solvatochromic Phenothiazinyl Merocyanine Dyes, *Chem. Eur. J.*, 17, 9984–9998 (DOI:10.1002/chem.201100592). (b) Sailer M., Gropeanu R.-A., Müller T. J. J. (2003), Practical Synthesis of Iodo Phenothiazines. A Facile Access to Electrophore Building Blocks, *J. Org. Chem.*, 68, 7509–7512 (DOI: 10.1021/jo034555z). (c) Krämer, C. S., Zeitler, K., Müller, T. J. J. (2000), Synthesis of Functionalized Ethynylphenothiazine Fluorophores, *Org. Lett.*, 2, 3723–3726 (DOI: 10.1021/ol0066328).
- [9] (a) Dhokale B., Gautam P., Mobin S. M., Misra R. (2013), Donor–acceptor, ferrocenyl substituted BODIPYs with marvelous supramolecular interactions, *Dalton Trans.*, 42, 1512–1518 (DOI: 10.1039/c2dt31632c). (b) Gautam P., Dhokale B., Mobin S. M., Misra R. (2012), Ferrocenyl BODIPYs: synthesis, structure and properties, *RSC Adv.*, 2, 12105–12107 (DOI: 10.1039/c2ra21964f). (c) Misra R., Dhokale B., Jadhav T., Mobin S. M. (2013), Donor–acceptor meso-alkynylated ferrocenyl BODIPYs: synthesis, structure, and properties, *Dalton Trans.*, 42, 13658–13666 (DOI: 10.1039/c3dt51374b).
- [10] Duvva N., Sudhakar K., Badgurjar D., Chitta R., Giribabu L. (2015), Spacer controlled photo-induced intramolecular electron transfer in a series of phenothiazine-boron dipyrromethene donor–acceptor dyads, *Journal of Photochemistry and Photobiology A: Chemistry*, 312, 8–19 (DOI: 10.1016/j.jphotochem.2015.07.007).
- [11] Leen V., Yuan P., Wang L., Boens N., Dehaen W. (2012), Synthesis of Meso-Halogenated BODIPYs and Access to Meso-Substituted Analogues, *Org. Lett.*, 14, 6150–6153 (DOI: 10.1021/ol3028225).
- [12] Chen Y., Zhao J., Guo H., Xie L. (2012), Geometry Relaxation-Induced Large Stokes Shift in Red-Emitting Borondipyrromethenes (BODIPY) and Applications in Fluorescent Thiol Probes, *J. Org. Chem.*, 77, 2192–2206, (DOI:10.1021/jo202215x).

- [13] (a) Dhokale B., Jadhav T., Mobin S. M., Misra R. (2016), Tetracyanobutadiene functionalized ferrocenyl BODIPY dyes, *Dalton Trans.*, 45, 1476-1483 (DOI: 10.1039/c5dt04037j). (b) Kato S.-I., Diederich F. (2010), Non-planar push-pull chromophores, *Chem. Commun.*, 46, 1994-2006 (DOI: 10.1039/b926601a). (c) Retenauer P., Kivala M., Jarowski P. D., Boudon C., Gisselbrecht J.-P., Gross M., Diederich F., New strong organic acceptors by cycloaddition of TCNE and TCNQ to donor-substituted cyanoalkynes, *Chem. Commun.*, 46, 4898-4900, (DOI: 10.1039/B714731G).
- [14] Frisch M. J., Trucks G. W., Schlegel H. B., Scuseria G. E., Robb M. A., Cheeseman J. R., Scalmani G., Barone V., Mennucci B., Petersson G. A., Nakatsuji H., Caricato M., Li X., Hratchian H. P., Izmaylov A. F., Bloino J., Zheng G., Sonnenberg J. L., Hada M., Ehara M., Toyota K., Fukuda R., Hasegawa J., Ishida M., Nakajima T., Honda Y., Kitao O., Nakai H., Vreven T., Montgomery J. A. Jr., Peralta J. E., Ogliaro F., Bearpark M., Heyd J. J., Brothers E., Kudin K. N., Staroverov V. N., Kobayashi R., J., Raghavachari K., Rendell A., Burant J. C., Iyengar S. S., Tomasi J., Cossi M., Rega N., Millam J. M., Klene M., Knox J. E., Cross J. B., Bakken V., Adamo C., Jaramillo J., Gomperts R., Stratmann R. E., Yazyev O., Austin A. J., Cammi R., Pomelli C., Ochterski J. W., Martin R. L., Morokuma K., Zakrzewski V. G., Voth G. A., Salvador P., Dannenberg J. J., Dapprich S., Daniels A. D., Farkas Ö., Foresman J. B., Ortiz J. V., Cioslowski J., Fox D. J. (2009), Gaussian 09, Revision C.01, Gaussian, Inc., Wallingford, CT.

Chapter 6

1,1,4,4-Tetracyanobuta-1,3-Diene (TCBD)- and Cyclohexa-2,5-Diene-1,4-Diylidene-Expanded TCBD-Substituted BODIPY-Phenothiazines: Tuning of HOMO-LUMO gap

6.1. Introduction

The development of synthetic supramolecular donor-acceptor (D-A) systems for mimicking the natural photosynthetic complexes, which harvests the solar light and convert it into storable chemical energy, have attracted the attention of researchers for the last couple of decades.^[1-6] Photosynthetic energy conversion is a crucial and fundamental process, which is initiated by the absorption of light from antenna systems and transport it to the reaction center to promote light induced sequential electron transfer events.^[7] In order to design the artificial supramolecular systems, significant efforts have been given to synthesize D-A molecular systems as their light harvesting properties could easily be tuned by varying the (i) D/A redox potentials, (ii) intramolecular distance, and (iii) nature of the linker. Our groups and others have explored a variety of D-A systems for light harvesting applications in recent years.^[1-6,8]

Among the most commonly studied chromophores for artificial photosynthesis, 4,4-difluoroboradiaza-s-indacene (BODIPY) have been largely employed as a building block of donor-acceptor systems.^[9, 10] BODIPYs reveal strong absorption with high molar extinction coefficient values, high fluorescence quantum yields along with tunable redox properties.^[9a-c] The photonic properties of BODIPYs can be modified by the incorporation of appropriate donor/acceptor groups at the *meso*- and the pyrrolic positions (α and β positions).^[11] On the other hand, S and N containing heterocyclic phenothiazine moiety is known for its high thermal and chemical robustness.^[12] Phenothiazines can easily be functionalized by electrophilic substitution reaction at the aromatic position, oxidation at sulfur and nucleophilic reaction at the N position.^[13] Furthermore, phenothiazine possesses low oxidation potential which make them useful electron donor chromophores in organic photonic materials.^[14] In contrast, the cyano-based

1,1,2,2-tetracyanoethylene (TCNE) and 7,7,8,8-tetracyanoquinodimethane (TCNQ) are known as the most commonly used strong acceptors.^[15] They react with the electron rich alkynes easily *via* [2+2] cycloaddition–electrocyclic ring-opening reaction.^[15] The resulted 1,1,4,4-tetracyanobuta-1,3-diene (TCBD) and cyclohexa-2,5-diene-1,4-ylidene-expanded TCBD (abbreviated as DCNQ = dicyanodiquinodimethane) substituted D–A systems show broad absorption along with strong intramolecular charge transfer (ICT) transitions, properties relevant in optoelectronic applications.^[8,16]

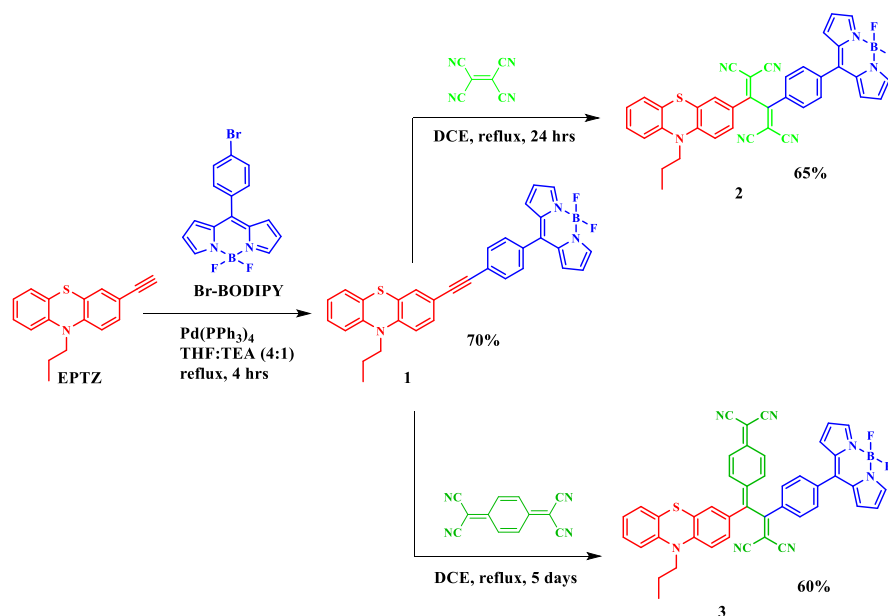
Diederich *et al.* have investigated a large array of TCBD and DCNQ derivatives and studied their photophysical and electrochemical properties.^[17] Michinobu *et al.* have explored a variety of TCBD and DCNQ substituted molecules for optoelectronic applications.^[18] Our groups have reported a variety of acetylene linked chromophores which were subjected to [2+2] cycloaddition–electrocyclic ring-opening reaction with TCBD and DCNQ and studied their photophysical and electrochemical properties for pertinent optoelectronic applications.^[8,19]

Herein, in this chapter we wish to report the design and synthesis of phenothiazine-BODIPY based TCBD and cyclohexa-2,5- diene-1,4-ylidene-expanded TCBD chromophores. We were interested to improve the photophysical properties of phenothiazine-BODIPY chromophore by incorporating TCNE and TCNQ acceptors in the molecular building block. We have also performed the theoretical calculations, in order to investigate the conformation and the photonic properties of the phenothiazines.

6.2. Results and Discussion

The synthetic route of phenothiazine-BODIPY derived donor-acceptors, **1–3** is shown in Scheme 6.1. The phenothiazine-BODIPY **1** was synthesized *via* Pd-catalyzed Sonogashira cross-coupling reaction of ethynyl phenothiazine (**EPTZ**) with **Br-BODIPY** in presence of THF in 70% yield. The Pd-catalyzed Sonogashira cross-coupling reaction of 3-bromo-10-propyl-10*H*-phenothiazine with TMS acetylene in THF, followed by deprotection with NaOH and methanol, resulted in intermediate **EPTZ**.^[11a] On the other hand, the condensation reaction

of 4-bromo-benzaldehyde and pyrrole followed by the oxidation with DDQ and complexation with BF_3 -etherate resulted in intermediate **Br-BODIPY**.^[20]



Scheme 6.1. Synthesis of phenothiazines **1**, **2** and **3**.

In order to investigate the photonic and electronic properties of strong electron acceptors on the phenothiazine-BODIPY **1**, TCNE and TCNQ were incorporated in between phenothiazine and BODIPY. The [2+2] cycloaddition–electrocyclic ring-opening reaction of **1** with TCNE at 83 °C for 24 h in dichloroethane resulted in compound **2** in 65% yield. The phenothiazine **1** underwent similar transformation in presence of TCNQ acceptor at 83 °C for 5 days in dichloroethane resulted in compound **3** in 60% yield. The donor-acceptor conjugates **1**, **2** and **3** were soluble in common organic solvents, such as dichloroethane, dichloromethane, tetrahydrofuran and chloroform. All the compounds were fully characterized by using ^1H and ^{13}C NMR spectroscopy and HRMS techniques.

6.3. Photophysical Properties

The absorption spectrum of the studied compounds **1–3** were recorded in dichloromethane at room temperature (Figure 6.1) and the data are compiled in

Table 6.1. The phenothiazine-BODIPY molecules **1–3** showed strong absorption in the 410–550 nm region (with peak maxima at 503 nm for **1**), and based on its similarity with other BODIPY compounds, this was attributed to the $S_0 \rightarrow S_1$ ($\pi \rightarrow \pi^*$) transition.^[9] In addition a weaker absorption band was observed in the range of 300–400 nm which could be due to the $S_0 \rightarrow S_2$ ($\pi \rightarrow \pi^*$) transition of BODIPY with contributions from phenothiazine entity. The TCBD incorporated derivative, **2** exhibited significant broadening in $S_0 \rightarrow S_1$ transition accompanied by a broad shoulder peak spanning 550–700 nm range. This was also the trend in the DCNQ incorporated derivative, **3** that showed broadening of the $S_0 \rightarrow S_1$ peak with a new broad peak covering the 550–900 nm range. The new broad peak observed in the case of **2** and **3** has been attributed to intramolecular charge transfer (ICT) resulting from strong D–A interactions, viz., TCBD and DCNQ interacting with spatially close phenothiazine and BODIPY entities.

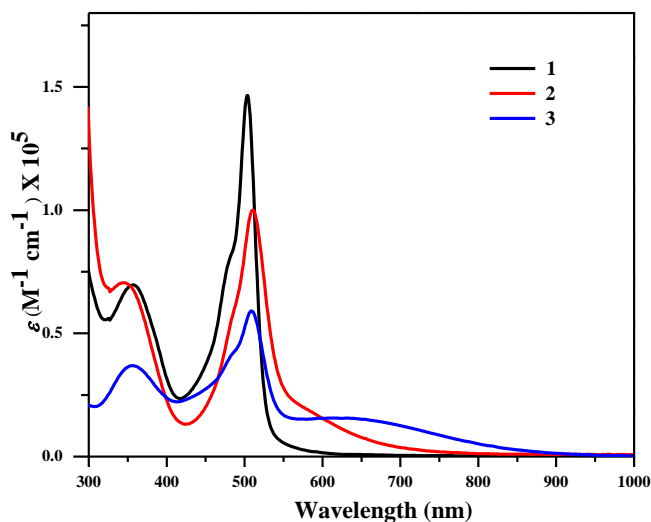


Figure 6.1. The electronic absorption spectra of phenothiazines **1**, **2** and **3** in dichloromethane (1×10^{-5} M).

The optical band gap of phenothiazines **1**, **2** and **3** follow the order **1**>**2**>**3**. The trend in the optical band gap signifies that the influence of cyclohexa-2,5-diene-1,4-ylidene-expanded TCBD on phenothiazine-BODIPY molecule leading to strong CT absorption and low optical band gap.

Table 6.1. Photophysical and theoretical properties of phenothiazines **1–3**.

| Phenothiazines | Photophysical data ^a | | Theoretical data ^c | |
|----------------|---------------------------------|--|--|------------------------------|
| | λ_{abs} (nm) | ϵ ($\text{M}^{-1} \text{cm}^{-1}$) | Optical Band Gap (eV) ^b | HOMO-LUMO energy gap (eV) |
| 1 | 503 | 146768 | 2.22 | 2.3 |
| | 357 | 69621 | | |
| 2 | 510 | 100043 | 1.71 | 2.11 |
| | 344 | 70532 | | |
| 3 | 666 | 147951 | 1.42 | 1.63 |
| | 509 | 59089 | | |
| | 356 | 37034 | | |

^a Absorbance measured in dichloromethane at 1×10^{-5} M concentration; λ_{abs} : absorption wavelength; ϵ : extinction coefficient. ^b determined from onset wavelength of the UV/Vis absorption; ^c obtained from density functional theory calculations at B3LYP/6-31+G** level.

6.4. Theoretical Calculations

The density functional theory calculation was performed on phenothiazines **1–3** to explore the structure and electronic properties at B3LYP/6-31+G** level for B, C, F, H, N, O and S.^[21] The energy diagram of the phenothiazines **1–3** is shown in Figure 6.2. The optimized structure of the phenothiazines showed nonplanar twisted geometry Figure 6.3. The HOMO energy levels of the phenothiazines **1–3** are mainly localized on the phenothiazine donor moiety. The LUMO energy level of compound **1** is localized on the BODIPY moiety. In case of compounds **2** and **3** the LUMO energy levels are mainly localized on the TCBD and cyclohexa-2,5-diene-1,4-ylidene-expanded TCBD acceptors. The theoretically calculated HOMO energy levels for phenothiazines **1**, **2** and **3** are -5.08 , -5.69 and -5.59 eV, respectively whereas the LUMO energy levels are -2.78 , -3.58 and -3.96 eV, respectively.

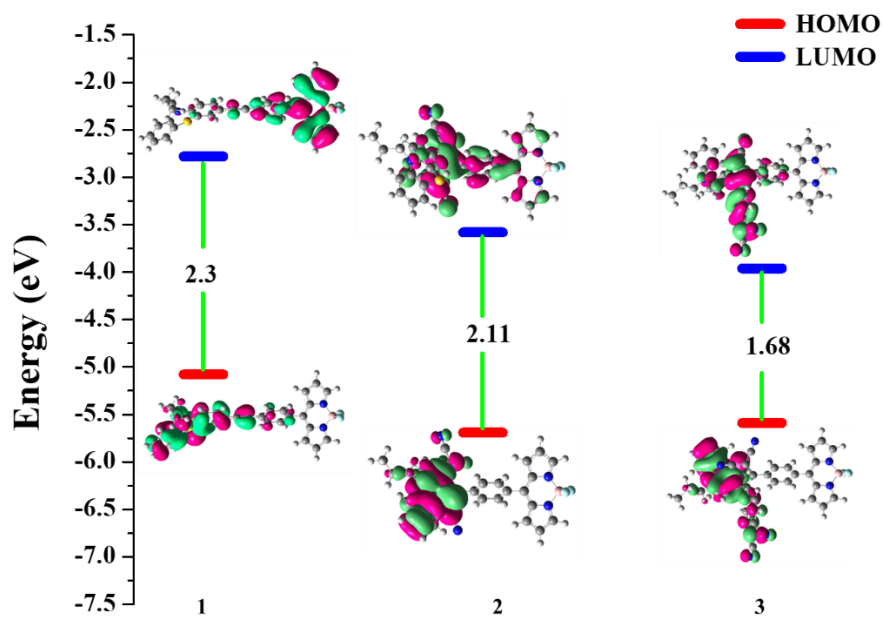


Figure 6.2. Energy diagram showing the HOMO and LUMO wave functions and energies of phenothiazines 1–3 as determined at B3LYP/6-31G** level.

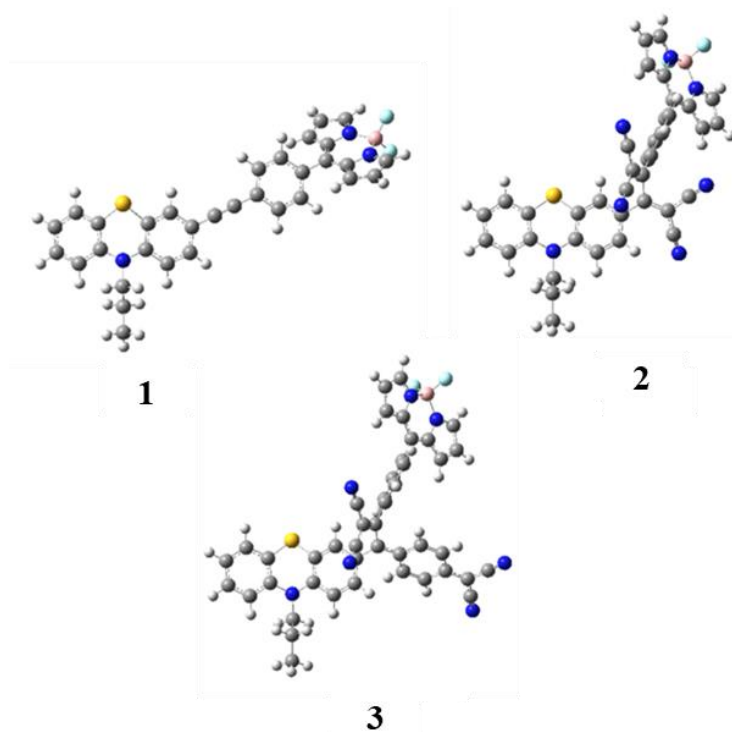


Figure 6.3. Theoretically optimized structures of phenothiazines **1–3** by B3LYP/6-31+G** basis set.

6.5. Experimental Section

General Methods. Chemicals were used as received unless otherwise indicated. All the oxygen or moisture sensitive reactions were carried out under argon atmosphere. ^1H NMR spectra were recorded using a 400 MHz spectrometer. Chemical shifts are reported in delta (δ) units, expressed in parts per million (ppm) downfield from tetramethylsilane (TMS) using residual protonated solvent as an internal standard $\{\text{CDCl}_3, 7.26 \text{ ppm}\}$. ^{13}C NMR spectra were recorded using a 400 MHz spectrometer. Chemical shifts are reported in delta (δ) units, expressed in parts per million (ppm) downfield from tetramethylsilane (TMS) using the solvent as internal standard $\{\text{CDCl}_3, 77.0 \text{ ppm}\}$. The ^1H NMR splitting patterns have been described as “s, singlet; d, doublet; t, triplet and m, multiplet”.

Synthesis of compound **1**.

In a 100 mL round bottomed flask Br-BODIPY (88.14 mg, 0.39 mmol) and 3-ethynyl-10-propyl-10H-phenothiazine **EPTZ** (100 mg, 0.39 mmol) were dissolved in THF–triethylamine (4 : 1, v/v; 5 ml). The reaction mixture was purged with argon, and $\text{Pd}(\text{PPh}_3)_2\text{Cl}_2$ (13.68 mg, 5 mol%), and CuI (3.6 mg, 5 mol%) were added. The reaction mixture was stirred at 70 °C for 4 h. Upon the completion of the reaction, the mixture was evaporated and purified by silica gel column chromatography with hexane/ CH_2Cl_2 (3:7) to get the desired compound **1** as a dark colored solid. (Yield: 140.0 mg, 70%). ^1H NMR (400 MHz, CDCl_3): δ = 7.95 (s, 2H), 7.64 (d, J = 6.6, 2H), 7.55 (d, J = 6.6, 2H), 7.35–7.31 (m, 2H), 7.17–7.11 (m, 2H), 6.95–6.92 (m, 3H), 6.87 (d, J = 6.4, 1H), 6.81 (d, J = 6.84, 1H), 6.56 (d, J = 4.4, 2H), 3.83 (t, J = 5.76, 2H), 1.88–1.80 (m, 2H), 1.02 (t, J = 5.88, 3H); ^{13}C NMR (100 MHz, CDCl_3): δ = 146.6, 145.9, 144.5, 144.2, 134.7, 133.2, 131.4, 130.9, 130.6, 130.3, 127.5, 127.4, 126.5, 125.0, 124.1, 122.9, 118.6, 116.3, 115.6, 115.1, 92.0, 88.3, 49.4, 20.1, 11.3; HRMS (ESI-TOF): m/z calculated for $\text{C}_{32}\text{H}_{24}\text{BF}_2\text{N}_3\text{S}$ = 532.183 $[\text{M}+\text{H}]^+$, measured 532.1764 $[\text{M}+\text{H}]^+$.

Synthesis of compound 2.

Tetracyanoethylene (TCNE) (19.2 mg, 0.15 mmol) was added to a solution of compound **1** (98.6 mg, 0.15 mmol) in C₂H₄Cl₂ (50 mL). The mixture was refluxed for 83 °C for 24 h. After the completion of the reaction the solvent was removed in vacuum, and the product was purified by column chromatography with CH₂Cl₂ as the eluent to yield compound **2** as a dark violet colored solid. (Yield: 80.0 mg, 65%); ¹H NMR (400 MHz, CDCl₃): δ = 7.98 (m, 2H), 7.83 (d, J = 8.5, 2H), 7.74 (d, J = 8.3, 2H), 7.43 (s, 1H), 7.21–7.18 (m, 1H), 7.10–7.00 (m, 2H), 6.93–6.84 (m, 4H), 6.58 (d, J = 2.76, 2H), 3.88 (t, J = 7.28, 2H), 1.92–1.83 (m, 2H), 1.06 (t, J = 7.28, 3H); ¹³C NMR (100 MHz, CDCl₃): δ = 151.6, 148.1, 145.5, 143.7, 141.7, 139.5, 134.4, 133.1, 131.6, 130.5, 129.3, 128.1, 127.7, 127.5, 125.9, 124.8, 123.8, 119.3, 116.3, 115.2, 50.1, 20.0, 11.1; HRMS (ESI-TOF): m/z calculated for C₃₂H₂₄BF₂N₃S = 659.1876 [M]⁺, measured 659.1881 [M]⁺.

Synthesis of compound 3.

Tetracyanoquinodimethane (TCNQ; 44.9 mg, 0.22 mmol) was added to a solution of compound **1** (98.8 mg, 0.22 mmol) in C₂H₄Cl₂ (50 mL). The mixture was refluxed for 83 °C for 5 days. After the completion of the reaction the solvent was removed in vacuum, and the product was purified by column chromatography with CH₂Cl₂ as the eluent to give compound **3** as a dark-brown solid (Yield: 82.0 mg, 60%); ¹H NMR (400 MHz, CDCl₃): δ = 7.96 (s, 2H), 7.77 (d, J = 7.76, 2H), 7.67 (d, J = 7.76, 2H), 7.48 (d, J = 9.52, 1H), 7.35–7.29 (m, 2H), 7.20–7.15 (m, 2H), 7.08 (t, J = 7.56, 2H), 7.01–6.98 (m, 2H), 6.87 (t, J = 6.52, 2H), 6.81 (s, 2H), 6.55 (s, 2H), 3.84 (t, J = 6.52, 2H), 1.88–1.83 (m, 2H), 1.03 (t, J = 7.04, 3H); ¹³C NMR (100 MHz, CDCl₃): δ = 169.8, 153.6, 148.9, 147.8, 145.3, 143.9, 142.7, 138.7, 135.7, 135.6, 134.6, 134.4, 133.9, 133.5, 131.7, 131.5, 131.3, 129.4, 129.2, 128.3, 127.9, 127.6, 126.7, 125.9, 124.0, 122.7, 119.2, 116.1, 115.4, 113.5, 112.3, 111.9, 88.8, 49.8, 20.0, 11.2; HRMS (ESI-TOF): m/z calculated for C₃₂H₂₄BF₂N₃S = 735.219 [M]⁺, measured 735.2192 [M]⁺.

6.6. Conclusions

In summary, BODIPY-phenothiazine, **1** was synthesized *via* Pd-catalyzed Sonogashira cross coupling reaction. Subsequently, the TCBD and DCNQ substituted molecules, **2** and **3** were synthesized by [2+2] cycloaddition–electrocyclic ring-opening reactions of compound **1** with TCNE and TCNQ, respectively. The photophysical data showed that the incorporation of TCBD and DCNQ acceptors in the BODIPY substituted phenothiazines resulted in strong D–A interactions which led to low HOMO–LUMO band gap in compounds **2** and **3** as compared to **1**. The UV-vis absorption spectra of compounds **2** and **3** showed ICT transitions along with significant broadening in $S_0 \rightarrow S_1$ transition. The theoretical calculations of compounds **1–3** revealed that the DCNQ substituted **3** stabilized the LUMO energy level to greater extent as compared to TCBD substituted phenothiazine **2**. This work provides a strategy for the design and synthesis of D–A based chromophores with low HOMO–LUMO gap for various optoelectronic applications.

6.7. References

- [1] (a) Wasielewski, M. R. (2009), Self-Assembly Strategies for Integrating Light Harvesting and Charge Separation in Artificial Photosynthetic Systems, *Acc. Chem. Res.*, 42, 1910-1921 (DOI: 10.1021/ar9001735); (b) Wasielewski, M. R. (1992), Photoinduced electron transfer in supramolecular systems for artificial photosynthesis, *Chem. Rev.*, 92, 435-461 (DOI: 10.1021/cr00011a005); (c) Gust, D., Moore, T. A., Moore, A. L. (2009), Solar Fuels via Artificial Photosynthesis, *Acc. Chem. Res.*, 42, 1890-1898 (DOI: 10.1021/ar900209b).
- [2] (a) Armaroli, N., Balzani, V. (2007), The future of energy supply: Challenges and opportunities, *Angew. Chem. Int. Ed.*, 46, 52-66 (DOI: 10.1002/anie.200602373); (b) Harriman, A., Sauvage, J. P. (1996), A strategy for constructing photosynthetic models: porphyrin-containing modules assembled around transition metals, *Chem. Soc. Rev.*, 25, 41-48 (DOI: 10.1039/CS9962500041); (c) Balzani, V., Juris, A., Venturi, M.,

- Campagna, S., Serroni, S. (1996), Luminescent and Redox-Active Polynuclear Transition Metal Complexes, *Chem. Rev.*, 96, 759-834 (DOI: 10.1021/cr941154y); (d) Blanco, M. J., Jiménez, M. C., Chambron, J. C., Heitz, V., Linke, M., Sauvage, J. P. (1999), Rotaxanes as new architectures for photoinduced electron transfer and molecular motions, *Chem. Soc. Rev.*, 28, 293-305 (DOI: 10.1039/A901205B).
- [3] (a) Sánchez, L., Nazario, M., Guldi, D. M. (2005), Hydrogen-Bonding Motifs in Fullerene Chemistry, *Angew. Chem.*, 117, 5508 (DOI: 10.1002/anie.200500321); (2005), Hydrogen-Bonding Motifs in Fullerene Chemistry, *Angew. Chem. Int. Ed.*, 44, 5374-5382 (DOI: 10.1002/anie.200500321); (b) Guldi, D. M. (2000), Fullerenes: three dimensional electron acceptor materials, *Chem. Commun.*, 321-327 (DOI: 10.1039/A907807J); (c) Mateo-Alonso, A., Guldi, D. M., Paolucci, F., Prato, M. (2007), Fullerenes: versatile building blocks for molecular machines, *Angew. Chem.*, 119, 8266-8272 (DOI: 10.1002/anie.200702725); (2007), Fullerenes: Multitask Components in Molecular Machinery, *Angew. Chem. Int. Ed.*, 46, 8120-8126 (DOI: 10.1002/anie.200702725); (d) Guldi, D. M. (2007), Nanometer scale carbon structures for charge-transfer systems and photovoltaic applications, *Phys. Chem. Chem. Phys.*, 9, 1400-1420 (DOI: 10.1039/B617684B); (e) Sgobba, V., Guldi, D. M. (2009), Carbon nanotubes—electronic/electrochemical properties and application for nanoelectronics and photonics, *Chem. Soc. Rev.*, 38, 165-184 (DOI: 10.1039/B802652C).
- [4] (a) Imahori, H., Fukuzumi, S. (2004), Porphyrin- and Fullerene-Based Molecular Photovoltaic Devices, *Adv. Funct. Mater.*, 14, 525-536 (DOI: 10.1002/adfm.200305172); (b) Fukuzumi, S. (2008), Development of bioinspired artificial photosynthetic systems, *Phys. Chem. Chem. Phys.*, 10, 2283-2297 (DOI: 10.1039/B801198M); (c) Torre, G. de La, Claessens, C. G., Torres, T. (2007), Phthalocyanines: old dyes, new materials. Putting color in nanotechnology, *Chem. Commun.*, 2000-2015 (DOI: 10.1039/B614234F); (d) Fukuzumi, S. (2007), New development of

- photoinduced electron-transfer catalytic systems, *Pure Appl. Chem.*, 79, 981-991 (DOI: 10.1351/pac200779060981); (e) Fukuzumi, S., Kojima, T. (2008), Photofunctional nanomaterials composed of multiporphyrins and carbon-based π -electron acceptors, *J. Mater. Chem.*, 18, 1427-1439 (DOI: 10.1039/B717958H).
- [5] (a) D'Souza, F., Ito, O. (2012), Photosensitized electron transfer processes of nanocarbons applicable to solar cells, *Chem. Soc. Rev.*, 41, 86-96 (DOI: 10.1039/C1CS15201G); (b) D'Souza, F., Ito, O. (2012) In *Multiporphyrin Array: Fundamentals and Applications*, (Ed. D. Kim), Pan Stanford Publishing: Singapore, Chapter 8, pp 389-437. (c) KC, C. B., D'Souza, F. (2016), Design and photochemical study of supramolecular donor-acceptor systems assembled via metal-ligand axial coordination, *Coord. Chem. Rev.*, 322, 104-141 (DOI: 10.1016/j.ccr.2016.05.012); (d) D'Souza, F., Sandanayaka, A. S. D., Ito, O. (2010), SWNT-Based Supramolecular Nanoarchitectures with Photosensitizing Donor and Acceptor Molecules, *J. Phys. Chem. Lett.*, 1, 2586-2593 (DOI: 10.1021/jz1009407).
- [6] (a) Sessler, J. S., Wang, B., Springs, S. L., Brown C. T. (1996) In *Comprehensive Supramolecular Chemistry* (Eds.: J. L. Atwood, J. E. D. Davies, D. D. MacNicol, F. Vogtle), Pergamon, New York, Chapter 9. (b) Sessler, J. L., Lawrence, C. M., Jayawickramarajah, J. (2007), *Chem. Soc. Rev.*, 36, 314-325 (DOI: 10.1039/B604119C).
- [7] (a) *The Photosynthetic Reaction Center* (Eds.: J. Deisenhofer, J. R. Norris), Academic Press, San Diego, (1993). (b) R. E. Blankenship, *Molecular Mechanisms of Photosynthesis*, Blackwell Sciences, Oxford, (2002). (c) *Photosynthetic Light Harvesting* (Eds.: R. Cogdell, C. Mullineaux), Springer, Dordrecht, (2008). (d) *Handbook of Photosynthesis*, 2nd ed. (Ed.: M. Pessarakli), CRC, Boca Raton, (2005).
- [8] (a) Gautam, P., Misra, R., Thomas, M. B., D'Souza, F. (2017), Ultrafast Charge-Separation in Triphenylamine-BODIPY-Derived Triads Carrying Centrally Positioned, Highly Electron-Deficient, Dicyanoquinodimethane or Tetracyanobutadiene Electron-Acceptors, *Chem. Eur. J.*, 23, 9192-9200

- (DOI: 10.1002/chem.201701604); (b) Sharma, R., Thomas, M. B., Misra, R., D'Souza, F. (2019), Strong Ground- and Excited-State Charge Transfer in C₃-Symmetric Truxene-Derived Phenothiazine-Tetracyanobutadine and Expanded Conjugates, *Angew. Chem. Int. Ed.*, 58, 4350-4355 (DOI: 10.1002/anie.201814388).
- [9] (a) Loudet, A., Burgess, K. (2007), BODIPY Dyes and Their Derivatives: Syntheses and Spectroscopic Properties, *Chem. Rev.*, 107, 4891-4932 (DOI: 10.1021/cr078381n); (b) El-Khouly, M. E., Fukuzumi, S., D'Souza, F. (2014), Photosynthetic Antenna–Reaction Center Mimicry by Using Boron Dipyrromethene Sensitizers, *ChemPhysChem*, 15, 30-47 (DOI: 10.1002/cphc.201300715); (c) Ziessel, R., Ulrich, G., Harriman, A. (2007), The chemistry of Bodipy: A new El Dorado for fluorescence tools, *New J. Chem.*, 31, 496-501 (DOI: 10.1039/B617972J); (d) Zatsikha, Y. V., Maligaspe, E., Purchel, A. A., Didukh, N. O., Wang, Y., Kovtun, Y. P., Blank, D. A., Nemykin, V. N. (2015), Tuning Electronic Structure, Redox, and Photophysical Properties in Asymmetric NIR-Absorbing Organometallic BODIPYs, *Inorg. Chem.*, 54, 7915-7928 (DOI: 10.1021/acs.inorgchem.5b00992); (e) Zatsikha, Y. V., Holstrom, C. D., Chanawanno, K., Osinski, A. J., Ziegler, C. J., Nemykin, C. J. (2017), Observation of the Strong Electronic Coupling in Near-Infrared-Absorbing Tetraferrocene aza-Dipyrromethene and aza-BODIPY with Direct Ferrocene– α - and Ferrocene– β -Pyrrole Bonds: Toward Molecular Machinery with Four-Bit Information Storage Capacity, *Inorg. Chem.*, 56, 991-1000 (DOI: 10.1021/acs.inorgchem.6b02806).
- [10] (a) Poddar, M., Gautam, P., Rout, Y., Misra, R. (2017), Donor–acceptor phenothiazine functionalized BODIPYs, *Dyes and Pigments*, 146, 368-373 (DOI: 10.1016/j.dyepig.2017.07.017); (b) Dhokale, B., Jadhav, T., Mobin, S. M., Misra, R. (2016), Tetracyanobutadiene functionalized ferrocenyl BODIPY dyes, *Dalton Trans.*, 45, 1476-1483 (DOI: 10.1039/C5DT04037J); (c) Dhokale, B., Gautam, P., Mobin, S. M., Misra, R. (2013), Donor–acceptor, ferrocenyl substituted BODIPYs with marvelous supramolecular

- interactions, *Dalton Trans.*, 42, 1512-1518 (DOI: 10.1039/C2DT31632C);
- (d) Misra, R., Dhokale, B., Jadhav, T., Mobin, S. M. (2013), Donor–acceptor meso-alkynylated ferrocenyl BODIPYs: synthesis, structure, and properties, *Dalton Trans.*, 42, 13658-13666 (DOI: 10.1039/C3DT51374B);
- (e) Gautam, P., Dhokale, B., Mobin, S. M., Misra, R. (2012), Ferrocenyl BODIPYs: synthesis, structure and properties, *RSC Adv.*, 2, 12105-12107 (DOI: 10.1039/C2RA21964F).
- [11] (a) Poddar, M., Sharma, V., Mobin, S. M., Misra, R. (2018), 1,8-Naphthalimide-Substituted BODIPY Dyads: Synthesis, Structure, Properties, and Live-Cell Imaging, *Chem. Asian J.*, 13, 2881-2890 (DOI: 10.1002/asia.201800816); (b) Carlotti, B., Poddar, M., Elisei, F., Spalletti, A., Misra, R. (2019), Energy-Transfer and Charge-Transfer Dynamics in Highly Fluorescent Naphthalimide–BODIPY Dyads: Effect of BODIPY Orientation, *J. Phys. Chem. C*, 123, 24362-24374 (DOI: 10.1021/acs.jpcc.9b05851).
- [12] (a) Bureš, F. (2014), Fundamental aspects of property tuning in push–pull molecules, *RSC Adv.*, 4, 58826-58851 (DOI: 10.1039/C4RA11264D); (b) Poddar, M., Misra, R. (2017), NIR-Absorbing Donor–Acceptor Based 1,1,4,4-Tetracyanobuta-1,3-Diene (TCBD)- and Cyclohexa-2,5-Diene-1,4-Ylidene-Expanded TCBD-Substituted Ferrocenyl Phenothiazines, *Chem. Asian J.*, 12, 2908-2915 (DOI: 10.1002/asia.201700879); (c) Hauck, M., Stolte, M., Schçnhaber, J., Kuball, H.-G., Müller, T. J. J. (2011), Synthesis, Electronic, and Electro-Optical Properties of Emissive Solvatochromic Phenothiazinyl Merocyanine Dyes, *Chem Eur J*, 17, 9984-9998 (DOI: 10.1002/chem.201100592); (d) Sailer, M., Gropeanu, R.-A., Müller, T. J. J. (2003), Practical Synthesis of Iodo Phenothiazines. A Facile Access to Electrophore Building Blocks, *J Org Chem*, 68, 7509-7512 (DOI: 10.1021/jo034555z).
- [13] (a) Franz, A. W., Rominger, F., Müller, T. J. J. (2008), Synthesis and Electronic Properties of Sterically Demanding N-Arylphenothiazines and Unexpected Buchwald–Hartwig Aminations, *J. Org. Chem.*, 73, 1795-1802

- (DOI: 10.1021/jo702389v); (b) Forrest, I., Forrest, F., Berger M. (1958), Free radicals as metabolites of drugs derived from phenothiazine, *Biochim. Biophys. Acta*, 29, 441 (DOI: 10.1016/0006-3002(58)90212-9).
- [14] (a) Peterson, B. M., Ren, D., Shen, L., Wu, Y.-C. M., Ulgut, B., Coates, G. W., Abruña, H. D., Fors, B. P. (2018), Phenothiazine-Based Polymer Cathode Materials with Ultrahigh Power Densities for Lithium Ion Batteries, *ACS Appl. Energy Mater.*, 1, 3560-3564 (DOI: 10.1021/acsaem.8b00778); (b) Salunke, J., Guo, X., Lin, Z., Vale, J. R., Candeias, N. R., Nyman, M., Dahlstrom, S., Osterbacka, R., Priimagi, V., Chang, J., Vivo, P. (2019), Phenothiazine-Based Hole-Transporting Materials toward Eco-friendly Perovskite Solar Cells, *ACS Appl. Energy Mater.*, 2, 3021-3027 (DOI: 10.1021/acsaem.9b00408); (c) Kamimura, T., Ohkubo, K., Kawashima, Y., Ozako, S., Sakaguchi, K.-i., Fukuzumi, S., Tani, F. (2015), Long-Lived Photoinduced Charge Separation in Inclusion Complexes Composed of a Phenothiazine-Bridged Cyclic Porphyrin Dimer and Fullerenes, *J. Phys. Chem. C*, 119, 25634-25650 (DOI: 10.1021/acs.jpcc.5b09147); (d) Lu, Y., Song, H., Li, X., Ågren, H., Liu, Q., Zhang, J., Zhang, X., Xie, Y. (2019), Multiply Wrapped Porphyrin Dyes with a Phenothiazine Donor: A High Efficiency of 11.7% Achieved through a Synergetic Coadsorption and Cosensitization Approach, *ACS Appl. Mater. Interfaces*, 11, 5046-5054 (DOI: 10.1021/acsaem.8b19077).
- [15] (a) Jordan, M., Kivala, M., Boudon, C., Gisselbrecht, J.-P., Schweizer, W. B., Seiler, P., Diederich, F. (2011), Switching the Regioselectivity in Cycloaddition-Retro-Electrocyclizations between Donor-Activated Alkynes and the Electron-Accepting Olefins TCNE and TCNQ, *Chem. Asian J.*, 6, 396-401 (DOI: 10.1002/asia.201000539); (b) Michinobu, T., Boudon, C., Gisselbrecht, J.-P., Seiler, P., Frank, B., Moonen, N. N. P., Gross, M., Diederich, F. (2006), Donor-Substituted 1,1,4,4-Tetracyanobutadienes (TCBDs): New Chromophores with Efficient Intramolecular Charge-Transfer Interactions by Atom-Economic Synthesis, *Chem. Eur. J.*, 12, 1889-1905 (DOI: 10.1002/chem.200501113); (c) Kivala, M., Boudon, C.,

- Gisselbrecht, J.-P., Enko, B., Seiler, P., Müller, I. B., Langer, N., Jarowski, P. D., Gescheidt, G., Diederich, F. (2009), Organic Super-Acceptors with Efficient Intramolecular Charge-Transfer Interactions by [2+2] Cycloadditions of TCNE, TCNQ, and F₄-TCNQ to Donor-Substituted Cyanoalkynes, *Chem. Eur. J.*, 15, 4111-4123 (DOI: 10.1002/chem.200802563).
- [16] (a) Sekita, M., Ballesteros, B., Diederich, F., Guldi, D. M., Bottari, G., Torres, T. (2016), Intense Ground-State Charge-Transfer Interactions in Low-Bandgap, Panchromatic Phthalocyanine–Tetracyanobuta-1,3-diene Conjugates, *Angew. Chem. Int. Ed.*, 55, 5560-5564 (DOI: 10.1002/anie.201601258); (b) Winterfeld, K. A., Lavarda, G., Guilleme, J., Sekita, M., Guldi, D. M., Torres, T., Bottari, G. (2017), Subphthalocyanines Axially Substituted with a Tetracyanobuta-1,3-diene–Aniline Moiety: Synthesis, Structure, and Physicochemical Properties, *J. Am. Chem. Soc.*, 139, 5520-5529 (DOI: 10.1021/jacs.7b01460).
- [17] (a) Breiten, B., Jordan, M., Taura, D., Zalibera, M., Griesser, M., Confortin, D., Boudon, C., Gisselbrecht, J.-P., Schweizer, W. B., Gescheidt, G., Diederich, F. (2013), Donor-Substituted Octacyano[4]dendralenes: Investigation of π -Electron Delocalization in Their Radical Ions, *J. Org. Chem.*, 78, 1760-1767 (DOI: 10.1021/jo301194y); (b) Kato, S.-i., Diederich, F. (2010), Non-planar push–pull chromophores, *Chem. Commun.*, 46, 1994-2006 (DOI: 10.1039/B926601A).
- [18] (a) Michinobu, T. (2008), Click-Type Reaction of Aromatic Polyamines for Improvement of Thermal and Optoelectronic Properties, *J. Am. Chem. Soc.*, 130, 14074-14075 (DOI: 10.1021/ja8061612); (b) Fujita, H., Tsuboi, K., Michinobu, T. (2011), High-Yielding Alkyne-Tetracyanoethylene Addition Reactions: A Powerful Tool for Analyzing Alkyne-Linked Conjugated Polymer Structures, *Macromol. Chem. Phys.*, 212, 1758-1766 (DOI: 10.1002/macp.201100198); (c) Michinobu, T., May, J. C., Lim, J. H., Boudon, C., Gisselbrecht, J.-P., Seiler, P., Gross, M., Biaggio, I., Diederich, F. (2005), A new class of organic donor–acceptor molecules with large

- third-order optical nonlinearities, *Chem. Commun.*, 737-739 (DOI: 10.1039/B417393G); (d) Michinobu, T. (2011), Adapting semiconducting polymer doping techniques to create new types of click postfunctionalization, *Chem. Soc. Rev.*, 40, 2306-2316 (DOI: 10.1039/C0CS00205D); (e) Li, Y., Tsuboi, K., Michinobu, T. (2010), Double Click Synthesis and Second-Order Nonlinearities of Polystyrenes Bearing Donor–Acceptor Chromophores, *Macromolecules*, 43, 5277-5286 (DOI: 10.1021/ma100869m).
- [19] (a) Misra, R., Gautam, P., Mobin, S. M. (2013), Aryl-Substituted Unsymmetrical Benzothiadiazoles: Synthesis, Structure, and Properties, *J. Org. Chem.*, 78, 12440-12452 (DOI: 10.1021/jo402111q); (b) Misra, R., Gautam, P. (2014), Tuning of the HOMO–LUMO gap of donor-substituted symmetrical and unsymmetrical benzothiadiazoles, *Org. Biomol. Chem.*, 12, 5448-5457 (DOI: 10.1039/C4OB00629A); (c) Rout, Y., Gautam, P., Misra, R. (2017), Unsymmetrical and Symmetrical Push–Pull Phenothiazines, *J. Org. Chem.*, 13, 6840-6845 (DOI: 10.1021/acs.joc.7b00991).
- [20] Basumatary, B., Sekhar, A. R., Reddy, R. V. R., Sankar, J. (2015), Corrole-BODIPY Dyads: Synthesis, Structure, and Electrochemical and Photophysical Properties, *Inorg. Chem.*, 54, 4257-4267 (DOI: 10.1021/ic502919s).
- [21] Frisch M. J., Trucks G. W., Schlegel H. B., Scuseria G. E., Robb M. A., Cheeseman J. R., Scalmani G., Barone V., Mennucci B., Petersson G. A., Nakatsuji H., Caricato M., Li X., Hratchian H. P., Izmaylov A. F., Bloino J., Zheng G., Sonnenberg J. L., Hada M., Ehara M., Toyota K., Fukuda R., Hasegawa J., Ishida M., Nakajima T., Honda Y., Kitao O., Nakai H., Vreven T., Montgomery J. A. Jr., Peralta J. E., Ogliaro F., Bearpark M., Heyd J. J., Brothers E., Kudin K. N., Staroverov V. N., Kobayashi R., J., Raghavachari K., Rendell A., Burant J. C., Iyengar S. S., Tomasi J., Cossi M., Rega N., Millam J. M., Klene M., Knox J. E., Cross J. B., Bakken V., Adamo C., Jaramillo J., Gomperts R., Stratmann R. E., Yazyev O., Austin A. J., Cammi

R., Pomelli C., Ochterski J. W., Martin R. L., Morokuma K., Zakrzewski V. G., Voth G. A., Salvador P., Dannenberg J. J., Dapprich S., Daniels A. D., Farkas Ö., Foresman J. B., Ortiz J. V., Cioslowski J., Fox D. J. (2009), Gaussian 09, Revision C.01, Gaussian, Inc., Wallingford, CT.

Chapter 7

Donor-Acceptor based 1,8-Naphthalimide Substituted Phenothiazines: Tuning of HOMO-LUMO gap

7.1. Introduction

Organic π -conjugated frameworks containing heteroatoms such as sulfur (S) and nitrogen (N) are of great interest of researchers in the view of their potential applications in the field of organic photonics and electronics.^[1] The incorporation of heteroatom-based moieties such as phenothiazine, thiazole, benzothiazole, benzothiadiazole *etc.* in donor-acceptor (D-A) chromophores have received substantial attention in the field of nonlinear optics (NLO), organic light-emitting diodes (OLEDs), organic photovoltaics (OPVs), *etc.*^[2] In order to fine tune the HOMO/LUMO energy levels, D-A based chromophores can be utilized by; (a) changing the donor or acceptor strength or (b) incorporation of different π -linkers.^[3] Therefore, our group is interested to design and synthesize push-pull based chromophores by modulating the donor and acceptor moieties for the application in optoelectronics.^[13d-h]

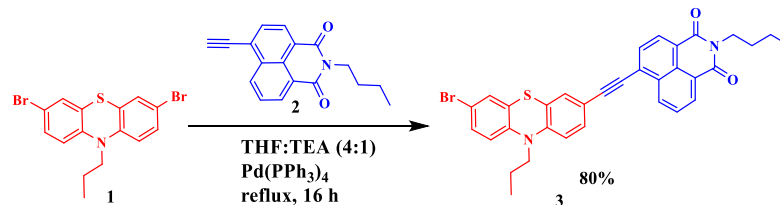
Phenothiazine has attracted the attention of researchers due to its well-conjugated heterocyclic ring system.^[4] Phenothiazine acts as a strong donor due to its electron rich nitrogen and sulphur atom.^[5] It possesses unique electronic and optical properties.^[6] The easy functionalization of phenothiazine chromophores and their higher chemical and thermal stability makes them an excellent prerequisite for optoelectronic applications.^[7] On the other hand, the 1,8-naphthalimide (NPI) is electron deficient fluorophore which acts as a strong acceptor.^[8] NPI exhibits high thermal and chemical stability, strong fluorescence quantum yield, good photostability and have been explored in the field of fluorescent dyes, laser dyes, metal sensors, pH sensors, bioimaging, optoelectronic materials and many more.^[9] We were interested to investigate the effect of the different donors such as phenothiazine, carbazole, ferrocene,

triphenylamine on the photophysical and electrochemical properties of NPI substituted phenothiazines (Figure 1). The electron rich molecules carbazole, ferrocene and TPA act as strong donors.^[10] Furthermore, cyano-based tetracyanoethylene (TCNE) acceptor was incorporated in the donor substituted NPI-phenothiazines.^[11] The TCNE acts as a strong acceptor which shows high chemical reactivity towards electron-rich reagents is frequently used to introduce strong acceptor moieties into organic molecules.^[12] TCNE reacts with the organo-donor-activated electron rich alkynes *via* [2+2] cycloaddition followed by electrocyclic ring-opening reaction to give 1,1,4,4-tetracyanobuta-1,3-diene (TCBD) substituted donor-acceptor molecular systems.^[11, 12] Our group has reported a wide variety of π -linked donor-acceptor-based chromophores as well as TCBD-substituted chromophores for optoelectronic properties.^[13]

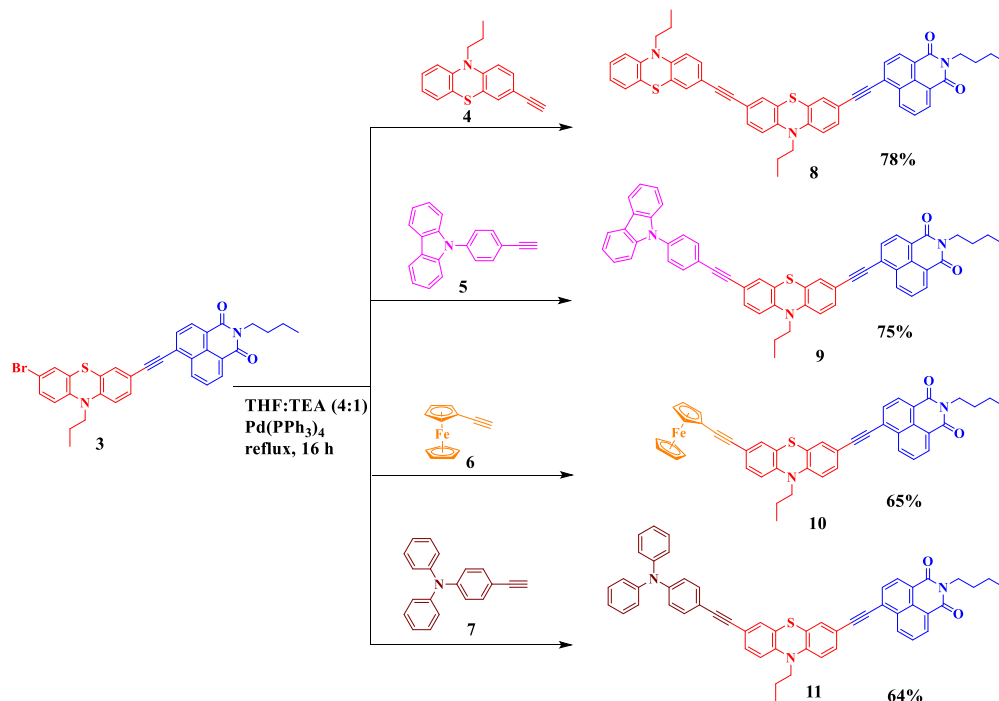
Herein in this chapter we wish to report the design and synthesis of D- π -D- π -A, D'- π -D- π -A, D-A'-D- π -A and D'-A'-D- π -A type of phenothiazine based molecular systems. In this work, our main objective was to modulate the photophysical and electrochemical properties of the donor-acceptor systems. We have also done comparative studies by varying different donors in the phenothiazine derivatives. In addition, we have explored the theoretical calculation to study the conformation and electronic properties of the phenothiazine derivatives.

7.2. Results and Discussion

Synthesis. The chromophores **8**, **9**, **10** and **11** were synthesized by Sonogashira cross-coupling reactions of PTZ-NPI precursor **3** with different ethynyl substituted donors. The PTZ-NPI precursor **3** was synthesized *via* Sonogashira cross-coupling reaction of 3,7-dibromo-10-propylphenothiazine and 4-ethynyl-1,8-naphthalimide in 80% yield (Scheme 7.1). The Pd-catalysed Sonogashira cross-coupling reactions of precursor **3** with the intermediates ethynyl phenothiazine (**4**), ethynyl carbazole (**5**), ethynyl ferrocene (**6**) and ethynyl TPA (**7**) at 60 °C for 16 h gave **8**, **9**, **10** and **11** in 78%, 75%, 65% and 64% yield, respectively (Scheme 7.2). The intermediates **4-7** were synthesized by the literature procedures.

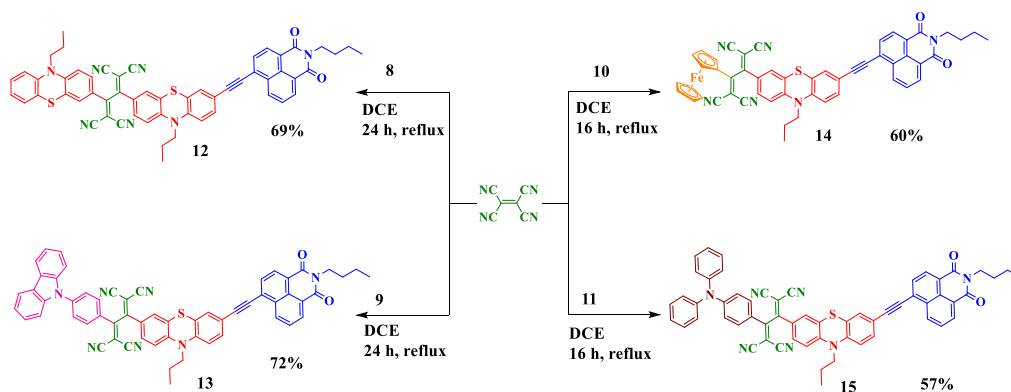


Scheme 7.1. Synthetic route of compound **3**.



Scheme 7.2. Synthetic route of compounds **8–11**.

In order to tune the HOMO–LUMO gap of the donor substituted PTZ–NPI based compounds **8–11**, TCBD acceptor introduced to obtain compounds **12 – 15** (Scheme 7.3). Compounds **8** and **9** undergo [2+2] cycloaddition–electrocyclic ring-opening reaction in presence of TCNE, using dichloroethane (DCE) as solvent, at reflux condition within 24 h to give TCBD substituted compounds **12** and **13** in 69% and 72% yield, respectively. Compound **10** underwent similar kind of conversion with TCNE in DCE within 24 h and gave compound **14** in 60% yield. The reaction of compound **11** with TCNE at similar condition within 24 h resulted in compound **15** which gave 57% yield.



Scheme 7.3. Synthetic route of compounds 12–15.

The PTZ-NPI based push-pull chromophores **3** and **8–15** are soluble in common organic solvents, such as dichloromethane, chloroform, tetrahydrofuran, and were well characterized by using ^1H and ^{13}C NMR spectroscopy and HRMS techniques. The compound **3** was characterized by single-crystal X-ray crystallography.

Crystal. The single crystals of the intermediate **3** was obtained by the slow diffusion of a mixture of dichloromethane and hexane solution (2:1) at room temperature. The molecule crystallizes in triclinic $P\bar{1}$ form. The front view and side view of the crystal structures are shown in Figure 7.1. The data refinement parameters Table 7.1. The intermediate **3** show butterfly like structure. The dihedral angle between the NPI and phenothiazine units in intermediate **3** is 22.2° .

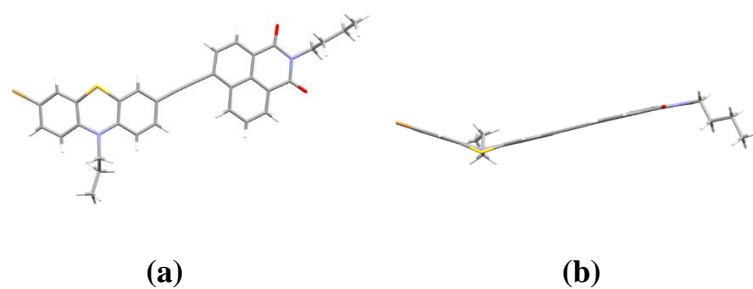


Figure 7.1. Crystal structures of compound **3**: (i) front view, (ii) side view.

Table 7.1. Crystal structure data and refinement parameters.

| Compound | 3 |
|---|--|
| Empirical formula | C ₃₃ H ₂₇ Br N ₂ O ₂ S |
| Formula weight | 595.53 |
| Temperature/K | 293(2) K |
| Wavelength/Å | 0.71073 Å |
| Crystal system | Triclinic |
| Space group | <i>P</i> $\bar{1}$ |
| a/Å | 8.2382(9) |
| α /° | 90.811(7) |
| b/Å | 8.5477(7) |
| β /° | 97.894(8) |
| c/Å | 21.8887(18) |
| γ /° | 115.390(10) |
| Volume Å ³ | 1374.7(2) |
| Z, Calculated density Mg/m ³ | 2, 1.439 |
| Absorption coefficient mm ⁻¹ | 1.605 |
| F(000) | 612 |
| Crystal size/mm | 0.330 x 0.260 x 0.210 |
| θ range for data collection/° | 2.882 to 32.236 |
| Reflections collected/unique | 18426 / 8921 [R(int) = 0.0805] |
| Completeness to θ | 99.8 % |
| Absorption correction | Semi-empirical from equivalents |
| Max. and min. transmission | 1.00000 and 0.31585 |
| Refinement method | Full-matrix least- squares on F ² |
| Data / restraints / parameters | 8921 / 0 / 355 |
| Goodness-of-fit on F ² | 0.905 |
| Final R indices [I>2sigma(I)] | R1 = 0.0665, wR2 = 0.1452 |
| R indices (all data) | R1 = 0.2046, wR2 = 0.2061 |
| Largest diff. peak and hole/e Å ⁻³ | 0.470 and -0.561 |

7.3. Photophysical Properties

The electronic absorption spectra of the compounds **8–11** and their TCBD conjugates **12–15** were recorded in dichloromethane at room temperature (Figure 7.2 and Figure 7.3), and the data are collected in Table 7.2.

The compounds **8, 9, 10** and **11** showed two absorption bands in the UV-Vis region. They exhibited intermolecular charge transfer band (ICT) with lower intensity at 445, 445, 448 and 446 nm, respectively which could be attributed to the donor–acceptor interactions. On the other hand, higher intensity π – π^* transitions were observed at 372, 341, 352 and 352 nm for the compounds **8, 9, 10** and **11**, respectively, which may be due to the presence of phenothiazine, carbazole, ferrocene, and triphenylamine donors.

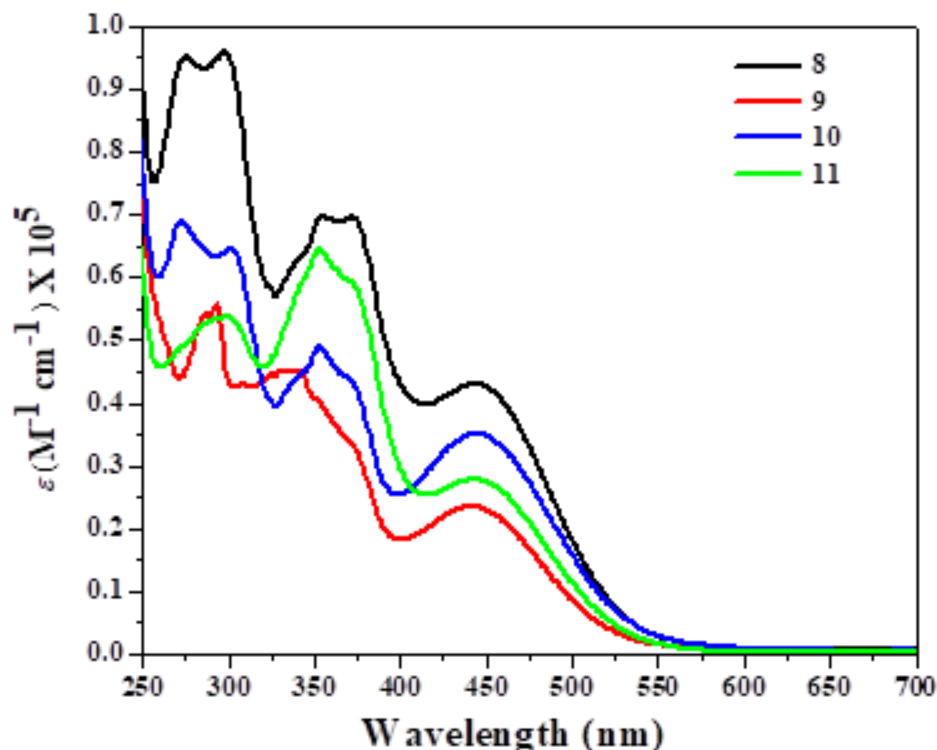


Figure 7.2. The electronic absorption spectra of phenothiazines **8–11** in dichloromethane (1×10^{-5} M).

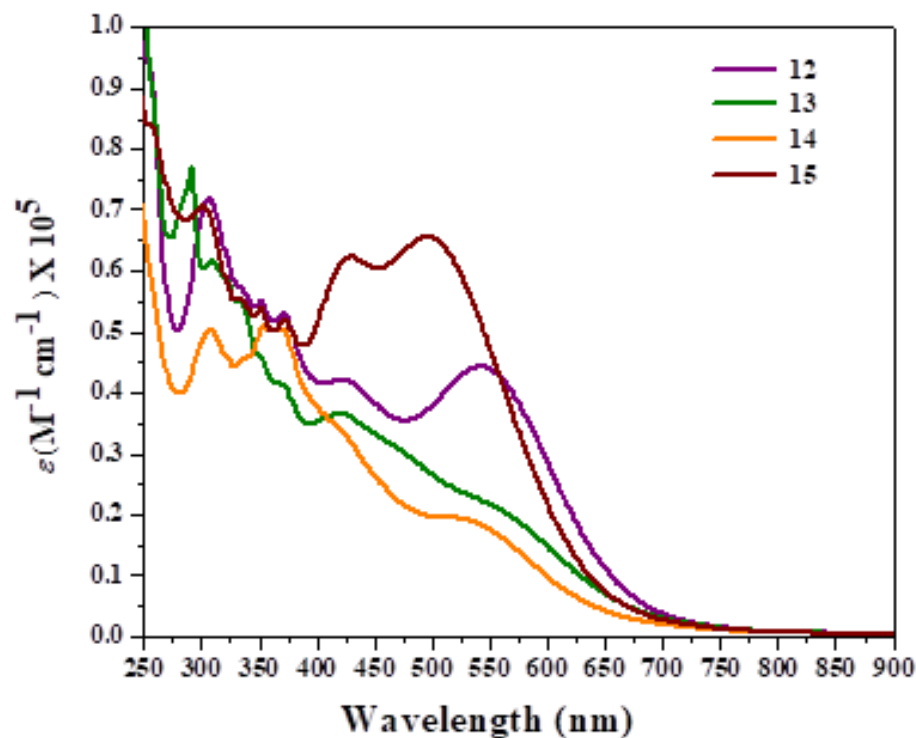


Figure 7.3. The electronic absorption spectra of phenothiazines **12–15** in dichloromethane (1×10^{-5} M).

The TCBD derivatives **12–15** resulted in red shifted absorption spectrum as compared to **8–11**, respectively. The compounds **12**, **13**, **14** and **15** showed ICT transition at 554, 548 nm, 539 nm and 495 nm respectively. Along with the ICT transition all the TCBD substituted **12–15** showed a shoulder bands in the range of 375–475 nm which may be due to the presence of two different donor moieties in the molecules. The introduction of different donors such as phenothiazine, carbazole, ferrocene and TPA in **8–11** resulted in almost similar absorption bands which implies that changing the donor strength do not have much effect on the absorption properties. Conversely, the incorporation of the TCBD acceptors in **12–15** resulted in strong donor–acceptor interaction which leads to red shifted absorption spectra and low HOMO–LUMO gap. The trend in the optical band gap follows the order $9 > 10 > 11 > 8 > 15 > 14 > 12 > 13$. The result was further explained by TD-DFT calculation in dichloromethane phase.

Table 7.2. Photophysical properties of compounds **8–15** in dichloromethane.

| Phenothiazines | Photophysical data ^a | | Theoretical | Electrochemical | | |
|----------------|---------------------------------|--|---|-----------------|--|--|
| | λ_{abs} (nm) | ϵ (M ⁻¹ cm ⁻¹) | Optical Band Gap (eV) ^b | data | HOMO- LUMO energy gap (eV) ^c | E _{ox} (V) E _{red} (V) |
| 8 | 445 | 43196 | 2.21 | 2.4 | 0.76 | -1.26 |
| | 372 | 69446 | | | 0.9 | |
| | 298 | 95876 | | | | |
| 9 | 445 | 23167 | 2.3 | 2.55 | 0.85 | -1.27 |
| | 341 | 44986 | | | 1.03 | |
| | 293 | 55613 | | | | |
| 10 | 448 | 34877 | 2.18 | 2.5 | 0.61 | -1.26 |
| | 352 | 49035 | | | 0.95 | |
| | 301 | 64281 | | | | |
| 11 | 446 | 27703 | 2.2 | 2.34 | 0.79 | -1.28 |
| | 352 | 64521 | | | 1.03 | |
| | 302 | 53440 | | | | |
| 12 | 554 | 44144 | 1.7 | 2.32 | 1.01 | -0.45 |
| | 424 | 41748 | | | -0.77 | |
| | 306 | 72173 | | | -1.27 | |
| 13 | 548 | 22555 | 1.69 | 2.22 | 1.07 | -0.36 |
| | 423 | 37001 | | | 1.33 | -0.73 |
| | 291 | 77416 | | | -1.26 | |

| | | | | | | |
|-----------|-----|-------|------|------|------|-------|
| 14 | 539 | 18651 | 1.76 | 2.56 | 0.92 | -0.57 |
| | 421 | 34325 | | | 1.04 | -0.84 |
| | 306 | 50136 | | | | -1.26 |
| 15 | 495 | 65592 | 1.77 | 2.4 | 1.07 | -0.47 |
| | 428 | 62616 | | | 1.28 | -0.77 |
| | 303 | 70507 | | | | -1.26 |

^a Absorbance measured in dichloromethane at 1×10^{-5} M concentration; λ_{abs} : absorption wavelength; ϵ : extinction coefficient. ^b determined from onset wavelength of the UV/Vis absorption; ^c obtained from density functional theory calculations at B3LYP/6-31+G** level; ^d recorded by cyclic voltammetry, in 0.1 M solution of TBAPF₆ in DCM at 100 mV s⁻¹ scan rate versus SCE electrode.

7.4. Electrochemical Properties

The electrochemical properties of compounds **8–11** and their TCBD conjugates **12–15** were explored by cyclic voltammetry (CV) in dry dichloromethane (DCM) solution at room temperature using tetrabutylammonium hexafluorophosphate (TBAPF₆) as a supporting electrolyte. The electrochemical data are compiled in Table 7.2, and the CV plots are shown in Figure 7.4 and Figure 7.5.

In general, the phenothiazine moiety shows one reversible oxidation wave and the NPI moiety shows one reversible reduction wave. The compounds **8–15** showed two oxidation waves due to the presence of two donor units in the molecules.

The compounds **8**, **9**, **10** and **11** showed two reversible oxidation potentials at +0.76, +0.9 V; +0.85, +1.03 V; +0.61, +0.95 V; and +0.79, +1.03 V, respectively. The first oxidation potentials of the **8–11** could be attributed to the terminal donor moieties such as, phenothiazine, carbazole, ferrocene, and TPA, respectively, whereas the second oxidation potentials could be due to the central phenothiazine moieties. On the other hand, compounds **8**, **9**, **10** and **11** exhibited reversible one electron reduction wave at -1.26, -1.27, -1.26 and -1.28 V, which could be attributed to the NPI moieties.

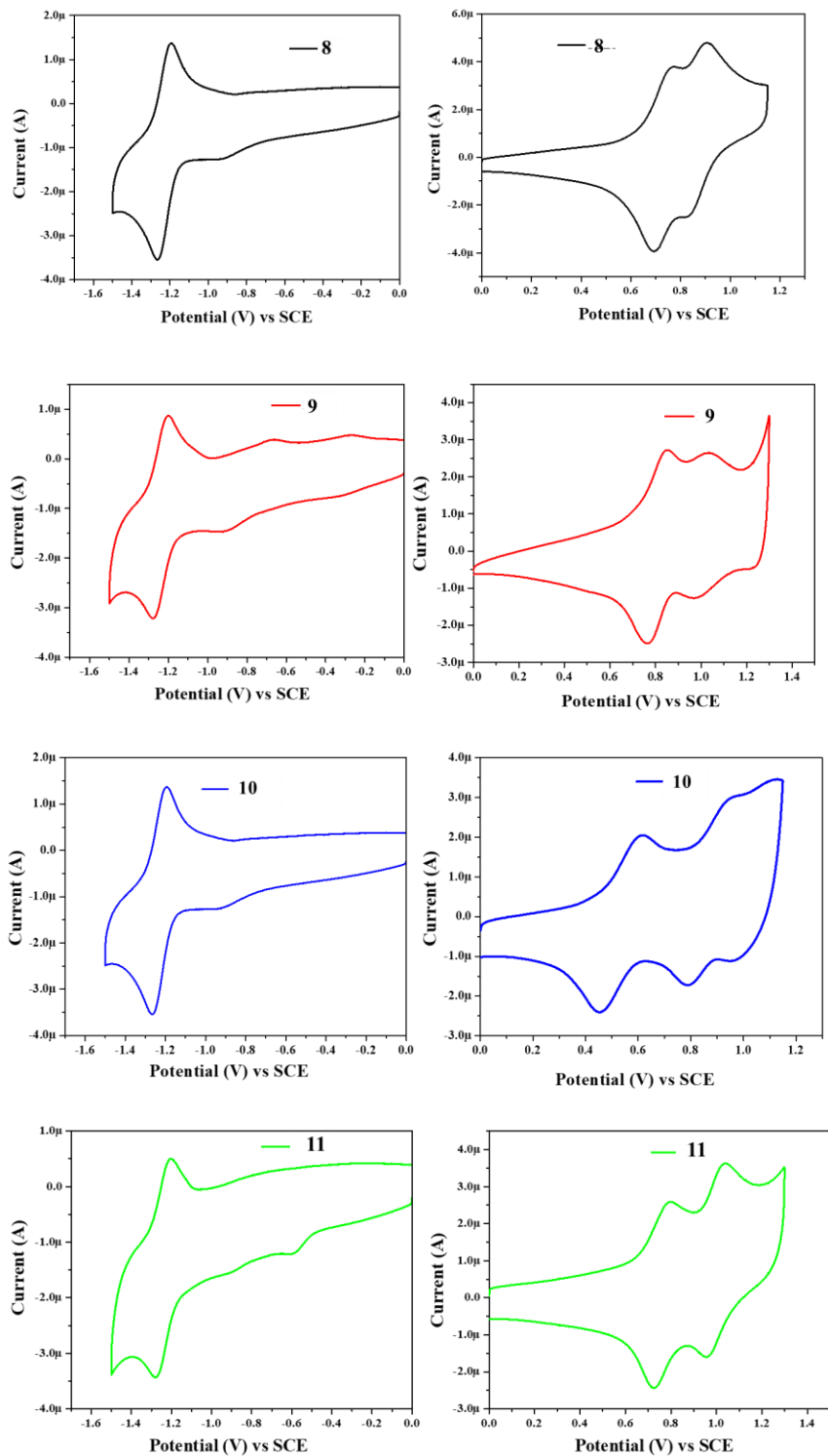


Figure 7.4. Cyclic voltammograms of phenothiazines **8–11** (0.01 M) in dichloromethane with 0.1 M TBAPF₆ at a scan rate of 100 mVs⁻¹ versus a standard calomel electrode (SCE) at 25 °C.

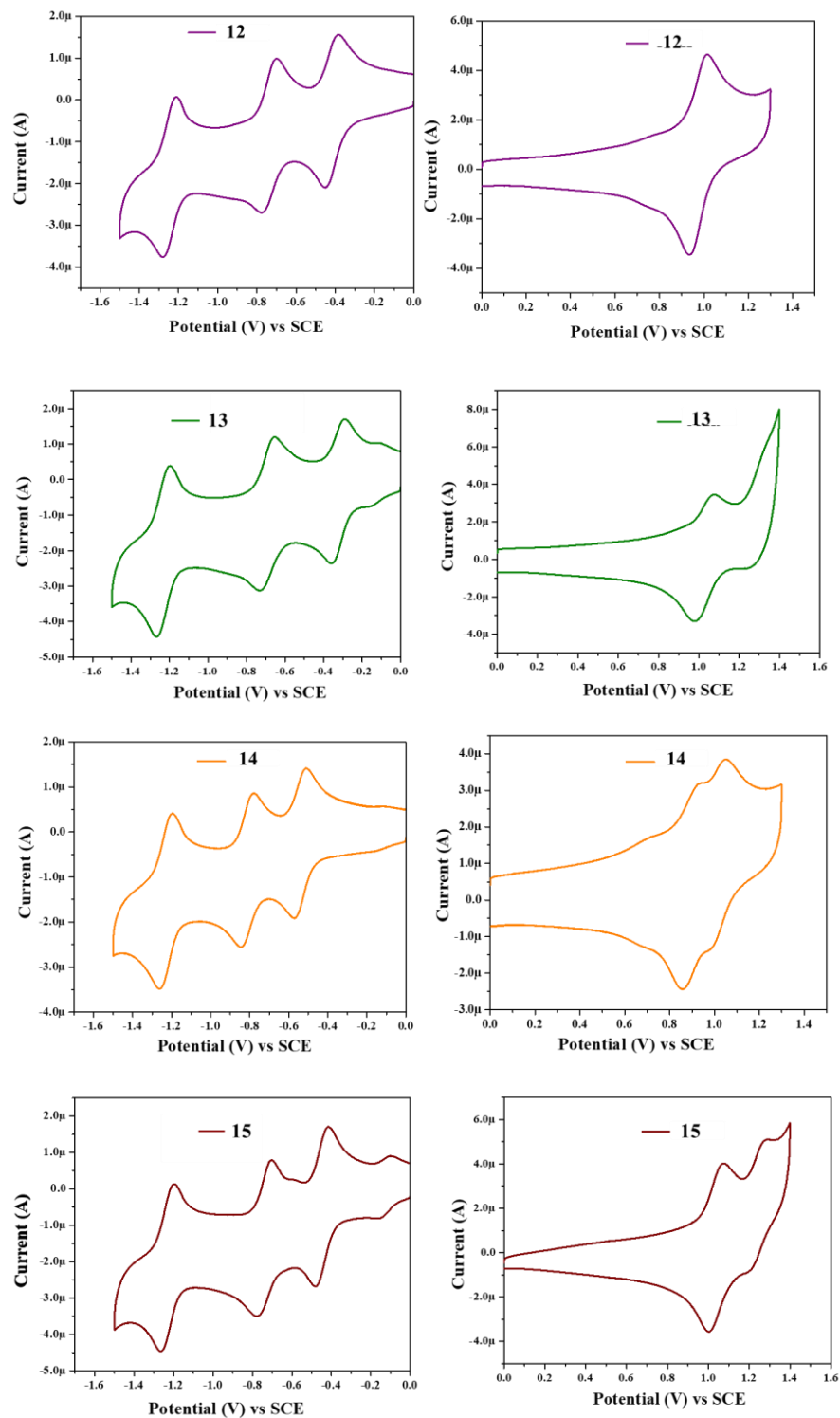


Figure 7.5. Cyclic voltammograms of phenothiazines **12–15** (0.01 M) in dichloromethane with 0.1 M TBAPF₆ at a scan rate of 100 mVs⁻¹ versus a standard calomel electrode (SCE) at 25 °C.

In case of TCBD substituted phenothiazines **13**, **14** and **15**, two oxidation waves were observed at +1.07, +1.33 V; +0.92, +1.04 V; and +1.07, +1.28 V, respectively, in which the first oxidation potentials could be due to the carbazole, ferrocene, and TPA moieties, respectively and the second oxidation potentials could be due to the central phenothiazine moieties. Compound **12** exhibited one reversible oxidation potential which could be to the simultaneous reversible oxidation potentials of the two phenothiazine donor moieties. The compounds **12–15** showed three reduction waves. The first and second reduction potentials of compounds **12**, **13**, **14** and **15** were observed at –0.45, –0.77 V; –0.36, –0.73 V; –0.57, –0.84 V; and –0.47, –0.77 V respectively, which may be due to the TCBD acceptors, whereas the third reduction potentials were observed at ~1.26 V for all the molecules due to the NPI moieties. The data showed that the TCBD substituted compounds **12–15** showed low first reduction potential values as compared to compounds **8–11** which reveals that the incorporation of TCBD acceptor in the former stabilized the LUMO energy level of the compounds **12–15** to greater extent resulting in a much lower HOMO–LUMO gap. The HOMO/LUMO energy levels calculated from the onset values of compounds **8**, **9**, **10**, **11**, **12**, **13**, **14** and **15** are as follows, –5.03/–3.29, –5.11/–3.29, –4.88/–3.3, –5.1/–3.28, –5.31/–4.11, –5.37/–4.18, –5.23/–3.97, –5.36/–4.07, respectively.

7.5. Theoretical Calculations

In order to explore the electronic structure and geometry of compounds **8–15**, density functional theory calculations were performed B3LYP/6-31+G** level for C, H, N, O, Fe and S.^[14] The optimised structure of compounds **8–15** showed nonplanar orientation with twisted geometry. The HOMO energy levels are mainly localized on the stronger donor moieties and the LUMO energy levels are localized on the stronger acceptor moieties. The data reveals that the incorporation of TCBD moiety in compounds **12–15** leads to a strong donor-acceptor interaction. The energy level diagram are shown in Figure 7.6.

In case of donor substituted PTZ-NPIs the HOMO–LUMO energy levels are localized as follows: (a) The HOMO of the phenothiazine substituted PTZ-

NPI (**8**) is localized on both the phenothiazine moieties. (b) Similarly, in case of carbazole substituted PTZ-NPI (**9**) the HOMO is distributed on the carbazole and phenothiazine moieties. (c) The HOMO of ferrocene substituted PTZ-NPI (**10**) is localized on both the ferrocene and phenothiazine moiety whereas for TPA substituted PTZ-NPI (**11**) the HOMO is localized on both the TPA and phenothiazine moiety. (d) In **8–11**, the LUMO energy levels of **8–11** are mainly localized on the NPI moiety and partially localized on the phenothiazine moiety.

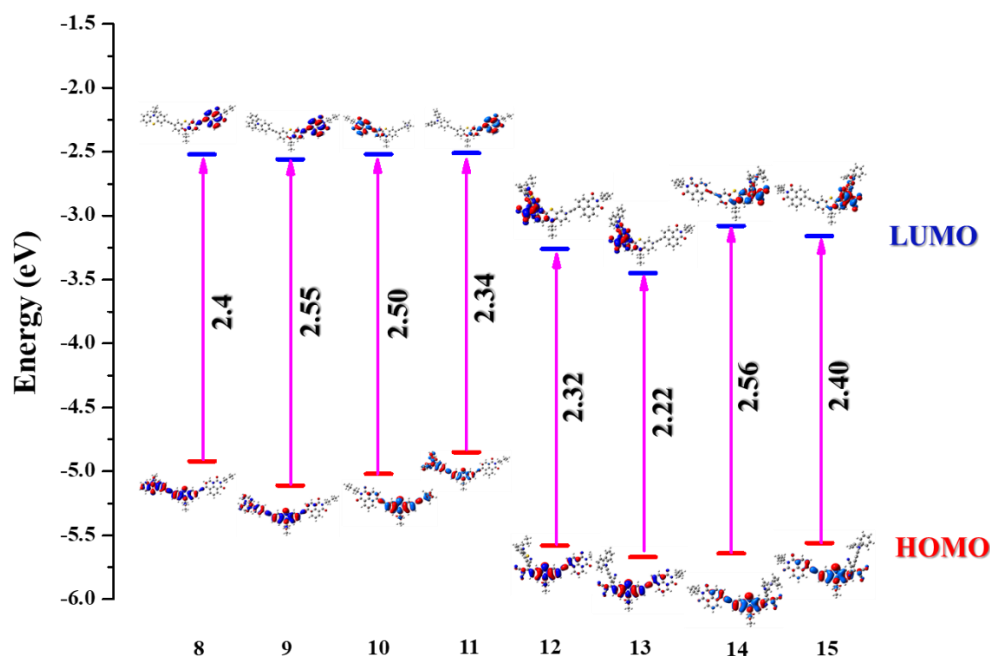


Figure 7.6. Energy diagram showing the HOMO and LUMO wave functions and energies of phenothiazines **8–15** as determined at B3LYP/6-31G** level.

On the other hand, the HOMOs of the TCBD substituted compounds **12–15** are mainly localized on the phenothiazine moieties whereas the LUMOs are localized on the TCBD moieties which resulted in a strong donor-acceptor interaction. The theoretically calculated HOMO energy levels of compounds **8, 9, 10, 11, 12, 13, 14** and **15** are -4.92 eV, -5.11 eV, -5.02 eV, -4.85 eV, -5.58 eV, -5.67 eV, -5.64 eV and -5.56 eV whereas the LUMO energy levels are -2.52 eV, -2.56 eV, -2.52 eV, -2.51 eV, -3.26 eV, -3.45 eV, -3.08 eV and -3.16 eV. The

data reveals that the LUMO energy levels of the TCBD substituted compounds **12–15** are much more stabilized as compared to the compounds **8–11**.

Table 7.3. Calculated electronic transition of compounds **8–15**.

| Compou nds | Wavelength | Composition | f^a | Assignme nt |
|---------------|------------|----------------------|-------|----------------|
| 8 | 413 | HOMO→LUMO (0.49) | 1.62 | ICT |
| | 321 | HOMO-2→LUMO (0.33) | 0.73 | $\pi-\pi^*$ |
| | 274 | HOMO-3→LUMO+1 (0.28) | 0.53 | $\pi-\pi^*$ |
| 9 | 411 | HOMO→LUMO (0.53) | 1.61 | ICT |
| | 315 | HOMO-3→LUMO (0.38) | 0.74 | $\pi-\pi^*$ |
| | 276 | HOMO-5→LUMO (0.35) | 0.28 | $\pi-\pi^*$ |
| 10 | 411 | HOMO→LUMO (0.55) | 1.40 | ICT |
| | 312 | HOMO→LUMO (0.35) | 0.22 | $\pi-\pi^*$ |
| | 277 | HOMO-1→LUMO+1 (0.27) | 0.51 | $\pi-\pi^*$ |
| 11 | 414 | HOMO→LUMO (0.43) | 1.66 | ICT |
| | 325 | HOMO-2→LUMO (0.38) | 0.89 | $\pi-\pi^*$ |
| | 274 | HOMO-2→LUMO+2 (0.23) | 0.34 | $\pi-\pi^*$ |
| 12 | 481 | HOMO→LUMO (0.61) | 0.75 | ICT |
| | 394 | HOMO→LUMO+1 (0.57) | 0.77 | $\pi-\pi^*$ |
| | 274 | HOMO→LUMO+7 (0.23) | 0.25 | $\pi-\pi^*$ |
| 13 | 489 | HOMO-1→LUMO (0.63) | 0.66 | ICT |
| | 399 | HOMO→LUMO+1 (0.59) | 0.72 | $\pi-\pi^*$ |
| | 283 | HOMO-4→LUMO+1 (0.4) | 0.16 | $\pi-\pi^*$ |
| 14 | 455 | HOMO→LUMO (0.64) | 1.03 | ICT |
| | 379 | HOMO→LUMO+2 (0.46) | 0.66 | $\pi-\pi^*$ |
| | 304 | HOMO-5→LUMO+1 (0.52) | 0.26 | $\pi-\pi^*$ |
| 15 | 473 | HOMO→LUMO (0.59) | 0.87 | ICT |
| | 390 | HOMO→LUMO+1 (0.57) | 0.77 | $\pi-\pi^*$ |
| | 269 | HOMO→LUMO+3 (0.37) | 0.28 | $\pi-\pi^*$ |

f^o oscillator strength

The TD-DFT calculations were performed at the CAM-B3LYP/6-31G (d, p) level for the optimization of compounds **8–15** in dichloromethane to evaluate the absorption properties. The transitions with composition, oscillator strengths, and assignments are as shown in Table 2. The molecular orbital diagrams are shown in Table S1–S3. The TD-DFT calculation showed three absorption bands for all the molecules. The compounds **8, 9, 10, 11, 12, 13, 14** and **15** showed absorption band at 413, 411, 411, 414, 481, 489, 455 and 473 nm respectively which could be attributed to the ICT transitions, where the absorption bands at the shorter wavelengths may be due to the π - π^* transitions. The ICT transitions occur from HOMO→LUMO for all the molecules. The TD-DFT calculation showed that the TCBD substituted compounds **12–15** are red shifted as compared to compounds **8–11**. The theoretical electronic absorption wavelengths were found to be lower than those of experimental values which might be due to various factors, e.g. solvent effect, dipole moment and temperature.

7.6. Experimental Section

General Methods. Chemicals were used as received unless otherwise indicated. All the oxygen or moisture sensitive reactions were carried out under argon atmosphere. ^1H NMR spectra were recorded using a 400 MHz spectrometer. Chemical shifts are reported in delta (δ) units, expressed in parts per million (ppm) downfield from tetramethylsilane (TMS) using residual protonated solvent as an internal standard $\{\text{CDCl}_3, 7.26 \text{ ppm}\}$. ^{13}C NMR spectra were recorded using a 100 MHz spectrometer. Chemical shifts are reported in delta (δ) units, expressed in parts per million (ppm) downfield from tetramethylsilane (TMS) using the solvent as internal standard $\{\text{CDCl}_3, 77.0 \text{ ppm}\}$. The ^1H NMR splitting patterns have been described as “s, singlet; d, doublet; t, triplet and m, multiplet”. UV/Vis spectrums of all compounds were recorded in dichloromethane solution. Cyclic voltammograms were recorded on electrochemical analyzer using Glassy carbon as working electrode, Pt wire as the counter electrode, and Saturated Calomel Electrode (SCE) as the reference electrode. The scan rate was 100mVs^{-1} for

Cyclic Voltammetry. A solution of tetrabutylammonium hexafluorophosphate (TBAPF₆) in CH₂Cl₂ (0.1M) was used as supporting electrolyte.

Crystallographic data

A single crystal X-ray structural study of compound **3** was performed on a CCD Agilent Technologies (Oxford Diffraction) SUPER NOVA diffractometer. Data were collected at 150(2) K using graphite-monochromated Mo K α radiation ($\lambda = 0.71073$ Å). The strategy for the Data collection was evaluated by using the CrysAlisPro CCD software. The data were collected by the standard ϕ - ω scan techniques, and were scaled and reduced using CrysAlisPro RED software. The structures were solved by direct methods using SHELXS-97, and refined by full matrix least-squares with SHELXL-97, refining on F². The positions of all the atoms were obtained by direct methods. All non-hydrogen atoms were refined anisotropically. The remaining hydrogen atoms were placed in geometrically constrained positions, and refined with isotropic temperature factors, generally 1.2U_{eq} of their parent atoms. The CCDC number 1997741 contain the supplementary crystallographic data for **3**. These data can be obtained free of charge via www.ccdc.cam.ac.uk (or from the Cambridge Crystallographic Data Centre, 12 union Road, Cambridge CB21 EZ, UK; Fax: (+44) 1223-336-033; or deposit@ccdc.cam.ac.uk).

Generalized Synthetic Procedure for the Compounds 8–11:

The intermediate phenothiazine-NPI **3** (100 mg, 0.22 mmol) and the corresponding alkynes (mg, 0.22 mmol) were dissolved in a mixture of dry THF (20 mL) and triethylamine (5 mL). The reaction mixture was purged with argon, followed by the addition of Pd(PPh₃)₂Cl₂ (15 mg, 5 mol %), and CuI (8.3 mg, 10 mol %). The reaction mixture was stirred at 60 °C for 12 h. After the completion of the reaction the solvent was removed in a vacuum, and the products were purified by column chromatography with n-hexane/CH₂Cl₂ (3:7) as the eluent by column chromatography on silica gel.

Characterization Data:

Compound **8**: Orangish Red Solid, Yield: 103.0 mg, 78%. ¹H NMR (400 MHz, CDCl₃): δ = 8.70 (1H, *J*=8.28, d), 8.64 (1H, *J*=7.04, d), 8.54 (1H, *J*=7.56, d), 7.90 (1H, *J*=7.52, d), 7.83 (1H, *J*=7.8, t), 7.43 (1H, *J*=8.56, d), 7.39 (1H, s), 7.29-7.24 (4H, m), 7.16-7.10 (2H, m), 6.93-6.89 (1H, m), 6.85-6.76 (4H, m), 4.18 (2H, *J*=7.52, d), 3.86-3.79 (4H, m), 1.88-1.80 (4H, m), 1.72-1.68 (2H, m), 1.50-1.42 (2H, m), 1.06-0.96 (9H, m); ¹³C NMR (100 MHz, CDCl₃): δ = 164.0, 163.8, 145.7, 145.2, 144.6, 143.9, 132.4, 131.5, 131.5, 131.4, 131.3, 130.7, 130.6, 130.4, 130.3, 130.1, 130.0, 128.1, 127.7, 127.4, 127.3, 127.2, 124.8, 124.4, 124.2, 123.8, 122.9, 122.7, 121.8, 118.0, 116.9, 116.1, 115.5, 115.3, 115.2, 115.0, 98.8, 89.1, 88.2, 86.6, 49.5, 49.3, 40.3, 30.2, 20.4, 20.1, 20.0, 13.8, 11.3, 11.2; LCMS (ESI-TOF): *m/z* calculated for C₅₃H₃₉N₃O₂S = 781.2758 [M]⁺, measured 781.2490 [M]⁺.

Compound **9**: Orangish Red Solid, Yield: 98.0 mg, 75%. ¹H NMR (400 MHz, CDCl₃): δ = 8.68 (d, *J*=8.28, 1H), 8.62 (d, *J*=7.04, 1H), 8.53 (d, *J*=7.52, 1H), 8.14 (d, *J*=7.52, 2H), 7.89 (d, *J*=7.52, 1H), 7.81 (t, *J*=7.8, 1H), 7.73 (d, *J*=8.04, 2H), 7.56 (d, *J*=8.28, 2H), 7.45-7.25 (m, 9H), 6.85 (t, *J*=8.04, 2H), 4.18 (t, *J*=7.28, 2H), 3.86 (t, *J*=7.0, 2H), 1.91-1.86 (m, 2H), 1.73-1.71 (m, 2H), 1.51-1.43 (m, 2H), 1.08-0.97 (m, 6H); ¹³C NMR (100 MHz, CDCl₃): δ = 163.9, 163.7, 145.5, 144.4, 140.5, 137.4, 132.9, 132.3, 131.5, 131.4, 131.0, 130.4, 130.2, 128.0, 127.6, 127.3, 126.8, 126.0, 124.3, 123.9, 123.5, 122.9, 122.2, 121.8, 120.3, 120.2, 117.5, 116.2, 115.3, 115.2, 109.7, 98.7, 89.5, 88.9, 86.7, 49.5, 40.3, 30.2, 20.4, 19.9, 13.8, 11.2; LCMS (ESI-TOF): *m/z* calculated for C₅₀H₄₁N₃O₂S₂ = 779.2635 [M]⁺, measured 779.2803 [M]⁺.

Compound **10**: Orangish Red Solid, Yield: 80.0 mg, 65%. ¹H NMR (400 MHz, CDCl₃): δ = 8.70 (d, *J*=8.0, 1H), 8.64 (d, *J*=7.04, 1H), 8.54 (d, *J*=7.56, 1H), 7.90 (d, *J*=7.76, 1H), 7.83 (t, *J*=7.8, 1H), 7.70 (t, *J*=5.76, 1H), 7.44 (d, *J*=7.0, 1H), 7.39 (s, 1H), 7.28-7.24 (m, 1H), 6.85 (d, *J*=7.92, 1H), 6.79 (d, *J*=8.52, 1H), 4.47 (s, 2H), 4.23 (s, 6H), 4.18 (t, *J*=7.56, 2H), 3.84 (t, *J*=7.04, 2H), 1.88-1.82 (m, 2H), 1.76-1.69 (m, 2H), 1.48-1.42 (m, 2H), 1.04 (t, *J*=7.28, 3H), 0.98 (t, *J*=7.28, 3H);

^{13}C NMR (100 MHz, CDCl_3): $\delta = 164.0, 163.7, 145.8, 143.6, 135.2, 132.3, 131.5, 131.3, 130.6, 130.4, 130.0, 128.0, 127.3, 124.5, 123.8, 122.9, 121.8, 118.5, 116.0, 115.3, 115.2, 98.8, 88.5, 86.6, 84.7, 71.3, 69.9, 68.8, 65.3, 49.5, 40.3, 30.2, 20.4, 19.9, 13.8, 11.2$; HRMS (ESI-TOF): m/z calculated for $\text{C}_{45}\text{H}_{36}\text{FeN}_2\text{O}_2\text{S} = 724.1842$ $[\text{M}]^+$, measured 724.1948 $[\text{M}]^+$

Compound **11**: Orangish Red Solid, Yield: 85.0 mg, 64%. ^1H NMR (400 MHz, CDCl_3): $\delta = 7.59$ (1H, d, $J = 7.28$ Hz), 7.30 (1H, s), 7.16 (1H, t, $J = 7.56$ Hz), 7.06 - 6.95 (2H, m), 6.87 - 6.81 (2H, m), 5.18 (1H, s), 4.95 (1H, s), 4.84 (1H, s), 4.70 (1H, s), 4.45 - 4.37 (5H, m), 3.82 (2H, t, $J = 7.04$ Hz), 1.85 - 1.79 (2H, m), 1.01 (3H, t, $J = 7.28$ Hz); ^{13}C NMR (100 MHz, CDCl_3): $\delta 173.3, 163.5, 150.8, 142.2, 129.7, 128.6, 127.9, 127.6, 127.5, 125.3, 124.3, 124.2, 122.6, 116.1, 114.9, 113.7, 112.8, 112.5, 80.3, 79.1, 75.5, 75.4, 74.9, 72.7, 72.5, 72.0, 71.9, 71.5, 49.9, 19.9, 11.1$; HRMS (ESI-TOF): m/z calculated for $\text{C}_{53}\text{H}_{41}\text{N}_3\text{O}_2\text{S} = 783.2914$ $[\text{M}]^+$, measured 783.297 $[\text{M}]^+$.

Synthesis of Compound 12. Tetracyanoethylene (TCNE) (13 mg, 0.1 mmol) was added to a solution of compound **8** (80.0 mg, 0.1 mmol) in $\text{C}_2\text{H}_4\text{Cl}_2$ (50 mL). The mixture was stirred at 80°C for 24 h. After the completion of the reaction the solvent was removed in a vacuum, and the product was purified by column chromatography with CH_2Cl_2 as the eluent to yield **12** as a dark violet colored solid. Yield: 65.0 mg, 69%; ^1H NMR (400 MHz, CDCl_3): $\delta = 8.68$ - 8.63 (2H, m), 8.54 (1H, $J = 7.8$, d), 7.91 (1H, $J = 7.52$, d), 7.83 (1H, $J = 7.76$, t), 7.71 - 7.67 (m, 2H), 7.47 - 7.44 (m, 1H), 7.37 - 7.35 (m, 3H), 7.17 (t, $J = 7.28$, 1H), 7.06 (d, $J = 6.52$, 1H), 6.99 (t, $J = 7.52$, 1H), 6.91 - 6.86 (m, 4H), 4.18 (t, $J = 7.56$, 2H), 3.90 - 3.84 (m, 4H), 1.92 - 1.83 (m, 4H), 1.76 - 1.68 (m, 2H), 1.50 - 1.40 (m, 2H), 1.09 - 0.96 (m, 9H); ^{13}C NMR (100 MHz, CDCl_3): $\delta = 164.2, 163.9, 163.8, 163.7, 151.3, 150.1, 142.9, 141.9, 132.2, 131.7, 131.6, 131.5, 130.6, 130.5, 130.4, 130.3, 128.0, 127.9, 127.7, 127.6, 127.4, 127.2, 125.5, 125.3, 124.9, 124.5, 124.4, 123.2, 123.0, 122.6, 122.2, 118.2, 116.2, 115.9, 115.5, 115.1, 112.9, 112.9, 112.7, 112.2, 111.9, 97.7, 87.4, 81.7, 80.5, 50.1, 49.9, 40.3, 30.2, 20.4, 20.0, 19.9, 13.8, 11.1$; LCMS (ESI-TOF): m/z calculated for $\text{C}_{59}\text{H}_{39}\text{N}_7\text{O}_2\text{S} = 909.2880$ $[\text{M}]^+$, measured 909.2247 $[\text{M}]^+$.

Synthesis of Compound 13. Tetracyanoethylene (TCNE) (13 mg, 0.1 mmol) was added to a solution of compound **9** (80 mg, 0.1 mmol) in C₂H₄Cl₂ (50 mL). The mixture was stirred at 80 °C for 24 h. After the completion of the reaction the solvent was removed in a vacuum, and the product was purified by column chromatography with CH₂Cl₂ as the eluent to yield compound **13** as a dark violet colored solid. Yield: 67.0 mg, 72%; ¹H NMR (400 MHz, CDCl₃): δ = 8.68-8.63 (m, 2H), 8.54 (d, *J*=7.76, 1H), 8.13 (d, *J*=7.52, 2H), 8.99 (d, *J*=8.52, 2H), 7.91 (d, *J*=7.8, 1H), 7.86 (d, *J*=8.8, 2H), 7.82 (d, *J*=7.76, 1H), 7.77-7.75 (m, 1H), 7.57 (d, *J*=8.28, 2H), 7.50-7.43 (m, 4H), 7.37-7.33 (m, 3H), 6.97 (d, *J*=8.8, 1H), 6.92 (d, *J*=8.56, 1H), 4.18 (t, *J*=7.28, 2H), 3.91 (t, *J*=7.04, 2H), 1.93-1.86 (m, 2H), 1.76 (m, 2H), 1.48-1.42 (m, 2H), 1.09 (t, *J*=7.28,), 0.98 (t, *J*=7.28, 3H); ¹³C NMR (100 MHz, CDCl₃): δ = 165.9, 163.9, 163.6, 163.4, 150.4, 143.9, 142.7, 139.4, 132.1, 131.7, 131.6, 131.4, 131.3, 130.6, 130.5, 130.3, 128.7, 128.0, 127.6, 127.4, 127.1, 126.9, 126.5, 125.2, 124.9, 124.3, 123.0, 122.2, 121.5, 120.6, 118.4, 116.1, 115.6, 112.6, 111.9, 111.3, 109.8, 97.5, 87.5, 86.6, 81.8, 53.4, 40.3, 30.2, 20.3, 19.9, 13.8, 11.1; LCMS (ESI-TOF): *m/z* calculated for C₅₆H₄₁N₇O₂S₂= 908.2836 [M]⁺, measured 908.2846 [M]⁺.

Synthesis of Compound 14. Tetracyanoethylene (TCNE) (14 mg, 0.11 mmol) was added to a solution of compound **10** (80 mg, 0.11 mmol) in C₂H₄Cl₂ (50 mL). The mixture was stirred at 80 °C for 16 h. After the completion of the reaction the solvent was removed in a vacuum, and the product was purified by column chromatography with CH₂Cl₂ as the eluent to yield compound **14** as a dark violet colored solid. Yield: 57.0 mg, 60%; ¹H NMR (400 MHz, CDCl₃): δ = 8.66 (t, *J*=8.76, 2H), 8.55 (d, *J*=7.56, 1H), 7.91 (d, *J*=7.52, 1H), 7.83 (t, *J*=7.8, 1H), 7.61-7.58 (m, 1H), 7.47-7.44 (m, 1H), 7.36 (s, 1H), 7.32 (s, 1H), 6.9-6.86 (m, 2H), 5.23 (s, 1H), 4.98 (s, 1H), 4.87 (s, 1H), 4.70 (s, 1H), 4.47 (s, 4H), 4.18 (t, *J*=7.52, 2H), 3.86 (t, *J*=7.28, 2H), 1.89-1.83 (m, 2H), 1.76-1.68 (m, 2H), 1.48-1.42 (m, 2H), 1.06 (t, *J*=7.28, 3H), 0.98 (t, *J*=7.28, 3H); ¹³C NMR (100 MHz, CDCl₃): δ = 173.1, 163.9, 163.7, 163.5, 149.8, 143.2, 132.2, 131.7, 131.6, 131.5, 130.6, 130.5, 130.3, 129.7, 128.1, 127.5, 127.4, 127.2, 124.9, 124.8, 123.2, 123.1, 122.2, 118.1, 115.9, 115.4, 113.6, 112.8, 112.6, 112.3, 97.6, 87.4, 81.3, 79.1, 75.6, 75.4, 75.0,

72.6, 72.1, 71.9, 50.0, 40.3, 30.2, 20.4, 19.9, 13.8, 11.1; LCMS (ESI-TOF): m/z calculated for $C_{51}H_{36}FeN_6O_2S= 853.2044 [M+H]^+$, measured 853.1518 $[M+H]^+$.

Synthesis of Compound 15. Tetracyanoethylene (TCNE) (13 mg, 0.5 mmol) was added to a solution of compound **11** (80 mg, 0.11 mmol) in $C_2H_4Cl_2$ (50 mL). The mixture was stirred at 80 °C for 8 h. After the completion of the reaction the solvent was removed in a vacuum, and the product was purified by column chromatography with CH_2Cl_2 as the eluent to yield compound **15** as a dark violet colored solid. Yield: 53.0 mg, 57%; 1H NMR (400 MHz, $CDCl_3$): $\delta = 8.68-8.63$ (m, 2H), 8.55 (d, $J=7.56$, 1H), 7.92 (d, $J=7.76$, 1H), 7.83 (t, $J=8.04$, 1H), 7.74-7.71 (m, 1H), 7.64 (d, $J=9.28$, 2H), 7.46 (d, $J=8.52$, 1H), 7.41-7.36 (m, 6H), 7.28-7.21 (m, 6H), 6.91 (t, $J=9.04$, 4H), 4.18 (t, $J=7.56$, 2H), 3.88 (t, $J=7.04$, 2H), 1.92-1.85 (m, 2H), 1.76-1.68 (m, 2H), 1.48-1.42 (m, 2H), 1.07 (t, $J=7.28$, 3H), 0.98 (t, $J=7.28$, 3H); ^{13}C NMR (100 MHz, $CDCl_3$): $\delta = 165.2, 163.9, 163.7, 153.8, 149.9, 144.5, 143.1, 132.2, 131.9, 131.6, 131.5, 130.6, 130.5, 130.4, 130.3, 130.1, 128.1, 127.9, 127.5, 127.2, 126.9, 126.7, 125.7, 124.8, 123.3, 123.1, 122.2, 121.5, 118.1, 118.0, 115.9, 115.4, 113.6, 112.8, 97.7, 87.4, 50.1, 40.3, 30.2, 20.4, 19.9, 13.8, 11.4, 11.1$; LCMS (ESI-TOF): m/z calculated for $C_{59}H_{41}N_7O_2S= 912.3115 [M+H]^+$, measured 912.2555 $[M+H]^+$.

7.7. Conclusions

A series of donor substituted phenothiazine-NPI based chromophores **8–11** and their TCBD analogues **12–15** were synthesized *via* Pd-catalyzed Sonogashira cross-coupling reaction and [2+2] cycloaddition–electrocyclic ring-opening reactions, respectively. The electronic absorption spectra of the TCBD substituted phenothiazines **12–15** showed strong ICT transition in the longer wavelength as compared to the donor substituted phenothiazines **8–11**. The electrochemical properties revealed that the incorporation of TCBD in phenothiazines facilitates the reduction process to greater extent resulting in a much stabilized LUMO energy levels. The DFT and TDDFT calculations revealed that the TCBD substituted phenothiazines **12–15** are having much lower HOMO–LUMO gap as compared to compounds **8–11**, which are in a good

agreement with the photophysical and electrochemical data. The work provides a broad understanding of the effect of the strength of donors/acceptors on the photonic and electronic properties of the chromophores, which could be helpful for the design and synthesis of the donor–acceptor chromophores for optoelectronic applications.

7.8 References

- [1] (a) Bent, H. A. (1968), Structural chemistry of donor-acceptor interactions, *Chem. Rev.*, 68, 587-648 (DOI: 10.1021/cr60255a003); (b) Reissig, H.-U., Zimmer, R. (2003), Donor-Acceptor-Substituted Cyclopropane Derivatives and Their Application in Organic Synthesis, *Chem. Rev.*, 103, 1151-1196 (DOI: 10.1021/cr010016n); (c) Wan, X., Li, C., Zhang, M., Chen, Y. (2020), Acceptor–donor–acceptor type molecules for high performance organic photovoltaics – chemistry and mechanism, *Chem. Soc. Rev.* (DOI: 10.1039/D0CS00084A); (d) Zhang, J., Jin, J., Xu, H., Zhang, Q., Huang, W. (2018), Recent progress on organic donor–acceptor complexes as active elements in organic field-effect transistors, *J. Mater. Chem. C*, 6, 3485-3498 (DOI: 10.1039/C7TC04389A); (e) Li, Y., Liu, J.-Y., Zhao, Y.-D., Cao, Y.-C. (2017), Recent advancements of high efficient donor–acceptor type blue small molecule applied for OLEDs, *Mater. Today*, 20, 258-266 (DOI: 10.1016/j.mattod.2016.12.003).
- [2] (a) Han, L., Chen, Y., Zhao, J., Cui, Y., Jiang, S. (2020), Phenothiazine dyes containing a 4-phenyl-2-(thiophen-2-yl) thiazole bridge for dye-sensitized solar cells, *Tetrahedron*, 76, 131102 (DOI: 10.1016/j.tet.2020.131102); (b) Sathiyam, G., Chatterjee, S., Sen, P., Garg, A., Gupta, R. K., Singh, A. (2019), Thiazolothiazole-Based Fluorescence Probe towards Detection of Copper and Iron Ions through Formation of Radical Cations, *ChemistrySelect*, 4, 11718–11725 (DOI: 10.1002/slct.201902994); (c) Seintis, K., Şahin, Ç., Sigmundová, I., Stathatos, E., Hrobárik, P., Fakis, M. (2018), Solvent-Acidity-Driven Change in Photophysics and Significant Efficiency Improvement in Dye-

- Sensitized Solar Cells of a Benzothiazole-Derived Organic Sensitizer, *J. Phys. Chem. C*, 122, 20122-20134 (DOI: 10.1021/acs.jpcc.8b05686); (d) Wang, J.-L., Xiao, Q., Pei, J. (2010), Benzothiadiazole-Based D- π -A- π -D Organic Dyes with Tunable Band Gap: Synthesis and Photophysical Properties, *Org. Lett.*, 12, 4164-4167 (DOI: 10.1021/ol101754q).
- [3] (a) Bures, F., Schweizer, W. B., May, J. C., Boudon, C., Gisselbrecht, J.-P., Gross, M., Biaggio, I., Diederich, F. (2007), Property Tuning in Charge-Transfer Chromophores by Systematic Modulation of the Spacer between Donor and Acceptor, *Chem. Eur. J.*, 13, 5378-5387 (DOI: 10.1002/chem.200601735); (b) Poddar, M., Sivakumar, G., Misra, R. (2019), Donor-acceptor substituted 1,8-naphthalimides: design, synthesis, and structure-property relationship, *J. Mater. Chem. C*, 7, 14798-14815 (DOI: 10.1039/C9TC02634G); (c) Jaswal, S., Kumar, J. (2020), Review on fluorescent donor-acceptor conjugated system as molecular probes, *Mater. Today*, (DOI: 10.1016/j.matpr.2019.12.161); (d) Misra, R., Gautam, P., Mobin, S. M. (2013), Aryl-Substituted Unsymmetrical Benzothiadiazoles: Synthesis, Structure, and Properties, *J. Org. Chem.*, 78, 12440-12452 (DOI: 10.1021/jo402111q); (e) Dhokale, B., Gautam, P., Misra, R. (2012), Donor-acceptor perylene-3,4,9,10-tetracarboxylic diimide-ferrocene conjugates: synthesis, photophysical, and electrochemical properties, *Tetrahedron Lett.*, 53, 2352-2354 (DOI: 10.1016/j.tetlet.2012.02.107); (f) Misra, R., Gautam, P., Jadhav, T., Mobin, S. M. (2013), Donor-Acceptor Ferrocenyl-Substituted Benzothiadiazoles: Synthesis, Structure, and Properties, *J. Org. Chem.*, 78, 4940-4948 (DOI: 10.1021/jo4005734); (g) Dhokale, B., Jadhav, T., Mobin, S. M., Misra R. (2015), Meso Alkynylated Tetraphenylethylene (TPE) and 2,3,3-Triphenylacrylonitrile (TPAN) Substituted BODIPYs, *J. Org. Chem.*, 80, 8018-8025 (DOI: 10.1021/acs.joc.5b01117); (h) Gautam, P., Misra, R., Siddiqui, S. A., Sharma, G. D. (2015), Unsymmetrical Donor-Acceptor-Acceptor- π -Donor Type Benzothiadiazole-Based Small Molecule for a Solution Processed Bulk Heterojunction Organic

- Solar Cell, *ACS Appl. Mater. Interfaces*, 7, 10283–10292 (DOI: 10.1021/acsami.5b02250).
- [4] (a) Sailer, M., Gropeanu, R.-A., Müller, T. J. J. (2003) Practical Synthesis of Iodo Phenothiazines. A Facile Access to Electrophore Building Blocks, *J. Org. Chem.*, 68, 7509–7512 (DOI: 10.1021/jo034555z); (b) Krämer, C. S., Müller, T. J. J. (2003), Synthesis and Electronic Properties of Alkynylated Phenothiazines, *Eur. J. Org. Chem.*, 3534–3548 (DOI: 10.1002/ejoc.200300250)
- [5] (a) Hauck, M., Stolte, M., Schçnhaber, J., Kuball, H.-G., Muller, T. J. J. (2011) Synthesis, Electronic, and Electro-Optical Properties of Emissive Solvatochromic Phenothiazinyl Merocyanine, *Dyes. Chem. Eur. J.*, 17, 9984–9998 (DOI: 10.1002/chem.201100592); (b) Krämer, C. S., Zeitler, K., Müller, T. J. J. (2000), Synthesis of Functionalized Ethynylphenothiazine Fluorophores, *Org. Lett.*, 2, 3723–3726 (DOI: 10.1021/ol0066328).
- [6] (a) Konidena, R. K., Thomas, K. R. J., Kumar, S., Wang, Y.-C., Li, C.-J., Jou, J.-H. (2015), Phenothiazine Decorated Carbazoles: Effect of Substitution Pattern on the Optical and Electroluminescent Characteristics, *J. Org. Chem.*, 80, 5812–5823 (DOI: 10.1021/acs.joc.5b00787); (b) Wang, W., Li, X., Lan, J., Wu, D., Wang, R., You, J. (2018), Construction of 3,7-Dithienyl Phenothiazine-Based Organic Dyes via Multistep Direct C–H Arylation Reactions *J. Org. Chem.*, 83, 8114–8126 (DOI: 10.1021/acs.joc.8b00915). (c) Poddar, M., Gautam, P., Rout, Y., Misra, R. (2017), Donor–acceptor phenothiazine functionalized BODIPYs, *Dyes and Pigments*, 146, 368–373 (DOI: 10.1016/j.dyepig.2017.07.017); (d) Poddar, M., Misra, R. (2017), NIR-Absorbing Donor–Acceptor Based 1,1,4,4-Tetracyanobuta-1,3-Diene (TCBD)- and Cyclohexa-2,5-Diene-1,4-Ylidene-Expanded TCBD-Substituted Ferrocenyl Phenothiazines, *Chem. Asian J.*, 12, 2908–2915 (DOI: 10.1002/asia.201700879); (e) Poddar, M., Jang, Y., Misra, R., D’Souza, F. (2020), Excited State Electron Transfer in 1,1,4,4-Tetracyanobuta-1,3-Diene (TCBD)- and Cyclohexa-2,5-Diene-1,4-

Diylidene-Expanded TCBD-Substituted BODIPY Phenothiazines Donor-Acceptor Conjugates, *Chem. Eur. J.* (DOI: 10.1002/chem.202000346).

- [7] (a) Luo, J.-S., Wan, Z.-Q., Jia, C.-Y. (2016), Recent advances in phenothiazine-based dyes for dye-sensitized solar cells, *Chinese Chemical Letters*, 27, 1304–1318 (DOI: 10.1016/j.ccllet.2016.07.002); (b) Thokala, S., Singh, S. P. (2020), Phenothiazine-Based Hole Transport Materials for Perovskite Solar Cells, *ACS Omega*, 5, 5608–5619 (DOI: 10.1021/acsomega.0c00065); (c) Huang, Z.-S., Meier, H., Cao, D. (2016), Phenothiazine-based dyes for efficient dye-sensitized solar cells, *J. Mater. Chem. C*, 4, 2404-2426 (DOI: 10.1039/c5tc04418a); (d) Al-Busaidi, I. J., Haque, A., Rasbi, N. K. A., Khan M. S. (2019), Phenothiazine-based derivatives for optoelectronic applications: A review, *Synthetic Metals*, 257, 116189 (DOI: 10.1016/j.synthmet.2019.116189).
- [8] (a) Zeng, W., Lai, H.-Y., Lee, W.-K., Jiao, M., Shiu, Y.-J., Zhong, C., Gong, S., Zhou, T., Xie, G., Sarma, M., Wong, K.-T., Wu, C.-C., Yang, C. (2018), Achieving Nearly 30% External Quantum Efficiency for Orange–Red Organic Light Emitting Diodes by Employing Thermally Activated Delayed Fluorescence Emitters Composed of 1,8-Naphthalimide-Acridine Hybrids, *Adv. Mater.*, 30, 1704961 (DOI: 10.1002/adma.201704961); (b) Oguzhan, E., Bilgili, H., Koyuncu, F. B., Ozdemir, E., Koyuncu, S. (2013), A new processable donor–acceptor polymer displaying neutral state yellow electrochromism, *Polymer*, 54, 6283-6292 (DOI: 10.1016/j.polymer.2013.09.033).
- [9] (a) Poddar, M., Sharma, V., Mobin, S. M., Misra, R. (2018), 1,8-Naphthalimide-Substituted BODIPY Dyads: Synthesis, Structure, Properties, and Live-Cell Imaging, *Chem. Asian J.*, 13, 2881–2890 (DOI: 10.1002/asia.201800816); (b) Carlotti, B., Poddar, M., Elisei, F., Spalletti, A., Misra, R. (2019), Energy-Transfer and Charge-Transfer Dynamics in Highly Fluorescent Naphthalimide–BODIPY Dyads: Effect of BODIPY Orientation, *J. Phys. Chem. C*, 123, 24362 (DOI: 10.1021/acs.jpcc.9b05851). (c) Banerjee, S., Veale, E. B., Phelan, C. M.,

- Murphy, S. A., Tocci, G. M., Gillespie, L. J., Frimannsson, D. O., Kelly, J. M., Gunnlaugsson, T. (2013), Recent advances in the development of 1,8-naphthalimide based DNA targeting binders, anticancer and fluorescent cellular imaging agents, *Chem. Soc. Rev.*, 42, 1601-1618 (DOI: 10.1039/C2CS35467E).
- [10] (a) Dhokale, B., Gautam, P., Mobin, S. M., Misra R. (2013), Donor–acceptor, ferrocenyl substituted BODIPYs with marvelous supramolecular interactions, *Dalton Trans.*, 42, 1512–1518 (DOI: 10.1039/c2dt31632c); (b) Rout, Y., Gautam, P., Misra, R. (2017), Unsymmetrical and Symmetrical Push–Pull Phenothiazines, *J. Org. Chem.*, 13, 6840-6845 (DOI: 10.1021/acs.joc.7b00991); (c) Misra, R., Jadhav, T., Dhokale, B., Gautam, P., Sharma, R., Maragani, R., Mobin, S. M. (2014), Carbazole-BODIPY conjugates: design, synthesis, structure and properties, *Dalton Trans.*, 43, 13076–13086 (DOI: 10.1039/c4dt00983e).
- [11] (a) Morioka, Y., Yoshizawa, N., Nishida, J.-i., Yamashita, Y. (2004), Novel Donor– π –Acceptor Compounds Containing 1,3-Dithiol-2-ylidene and Tetracyanobutadiene Units. *Chem. Lett.*, 33, 1190–1191 (DOI: 10.1246/cl.2004.1190); (b) Michinobu, T., Boudon, I., Gisselbrecht, J.-P., Seiler, P., Frank, B., Moonen, N. N. P., Gross, M., Diederich, F. (2006), Donor-Substituted 1,1,4,4-Tetracyanobutadienes (TCBDs): New Chromophores with Efficient Intramolecular Charge-Transfer Interactions by Atom-Economic Synthesis. *Chem.–Eur. J.*, 12, 1889–1905 (DOI: 10.1002/chem.200501113).
- [12] (a) Krauß, N., Kielmann, M., Ma, J., Butenschön, H. (2015), Reactions of Alkynyl- and 1,1'-Dialkynylferrocenes with Tetracyanoethylene – Unanticipated Addition at the Less Electron-Rich of Two Triple Bonds. *Eur. J. Org. Chem.*, 2622–2631 (DOI: 10.1002/ejoc.201500105); (b) Kato, S.-i., Noguchi, H., Jin, S., Nakamura, Y. (2016), Synthesis and Electronic, Optical, and Electrochemical Properties of a Series of Tetracyanobutadiene-Substituted Carbazoles. *Asian J. Org. Chem.*, 5, 246–256 (DOI: 10.1002/ajoc.201500431).

- [13] (a) Gautam, P., Sharma, R., Misra, R., Keshtov, M. L., Kuklin, S. A., Sharma, G. D. (2017), Donor–acceptor–acceptor (D–A–A) type 1,8-naphthalimides as non-fullerene small molecule acceptors for bulk heterojunction solar cells. *Chem. Sci.*, 8, 2017–2024 (DOI: 10.1039/C6SC04461A); (b) Patil, Y., Misra, R., Singhal, R., Sharma, G. D. (2017), Ferrocene-diketopyrrolopyrrole based non-fullerene acceptors for bulk heterojunction polymer solar cells. *J. Mater. Chem. A*, 5, 13625–13633 (DOI: 10.1039/C7TA03322B). (c) Gautam, P., Misra, R., Thomas, M. B., D’Souza, F. (2017), Ultrafast charge separation in triphenylamine-BODIPY derived triads carrying centrally positioned, highly electron deficient, dicyanoquinodimethane or tetracyanobutadiene electron acceptors, *Chem. Eur. J.*, 23, 9192 (DOI: 10.1002/chem.201701604).
- [14] Frisch M. J., Trucks G. W., Schlegel H. B., Scuseria G. E., Robb M. A., Cheeseman J. R., Scalmani G., Barone V., Mennucci B., Petersson G. A., Nakatsuji H., Caricato M., Li X., Hratchian H. P., Izmaylov A. F., Bloino J., Zheng G., Sonnenberg J. L., Hada M., Ehara M., Toyota K., Fukuda R., Hasegawa J., Ishida M. Nakajima T., Honda Y., Kitao O., Nakai H., Vreven T., Montgomery J. A. Jr., Peralta J. E., Ogliaro F., Bearpark M., Heyd J. J., Brothers E., Kudin K. N., Staroverov V. N., Kobayashi R., Normand J., Raghavachari K., Rendell A., Burant J. C., Iyengar S. S., Tomasi J., Cossi M., Rega N., Millam N. J., Klene M., Knox J. E., Cross J. B., Bakken V., Adamo C., Jaramillo J., Gomperts R., Stratmann R. E., Yazyev O., Austin A. J., Cammi R., Pomelli C.; Ochterski J. W., Martin R. L., Morokuma K., Zakrzewski V. G., Voth G. A., Salvador P., Dannenberg J. J., Dapprich S., Daniels A. D., Farkas O., Foresman J. B., Ortiz J. V., Cioslowski J., Fox D. J. (2009), *Gaussian 09, revision A.02*; Gaussian, Inc.:Wallingford, CT.

Chapter 8

Conclusions and Future Scope

8.1. Conclusions

Phenothiazine is an excellent class of heterocyclic molecule containing nitrogen (N) and sulfur (S) heteroatoms.^[1] It is an electron rich organic molecule which acts as strong donor.^[2] It possesses strong absorption with high molar extinction coefficient and intense luminescence along with a π -conjugated molecular backbone.^[3] The photonic and electronic properties of phenothiazines can be easily tuned by functionalizing with different donor/acceptor substituents.^[4] We have designed and synthesized donor-acceptor functionalized phenothiazines and investigated their photophysical, electrochemical and theoretical properties.

In Chapter 3, we have functionalized the phenothiazine core with a series of aryl (benzene, naphthalene, anthracene, phenanthrene, pyrene) substituents through π -linker *via* Pd-catalyzed Sonogashira cross-coupling reactions. The fluorescence study of the phenothiazines shows that all of them are highly emissive with remarkable quantum yields. The investigated molecules exhibit large Stokes shift values in solution, with the anthracene functionalized phenothiazine featuring strong positive fluorosolvatochromism and thus the largest Stokes shift in polar solvents (7350 cm^{-1} in DMF). These fluorescent compounds are also highly emissive in the solid-state where the phenothiazines substituted with the largest aryl groups show marked red shifts of the emission maxima as compared to the solution, indicating considerable π - π stacking interactions. In particular, the anthracene substituted phenothiazine exhibits strongly redshifted absorption and emission wavelengths both in solid-state and in solution which implies pronounced electronic communication in this fluorophore. This finding agrees with the charge displacement predicted by the TD-DFT calculations as well as with the results of the cyclic voltammetry measurements.

In Chapter 4, a series of TCBD and cyclohexa-2,5-diene-1,4-ylidene-expanded TCBD substituted ferrocenyl phenothiazines were designed and

synthesized by [2+2] cycloaddition–electrocyclic ring-opening reactions. Their electrochemical properties reveal that the incorporation of strong acceptors TCBD and cyclohexa-2,5–diene-1,4–ylidene–expanded TCBD facilitates the reduction process of the ferrocenyl-phenothiazines which leads to low HOMO–LUMO gap. The electronic absorption spectra exhibit strong ICT at longer wavelength and strong donor–acceptor interactions. In particular, DFT and TDDFT calculations reveal a broad understanding of the electronic structure and absorption spectra of the phenothiazine chromophores which reveal that the incorporation of TCBD and cyclohexa-2,5–diene-1,4–ylidene–expanded TCBD acceptor group perturbs HOMO–LUMO gap of the phenothiazines to a greater extent which is in a good agreement with the experimental values.^[5]

In Chapter 5, we have described the design and synthesis of a series of donor-acceptor phenothiazine functionalized BODIPYs *via* the condensation and Pd-catalyzed Sonogashira cross-coupling reaction. The photophysical and electrochemical studies show strong donor-acceptor interactions between phenothiazine and BODIPY. The optimized structure of acetylene linked phenothiazine BODIPY shows co-planar orientation of the phenothiazine donor and the BODIPY acceptor units which leads to extension of conjugation and significant red shift of the absorption bands in 7a and 7b. The calculated HOMO–LUMO gap values were lower in acetylene linked phenothiazine BODIPYs. The increase in acceptor units of phenothiazine functionalized BODIPYs lowers the thermal stability.^[6]

In Chapter 6, we have synthesized BODIPY-phenothiazine *via* Pd-catalyzed Sonogashira cross coupling reaction. Subsequently, the TCBD and DCNQ substituted BODIPY-phenothiazine were synthesized by [2+2] cycloaddition–electrocyclic ring-opening reactions. The photophysical and electrochemical data showed that the incorporation of TCBD and DCNQ acceptors in the BODIPY substituted phenothiazines resulted in strong D–A interactions which led to low HOMO–LUMO band gap. The UV-vis absorption spectra of TCBD and DCNQ substituted BODIPY-phenothiazine showed ICT transitions along with significant broadening in $S_0 \rightarrow S_1$ transition. The theoretical

calculations of all the molecules revealed that the DCNQ substituted BODIPY-phenothiazine stabilized the LUMO energy level to greater extent as compared to TCBD substituted BODIPY-phenothiazine.^[7]

In Chapter 7, we have designed and synthesized a series of donor substituted phenothiazine-NPI based chromophores and their TCBD analogues *via* Pd-catalyzed Sonogashira cross-coupling reaction and [2+2] cycloaddition–electrocyclic ring-opening reactions, respectively. The electronic absorption spectra of the TCBD substituted phenothiazines showed strong ICT transition in the longer wavelength as compared to the donor substituted phenothiazines. The electrochemical properties revealed that the incorporation of TCBD in phenothiazines facilitates the reduction process to greater extent resulting in a much stabilized LUMO energy levels. The DFT and TDDFT calculations revealed that the TCBD substituted phenothiazines are having much lower HOMO–LUMO gap as compared to, which are in a good agreement with the photophysical and electrochemical data.

8.2. Future scope

The thesis highlights an important strategy for design and synthesis of donor–acceptor functionalized phenothiazine molecules with tunable photonic properties and low HOMO–LUMO gap. The HOMO–LUMO gap of the donor–acceptor functionalized phenothiazines can be modified by (a) varying the number of donor/acceptors attached, (b) enhancing the conjugation length and (c) changing the π -linker. The variation in the donor/acceptor strength perturbs the HOMO–LUMO gap to greater extent. The incorporation of TCNE and TCNQ based acceptors can also improve the donor–acceptor interactions in the phenothiazines resulting in strong intramolecular charge-transfer at longer wavelength which could be extended to the near infrared region. The donor–acceptor chromophores with strong absorption and low band gap could be promising candidate for optoelectronic applications. The phenothiazine based fluorophores with high fluorescence quantum yield and large stokes shift values could be excellent prerequisites for their possible use as promising fluorescent probes in bioimaging.

8.3. References

- [1] Al-Busaidi, I. J., Haque, A., Rasbi, N. K. A., Khan M. S. (2019), Phenothiazine-based derivatives for optoelectronic applications: A review, *Synthetic Metals*, 257, 116189 (DOI: 10.1016/j.synthmet.2019.116189).
- [2] Simokaitiene, J., Danilevicius, A., Grigalevicius, S., Grazulevicius, J. V., Getautis, V., Jankauskas, V. (2006), Phenothiazinyl-based hydrazones as new hole-transporting materials for electrophotographic photoreceptors, *Synth. Met.* 156 (14), 926–931 (DOI: 10.1016/j.synthmet.2006.05.011).
- [3] (a) Thokala, S., Singh, S. P. (2020), Phenothiazine-Based Hole Transport Materials for Perovskite Solar Cells, *ACS Omega*, 5, 5608–5619 (DOI: 10.1021/acsomega.0c00065); (b) Hauck, M., Stolte, M., Schønhaber, J., Kuball, H.-G., Müller, T. J. J. (2011) Synthesis, Electronic, and Electro-Optical Properties of Emissive Solvatochromic Phenothiazinyl Merocyanine, Dyes. *Chem. Eur. J.*, 17, 9984–9998 (DOI: 10.1002/chem.201100592); (c) Khan, F., Ekbote, A., Misra, R. (2019), Reversible mechanochromism and aggregation induced enhanced emission in phenothiazine substituted tetraphenylethylene, *New J. Chem.*, 43, 16156–16163 (DOI: 10.1039/C9NJ03290H); (d) Ekbote, A., Mobin, S. M., Misra, R. (2020), Stimuli-responsive phenothiazine-based donor–acceptor isomers: AIE, mechanochromism and polymorphism, *J. Mater. Chem. C*, 8, 3589–3602 DOI: 10.1039/C9TC05192A (DOI: 10.1039/C9TC05192A).
- [4] Huang, Z.-S., Meier, H., Cao, D. (2016), Phenothiazine-based dyes for efficient dye-sensitized solar cells, *J. Mater. Chem. C*, 4, 2404–2426 (DOI: 10.1039/c5tc04418a).
- [5] Poddar, M., Misra, R. (2017), NIR-Absorbing Donor–Acceptor Based 1,1,4,4-Tetracyanobuta-1,3-Diene (TCBD)- and Cyclohexa-2,5-Diene-1,4-Ylidene-Expanded TCBD-Substituted Ferrocenyl Phenothiazines, *Chem. Asian J.*, 12, 2908–2915 (DOI: 10.1002/asia.201700879).

- [6] Poddar, M., Gautam, P., Rout, Y., Misra, R. (2017), Donor–acceptor phenothiazine functionalized BODIPYs, *Dyes and Pigments*, 146, 368-373 (DOI: 10.1016/j.dyepig.2017.07.017).
- [7] Poddar, M., Jang, Y., Misra, R., D'Souza, F. (2020), Excited State Electron Transfer in 1,1,4,4-Tetracyanobuta-1,3-Diene (TCBD)- and Cyclohexa-2,5-Diene-1,4-Diylidene-Expanded TCBD–Substituted BODIPY Phenothiazines Donor-Acceptor Conjugates, *Chem. Eur. J.* (DOI: 10.1002/chem.202000346).